MECHANISMS OF REPLICATIVE SENESCENCE IN WERNER'S SYNDROME CELLS

Badr Ibrahim

PhD

2012

MECHANISMS OF REPLICATIVE SENESCENCE IN WERNER'S SYNDROME CELLS

Badr Ibrahim

A thesis submitted in partial fulfilment of the requirements of the University of Brighton for the degree of Doctor of Philosophy

September 2012

Declaration

I declare that the research contained in this thesis, unless otherwise formally indicated within the text, is the original work of the author. The thesis has not been previously submitted to this or any other university for a degree, and does not incorporate any material already submitted for a degree.

Signature

Date

Abstract

One of the causes of ageing is thought to be the accumulation of senescent cells. Since normal ageing is very complex, diseases with single gene mutations (progeroid syndromes) which show many features of normal ageing have been used as models in ageing research. Werner's syndrome is the progeroid syndrome which mimics most of the features of normal ageing. It is caused by a mutation of the WRN gene that encodes a RecQ helicase/exonuclease involved in DNA fork stabilization and repair during synthesis. Werner's syndrome fibroblasts have been shown to exit their replicative lifespan three to five times more rapidly than normal fibroblasts. The mechanisms of Werner's syndrome senescence have been extensively studied in fibroblasts. However, it is clear that accelerated replicative senescence is not a universal feature of the disease in all tissues. Thus, it is important to study the relationship between Werner's syndrome senescence in different tissue lineages. Donor to donor differences in replicative potential are also known to occur, thus it would be advantageous if replicative lifespan could be studied in cells with isogenic backgrounds.

Accordingly, this thesis describes an attempt to knockdown the WRN gene in normal cell lines to produce $WRN^{-/-}$ isogenic cell lines. RNAi knockdown using shRNA and hammerhead ribozymes was carried out previously but did not demonstrate a reduction in protein levels. However, an increased sensitivity to camptothecin was demonstrated by Comet assay. Therefore, we expressed both the shRNA and the ribozyme in a single cell line in order to improve the knockdown. The work was initially carried out on cell lines to test whether the RNAi method was effective prior to applying it to irreplaceable primary cell strains. This would have helped elucidate whether premature senescence in Werner's syndrome fibroblasts is due to DNA replication fork stalling or due to telomere erosion.

In normal individuals, keratinocyte senescence has been shown to occur by either telomere dependent or independent senescence depending on culture conditions. Thus, we have used keratinocytes from Werner's syndrome to explore the relationship between loss of WRN and replicative senescence in vitro. This was carried out using standard cytokinetic tests in the presence and absence of SB203580, a selective inhibitor of p38 MAP kinase which plays an important role in Werner's syndrome fibroblasts.

Table of contents

Chapter 2

Materials and methods

List of figures

List of tables

Acknowledgment

I would like to offer my deepest gratitude to all of those who helped me achieve the work required to produce this thesis. I would like to start by thanking those whose contributions can not be forgotten and without them completion of this thesis would not have been possible. These include my supervisor, Dr. Katrin Jennert-Burston for her guidance and continuous advice throughout the years of this PhD programme, Prof. Richard Faragher who has introduced me to cellular senescence and taught me how to conduct research, Dr. Angela Sheerin for teaching me laboratory techniques in molecular biology and ensuring that I achieve my goals, Dr. Elizabeth James for teaching me how to culture keratinocytes and optimise culture conditions.

I would like to thank Dr. Joseph Bird for teaching me the basics of many procedures carried out in this thesis and Dr. Dawn Jones for taking me through the procedures of sub-cloning. I will not forget the support I had from Dr. Iain Alan. I would like to thank Dr. Dominik Burton for his help and the many discussions we had over several topics covered in this thesis. I would like to thank Kevin and Leanne Butler for their assistance with statistics. I would like to thank Dr. Tomader Ali, Michelle Barry, Yishan Zheng and Sandeep Kumar for their help in the laboratory.

Chapter 1

Introduction

1.1 The cell cycle

The cell cycle is controlled by several factors and complex mechanisms that decide the cell's fate. Replicative senescence is a consequence of the exit from the cell cycle and is thought to be the main contributor in organismal ageing (Faragher *et al.* 1998). The principal cause of the symptoms of premature ageing featured in Werner's syndrome patients is hypothesised to be the premature replicative senescence of cells (Kipling *et al.* 2004). Cell cycle regulatory proteins are involved in most of the sections discussed in this thesis. Therefore, it is suitable to start with an introduction of the cell cycle.

1.1.1 Introduction to the cell cycle and cell cycle check points

The mammalian cell cycle is composed of four phases: G1 (gap1), S (DNA synthesis), G2 (gap2) and M (mitosis) (Howard *et al.* 1953; Voorhees *et al.* 1976). At G1, RNA and proteins are synthesized in preparation for DNA replication (Prescott 1968). DNA replication takes place during S phase, undergoing one cycle of replication only. Transition into G2 does not occur until nuclear DNA replication is completed. At G2, cells have twice the content of DNA that was present in G1. The cell then enters mitosis where chromosomal division occurs followed by division of the cell body through cytokinesis (Lewin 2000).

Cells *in vivo*, are usually present in a non cycling state termed quiescence or G0 until they are stimulated to proliferate and enter the cell cycle (Patt *et al.* 1963). *In vitro*, mitogenic stimulation, including nutrients and growth factors, is required for cells to proceed through the cell cycle, whereas serum depravation, contact inhibition and loss of adhesion lead the cells into quiescence (reviewed in (Blomen *et al.* 2007).

Rao and Johnson fused nuclei from two separate cells at different cell cycle phases into one cell to study cell cycle regulation. When an S phase nucleus was fused into a cell with a G2 phase nucleus (S / G2 Cell), the S nucleus continued to replicate DNA and progressed to M phase but the G2 nucleus did not reinitiate DNA synthesis. However, progression of the S phase nucleus into M was accelerated in the S / G2 cell, indicating that G2 contains factors that affect the S phase nucleus. Similarly, fusion of an S phase nucleus with a G1 nucleus led to the rapid induction of DNA synthesis in the G1

nucleus. These results demonstrate the presence of factors that drive the progress of the cell cycle in a unidirectional way (Rao *et al.* 1970).

Entry into S phase and the decision to undergo mitosis is made at the restriction point (R point) which occurs in mid to late G1 phase. Once the cell is committed to progress through the restriction point, it is committed to continue onto the other phases of the cell cycle. Under physiological conditions, cell cycle inhibitory signals past the restriction point do not prevent the progression of the cell into the S phase (Pardee 1974; Lewin 2000). Successful progression through all the cell cycle phases allows for division of the cell. Exit from the cell cycle at specific points leads the cells into either quiescence, differentiation, senescence or apoptosis (Blomen *et al.* 2007).

1.1.2 Cyclins and cyclin dependent kinases

Cyclins and cyclin dependent kinases are the most important proteins that regulate progression of the cell cycle. Cyclins are the activator subunits that bind to and activate cyclin dependent kinases (CDK) which act as the catalytic subunits of the complex. There are 16 identified cyclins in mammals (cyclin A, B1, B2, C, D1, D2, D3, E, F, G1, G2, H, I, K, T1 and T2) and 9 CDKs (CDK 1-9) (Johnson *et al.* 1999). Levels of cyclins fluctuate whilst CDKs remain relatively constant throughout the cell cycle. Cyclins are synthesized prior to entry into the cell cycle phase where they are required, and are degraded by proteolysis when the cell exits that phase (Randall *et al.* 1996). Progression through G1 requires CDK4 and CDK6 that are activated by cyclin D1, D2 and D3. Entry into and progression through S phase requires CDK2 which is activated by cyclin E and A (Johnson *et al.* 1999; Lewin 2000). Conditional overexpression of cyclin D1 and E in cells at G1 demonstrated the important role of these cyclins by reducing the duration of G1 to S phase transition (Resnitzky *et al.* 1994). G2 to M phase is regulated by CDK1 activated by cyclin A, B1 and B2 (Johnson *et al.* 1999; Lewin 2000). CDK complexes phosphorylate serine and threonine residues in target proteins, activating or inactivating them, in order to facilitate progression of the cell cycle.

1.1.3 E2F and its regulation by tumour suppressor retinoblastoma

The family of E2F transcription factors are the most important proteins regulated by CDKs. E2Fs regulate expression of proteins involved in the cell cycle (such as cyclin E, cyclin A and CDK1) and DNA synthesis (such as DNA polymerase α, dihydrofolate reductase and thymidine kinase) (Johnson *et al.* 1998).

The gene that codes the retinoblastoma protein (Rb) was named after being discovered as the primary mutation in the rare childhood eye cancer, retinoblastoma (Harbour 2006). Rb is a tumour suppressor protein and its most important function in cell cycle regulation is to bind and inactivate E2F transcription factors. CDK complexes phosphorylate Rb preventing it from interacting with E2F thus facilitating cell cycle progression. When the activity of the CDK complexes are inhibited, Rb remains in its dephosphorylated form bound to E2F (Sherr 1996; Harbour 2006).

1.1.4 The p53 tumour suppressor protein

P53 is the most important tumour suppressor in human cells. More than 50 % of human cancers involve a mutation of the p53 gene (Levine 1997). The p53 protein is a transcription factor that contains 393 amino acids. The first 42 amino acids at the N terminus of the protein carry the transcriptional activation domain. This transcriptional activation property is regulated by the MDM2 protein. Amino acids 102-292 contain the sequence specific DNA binding domain. Amino acids 324-355 are responsible for oligomerization of the p53 protein and are linked to the sequence specific DNA binding domain by a flexible linker with amino acids 287-323. The last 26 amino acids of the C terminus of p53 contain an open domain of 9 amino acid residues that can be activated to readily bind DNA and RNA (Levine 1997).

Mainly activated in response to DNA damage, p53 leads the cell into arrest by transcriptional activation of several proteins. Proteins that are transcriptionally activated by p53 include p21 that inhibits cyclin dependent kinases and binds PCNA and results in cell cycle arrest. GADD4 is a protein that is directly involved in DNA nucleotide excision repair. When GADD4 is triggered by p53 as a result of DNA damage, it binds PCNA to arrest the cell cycle. Apoptosis is promoted through p53 activation of Bax a member of the BCL2 family. p53 is also involved in blocking signalling of mitogenic growth factors by activating IGF-BP3 (insulin like growth factor binding protein 3) (Levine 1997).

1.1.5 Cyclin dependent kinase inhibitors

These are proteins that bind to a CDK-cyclin complex and maintain it in an inactive form. There are two classes of cyclin dependent kinase inhibitors. The INK4 family includes $p16^{INK4a}$, p15, p18 and $p19^{ARF}$ which are specific for CDK4 and CDK6. The KIP family (or cip-kip family) comprises p21, p27 and p57 which inhibit all G1 and S phase cyclin dependent kinase activity.

P16^{INK4a} is a specific inhibitor of cyclin D/CDK4. The specificity of p16^{INK4a} was tested in a study performed on yeast cells which contained proteins that associate with human CDKs. Two separate domains the GAL4$_{ad}$ and GAL4$_{db}$ found in yeast cells hybridize to reconstitute a transcriptional activator in the presence of histidine. Yeast cells were co-transformed with a plasmid containing GAL4$_{ad}$ –p16^{INK4a} fusion and a plasmid containing GAL$_{4db}$ fusion with different CDKs. Growth occurred in the absence of histidine only in cells that contained GAL4$_{ad}$ -p16^{INK4a} fusion and GAL$_{4db}$ –CDK4 fusion (Serrano *et al.* 1993).

P21 suppresses CDKs from phosphorylating retinoblastoma which inhibits factor E2F activity preventing the cell cycle transition from G1 into S phase. A study performed on the level of p21 mRNA in early passage Li-Fraumeni cells that are heterozygous for p53, showed similar levels of p21 mRNA seen in normal fibroblasts. On the other hand, p21 mRNA levels in Li-Fraumeni cells homozygous for p53 mutation were not detected (Li Y 1994). This study suggests that p21 is activated by p53. Cell cycle that is inhibited through p53 by activating p21 inhibits CDK2-cyclin A, CDK2- cyclin B and CDK4-cyclin D1 complexes (Ko *et al.* 1996; Puri *et al.* 1999). The p21 protein has also been reported to be a universal inhibitor of cyclin kinases. Cloning of p21 and reconstituting it with cell cycle kinase complexes showed that p21 inhibits the activity of each member of the cyclin /CDK family (Xiong *et al.* 1993).

1.2 Cellular Senescence

1.2.1 A brief history of cellular senescence

Attempts to grow isolated animal cells *in vitro* were first carried out in 1885 by Wilhelm Roux. The procedure involved removing a portion of tissue from the medullary plate of a chick embryo and maintaining it in warm saline solution. In 1907, Ross Harrison grew frog spinal cord tissue in clotted lymph fluid and observed elongation of nerve fibres. The growth of the cells was very slow and susceptible to bacterial contamination but cells had survived and Harrison's attempt had set the foundations for cell culture (Harrison *et al.* 1907). Alexis Carrel improved animal cell culture techniques significantly in 1912. Carrel's study was carried out on chick embryo tissue. Carrel succeeded in prolonging the life span of cells *in vitro* by enhancing cellular growth conditions and carrying out effective aseptic techniques to prevent contamination (Carrel 1912).

For many decades, cells were thought to have an indefinite lifespan *in vitro* if provided with the optimum culture conditions. It was not until 1961, when Hayflick and

Moorehead confirmed that cells have a finite lifespan. The study was carried out on normal diploid fibroblasts to assess their growth characteristics and chromosomal alterations during serial cultivation. The results showed that the cells maintained diploidy throughout their time in culture until they stopped proliferating. Hayflick and Moorehead described cultures of diploid fibroblasts in three phases. Phase I is the isolation of the cells from the tissue and growth of cells to confluency. Phase II is the proliferative life of the cells during which they replicate actively for two to ten months with gradual decrease in division with time. Phase III is the terminal phase at which cells stop mitotic activity and the culture is characterised by accumulation of debris (1961). The Hayflick limit states that normal diploid somatic cells have a limited capacity to divide, and that the indefinite lifespans described in past studies were observed in abnormal heteroploid cells. Hayflick carried out further studies on cultured cells and proposed that the finite lifespan of cells *in vitro* is cellular senescence (Hayflick 1965; 2003). It has been proposed that senescent cells accumulate leading to tissue ageing (Martin *et al.* 1970). This hypothesis can be illustrated by a study on the *in vitro* lifespan of human fibroblasts collected from individuals of various ages ranging from newborn to 93 year old. The results demonstrated a decline in cellular lifespan with increasing donor age (Allsop *et al.* 1992).

1.2.2 Mechanisms of cellular senescence

Cellular senescence is a state of irreversible exit from the cell cycle. A senescent cell remains in G1 stage of the cell cycle and cannot proliferate or progress to the next stage. Senescence occurs as a result of intrinsic stimuli to control proliferation (replicative senescence) and in response to various stresses triggered by build up of reactive oxygen and other external factors including the environment (stress induced premature senescence) (Ben-Porath *et al.* 2005). Cellular senescence is triggered by cell cycle inhibitors. These inhibitors act as barriers preventing immortalisation of cells and protect against tumourigenesis.

Fibroblasts infected using, the simian virus 40 (SV40) adenovirus or human papilloma virus, demonstrated an increase in growth rate, abnormal morphology followed by a rapid development of aneuploidy and eventually crisis. In crisis the cells express a balanced rate of division and death for a while. This is followed by death of the culture. However, rare rapidly growing cells arise forming an established immortal cell line. The mechanism of immortalisation occurs through inactivation of Rb and p53. SV40 binds to both p53 and Rb by large T antigen. Adenovirus binds to Rb by E1A protein and to p53

by E1B protein. Papilloma virus binds to p53 by E6 and binds Rb by E7 (Wright *et al.* 1992).

For cells to become immortal, they need to bypass two mortality stages M1 and M2. A cells normal proliferative lifespan in culture is controlled by replicative senescence which is M1. When cellular senescence (M1) is bypassed due to a mutation or inactivation of a cell cycle control gene, the cell enters a state of crisis (M2) where it has chromosomal instability and becomes apoptotic (Wright *et al.* 1992). The senescence checkpoint (M1) and crisis checkpoint (M2) have been collectively termed the proliferative lifespan barriers. When fibroblasts are infected with large T antigen, E1A in conjunction with E1B and E6 in conjunction with E7 they overcome M1 and enter crisis in M2 (Wright *et al.* 1992). An intermediate stage M^{int} between M1 and M2 takes place when either E6 or E7 is separately expressed in a cell abolishing the activity of either P53 or Rb respectively (Bond *et al.* 1999) (figure 1.1).

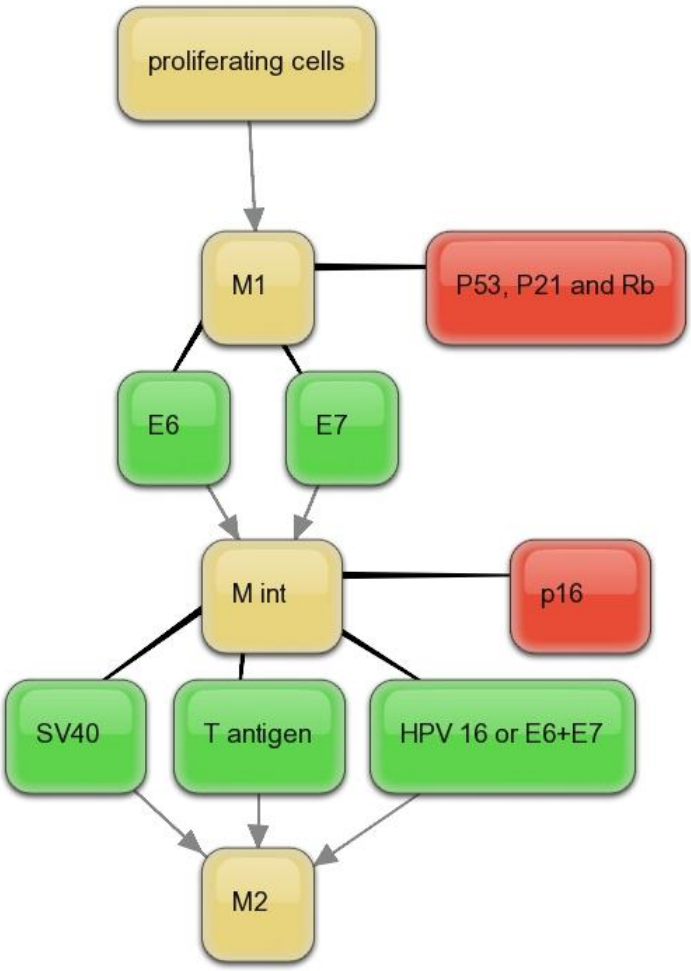

Figure 1.1 Cell proliferation barriers The diagram describes the order of proliferation barriers (M1, M^{int} and M2), the main proteins that stabilize the barrier stages (red boxes) and the factors that cause the cell to overcome the barriers (green boxes).

1.2.2.1 Replicative senescence

Replicative senescence is the stage cells reach in which they are no longer capable of division as a result of decline in replicative capacity with progressive proliferation. The number of times a cell divides is estimated by the number of doublings of the whole population (population doublings or PD). The measurement of replicative age *in vitro* is usually measured by the calculation of cumulative population doublings (CPD) or by number of generations of colony forming cells. Most of the literature in this thesis quotes the CPD of the samples. Cell generations have been used by some studies and are quoted where used.

When replicative cells become senescent, their functional properties change, this is due to over expression of secreted molecules and altered protein synthesis. Senescent cells remain metabolically active but do not replicate and are functionally impaired (Faragher *et al.* 1998; 2003). When the cell reaches its finite capacity for dividing, tumor inhibitors and cell cycle inhibitors are triggered to inactivate transcription factors required for the transition of the cell from G1 to S phase. Two mechanisms for replicative senescence have been classified, telomere dependent senescence and telomere independent senescence.

1.2.2.1.1 Telomere dependent senescence

Telomeres are short repeat sequences of DNA located at the terminals of a linear chromosome. Telomeres protect chromosomal ends from crossing over, non-homogenous recombination and DNA double strand breaks. In humans, the telomere sequence is a repeat of TTAGGG and is about 8-10 kb long in many somatic cells (Moyzis *et al.* 1988; McElligott *et al.* 1997). The end of telomere sequences contain a single strand of a 3' overhang that forms D-loop and T-loop structures with the rest of the duplex telomere sequence (Greider 1999).

The emergence of the Hayflick limit had prompted Olovnikov to speculate on the mechanistic basis of cellular senescence. In 1971, Olovnikov hypothesized that the ends of DNA are under-replicated with progressive cell division. After losing a critical portion of DNA terminal sequences the cell changes from its normal phenotype to the senescent phenotype. Olovnikov also postulated that prokaryotic DNA had a form of protection against the under-replication problem because it is circular and has no ends (Olovnikov 1996) (Olovnikov 1971). Watson had also theorised on the end replication problem by observing the replication of bacteriophage T7 in *Escherichia coli* (reviewed in (Greider 1998).

Telomere lengths decrease with serial passage of cultured human fibroblasts (Harley *et al.* 1990). Young fibroblast cultures have longer telomere sequences than senescent fibroblast cultures. This suggested that the replicative capacity is directly proportional to telomere lengths (Allsop *et al.* 1995). The telomere sequences are lost with progressive replication of the cells (Levy *et al.* 1992). Telomere shortening can be described as an intrinsic division counter mechanism for the lifespan of the cell. During S phase, DNA is replicated by polymerase III moving in 5'→3' direction. Polymerase III requires an RNA primer to attach to the template so it could add nucleotides to the 3'OH of the primer and extend resulting in the formation of a daughter strand. When complimentary daughter strands (lagging strands) are added, the primers are replaced by DNA fragments by the action of polymerase I. The terminus does not provide a free 3' OH for the addition of nucleotides, which results in the loss of the sequence. Short sequences of telomere strands fail to replicate each time new DNA is synthesized due to the loss of terminal primer sequence. This is called the end replication problem (Levy *et al.* 1992; Kipling 2001).

Telomere overhangs are protected by forming a knot like structure called the t-loop. This structure is described by having the single strand of the telomere tucked into adjacent double stranded telomere sequences. The t-loop has further protection of the single strand by base pairing with homologous double stranded DNA and forming a D loop (Greider 1999).

When telomeres shorten to a certain level, 6-8 kb (Herbig *et al.* 2004), they fail to fulfil their normal protective function and result in DNA double strand breaks that activate DNA damage check points. A study for the measurement of telomere lengths were carried out on human diploid fibroblasts (HDF) using quantitative fluorescence in situ hybridization. The study estimated the rate of loss of telomere lengths in HDF to about 50-150 bp / PD. The senescent cells had final telomere lengths of 1-2 kb (Martens *et al.* 2000).

DNA damage check points stimulate the DNA damage response proteins leading to cell senescence. Molecular markers of cells with DNA double strand breaks have been detected by immunofluorescence in senescent fibroblasts. Nuclear foci of phosphorylated histone H2AX were detected in association with DNA repair and DNA damage checkpoint factors (53BP1, MDC1, MBS1) (D'Adda *et al.* 2003). These trigger a p53 response that results in cellular senescence.

Telomerase is a reverse transcriptase enzyme responsible for maintaining telomere lengths. Telomerase is formed of two subunits, the RNA subunit hTERC which acts as a template for telomere synthesis and the protein subunit hTERT which carries out

the catalytic activity of the enzyme. Cells of all tissue types express hTERC but rarely express hTERT (reviewed in (Cong *et al.* 2002). Telomerase is normally active in male germ cells, stem cells, progenitor cells but is absent in most somatic cells due to hTERT repression (Reviewed in (Cong *et al.* 2002; Oeseburg *et al.* 2010)). Progenitor cells include haematopoetic progenitor cells and neuronal precursor cells. In addition, somatic cells that have a high expansion rate including activated lymphocytes and epidermal keratinocyte stem express telomerase (Taylor *et al*. 1996; Shay *et al*. 1997; Hiyama *et al*. 2007).

Ectopic introduction of hTERT increases telomere lengths and immortalises telomerase negative cells such as retinal pigment epithelial cells, foreskin fibroblasts (Bodnar *et al.* 1998), human large vessel and microvascular endothelial cells (Yang *et al.* 1999). These results anticipate potential therapeutic applications for telomerase in regenerative medicine. However, a study has demonstrated a rise of a transformed variant in telomerase expressing cells that have been in culture for long periods pointing out the tumourigenic risks of hTERT expression (Rea *et al.* 2006).

1.2.2.1.2 Telomere independent senescence

Although presence of telomerase maintains normal telomere lengths and overrides senescence in cells such as human fibroblasts and vascular endothelial cells, evidence from other cell types is consistent with the existence of a telomere independent pathway that leads to cellular senescence despite the presence of telomerase. Senescence has shown to be associated with increased levels of $p16^{INK4A}$ in mammary epithelial cells (Brenner *et al.* 1998), bladder urothelial cells (Puthenveettil *et al.* 1999), prostate epithelial cells (Jarrard *et al.* 1999) and keratinocytes (Rheinwald *et al.* 2002).

Expression of hTERT in human astrocytes *in vitro* did not result in the bypass of replicative senescence which occurred at approximately 20 CPD. However, inactivation of p53 by the expression of E6 led to an increase of 12 PD in the cells lifespan demonstrating bypass of the M1 proliferative lifespan barrier. A second cell cycle arrest took place as a result of elevated p16 levels (M_{int}). A population of cells had escaped M_{int} and had demonstrated downregulated p16 achieving 25 more population doublings until crisis (M2). Expression of telomerase prior to M2 resulted in the immortalisation of the cells (Evans *et al.* 2003).

Overexpression of CDK4 in human epidermal keratinocytes and mammary epithelium prevented $p16^{INK4a}$ dependent growth arrest. UV irradiation in control cells showed a slight upregulation of p53 and p21 that peaked one day after UV exposure but then returned to normal levels, but an upregulation in $p16^{INK4a}$ levels increased four days

after UV exposure and remained elevated. In contrast, UV irradiation in the CDK4 overexpressing cells showed no sign of $p16^{INK4a}$, p21 or p53 increase. This demonstrated that CDK4 overexpression effectively interacted with the cyclin dependent kinase inhibitors p16 and p21. After a 70 PD increase in the epidermal keratinocytes lifespan, and an 82 PD increase in the mammary epithelium life span, a second stage senescence took place. However, with co-expression of CDK4 and hTERT these cells overcame the second stage senescence and immortalized. This suggests that with the continuation of telomere erosion the cells come to a second stage of senescence which requires telomerase to achieve immortalization (Ramirez *et al.* 2003).

It is still not clear what triggers telomere independent senescence, and whether or not it depends on an intrinsic cell division counting mechanism. The study by Ramirez *et al* (2003) discussed above suggests that senescence in the keratinocytes and mammary epithelium was principally driven by a $p16^{INK4a}$ dependent mechanism. A study carried out by Itahana *et al* (2003) demonstrated that $p16^{INK4a}$ is controlled by a polycomb protein, Bmi-1 which represses the $p16^{INK4a}$ producing INK4α locus. Downregulation of Bmi-1 caused an increase in $p16^{INK4a}$ levels which led to cellular senescence. This demonstrates a role for Bmi-1 in the control of p16 dependent senescence.

Mammary epithelial cells that were grown in serum free medium achieved 3-7 CPD entered a temporary growth arrest state for several days (selection period) before they started to proliferate again. The reinitiated proliferation lasted for 10-34 CPD before the cells senesced. Levels of p16 were measured in the pre selection period and the post selection period and were compared to fibroblasts. Levels of p16 remained unchanged throughout the lifespan of fibroblasts whilst dropping to undetected levels in post-selected mammary epithelial cells. These results suggest that mammary epithelial cell proliferation is primarily controlled by p16 until a selection stage at where p16 is methylated. Telomere erosion is the secondary proliferation control mechanism which takes place after selection (Huschtscha *et al.* 1998).

1.2.2.2 Reactive senescence

Cell senescence is not only caused intrinsically as a result of progressive division but is also prematurely activated in response to damage by external factors. In studies expressing the ras oncogene in human cells, an accumulation of p53 and $p16^{INK4a}$ was observed and cellular senescence was induced. Inactivation of p53 and $p16^{INK4a}$ in ras expressed cells bypassed senescence. This suggests that ras induces an increase in levels of p53 and $p16^{INK4a}$ which triggered cellular senescence (Serrano *et al.* 1997).

Retroviral transfection of human fibroblasts with an activated ras gene showed increase in intracellular reactive oxygen species. When the ras expressing cells were placed in a low oxygen environment, ras was not able to trigger senescence. In a 20% oxygen environment, cell senescence took place, suggesting that ras oncogene stimulated an increase in reactive oxygen species. And an increase in H2O2 mediated the signalling for the activation of p21 and $p16^{INK4a}$ that led to premature cell senescence (Lee *et al.* 1999).

A study by Elmore *et al* (2002), shows that telomere damage induced in p53 wild type breast cancer cells causes them to enter senescence, whereas, telomere damage induction in cells lacking p53 leads to apoptosis. The study used driamycin (doxorubicin), which is an anthracycline antibiotic drug known to induce apoptosis in various p53 mutant cancer cell lines (Skladanowski *et al.* 1993; Gewirtz 1999), as a DNA damaging agent (Fornari *et al.* 1994). Adriamycin treatment of $p53^{+/+}$ breast tumour cells (MCF-7) resulted in an increase in p53 expression followed by senescence. Application of adriamycin to MCF-7 cells following E6 degradation of p53 caused the cells to bypass senescence and enter delayed apoptosis. Introduction of hTERT to wild type p53 MCF-7 (MCF-7.hTERT) resulted in increased telomerase activity and telomere lengths. Adriamycin treatment of MCF-7.hTERT cells demonstrated telomere damage and increased p53 expression that led to cellular senescence (Elmore *et al.* 2002). These findings indicate that induced telomere damage triggers p53 activity and absence of p53 in the event of telomere damage results in a delayed apoptosis in mammary epithelial cells.

1.2.4 Senescence associated-β-galactosidase assay (SA β-Gal)

Currently the most widely used test to detect senescence is the β-galactosidase activity in senescent cells specifically at pH 6.0 (SA β-Gal). Most cells stain positively for β-Gal at pH 4.0 and only senescent cells are β-Gal positive at pH 6.0. SA β-Gal has a characteristic of peri-nuclear staining and the numbers of stained cells increase exponentially with successive passages. This was demonstrated in a study by Dimri et al (1995) where fibroblast and keratinocyte cultures were treated with [^{3}H] thymidine, for autoradiography detection of dividing cells, in conjunction with β-Gal labelling at early, middle and late passages. Cells that were positive for β-Gal did not label with [^{3}H] thymidine. Exponential increase in β-Gal staining and decrease in [^{3}H] thymidine was observed with increasing passages. Cells induced to enter quiescence by serum starvation did not stain for β-Gal at pH 6.0. Other cell types tested using the SA β-Gal assay

included umbilical vein endothelial cells, human mammary epithelial cells and neonatal human melanocytes (Dimri *et al.* 1995).

Despite the specificity of β-galactosidase expression in many senescent cells at pH 6.0., it does not have a direct role in cellular senescence. This was demonstrated by the ability of cells with defective β-galactosidase to enter replicative senescence. SA β-Gal is most likely to be lysosomal β-galactosidase that has accumulated in cells with time. Young and senescent cultures of fibroblasts from G_{M1}- gangliosidosis patients, an autosomal recessive disease with defective lysosomal β-galactosidase, do not stain for β-galactosidase at pH 4.0 or pH 6.0. Furthermore, fibroblasts that expressed shRNA targeting GLB1 (the lysosomal β-galactosidase gene) had reduced staining of β-galactosidase at pH 6.0 (Lee *et al.* 2006).

1.3 Werner's syndrome

1.3.1 Introduction to Werner's syndrome

Clinical features of a cataract in conjunction with scleroderma like skin changes were described by Carl Wilhelm Otto Werner in his doctoral dissertation in 1904. Werner observed four siblings from one family; all four siblings had cataracts, skin changes that resemble scleroderma and features of premature ageing (Werner 1904).

In 1934 Werner's research came to the attention of Oppenheimer and Kugel when they observed clinical conditions that matched those reported in Werner's dissertation. They were first to name the disease "Werner's syndrome" dedicating it to Otto Werner (Oppenheimer *et al.* 1934).

Werner's syndrome has a rate of onset of 1 to 45 per million worldwide (Goto 1997). The highest occurring incidents were reported at a rate of 1:202,766 in Sardinia, Italy (Cerimele *et al.* 1982). In the whole country of Japan, the rate of occurrence is approximately 1:300,000 (Goto *et al.* 1981).

Normal ageing is affected by many external factors including the environment and diet. The genes that may lead to normal ageing range from several hundreds to many thousands (Salk *et al.* 1985; Kipling *et al.* 2004). Due to the complexity of normal ageing, the aid of a model system is required for understanding what causes it. Werner's syndrome is caused by a known single-gene mutation and has shown to have many features that mimic normal ageing. In addition, studies revealed that biochemical pathways lead to cellular senescence in Werner's syndrome have similarities to the pathways that lead to cellular senescence in normal individuals (Kipling *et al.* 1997; Davis *et al.* 2004).

Kipling and co-workers (2004) suggested three possibilities on what can be learnt from Werner's syndrome about ageing. First, nothing can be concluded on normal ageing because the premature ageing features in Werner's syndrome are caused by the mutator phenotype (elevated levels of deletional mutations due to impaired DNA repair) and has nothing to do with ageing. Second, the cause of the disease in Werner's syndrome and normal ageing is the decline in genomic integrity. Third, premature replicative senescence seen in Werner's syndrome can be the cause of ageing (Kipling *et al.* 2004). In the clinical section of the literature review, an overview of Werner's syndrome pathology will be discussed to highlight the similarities and differences of the disease to normal ageing.

1.3.2 Basic clinical features

Werner's syndrome is an autosomal recessive disease characterized by symptoms of premature ageing. The disease is prevalent in communities where consanguineous marriage is common, and where a large number of the population are heterozygous for the disease. Most symptoms of the disease usually become apparent at adolescence at an age range between 15 and 30 years and hence, classified as "adult progeria". A detailed study describing various clinical features of Werner's syndrome was carried out by Epstein *et al* (1966). The study involved analysing 125 definite cases of Werner's syndrome. More recent studies on the Werner's syndrome pathology were carried out by Makoto Goto in 1997. In his study he described the clinical conditions that manifest in Werner's syndrome patients by grouping them into the systems that are affected in chronological order. The conditions were grouped as connective tissue, endocrine metabolic, immune, nervous systems and disorders of a mixture of systems, which are mainly cancer and atherosclerosis (Goto 1997).

One of the earliest symptoms recognised is shortness of stature and growth retardation, this is usually observed at an age range from 10 to 18 years (The average height for males is 157 cm and the average for females is 146 cm) (Epstein *et al.* 1966). Patients usually show a characteristic habitus, with slender extremities. Greying of the hair takes place at an average age of 20 years. Alopecia, including loss of body hair is commonly seen at an early age. Atrophy of the skin and muscle is also observed at an early stage with continuous degeneration with age progress. Juvenile bilateral cataract is a cardinal feature of Werner's syndrome. An abnormal high pitched voice was reported in most of the patients due to atrophy of the vocal cords. Osteoporosis and calcification of soft tissue are two important characteristics of the disease. Fibrosis is reported in many cases.

Soft tissue calcification: subcutaneous calcification of 35 out of 41 major joints. Refractory skin ulcers were seen at areas of some of these calcified joints. Scleroderma like skin appearance is caused due to such changes of the underlying dermis and subcutaneous layer rather than direct alterations in keratinocytes.

Atrophy and tightening of skin takes place in the cutaneous lesions whilst sclerosis mainly occurs in distal extremities especially in the feet and legs. Fibroblasts show increased levels of collagen type I and III and elevated levels of collagenase but reduced levels of collagen type IV as opposed to scleroderma (Jabionska *et al.* 1998).

Diabetes mellitus type II has been reported in 70% of Werner's syndrome patients. Hypogonadism is observed in most of the patients in both males and females. The occurrence of hyperlipidemia is high in Werner's syndrome patients, and is considered a hallmark for this disease. Hyperurecemia, a feature rarely seen in normal elderly individuals has been reported in Werner's syndrome patients.

Cases of patients with Werner's syndrome with weak immune responses, or increased tendencies towards infectious diseases have not been reported. However, studies comparing NK (natural killer cells) activity of 14 individuals with Werner's syndrome to 187 normal individuals was carried out. Results obtained demonstrated that Werner's syndrome patients had an overall reduced NK activity (19.06 ± 3.13%) as compared to normal individuals (37.41 ± 11.51%) (Goto *et al.* 1982).

Neurological tests carried out on Werner's syndrome patients showed varying results. Early studies have reported some rare cases of WS patients that demonstrated defects in the nervous system such as dementia and accumulation of corpora amylacea in the subpial regions of the central nervous system.

A later more extensive study on the brains of two Werner's syndrome patients was carried out. Brain morphology examination was carried out using magnetic resonance imaging (MRI) and angiography (MRA). Results of these studies revealed that the brain morphology and function is not defective in WS (Postiglione *et al.* 1994).

Werner's syndrome patients are predisposed to different types of cancers with sarcoma as the highest occurring malignancy. Goto's review reported a single individual with Werner's syndrome carrying five different neoplasms including: soft tissue sarcoma, thyroid carcinoma, osteosarcoma, acral lentigenous melanoma, and meningioma (Goto M 1996). Atherosclerosis and its complications (such as cardiac failure and myocardial infarction) affect 50% of Werner's syndrome patients under the age of 40 (Goto 1997).

According to statistical analysis carried out by Epstein *et al* (1966) death in Werner's syndrome patients occurs at a median age of 46 years and 48 years in a study carried out by Goto *et al* (1997). The main causes of death in Werner's syndrome are

cancer and atherosclerosis. A case study that analysed reported causes of death in Werner's syndrome patients from 1916 to 2002 revealed that out of 47 deaths 25 were caused by malignant tumours, 8 were caused by cardiac failure and myocardial infarction, 3 as a result of pneumonia, 3 due to respiratory failure, 2 due to disseminated intravascular coagulation, 2 due to hepatic failure, 2 by renal failure and 2 caused by a cerebrovascular disorder (Yamamoto *et al.* 2003).

1.3.3 Criteria for diagnosis of Werner's syndrome

Different researchers have established criteria for the diagnosis of Werner's syndrome. The most widely used criteria are those developed by Goto and the Werner's syndrome registry. In Goto's criteria for diagnosing Werner's syndrome in individuals under the age of 35, four out of the following five features must be observed: consanguinity, characteristic bird like appearance and body habitus, premature senescence, scleroderma like skin changes and endocrine metabolic disorders (Goto 1997) (described in more detail in table 1.1). The international registry of Werner syndrome classifies the disease using a slightly different criterion which includes the features covered in Goto's criteria, but in a different order described in detail in table 1.1 (www.wernersyndrome.org). A detailed list of the clinical features used by in both criteria and the link between both criteria is shown in details in table 1.1. Further laboratory tests were performed in over 100 Werner's syndrome patients to confirm the clinical diagnosis. These tests include hyaluronuria (Goto *et al.* 1978), reduced replicative capacity in skin fibroblasts (Martin *et al.* 1970), autoantibodies (Goto *et al.* 1982) and reduced natural killer cell activity (Goto *et al.* 1982). The most definite test to confirm the diagnosis is the presence of the mutation in the gene responsible for the disease (the WRN gene) (Yu *et al.* 1996).

Goto Criteria: Four out of five of the following Categories	Signs and symptoms	Werner's syndrome registry criteria:
		Definite: All the following cardinal signs and two others. **Probable:** Numbers 2 and 3 of the cardinal signs and any two others. **Possible:** Either cataracts or dermatological alterations and any four others. **Exclusion:** Onset of signs and symptoms before adolescence except stature.
Consanguinity	1.parental consanguinity (3rd cousin or greater) or affected sibling.	Cardinal signs and symptoms
Characteristic habitus and stature	2.bird like appearance, short stature, light body weight and slender extremities.	
Premature senility	3.cataracts, 4.Grey hair and 5.alopecia.	
	6.hoarseness of voice, 7.hearing loss, 8.osteoporosis, 9.atherosclerosis and 10.malignancy.	Further signs and symptoms
Skin changes	11. atrophic skin, skin sclerosis, skin ulcer, hyperkeratosis, hyperpigmentation, hypopigmentation, telangectasia and subcutaneous calcification.	
Endocrine and metabolic disorders	12.Diabetes mellitus, 13.hypogonadism, 14.thyroid dysfunction, 15.hyperuricemia and 16.hyperlipidemia.	

Table 1.1 Overlapping list of the criteria set by Goto and the criteria by the Werner's syndrome registry for the diagnosis of Werner's syndrome Criteria for diagnosing Werner's syndrome: overlap of Goto's criteria (1997) for the clinical diagnosis of Werner's syndrome with the Werner's syndrome registry (www.wernersyndrome.org, last updated 7 September 2007).

1.3.4 Comparison of the clinical features observed in Werner's syndrome to normal ageing

Werner's syndrome has been characterised as the progeroid syndrome that best mimics features of normal ageing. Nevertheless, Werner's syndrome consists of features that are not common in normal ageing hence it gained the title segmental progeria. Features that are common in both Werner's syndrome and ageing include vascular diseases mainly atherosclerosis, greying of the hair, hypermelanosis, lymphoid depletion and thymic atrophy (Epstein *et al.* 1966). Features that may occur in normal ageing but are characteristic of Werner's syndrome include valvular calcification, osteoporosis, testicular atrophy and atrophy of the skin appendages (Epstein *et al.* 1966). Features commonly seen in normal ageing but are rare in Werner's syndrome include senile keratosis, senile elastosis, hyalinization of pancreatic islets, deposition of lipofuscin pigment, and the presence of corpora amylacea in the brain and spinal cord.

Major differences between Werner's syndrome and normal ageing are mainly in the pathologic features of the disease. This includes skin ulcers, atrophy of the distal extremities, hyaloronic aciduria and increased rate of noncarcinomatous neoplasia (Epstein *et al.* 1966). As mentioned above that cancer predisposes in Werner's syndrome patients but ratios of cancer types differ than what is observed in normal patients. The ratio of carcinoma of the mesenchymal tissue to sarcoma of epithelial tissue is 1:10 in normal individuals where in Werner's syndrome the ratio is 1:1 (Goto *et al.* 1996). In the general elderly population the highest occurring cancers are lung, gastrointestinal, prostate cancer in men and breast cancer in women (Hansen 1998; Ramesh *et al.* 2005).

1.3.5 Treatment of WS

Attempts at elucidating the pathways that cause the symptoms observed in WS are ongoing. Currently there are no specific treatments for the disease. However, medications are being prescribed to WS patients for some of their symptoms. Statins (hydroxyl methylglutaryl-coenzyme A reductase inhibitors) and pioglitazone (peroxisome proliferator- activated receptor- gamma agonist) are the medications prescribed to WS patients to date. Increased lifespans of Werner's syndrome patients in recent years coincides with the period these treatments were introduced (Yokote *et al.* 2008).

1.3.6 Molecular biology of Werner's syndrome

1.3.6.1 The Werner's syndrome protein (WRN)

Werner's syndrome is caused by loss of function mutations in the WRN gene. WRN was located by positional cloning on chromosome 8 at locus p11-12 (Yu *et al.* 1996). The WRN gene is 165 kb and consists of 35 exons.

The protein product; WRNp is composed of 1432 amino acids and has molecular mass of approximately 163 kDa. WRNp belongs to the RecQ helicase family and is also known as RecQ3 (or RecQL2). Other members of the RecQ family include the human RecQL, RecQ4, RecQ5 and BLM (mutated in Bloom's syndrome), and the *Saccharomyces cerevisiae* Sgs1 protein (Chakraverty *et al.* 1999). All of the mentioned members of the RecQ family are capable of catalyzing a helicase activity.

WRN protein is composed of several functional domains (figure 1.2). The helicase domain of WRN is located at the centre of the protein at exons 14-21 (amino acids 569 to 869) (Gray *et al.* 1997). The helicase domain consists of seven motifs with motif I containing the ATPase activity (Matsumoto *et al.* 1997). WRNp carries a nuclear localization domain at its C terminus (amino acids 1370-1375) (Matsumoto *et al.* 1997b). The RecQ C-terminal domain (RQC) is located between amino acids 949-1079 (Hu *et al.* 2005). The helicase and ribonuclease D-C terminal protein (HRDC) is located between amino acids 1142-1242 (Kitano *et al.* 2006). WRNp as opposed to other members of the RecQ helicase family has an exonuclease activity, which is located at its N terminus (amino acids 78 to 219) (Huang *et al.* 1998). DNA and protein binding domain (DPBD) is a 144 amino acid domain located in the C terminus (amino acids 949-1092) and has shown to be a multifunctional DNA and protein binding site. DPBD in association with NLS has shown to be responsible for the WRN localisation. In addition DPBD acts as a protein – protein binding site for WRN with other functional proteins (Hu *et al.* 2005).

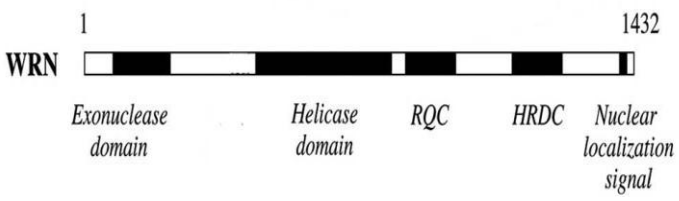

Figure 1.2 WRN protein domains The diagram illustrates the WRN protein structure with its various domains (modified from (Lee *et al.* 2005)).

The following studies demonstrate nuclear localisation of WRNp. Expression of WRN cDNA using a recombinant baculovirus system was carried out in *Spodoptera frugiperda* (Sf21) cells and the distribution of WRNp was examined in the Sf21 cells. WRNp was shown to be present exclusively in the nucleoplasm of the cells (Suzuki *et al.* 1997). A pcDNA3 vector designed to yield WRNp with an N terminal FLAG peptide expressed in HeLa cells showed that WRNp was exclusively transported to the nucleoplasm of the cells. The presence of WRNp exclusively in the nucleoplasm suggests that WRNp functions in DNA metabolism and does not function else where (Suzuki *et al.* 1997). Matsumoto *et al* (Matsumoto *et al.* 1997) identified the nuclear localisation domain of WRN at amino acids 1358-1452. von Kobbe *et al* (2002) used enhanced green fluorescence protein (EGFP) to tag WRN protein and analysed the proteins intracellular distribution by confocal microscopy. They identified a nuclear targeting sequence (NTS) at amino acids 949-1092 of the WRN protein. Both NTS and NLS were needed for the nucleolar localisation of WRN (vonKobbe *et al.* 2002).

Suzuki *et al* (1997) demonstrated the unwinding property of the helicase domain in WRNp. Complexes comprised of a substrate M13 DNA and a 5'-^{32}P-labelled oligodeoxynucleotide of two different sizes (24-mer, 40-mer) were incubated with purified WRNp. Unwinding of the DNA strands increased with increasing WRNp levels. Better activity with the smaller 24-mer than with the larger 40-mer oligodeoxynucleotide was evident. The addition of unpaired 10-mer oligodeoxynucleotides to each end of the 40-mer oligodeoxynucleotide increased the efficiency of WRNp to unwind the 40-mer to the same level of unwinding of 24-mer oligodeoxynucleotide. These results suggest that WRNp helicase preferentially unwinds DNA strands with unpaired ends indicating that single strands of DNA are required to increase the efficiency of WRNp (Suzuki *et al.* 1997). The directionality of WRNp helicase was analyzed in an experiment that involved employing the blunt-ended terminus of a linear single-stranded M13 DNA substrate with a labelled 19 bp strand at the 5’ end and a labelled 34 bp strand at the 3’ end. The addition of WRNp to the substrate, lead to the displacement of the 19mer but not the 34mer. This suggests that the WRNp helicase functions in a 3’→ 5’ directionality (Shen *et al.* 1998).

An important role of WRN helicase is the unwinding of alternate DNA structures such as tetra- and triple- helical DNA, duplex DNA containing a single-strand bubble, DNA-RNA duplexes and 4-way X junction DNA. *In vitro* studies have demonstrated that WRN helicase preferentially unwinds alternate DNA structures. Tetraplex DNA structures are formed of guanine quartets that are stabilized by non-Watson-Crick hydrogen bonds. Bimolecular tetraplex structure of the d(CGG)n repeat sequence yields

(G'2 d(CGG)n) which engenders fragile X syndrome. Incubation of WRNp in a helicase reaction mixture in the presence of hydrolysable ATP and Mg^{2+} unwound ^{32}P-5'-labeled G'2 5'-tail $d(CGG)_7$ and G'2 3'-tail $d(CGG)_7$. However, WRNp failed to unwind G'2 $d(CGG)_7$ structures that lacked a single stranded tail, and other blunt ended tetraplex structures. It also failed to unwind 5'-tailed G'2 bimolecular tetraplex forms of the telomeric sequence TeR2 and 5'-tailed G4 four-molecular tetraplex forms of the IgG switch sequence Q (Fry *et al.* 1999).

Holliday junctions are four strand DNA structures formed by the unwinding and subsequent annealing of the leading and lagging strands at a DNA fork. Holliday junctions are formed to restart a stalled replication fork after the damaged sequence has been repaired (Constantinou *et al.* 2000). In an experiment, α structures were prepared *in vitro* involving a gapped circular and chimeric 3'-^{32}P labelled linear duplex DNA to resemble Holliday junctions. WRNp in the presence of ATP resolves α structures. However, when RuvAB (a Holliday junction migrating protein) is introduced, it competes with WRNp with a higher affinity to resolve α structures. This suggests that WRNp is not a specific Holliday junction unwinding protein (Constantinou *et al.* 2000).

Significant similarities between WRN and exonuclease sequences were observed using statistical sequence analysis. Exonuclease activity was tested by incubating double stranded DNA substrates that are either labelled at there 5' or 3' with wild type WRNp or a mutant phenotype WRNp. The mutated WRNp control did not degrade the substrates. Wild type WRNp degraded the 5' labelled substrate yielding a series of smaller labelled fragments. Whilst degrading the 3' labelled substrate to a single labelled fragment that migrated as a mononucleotide. This test confirmed the exonuclease activity of WRN and demonstrated 3'→ 5' directionality (Huang *et al.* 1998).

In a study to determine the WRNp ATPase activity, WRNp was incubated with [[gamma]-^{32}P] ATP in the presence of DNA, and the reaction products were analyzed by PEI-thin layer chromatography. Radiolabelled phosphates were released as Pi. On the other hand, Incubation of WRNp with DNA substrate and [[alpha]-^{32}P] ATP yielded [^{32}P] ADP, but did not release any Pi. This suggests that WRNp acts as a [gamma]-ATPase that removes only the [gamma]-phospate of ATP.

Preliminary kinetics assays demonstrated that the WRNp ATPase hydrolyzes ATP at a rate of 6.7 [mu]mol/[mu]g protein/min under the standard conditions (Suzuki *et al.* 1997).

1.3.6.2 Functions of WRNp

Characterization of the catalytic activities of WRNp is not enough to identify the main function that is responsible for maintaining normal cellular lifespan and

chromosomal integrity. Therefore, studies that involve WRNp interactions with other proteins may shed light on the various functions of WRNp. Physical interaction and functional assay have identified a series of WRNp interacting proteins. They include DNA replication proteins FEN-1 (BroshJr *et al.* 2001), RPA (Doherty *et al.* 2005), PCNA (Lebel *et al.* 1999; Rodriguez-Lopez *et al.* 2003), DNA Polymerase δ (Kamath-Loeb *et al.* 2000), Topoisomerase I (Lebel *et al.* 1999) and II (Franchitto *et al.* 2003), EXO-1 (Sharma *et al.* 2003), WHIP/WRNIp1 (Kawabe *et al.* 2001), PARP-1 and MRE11 (Franchitto *et al.* 2004). WRN has shown to interact with p53 suggesting it has a role in tumor prevention (Sommers *et al.* 2005). The WRN proteins interactions with homologous recombination and repair proteins (RAD51, RAD52, RPA) (Sakamoto *et al.* 2001; Saintigny *et al.* 2002; Baynton *et al.* 2003), and non-homologous end joining proteins (DNA-PK_{cs}, Ku) (Yannone *et al.* 2001) suggests that WRN plays a role in DNA repair.

Altered cellular phenotypes seen in Werner's syndrome indicate that WRNp is involved in DNA replication. These alterations include a reduced replicative lifespan, an extended S phase and a reduced frequency of replication initiation sites. The WRN proteins catalytic activity was tested on a 69 bp DNA duplex in the presence and absence of a single stranded binding protein (SSB). In the absence of an SSB WRNp did not unwind the DNA duplex. When human replication protein A was added to the reaction, WRNp unwound 95% of the substrate. WRNp can catalyse the unwinding of an 849 bp DNA duplex in the presence of hRPA. This was demonstrated in a time dependent manner experiment. 14% of the 849 bp DNA duplex was unwound in one hour, whilst 31% was unwound in two hours (more on mechanism) (BroshJr *et al.* 1999).

Physical interactions of WRNp with human 5' flap endonuclease/ 5'-3' exonuclease (FEN-1) was demonstrated in an immunoprecipitation from a HeLa cell lysate and in affinity pull-down experiments. Results showed that FEN-1 associates with a non catalytic domain of WRNp on the C terminal. This domain is possibly glutathione S- transferase (GST)-$WRN_{949-1432}$ (BroshJr *et al.* 2001).

A protein complex, MRE11 has shown to play an important role in maintaining genome stability during DNA replication. MRE11 complex consists of MRE11, RAD50 and NBS1. Mutations of MRE11 and NBS1 of the MRE11 complexes result in chromosome instability syndromes Nijmegen breakage syndrome (NBS) and Ataxia telangiectasia-like disorder (ATLD) (Franchitto *et al.* 2004). WRN associates with MRE11 complex following stalled replication forks during DNA synthesis. This was demonstrated in a study which involved altering the functions of either WRN or MRE11 which resulted in an increase in chromosomal breakage during DNA synthesis. Knocking

out MRE11 in the absence of WRN did not accelerate chromosomal breakage. This suggests that WRN and MRE11 function together to resolve stalled replication forks (Franchitto *et al.* 2004).

Base excision repair (BER) involves excision of a damaged DNA base by means of a DNA glycosylase followed by incision of the resulting abasic site. The remaining 3' or 5' residue of the abasic site is also removed. The gap is then filled and ligated. DNA polymerase β is the predominant gap filling protein in short patch (single nucleotide) BER. Whilst in long patch (more than one nucleotide) BER, DNA polymerase β, polymerase δ and polymerase ε are involved (Lee *et al.* 2005). In a WRN knockdown in chicken B-cell line DT40, hypersensitivity of the cells to methyl methanesulphonate (MMS) was observed. MMS is considered to cause DNA damage that is repaired via BER. This suggests that BER is compromised in the absence of WRN (Imamura *et al.* 2002).

WRN is associated in recombinational repair. Cell proliferation is reduced in Werner's syndrome cells after mitotic recombination, and fewer gene conversion-type recombinants are formed (Prince *et al.* 2001). Resolving recombinational intermediates has shown to improve proliferation of Werner's syndrome cells. This was demonstrated by expressing a nuclear-targeted bacterial Holliday junction endonuclease (RusA) in Werner's syndrome fibroblasts. RusA expression restored DNA replication capacity and enhanced cell proliferation in the Werner's syndrome fibroblasts (Rodriguez-Lopez *et al.* 2007). Two functions of RecQ from *E. coli* have been reported, initiation of homologous recombination, and breakdown of aberrant recombination (Harmon *et al.* 1998). Homologues of WRN, the *E. coli* RecQ and *S.cerevisiae* Sgs1 have shown to suppress illegitimate recombination through homologous recombination (HR). In a mutation of Sgs1 in *S.cerevisiae* elevated rates of homologous recombination was seen. These elevated levels of HR were suppressed by the expression of WRN (Yamagata *et al.* 1998).

Double strand breaks (DSB) take place during normal DNA metabolism or exogenous factors such as oxidative stress. Non homologous end joining (NHEJ) is one of the pathways involved in repairing DSB. NHEJ pathway includes the DNA dependent protein kinase complex (DNA-PK) which consists of a catalytic subunit (DNA-PK_{CS}) and the Ku70/80 heterodimer. WRN has been shown to interact with Ku70/80 heterodimer. This was demonstrated by incubating HeLa nuclear extracts with flag-tagged WRN protein. Results analysed by SDS-PAGE and silver staining showed two polypeptides with sizes 65 kDa and 90 kDa eluted from the flag-WRN resin. These two polypeptides were then sequenced and were identical to Ku70 and Ku80. Further tests were carried out

to determine which subunit of Ku binds specifically to WRN. This was performed by co-infecting flag-tagged WRN with Ku70, Ku80 or Ku70/80 in SF9 cells by means of baculovirus vector. Ku70/80 and Ku80 co-immunoprecipitated with flag-WRN but Ku70 did not. This suggests that Ku80 binds to WRN and mediates its association with the Ku heterodimer (Li *et al.* 2000).

1.3.6.3 Mutations of WRN

Two WRN mRNAs have been identified, a 5.8 Kb and 8.1 Kb strand. The 5.8 Kb strand was shown to be the more robust strand and is expressed in different tissues at different levels (Yu *et al.* 1996). Yu *et al*. had listed four mutations in their study of positional cloning of the WRN gene. Two of the mutations were splice junctions which lead to the exclusion of an exon from the mRNA. One of these two leads to a frameshift and truncation of the protein (mutation 4) and is found in 50.8 % of the Japanese Werner's syndrome patients. The other two mutations described in the study by Yu *et al* (1996) were nonsense mutations. Another six mutations have been identified by Goto *et al* (Matsumoto *et al.* 1997) including the second most common mutation amongst Japanese Werner's syndrome patients (mutation 6) occurring at a rate of 17.5 %. According to a 1999 survey by Moser *et al*. of 19 Werner's syndrome mutations, 63 % of the mutations take place in the C terminal half of the protein. Only one of the mutations took place in the N terminal domain, whereas six mutations specifically affect exons encoding the HRDC domain (Moser *et al.* 1999).

Many more mutations had been identified and include stop codons, insertions or deletions that lead to a frame shift, splicing donor or acceptor site mutations resulting in an exon skip which also causes a frame shift. These mentioned mutations subsequently lead to truncation of the WRN protein (Chen *et al.* 2002). Table 1.2 shows the Werner's syndrome Registry list of the presently known Werner's syndrome gene mutations (www.wernersyndrome.org).

Mutation	Consequence	Exon	Domain
c.95A>G	p.K32R	3	
c.107G>A	p.R36Q	3	
c.123delA	p.E41fsX47	3	
c.171C>G	p.Y57X	3	
c.340G>A	p.V114I	3	

Table 1.2 List of Werner's syndrome mutations Werner's syndrome mutational database from the Werner's syndrome registry (www.wernersyndrome.org). Last updated 7 September 2007. **(continued pages 23-26).**

Mutation	Consequence	Exon	Domain
c.356_366del11	p.S118fsX125	5	exonuclease
c.356-2A>C	exon 5 skip	5	exonuclease
c.375A>T	p.K125N	5	exonuclease
c.403A>G	p.K135E	5	exonuclease
c.406G>A	p.A136T	5	exonuclease
C.474delT	p.F158fsX161	5	exonuclease
c.487_489delGATinsC	p.T162fsX166	5	exonuclease
c.502_503delAA	p.K167fsX177	5	exonuclease
c.655-1G>A r.655_724del70	p.Y218fsX227	7	exonuclease
c.867_874delAGAAAATC	p.I288fsX301	9	
c.970A>G	p.T324A	9	
c.986A>G	p.Q329R	9	
c.1027G>A	p.E343K	9	
c.1105C>T	p.R369X	9	
c.1123_1124delGAinsC	p.F374fsX378	9	
c.1147G>T	p.L383F	9	
c.1161G>A	p.M387I	9	
c.1165delA	p.E388fsX392	9	
c.1250_1253delTTGC	p.D416fsX436	9	
c.1278_1279insATCT	p.S246fsX430	10	
c.1389T>A	p.Y463X	11	
c.1462G>T	p.E488X	12	
c.1486A>T	p.K496X	12	
c.1486_1489delAAAA	p.L495fsX555	12	
c.1598A>G	p.N533S	13	
c.1674_1677delTTCA	p.I557fsX560	14	Helicase
c.1799_1800delCT	p.1599fsX609	15	Helicase
c.1835C>G	p.S612C	16	Helicase
c.1909A>T	p.R637>W	17	Helicase
c.2003delAT (ms: AC)	p.D668fsX674	18	Helicase
c.2088_2089ins105	p.M696fsX709	18-19	Helicase
c.2089_2825del	p.M696fsX705	19-23	Helicase
c.2102_2103delCA	p.V700fsX30	19	Helicase
c.2103_2104delAC	p.V700fsX30	19	Helicase
c.2123C>T	p.S708F	19	Helicase
c.2131C>T	p.R711W	19	Helicase
c.2179dupT	p.T726fsX731	19	Helicase
c.2194C>T	p.R732X	19	Helicase
c.2242C>T	p.Q748X	19	Helicase

Table 1.2 List of Werner's syndrome mutations Werner's syndrome mutational database from the Werner's syndrome registry (www.wernersyndrome.org). Last updated 7 September 2007. **(continued pages; 23-26).**

Mutation	Consequence	Exon	Domain
c.2283G>A	p.W761X	20	Helicase
c.2342C>T	p.T781I	20	Helicase
c.2448+1G>T r.2274_2448del	p.T757fsX760	IVS20	Helicase
c.2103_2104delAC	p.V700fsX30	19	Helicase
c.2123C>T	p.S708F	19	Helicase
c.2131C>T	p.R711W	19	Helicase
c.2179dupT	p.T726fsX731	19	Helicase
c.2194C>T	p.R732X	19	Helicase
c.2242C>T	p.Q748X	19	Helicase
c.2283G>A	p.W761X	20	Helicase
c.2342C>T	p.T781I	20	Helicase
c.2448+1G>T r.2274_2448del	p.T757fsX760	IVS20	Helicase
c.2500C>T	p.R834C	21	Helicase
c.2581C>T	p.Q861X	21	Helicase
c.2665C>T	p.R889X	22	
c.2735T>G	p.I912S	23	
c.2773delG	p.K924fsX973	23	
c.2828-1G>C r.2826_2967del142	p.S941fsX975	IVS23	RQC
c.2884C>T	p.Q962X	24	RQC
c.2959C>T	p.R987X	24	RQC
c.3028_3031delCAAA	p.D1009fsX1021	25	RQC
c.3030_3033delAACA	p.D1009fsX1021	25	RQC
c.3033_3034delAG	p.Q1010fsX1024	25	RQC
c.3034_3035delGA	p.T1011fsX1024	25	RQC
c.3130dupA	p.L1043fs1048	25	RQC
c.3139-1G>C r.3139_3233del95	p.K1046fs1060	IVS25	
c.3222G>T	p.L1074F	26	
c.3233+1G>C r.3139_3233del95	p.K1046fs1060	IVS26	
c.3233+1G>T r.3310_3383del74	p.K1103fsX1139	IVS28	
c.3236C>T	p.S1079L		
c.3244_3245delGT	p.V1082fsX1091	28	
c.3319G>T	p.E1107X		
c.3397T>G	p.S1133A	29	

Table 1.2 List of Werner's syndrome mutations Werner's syndrome mutational database from the Werner's syndrome registry (www.wernersyndrome.org). Last updated 7 September 2007. **(continued pages; 23-26).**

Mutation	Consequence	Exon	Domain
c.3446delA	p.Q1148fsX1161	29	
c.3460-7T>A	p.Q1153fsX1163	IVS29	
c.3460-2A>G	p.Q1153fsX1158	IVS29	HRDC
c.3493C>T	p.Q1165X	30	HRDC
c.3496A>T	p.K1166X	30	HRDC
c.3572+2T>A r.3460_3572del113	p.Q1153fsX1158	IVS30	HRDC
c.3587delA	p.V1195fsX1198	31	HRDC
c.3665T>G	p.F1222C	31	HRDC
c.3688_3691delACAG	p.Q1229fsX1246	IVS31/32	
c.3690_3693delAGAC	p.T1230fsX1246	32	
c.3789C>G	p.Y1263X (ms:W)	32	
c.3913C>T	p.R1305X	33	
c.3915dupA	p.R1305fsX1318	33	
c.3961C>T	R1321X	33	
c.4015G>A	p.V1339I	34	
c.4099T>C	p.C1367R	35	
c.4216C>T	p.R1406X	36	

Table 1.2 List of Werner's syndrome mutations Werner's syndrome mutational database from the Werner's syndrome registry (www.wernersyndrome.org). Last updated 7 September 2007. **(continued; pages 23-26)**

Single nucleotide polymorphisms (SNP) in the WRN gene were studied by means of denaturing high pressure liquid chromatography (DHPLC). Samples from 93 worldwide normal individuals were tested and a total of 58 SNPs were identified in the 12,839 bp region studied around the coding region of 3558 bp. Out of these nucleotide changes, 34 were tranisitions, 20 transversions, three or four single nucleotide deletion and one insertion. Out of the total, 15 nucleotide changes occurred in the coding region. Ten of these caused amino acid substitution, one caused premature termination of the protein and four were synonymous. There were no mutations detected in the nuclear localisation domain (amino acids 1370-1375) in normal individuals. However, several polymorphisms were detected in the vicinity of the nuclear localisation domain including a Cys1367Arg polymorphism that has been reported to be involved in myocardial infarction resistance and is also proposed to interfere with the nuclear localisation signal. The total nucleotide diversity was estimated to be 5.226×10^{-4}. There was no significant difference in nucleotide diversity estimates between the coding and non coding regions.

The study of polymorphism can be useful in identifying the association of the different alleles of the WRN gene and complex traits (Chen *et al.* 2002).

1.3.7 Cellular characteristics of Werner's syndrome

1.3.7.1 Growth dynamics of Werner's syndrome cells

Cell culture studies have demonstrated that Werner's syndrome fibroblast cultures have a characteristically reduced rate of population doubling when compared to normal cells (Holliday *et al.* 1985). Werner's syndrome fibroblasts took approximately seven days for the population to double whilst normal fibroblasts double in three to four days. The population doubling of Werner's syndrome fibroblasts remained low throughout their lifespan in culture and was not at a constant rate (Holliday *et al.* 1985). Flow cytometery measurement of 5-bromodeoxyuridine labelled cells demonstrated that Werner's syndrome lymphoid cells remain 2.5 hours longer in S phase than normal lymphoid cells. The ratio of cells arrested in S phase was also higher in Werner's syndrome compared to normal lymphoid cells (Poot *et al.* 1992). Cultures of Werner's syndrome cells also show a reduced lifespan compared to normal cells. Salk *et al* (1981) studied fibroblasts like cells from Werner's syndrome patients, and observed that they had an average lifespan of only about 14.6 population doublings (range= 3.8-27.8 PD) as opposed to fibroblast like cells from normal individuals which maintained an average lifespan of around 54.3 population doublings (range= 37.0-70.6 PD). Faragher *et al* (1993) showed that the reduced replicative lifespan of Werner's syndrome fibroblasts is due to the enhanced rate of loss of cycling fraction of these cells. This was demonstrated by measuring the rate of decrease in S-phase cells with successive population doublings in Werner's syndrome cells and comparing it to normal cells. The fraction of S-phase cells was determined during the *in vitro* lifespan of fibroblasts from Werner's syndrome and normal individuals by BrdUrd staining. A continuous decline of the S-phase cell fraction, in both normal and Werner's syndrome fibroblasts was observed, but a significantly higher rate of decline took place in Werner's syndrome fibroblasts. S-phase decline in normal fibroblasts ranged from -0.00446 to -0.00599 per population doubling, whilst in Werner's syndrome S-phase decline was between -0.0197 and -0.0224 per population doubling (Faragher *et al.* 1993). Furthermore, measurement of proliferation specific antigen expressing fraction of cells demonstrated a five to six fold higher rate of decline in Werner's syndrome fibroblasts when compared to normal fibroblasts (Kill *et al.* 1994). This concludes that Werner's syndrome fibroblasts have a reduced replicative lifespan due to elevated loss of the cycling fraction of cells.

1.3.7.2 Variegated translocation mosaicism (VTM)

WRN mutation and loss of its function result in the genetic instability seen in Werner's syndrome. One of the main features of genetic instability in Werner's syndrome is variegated translocation mosaicsm (VTM). VTM is described as the repeated occurrence of multiplicity of chromosomal rearrangements in a cell (Hoehn *et al.* 1975). Salk *et al* (1981b) determined the frequency of VTM in Werner's syndrome cells compared to normal cells. In 29 different strains obtained from five Werner's syndrome patients, 92% of the cultures demonstrated VTM. On the other hand, only 8.4% of 95 non Werner's syndrome cultures demonstrated VTM. Moreover, VTM occurs throughout the Werner's syndrome cellular lifespan, whilst in normal fibroblasts VTM has been observed in terminal stages. Co-cultivation of Werner's syndrome fibroblasts with fibroblasts from normal individuals did not induce VTM in the normal fibroblasts (Salk *et al.* 1981b) suggesting it is a clonal feature of the disease. Salk *et al* (1981c) demonstrated attenuation and clonal succession in a growing Werner's syndrome cell culture population. This study involved cytogenetic analysis of fibroblast like cell strains from Werner's syndrome patients throughout their lifespan, and examining their clonal behaviour. What had been observed was a correlation between clonal expansion and attenuation in the replicating cell strains. It has also been shown that Werner's syndrome fibroblasts *in situ* from primary skin explants demonstrate VTM indicating that VTM is expressed *in vivo* (Scappaticci *et al.* 1982).

These results suggest that VTM is a characteristic feature of Werner's syndrome and can be used to distinguish Werner's syndrome cells from others. 1,538 metaphases were carried out from 29 strains collected from 5 different patients. The majority of these metaphases show pseudodiploidy. The chromosomal rearrangements due to VTM examined in 1,005 metaphases show 10 breakpoints that account for 27 % of the overall chromosomal rearrangements (Salk *et al.* 1981b). Other points have been reported to recur constantly in Werner's syndrome cultures. These repeated points have been described by Salk D *et al* (1982) as "hotspots" of VTM and are 1q12, 1q44, 5q12 and 6Cen. Preferential occurrence of rearrangements were also observed in the Scappaticci *et al*. study demonstrating the repeats of rearrangements in chromosome 1p, 1q, 12q and 3q in two clones of fibroblast cultures, and X chromosome in other two cultures. The first three are known translocation points causing chromosomal aberrations in neoplastic and adenovirus infected cells. VTM may be the main cause of increased predisposition to cancers seen in Werner's syndrome.

Scappaticci *et al*. (1982) demonstrated that VTM was present in blood lymphocytes cultured for 72 hours. Multiple numerical and structural chromosomal

abnormalities in cultured lymphocytes from four Werner's syndrome patients were seen. The study demonstrated 30-44 % of all metaphases showing structural and/or numerical chromosomal aberrations, several of them were clonal. These results point out that VTM occurs in lymphocytes as well as in fibroblasts, however, the incidence of structural rearrangements of chromosomes observed in fibroblasts was much higher than in the lymphocytes (Scappaticci *et al.* 1990).

1.3.7.3 Hyper sensitivity of Werner's syndrome cells to DNA damaging agents

The absence of the repair functions of WRN in Werner's syndrome cells results in defective DNA damage response. Experiments using clastogens that produce replication associated DNA damage or inhibit replication fork progression have answered some of the questions about the normal intra-cellular functions that are absent in Werner's syndrome patients. One of the clastogens widely used is camptothecin, a substance that interferes with replication fork progress by binding topoisomerase I, a DNA unwinding enzyme. As a consequence, double strand breaks accumulate leading to cell death. Comet analysis of Werner's syndrome fibroblasts followed by camptothecin treatment demonstrated increased sensitivity to DNA damage when compared to normal cells (Lowe *et al.* 2004).

A study on Werner's syndrome lymphocytes showed increased levels of chromosomal breaks compared to normal cells. However, introduction of diepoxybutane, isonicotinic acid hydrazide, 4-nitroquinoline-1-oxide (4NQO), and bleomycin as standard clastogens to the Werner's syndrome lymphocytes did not accelerate the chromosomal breaks compared to untreated Werner's syndrome lymphocytes. Furthermore, labelling of the Werner's syndrome cells with BrdU did not show significant reduction in their proliferation rates (Gebhart *et al.* 1985). These results suggest that lymphocytes from Werner's syndrome have higher levels of chromosome breaks when compared to normal cells, but do not have a reduced response towards damage induced by the clastogens. Studies showed that SV40 immortalised WS fibroblasts (WS780) were hypersensitive to damage induced by 4NQO whereas WS fibroblasts (PSV811 and W-V) did not have any increased damage caused by treatment with 4NQO. An attempt to functionally complement SV40 immortalised cells that were hypersensitive to damage induced by 4NQO with chromosome 8 did not reverse the increased sensitivity (Kodama *et al.* 1998). However, when WS cells were immortalised by the expression of hTERT, they became susceptible to phenotype correction by the introduction of a normal chromosome 8 (Ariyoshi *et al.* 2009).

1.3.8 Mechanisms of cellular senescence in Werner's syndrome

1.3.8.1 Telomere dynamics in Werner's syndrome fibroblasts

A study measuring telomere restriction fragments (TRF) showed that serially passaged Werner's syndrome skin fibroblasts undergo accelerated telomere loss when compared to normal skin fibroblasts, but the mean telomere lengths in senescent Werner's syndrome skin fibroblasts were longer than in normal senescent skin fibroblasts (Schulz *et al.* 1996). This indicates that WRN may trigger an alternative senescence mechanism to telomere erosion. However, introduction of telomerase activity in Werner's syndrome fibroblasts by expressing hTERT prevented premature senescence of these cells (Wyllie *et al.* 2000). These results suggest that telomere erosion plays an important role in the senescence of Werner's syndrome fibroblasts. These findings also suggest that telomere integrity may be affected by the absence of WRNp. Telomere measurements were carried out in primary IMR90 fibroblasts and HeLa cells that expressd a dominant negative WRN allele with an inhibitory mutation in the helicase domain (K577M). The cells were compared to their wild types that are $WRN^{+/+}$. Measurements of metaphase telomeres in both cell types were carried out by fluorescence in situ hybridisation (FISH). The telomeric signals were detected at a single chromatid termed sister telomere loss (STL). HeLa cells expressing the wild type WRNp demonstrated low levels of STL (0.8 events per cell), whilst HeLa cells expressing the mutated WRNp showed a significant increase in STL (2.2 events per cell). Further increase in STL (4.3 events per cell) was observed when telomerase activity was inhibited in HeLa cells expressing the mutant WRNp. Similarly, the telomerase deficient IMR90 fibroblasts expressing the mutant WRN were high in STL (4.1 events per cell) (Crabbe *et al.* 2004).

Single telomere length analysis (STELA) demonstrated that telomere erosion in WS cells ranged between that of normal cells (99 bp/ PD) and four times the normal cells (355 bp/ PD). Observations in this study provided data that suggests the telomere dynamics at the single cell stage in WS cells are not significantly different from the normal cells. Results from this study suggest that premature senescence in WS cells is not mainly caused by accelerated telomere erosion due to the absence of WRNp, but is due to telomere erosion due to increased cell turnover (Baird *et al.* 2004). This could be as a result of reduced DNA damage repair and accumulation of cells with stalled replication forks as a consequence of WRNp deficiency. Consequently, an increase in cellular production and DNA replication takes place which accelerates telomere erosion leading to cellular senescence.

1.3.8.2 Senescence signalling pathway in Werner's syndrome fibroblasts

The signalling pathway for cellular senescence has been studied by researchers to determine whether the premature senescence phenotype in Werner's syndrome is an accelerated normal ageing process, or is a consequence of a distinctive defect in the biochemistry of the cell. A protein analysis study of senescent Werner's syndrome fibroblasts has demonstrated similarities in changes of protein levels to those seen in normal cells. Werner's syndrome fibroblasts (AG03141) were cultured at 12 population doublings until senescence (20.5 CPD). Levels of three different cyclin dependent kinase inhibitors (CdkI); $p16^{Ink4a}$, $p21^{Waf1}$ and $p27^{Kip1}$ were measured. Results showed low and moderate levels of $p16^{Ink4a}$ and $p21^{Waf1}$ respectively in proliferating cells and increased levels when cells reached senescence. Levels of $p27^{Kip1}$ did not change from dividing cells to senescent cells. These patterns of CdkI expression resembled the pattern seen in normal HCA2 cells (Davis *et al.* 2003).

Infection of WS fibroblasts with HPV 16 E6 resulted in an increase in their overall proliferative lifespan. The increased proliferation of E6 expressing WS fibroblasts resulted from bypassing the usual senescence point (M1) at ~20 PDs. The E6 expressing fibroblasts then entered a second senescence-like stage (M^{int}) at 15-25 PDs post infection. The cells then entered a stage that resembles crisis (M2). Bypass of M1 senescence as a result of E6 expression concludes that senescence in WS fibroblasts is initiated by p53 and backed by $p21^{Waf}$. However, P53 was not detected in E6 expressing WS fibroblasts suggesting that $p21^{Waf}$ was also low. This is because HPV 16 E6 may target other proteins as well as p53. Therefore, microinjection of WS fibroblasts with a p53-neutralizing antibody was carried out to determine the direct role of p53 in Werner's syndrome cellular senescence. As a result, Werner's syndrome fibroblasts bypassed M1, confirming that M1 senescence is p53 dependent. Furthermore, ectopic expression of hTERT in post M1 cells led the cells to overcome M^{int} and immortalize. These findings suggest that M^{int} is p53 independent and is caused by telomere erosion (Davis *et al.* 2003).

1.3.8.3 Replicative senescence in Werner's syndrome T- Lymphocytes

Human T lymphocytes selectively express telomerase (reviewed in (Kaszubowska 2008)). Cultured T lymphocytes show telomerase activity until they reach 10-20 population doublings. After that, the levels of telomerase decline until it stops being produced and subsequently telomeres shorten causing the cells to senesce.

To date, T-lymphocytes cells from Werner's syndrome patients are the only cells studied that naturally express telomerase. The proliferative capacity of WS T-lymphocytes from

three patients were measured and compared to results from normal T lymphocytes collected from seven individuals. The cells were grown under short term culture conditions which involve incubation of cells with a single treatment with the mitogenic stimulant phytohaemaglutinin (PHA). WS T lymphocytes had a mean lifespan of 13.29 ± 0.6 PD, which was within range of the mean lifespan of normal T lymphocytes, 13.5 ± 2.5 PD. Long term culture conditions were applied to confirm the results were not due to an artefact. This involved co-culturing the T lymphocytes with lethally irradiated TK6 B lymphoblastoid cells. As a result, the lifespans of both normal and WS T lymphocytes were extended to 50-60 PD (James *et al.* 2000). The normal lifespan of Werner's syndrome T lymphocytes despite genetic instability (Scappaticci *et al.* 1990) suggests that replicative senescence is not caused by the mutator phenotype.

1.3.8.4 *In vivo* studies (using mouse models)

Mouse models have been used for studying the effect of WRN mutations *in vivo*. An attempt that conducted homozygous deletions of the helicase domain of the WRN gene in mice did not express the *in vivo* characteristics of Werner's syndrome that are observed in human patients. However, cultured fibroblasts from the WRN-/-mice demonstrated a shortened replicative lifespan. Furthermore, increased sensitivity of cells treated with camptothecin was observed in samples obtained from the WRN-/- mice. Cytogenetic analysis had also demonstrated VTM, a characteristic feature of Werner's syndrome cells, in the WRN-/- mouse cells (Lebel *et al.* 1998).

Chang et al (2004) carried out an experiment using a mouse model with a more diverse selection of knockout genes to elaborate the role of telomere erosion in the Werner's syndrome pathology of mice. The experiment involved two different knockout genes in one population of mice (WRN-/-, TERC-/-) and a single knockout in another population (WRN+/+, TERC-/-). The starting generation (G0) of the knock out mice was produced by crossing (WRN-/-, TERC+/+) mice with 3rd generation (G3) (WRN+/+, TERC-/-) mice. The starting G0 mice were (WRN+/-, TERC+/-) mice. The G0 (WRN+/-, TERC+/-) mice and later generations were intercrossed to produce a final (WRN -/-, TERC -/-) phenotype. Intercrossing of the same generation mice was continued until G6 mice were produced.

The (WRN-/-, TERC-/-) mice were monitored through successive generations and were compared with aged matched G0 mice. In G1 and G2 mice, none of the pathological features of Werner's syndrome were apparent and there was no effect on there lifespan. On the other hand, G4-G6 mice had significant body weight loss, and a median lifespan that is reduced to almost one quarter of the median lifespan of G0 mice (G6 median

lifespan= 24 weeks, G0 median lifespan= 94 weeks). The G4-G6 mice appeared to be healthy during there early adulthood and started to show clinical features of Werner's syndrome premature ageing in approximately 63 % of the population at ages from 12-16 weeks. These clinical features included hair loss, cataract formation and severe hypogonadism. The mice that manifested the premature ageing features of Werner's syndrome had also demonstrated shortened telomeres. This implies that telomere erosion is required alongside the Wrn mutation to cause premature senescence in the mice (Chang *et al.* 2004).

Further work was carried out involving individual and combined knockouts of WRN, BLM and TERC. Similar to the previous study, mutant mice were cross linked to yield G1 mice with $WRN^{-/-}$ (*w*), $BLM^{M3/M3}$ (*b*), $TERC^{-/-}$ (*t*), $WRN^{-/-}$ $BLM^{M3/M3}$ (*wb*) and $WRN^{-/-}$ $BLM^{M3/M3}$ $TERC^{-/-}$ (*wbt*). The *wbt* mutant mice at G3 had a significantly reduced median lifespan of seven months as opposed to the wild type and other genotypes which had median lifespan of more than 10 months. The median lifespan of G3 *bt* mice was also significantly lower than the other genotypes, but was higher than *wbt* mice. Fertility tests showed that *wbt* mutant mice had become sterile at G4, whereas *wb* and *t* mutant mice generated offspring until G7 (Chang *et al.* 2004).

These findings demonstrate that telomere erosion is essential for the manifestation of the premature ageing phenotype and the reduction of lifespan in WRN mutant mice. They also demonstrate that premature ageing in Werner's syndrome takes place through a separate mechanism to the mutator phenotype.

1.4 Objectives

Despite the extensive studies performed on Werner's syndrome fibroblasts, the principal mechanisms by which they senesce are not completely understood. The aim of this project is to study mechanisms by which Werner's syndrome cells senesce. The main approach involves studying replicative senescence in a non-fibroblastoid cell lineage. The selected cell strains were keratinocytes because their mechanism of senescence has not been previously studied in Werner's syndrome. Experiments for the investigation of growth dynamics, growth kinetics and cell cycle control in Werner's syndrome keratinocytes will be performed. Additionally, treatment of Werner's syndrome fibroblasts with SB203580 (Davis *et al*, 2006) will be carried out in order to optimise the experiment for application in other Werner's syndrome cell types.

Due to the small population affected by Werner's syndrome, silencing WRN in abundant cells would provide more material for studying selected phenotypes of the disease. Furthermore, WRN silenced cell strains can be compared to wild type cells of isogenic backgrounds. The silencing procedure will be initially carried out in SV40 immortalised cell lines to investigate feasibility of the approach.

Chapter 2

Materials and methods

2.1 Cell culture

All cells were grown as attached cells in tissue culture flasks (25 cm^2 or 75 cm^2, Iwaki and Greiner). Cell culture work including subculture and treatment of cells were carried out Class II tissue culture cabinets (Contained Air Solutions, CAS). The microscopes used for monitoring the cells and carrying out cell counts were inverted phase microscopes (Axiovert 25 Carl Zeiss and Motic AE31).

2.1.1 Cell lines and cell strains

This section presents all cell types studied, their source and culture conditions. Table 2.1 summarizes this information.

2.1.1.1 Human fibroblasts

Human fibroblasts used; primary Werner's syndrome fibroblasts AG03141 (Coriell Cell Repository, Camden, NJ), telomerase immortalised normal (HCA2/hTERT) and Werner's syndrome (AG03141/hTERT) fibroblasts (provided by Dr. Terence Davis, Cardiff University), SV40 immortalized normal (1BR.3neo) and Werner's syndrome (WV-1) fibroblasts.

All human fibroblast cell lines and strains were grown in Minimal Essential Medium (MEM) (GIBCO) supplemented with 10 % foetal calf serum (FCS) (heat inactivated, PAA), 2mM glutamine (PAA), 50 units/L penicillin (PAA) and 50μg/L streptomycin (PAA). Cells were grown at 37°C in a humid incubator (95% air, 5% CO_2, Hera Cell, Heraeus).

2.1.1.2 Virus packaging cell lines (producer cell lines)

ΩE ecotropic and Ψ Crip amphotropic retroviral producer cell lines were grown in MEM (GIBCO) with 10 % donor herd serum (GIBCO), 2mM glutamine (PAA), 50u/L penicillin and 50μg/L streptomycin (PAA). Both cell lines were treated in separate hoods and were kept isolated from each other to avoid risk of cell cross contamination and viral infection. Cells were grown at 37°C in a humid incubator (95% air, 5% CO_2, Hera Cell, Heraeus).

2.1.1.3 Mouse embryonic cells (3T3)

3T3 cells (National Institute for Biological Standards and Control) were routinely cultured in Dulbecco's Modified Eagle's Medium (DMEM) (GIBCO) with 10 % FCS. Cells were grown at 37°C in a humid incubator (90% air, 10% CO_2, Hera Cell 150, Thermo Electra).

2.1.1.4 Primary human keratinocytes

Samples of primary keratinocytes were isolated from skin tissue by Dr. Elizabeth James. SK206AK are primary keratinocytes isolated from skin obtained from routine surgical tissue from the abdomen of a normal male patient aged 26.

SKK372 primary keratinocytes were obtained from skin tissue of a normal patient.

WSK368 primary keratinocytes were extracted from a tissue sample collected from a 26 year old female with Werner's syndrome from Sardinia, Italy. WSK369 primary keratinocytes were from a separate Werner's syndrome skin sample.

Keratinocytes were routinely co-cultured with γ-irradiated 3T3 cells. The media used was Rheinwald and Green culture medium (Rheinwald *et al.* 1977) which consists of 60% Dulbecco's modified Eagle's medium (DMEM) (GIBCO), 20% Ham's F12 (GIBCO) and 20% Foetal Bovine Serum (GIBCO) supplemented with 10 ng/ml epidermal growth factor (EGF) (Sigma), 400 ng/ml hydrocortisone (Sigma), and 10^{-10} M cholera toxin (Sigma). Keratinocytes cultures were maintained at 37°C in a humid incubator (90% air, 10% CO_2, Hera Cell 150, Thermo Electra).

Cultures of keratinocytes were transferred to defined keratinocyte serum free media (GIBCO) to test the reactions of cells to change in culture condition.

Cell name	Cell type and source	Cell strain/ cell line	Experiments used for	Obtained from or provided by
HCA2/hTERT	Human fibroblasts from neonatal foreskin	hTERT immortalised	Effect of P38 inhibitor SB203580	Dr. T. Davis, Cardiff University.
AG03141 /hTERT Clone 8	Human fibroblasts from a Werner's syndrome patient	hTERT immortalised	Effect of P38 inhibitor SB203580	Dr. T. Davis, Cardiff University
1BR.3NEO	Human fibroblasts	SV40 immortalised	Control for WRN knock down experiment	
WV-1	Human fibroblasts from Werner's syndrome patient	SV40 immortalised	Control for WRN knock down experiment	
AG03141A	Human fibroblasts from Werner's syndrome patient	Primary cells	Effect of P38 inhibitor SB203580	Coriell Cell Repository (Camden, NJ)
3T3	Mouse embryonic fibroblasts	Primary cells	Irradiated and used as feeder layer for Keratinocyte cultures	National institute for biological standards and control (NIBSC).
SK206 AK	Normal human keratinocytes	Primary cells	Keratinocytes growth dynamics and kinetics	Keratinocytes isolated by Dr. E. James.
SKK 372	Normal human keratinocytes	Primary cells	Keratinocytes growth dynamics	Cells isolated by Dr. E. James.
WSK 368	Werner's syndrome keratinocytes	Primary cells	Keratinocytes growth dynamics and kinetics	Cells isolated by Dr. E. James.
WSK 369	Werner' syndrome keratinocytes	Primary cells	Keratinocytes growth dynamics	Cells isolated by Dr. E. James.

Table 2.1 Summarised information of all the cell strains and cell lines studied in this thesis.

2.1.2 Routine maintenance of cell cultures

2.1.2.1 Media replacement

Cell culture media was routinely replaced every 48 to 72 hours in all cell cultures. All cell culture media were stored at 4° C and pre warmed to 37° C prior to adding to cells. Preparation of cell culture media was carried out in cell culture hoods under sterile conditions. Bottles for media storage were autoclaved. Supplements added to cell culture were sterilized by suppliers or were filter sterilized prior to adding to the media.

2.1.2.2 Passaging human fibroblasts and 3T3 cells

Cells were passaged when they had reached approximately 80 % confluence. The cells were washed with PBS (phosphate buffered saline). They were then treated with trypsin /EDTA (PAA) for 2 to 5 minutes at 37°C. The suspension was neutralised with at least double its volume of culture media containing FCS. The cell suspension was centrifuged for 5 minutes at 500 g (BS400, Denley or Heraeus Labofuge 400, Thermo) the supernatant was aspirated off and the cell pellet was re-suspended with fresh media. Cell counts were performed (see section 2.1.2.4) prior to re-seeding the cells (at $4x10^3$ cells/cm^2) or freezing them down (at 10^6 cells/ml).

2.1.2.3 Passaging keratinocytes

In culture, the keratinocytes attach tightly to the tissue culture treated plastic surface of the flask and are difficult to remove, whilst the γ irradiated 3T3s are loosely attached. Cell cultures of keratinocytes were washed three to four times with PBS by applying pressure onto the cultured surface of the flask forcing the γ irradiated 3T3 cells to detach leaving colonies of keratinocytes that remain adhered to the flask. Trypsin/ EDTA (1ml) was added to the culture for 20 – 50 minutes to detach the keratinocytes from the flask. Trypsin/ EDTA was neutralised with twice its volume of cell culture media. The cells were counted (as in section 2.1.2.4) and were reseeded between 1.2 x 10^4 and 2 x 10^4 cells / cm^2 in combination with a layer of γ irradiated 3T3 feeder cells seeded at $2.4x10^4$-$4x10^4$ cells / cm^2 or without the feeder layer in defined K-SFM (keratinocyte serum free media).

2.1.2.4 Cell counts and population doubling

Cell suspensions were mixed well and a sample from the suspension was placed onto a bright-lined haemocytometer (Fisher Scientific). The cells on the haemocytometer were viewed using an inverted light microscope. Cells in the four large outer grids of the counting chamber of the haemocytometer were counted as illustrated in the diagram below (figure 2.1). Each one of the large four grids equals 0.1µl in volume and is subdivided into 16 smaller squares. To obtain a cell count per 1ml, the total cell count in four grids are divided by 4 to obtain the average, and multiplied by 10^4.

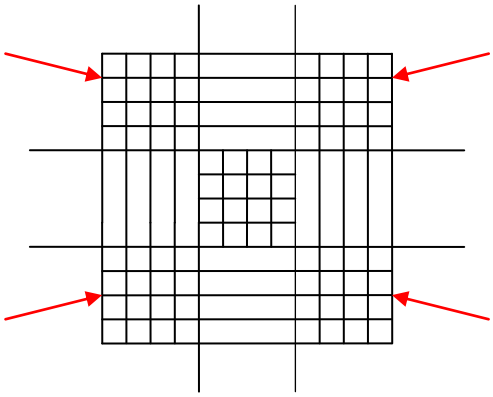

Figure 2.1 Schematic diagram of a haemocytometer chamber Cell counts were carried out in the four large squares which contain 16 smaller squares marked by the red arrows in the diagram.

The cell counts were used to calculate the population doublings achieved by cell division at each passage using the following formula:

Cell population doubling = [1 / Log 2] x [(Log (number of cells harvested) – Log (number of cells seeded)].

The results were plotted on a graph showing the cumulative population doublings achieved against the number of days in culture. Corrections were not made to the cell counts for dividing and non-dividing cells. Total counts were obtained indiscriminately.

2.1.2.5 Cryopreservation

Cells were detached from the surface of the flask by routine passaging methods and centrifuged at 500 g for 5 minutes (BS400, Denley or Heraeus Labofuge 400, Thermo). The cell pellets were re-suspended in freezing down media (60% culture media, 30% Foetal Calf Serum and 10% dimethyl sulfoxide (DMSO) (Sigma) for all cells except 3T3 cells and keratinocytes which were frozen in 90% culture media and 10% DMSO Cells in freezing down media were transferred to cryovials (Nunc or Fisher Scientific)

and placed in freezing pots containing isopropanol (Thermo Scientific Nalgene) and stored at -80°C for a minimum of 24 hours. Cells were then transferred to the liquid nitrogen tank for long term storage.

2.1.2.6 Thawing of cryo-preserved cells

Cryovials containing the required cells were carefully removed from the liquid nitrogen tank and held in hand or placed in water-bath at 37°C until thawed. The cell suspension was transferred to a universal tube as soon as it thawed and culture media was added to the suspension to make it up to 10 ml immediately to neutralise the damaging effects of DMSO. The suspension was centrifuged at 500 g for 5 minutes (BS400, Denley or Heraeus Labofuge 400, Thermo) (except for keratinocytes which were seeded immediately after neutralising and counting without centrifugation), the supernatant was aspirated off and the pellet was resuspended in cell culture media. The cells were counted (see section 2.1.2.4) and seeded at the recommended seeding density.

2.1.3 Treatment and manipulation of cells in culture

2.1.3.1 Mitosis inactivation in 3T3 cells by γ irradiation

3T3 (mouse embryonic fibroblasts, NIBSC) were γ irradiated for them to be permanantly mitotically inactive to be used as feeder layers for the culture of primary human keratinocytes. Cells were harvested and collected in 15 ml tubes (Falcon). The γ source used was Cesium137 which is situated permanently in the stator section of the biological shield of the instrument (γ cell 1000, Centre for Genome Damage and Stability, University of Sussex). Exposure to γ rays was measured in units of rad (radiation absorbed dose). The exposure of cells in the chamber to the rays varies slightly at different heights of the tube. Prior to setting the dosage for the experiments, the cells were exposed to different dosages and were kept in culture. The best killing dose was selected to use for routine experiments. For best results, the instrument was set to 750 rad / minute and the 3T3 cells were irradiated for 12 minutes exposing them to a maximum dose of 9000 rad.

2.1.3.2 P38 inhibition by treatment with SB203580

SB203580 ($C_{21}H_{16}FN_3OS$) (Sigma) is a pyridinyl imidazole and acts as a cytokine suppressive anti-inflammatory drug that interferes with the activation of MAPKAP kinase-2 pathway. SB203580 mainly inhibits p38 but also targets upstream regulators of the MAPKAP kinase pathway. The use of SB203580 in this project was to study its effect

on Werner's syndrome cells lifespan and growth rates. SB203580 was prepared as a working stock at 10 mM in DMSO (Sigma) and stored in aliquots at -20°C. A dose response study comparing untreated cells, 0.2% DMSO treated and SB203580 treatments at final concentrations of 2 µM, 5 µM, 10 µM, 15 µM and 20 µM was carried out. Untreated and 10 µM SB203580 treated cells were cultured for an extended period. Treatment was carried out with the reintroduction of SB203580 with fresh media on a daily basis.

2.1.3.3 Camptothecin treatment

Camptothecin ($C_{20}H_{16}N_2O_4$) (Sigma) is a cytotoxic alkaloid that acts as a topoisomerase I inhibitor. Camptothecin treatment was used to damage DNA and test recovery of the cells by performing COMET assay. Camptothecin was prepared at a working concentration of 10 mM in DMSO (Sigma) and stored in -20° C.

2.1.3.4 Adriamycin (doxorubicin) treatment

Adriamycin (doxorubicin) ($C_{27}H_{29}NO_{11}$) (Sigma) is an anthracyclin antitumour antibiotic. It is an inhibitor of reverse transcriptase and RNA polymerase and an immunosuppressive agent that intercalates in DNA. Stocks of adriamycin were prepared at concentrations of 100 µM in sterile dH2O and stored at 4° C. Acute adriamycin treatment was performed on cells by applying 1 µM of the drug for two hours followed by replacement with drug free media.

2.1.3.5 Anchorage independence assay

Cells at a density of 2 - 3 x 10^5 were suspended in 5ml Rheinwald and Green culture medium containing 1.68 % methylcellulose (Celacol). The suspension was spread over agar (Oxoid) in a 60 mm dish and incubated in 37° C with 10 % CO_2. Replenishment with 1ml Rheinwald and Green medium was carried out weekly. The cells were harvested and counted after 3 weeks.

2.1.3.6 Senescence-associated β-galactosidase staining (SA-β-Gal)

The senescence associated β-galactosidase stain (Dimri *et al.* 1995) is formed of 1 mg of 5-bromo-4-chloro-3-indolyl β-D-galactoside (X-Gal) per ml (stock dissolved at 20 mg / ml in dimethylformamide), 40 mM citric acid / 80 mM Na_2HPO_4 buffer at pH 6.0, 5 mM potassium ferrocyanide, 5 mM potassium ferricyanide, 150 mM NaCl, 2 mM $MgCl_2$) (all chemicals used in the preparation of β-galactosidase stain solution were from Sigma).

Cells were grown in a 12 well plate (Iwaki) at 4 x 10^3 cells per cm^2 for at least48 hours prior to fixing. Cells were washed with PBS and fixed with 3 % formalin (Sigma) for 10 minutes at room temperature. The fixative was removed and the cells were washed with PBS. The senescence-associated β-galactosidase stain solution (pH 6.0) was added to the cells and incubated for 16hrs at 37^0C. Positive control was achieved by staining cells with β-galactosidase stain solution prepared as above except with the 40 mM citric acid / 80 mM Na_2HPO_4 buffer adjusted to pH 4.0.

2.2 Subcloning and gene transduction

This section describes the methods used to subclone the U1 stabilised ribozyme (Rib3) into a pMSCVhyg vector and stably express it in 1Br.3neo.WRN4 by retroviral infection. All enzymes and buffers used were from Promega unless stated otherwise. The subcloning methods are described in the following sections.

In summary, the pU1-Rib3 and the pMSCVhyg plasmids were extracted from *E.coli*. Following restriction digestion, the U1-Rib3 cassette was ligated into the pMSCVhyg vector. Transformants were isolated and recombinants identified using PCR. pMSCVhyg-Rib3 plasmids were initially transfected into an ecotropic producer line (ΩE). The resulting packaged virus was then introduced into an amphotropic producer cell line (ΨCrip). The packaged viruses carrying amphotropic envelopes were used to infect the target cell line (1Br.3neo.WRN4) to produce 1Br.3neo.WRN4-Rib3.

2.2.1 Plasmid vectors

The pU1-Rib3 plasmid was supplied by Dr. Katrin Jennert Burston (Bird *et al.* 2012) and carries a zeocin resistance cassette. The construct contains an anti WRN hammerhead ribozyme (Rib3). This is composed of a 24 base pair consensus hammerhead that lies between a 14 base complementary sequence 5' of the target and a 15 base complementary sequence 3' of the target (Montgomery *et al.* 1997; Bird *et al.* 2012). pMSCV-hygro, a vector containing murine stem cell virus long terminal repeats (LTRs) with a hygromycin resistance cassette (Clontech) (figure 2.2) was used for introducing and expressing the Rib3 gene in the target cell line (1Br.3neo.WRN4).

2.2.2 Competent bacteria

The competent bacteria cells used in these experiments were *E.coli* JM109 (genotype: endA1, recA1, gyrA96, thi, hsdR17 (r_k^-, m_k^+), relA1, supE44, Δ(lac-proAB), [F´ traD36, proAB, $laqI^qZ\Delta M15$]) (Promega), a routine strain used for cloning and

subcloning procedures. Bacterial strains were cultured in LB (Luria-Bertani, BD) broth (10 g/ L tryptone, 5 g/ L yeast extract, 5 g / L NaCl) or on LB agar (same as broth with 15 g / L agar).

Bacterial cells that contain a specific plasmid, post transformation, were selected either on ampicillin at 100 µg / ml for pMSCV-based plasmids or Zeocin at 50 µg / ml in the case of pU1-Rib3 plasmids.

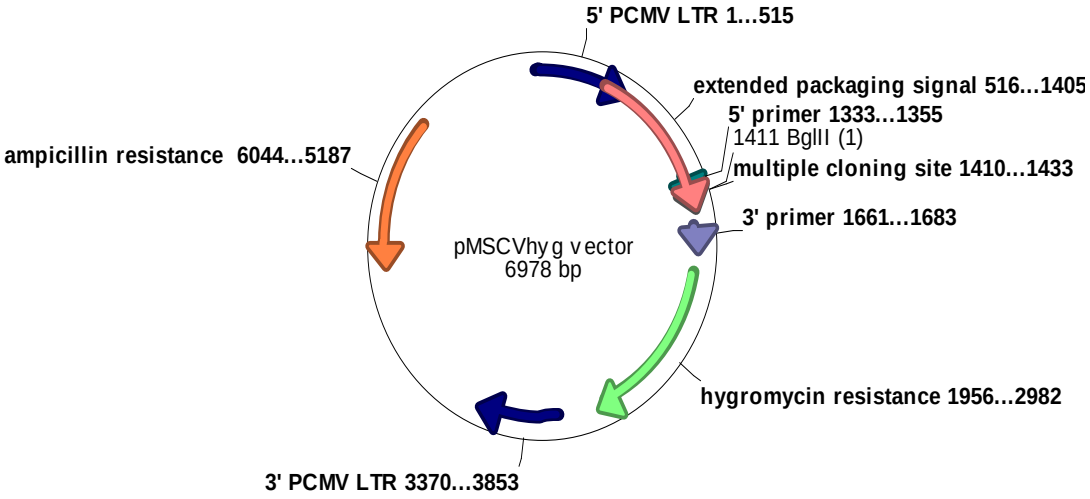

Figure 2.2 Vector map for pMSCVhyg The map for pMSCVhyg, displaying primer sites, *Bgl* II restriction site, antibiotic resistance genes and multiple cloning sites.

2.2.3 DNA extraction

2.2.3.1 Small scale plasmid extraction

Small scale plasmid DNA extraction was carried out using a Qiagen miniprep kit (Qiagen). Single colonies of *E.coli*, containing the plasmid of interest, were inoculated in 2 mls of LB broth and cultured overnight for 16 hours prior to extraction. Extraction of the plasmid was carried out according to the manufacturer's schedule. Purified plasmid DNA was eluted in 100 µl of nuclease free water.

2.2.3.2 Large scale Endotoxin free plasmid extraction

The centrifugation method of the Pure Yield plasmid midiprep system kit (Promega) was used for large scale endotoxin free plasmid extraction. The bacterial clone of choice was picked from the plate and subcultured in LB broth (Luria-Bertani, BD) supplemented with 100 µg / ml ampicillin overnight prior to plasmid extraction. The plasmid extraction was carried out according to the manufacturer's instructions.

The filtrate was collected and stored in a 1.5 ml eppendorf tube at -20°C.

2.2.4 Subcloning

2.2.4.1 Restriction digestion

Restriction enzymes *Bgl* II (AGATCT) and *Bam*H I (GGATTC) were added at 0.1 u / µl to the samples containing pMSCVhyg and pU1-Rib3 respectively.

2.2.4.2 Agarose gel electrophoresis

Agarose gels at 0.8 % to 1.5 % in TBE (45 mM Tris base, 45 mM boric acid, 1 mM EDTA pH 8.0) and at 1.8 % in TAE (20 mM Tris acetate, 1 mM EDTA pH 8.0) containing ethidium bromide (0.5 µg / ml) were prepared for analytical and preparatory gel electrophoresis. Samples mixed with loading dye (0.03% bromophenol blue, 0.03% xylene cyanol FF, 60% glycerol) and electrophoresed at 120 V (Power Pack 300, Bio-Rad) for 30 minutes.

2.2.4.3 DNA purification from agarose gels

The digested DNA was observed using an ultra violet light box. The specific band corresponding to the DNA sequence of interest was carefully excised from the gel using a scalpel. This was then placed in a 50 ml tube and stored at -20º C overnight.

Then, two pieces of filter paper were wetted, using molecular biology grade deionised water, and placed in a 10ml syringe. The gel containing the DNA sample was then syringed through the filter paper until most of the fluid passed through into eppendorf tubes and most of the gel remained in the syringe. The crude extract was then ethanol precipitated.

2.2.4.4 Ethanol precipitation

Ethanol precipitation was performed to concentrate and purify the DNA samples. The salt concentration was adjusted by adding 3 M sodium acetate to the eppendorf tubes at a 1:10 dilution (final concentration of 0.3 M). Pre-cooled 100 % ethanol was added at twice the volume of the total mixture. The tubes were placed in -20º C for a minimum of one hour. The tubes were centrifuged at 13,000 g at 4º C for 10 minutes. The supernatant was aspirated carefully leaving the pellet at the bottom of the tube. The pellet was resuspended with pre-cooled 70 % ethanol and centrifuged at 13,000 g at 4º C for 5 minutes. The supernatant was aspirated carefully leaving a pellet at the bottom of the tube. The wash step with pre-cooled 70 % ethanol was repeated and the pellet was placed on a heat block to air dry. The pellet was then resuspended in 100 µl molecular biology grade deionised water.

2.2.4.5 DNA ligation

The number of moles of the ends of double stranded DNA fragments was calculated using the following formula:

Number of moles= 2 x (DNA weight in grams) / (number of DNA bases x 660 Da / bp).

The vector digest was treated with BAP (bacterial alkaline phosphatase) (Invitrogen) for one hour prior to ligation, to prevent self-ligation. Ligation was carried out at molar vector-to-insert ratios of 1:1, 1:3 and 1:5 using T4 DNA ligase. The ligation mixture was incubated for 24 hours at 4 º C.

2.2.4.6 Transformation of competent bacteria

E.coli JM109 competent cells were thawed. 1 µl of plasmid DNA or ligation mix and 100 µl of *E.coli* competent cell suspension were added to an eppendorf tube. The suspension was gently mixed and the tube was placed on ice for 10 minutes. The tube was then transferred to a pre-heated water bath at 42 ºC for 45-50 seconds to heat shock the competent cells. The tube was placed on ice for two minutes. 900 µl of SOC medium (2 g tryptone, 0.5 g yeast extract, 10 mM NaCl, 10 mM KCl, 20 mM Mg^{2+}, 20 mM glucose) was added to the mixture and the tube was incubated on a shaker at 37 ºC for 60 minutes. Transformed cells were plated on LB agar containing the appropriate selection.

2.2.5 Identification of recombinant clones by PCR

Polymerase chain reaction (PCR) was performed to identify recombinant plasmids containing the desired gene. PCR mixtures contained 1.5 mM $MgCl_2$, 10 mM of each dNTP, 100 pmol of forward primer (pMSCV 3': 5'-GAGACGTGCTACTTCCATTTGTC-3') and 20 pmol of reverse primer (U1 5': 5' ATACTTACCTGGCAGGGGAGAT 3') and one unit of Taq DNA polymerase. Either bacterial colonies or purified DNA samples were added to the mixture. The mixtures were placed in thin walled 200 µl micro eppendorf tubes and the reactions were carried out in a Techne Genius (model: FGEN 02 TD) thermal cycler. An initial hot start at 95º C for 5 minutes was carried out followed by 30 to 32 cycles of denaturation (95º C for one minute), annealing (5º C below the melting temperature of the primer with the lowest melting temperature for one minute), extension or elongation (72º C for one minute). A final extension step (72 º C for 10 minutes) was carried out when the cycles were completed. PCR products were resolved using agarose gel electrophoresis (see 2.2.4.2).

2.2.6 DNA sequencing

To confirm integrity of the Rib3 containing region of the plasmid vector (pMSCVhyg.Rib3) DNA sequencing was performed at MWG Biotech (Milton Keynes, UK). Air dried samples of plasmid DNA from a forward and reverse primer PCR were sent to MWG Biotech for sequencing. The results obtained were compared to sequences from the NCBI nucleotide database using the multiple alignment construction and analysis workbench software (MACAW 2.05) (Schuler *et al.* 1991) or GENtle V 1.9.4.

2.2.7 Retroviral transduction

The recombinant vector generated above was transduced into retroviral packaging cell lines in order to generate a retrovirus capable of infecting human cell strains. This follows a two-step process involving an ecotropic producer followed by an amphotropic producer as described below.

2.2.7.1 Safety precautions for handling retrovirus

Additional safety precautions were applied for the handling of retroviruses. A separate working area, tissue culture hood and incubator are designated for retroviral infection procedures and a warning sign is placed near the area. An apron was worn over the lab coat and was protected with a second lab coat. Goggles and Mask were worn to protect the eyes and from inhalation of infected material. Double gloves were worn as an extra protective measure and no sharps were used during retroviral infection and culture of infected cells. All items for disposal were sleeved with plastic wrapping prior to discarding them in a biohazard lidded bin. Biological waste was treated with 5% Virkon overnight. All tissue culture vessels were placed in a second outer vessel for incubation.

2.2.7.2 Transfection of ecotropic producer cells using lipofectamine

Transfection was carried out to package the vector (MSCV-WRN Rib3.hygro) in the ΩE ecotropic retroviral producer cell line using lipofectamine (Invitrogen). The ΩE ecotropic retroviral producer cell line packaged viruses are capable of infecting mouse and rat cells only. Following the manufactures procedures, 8 µg of the vector DNA in 500 µl of OptiMEM (reduced serum medium, Invitrogen) and a suspension containing 200 µl of lipofectamine in 500 µl of OptiMEM were prepared and incubated at room temperature for five minutes. The OptiMEM suspensions containing the DNA and lipofectamine were mixed together and incubated at room temperature for 20 minutes to allow the DNA to be enclosed by liposomes.

Standard cell culture media were replaced with 5 ml of OptiMEM in the ΩE cell culture. The lipofection mixture was then added to the cells. The lipofection reaction was incubated at 37°C with 5% CO_2 for five hours. OptiMEM was replaced with standard cell culture media and the cell culture was returned to the incubator.

2.2.7.3 Harvesting viral particles

Viral particles were reproduced and packaged in the host producer cell lines. Supernatants from the producer cell lines containing the free packaged and infectious viral particles were syringed through a 0.2 μm filter to remove any remaining cells. The virus supernatants were collected in a cryovial and snap frozen in a liquid nitrogen filled canister. The virus supernatants were transferred to a -80º C freezer for long term storage.

2.2.7.4 Generation of amphotropic producer cells and retroviral infection of target cells

Retroviral infection of the vector into the Ψ^+ amphotropic retroviral producer cell line was carried out in order to stably produce viruses capable of infecting cultures of human cells. The packaged viruses were then used for the stable introduction of Rib3 into 1Br.3neo.WRN4 cells. The procedure carried out to infect both the Ψ^+ retroviral producer and 1Br.3neo.WRN4 target cells was the same. The target cells including one negative control were pretreated with polybrene at 8 μg/ ml. The virus supernatant was syringed through a 0.2 μm filter (Iwaki) and suspended in media containing 2 μg/ml polybrene. The media from the cells was replaced by the suspension containing the virus and 2 μg/ml polybrene. Media containing polybrene without the virus supernatant was added to the negative controls. After 2 hour incubation, the virus suspension was diluted with cell culture media up to a volume of 5 ml. The cells were incubated for 24 hours in 37°C and 5% CO_2 (S410 NAPCO). The virus containing media was replaced with virus free routine cell culture media. Retroviral infected cells were selected from the culture by the addition of 2.5 μg/ml puromycin and 200 μg/ml hygromycin to the cell cultures. Cells that have undergone retroviral infection are kept under antibiotic selection indefinitely.

The virus supernatant from the Ψ^+ amphotropic retroviral producer cells generated above was harvested as described in section 2.2.7.3 and used to infect 1BR.3neo.WRN4. Cells were passaged with a high level of precaution for one week post infection. After one week, the cells were routinely passaged as described in section 2.1.1.2.

2.2.8 RNA extraction

Cells were seeded in either 25 cm^2 or 75 cm^2 flasks at a final density of 7000 cells/cm^2. Target cells were not fed for 72 hours, prior to RNA extraction.

RNA working area and instruments were cleaned thoroughly with RNAse Away (Fisher, UK) prior to extraction. Cells were washed once in warm (37^oC) PBS and then lysed immediately in 1.5ml cold (4^oC) TRIzol (Invitrogen). The cell lysate was harvested using a cell scraper and transferred into two Eppendorf tubes. The suspension was left at room temperature for five minutes to lyse completely. Following the addition of 175µl of chloroform, tubes were shaken vigorously for 15 seconds and incubated at room temperature for three minutes. The whole RNA extraction mixture was transferred into a heavy phase lock gel column (Eppendorf). Following centrifugation at 13,000g for two minutes, the upper aqueous layer was transferred to a separate tube and an equal volume of isopropanol and 1µl of Pellet paint NF co-precipitant (Merck) was added. The solution was left to precipitate at room temperature for ten minutes and centrifuged at 13,000g for 20 minutes at 4ºC. The pellet was washed in 0.5ml of 75% ethanol and centrifuged for a further 10 minutes at 13,000g at 4ºC. The supernatant was removed and the pellet air-dried for 5 minutes. The pellet was then resuspended in 15µl of RNAse free dH_2O. The suspension was heated to 65ºC for 5 minutes, centrifuged briefly and left on ice for 30-60 minutes. Duplicate tubes were pooled and the RNA samples stored at –80^oC until required.

2.2.9 Reverse transcriptase PCR

Reverse transcriptase PCR was carried out using the OneStep RT-PCR kit (QIAGEN). The reaction mix contained 5 µl One Step RT-PCR buffer, 10 mM of each dNTP, 0.6 µM of forward primer (U1 5': 5'-TCCACTGTAGGATTAACAACTAAG-3'), 0.6µM of reverse primer (U1 3': 5'-ATACTTACCCTGGCAGGGGAGAT-3'), 1 µl RT-PCR enzyme mix and 0.5 µg template RNA. The mixtures were placed in thin walled 200 µl micro eppendorf tubes and the reactions were carried out in a Techne Genius (model: FGEN 02 TD) thermal cycler. Reverse transcription at 50° C for 30 minutes was carried out followed by reverse transcriptase inactivation at 95° C for 15 minutes. The following reactions were carried out over 40 cycles of denaturation (94º C for 30 seconds), annealing (5º C below the melting temperature of the primer with the lowest melting temperature for 30 seconds), extension or elongation (72º C for one minute). A final

extension step at 72 º C for 10 minutes was carried out when the cycles were completed. PCR products were isolated by agarose gel electrophoresis (see 2.2.4.2).

2.3 Chromosome analysis

2.3.1 Metaphase preparation

Cells were treated with 50 nM colcemid and incubated for 30 minutes at 37° C. Cells were trypsinised, neutralised and collected as per routine passage procedure (section 2.1.2). The suspension was then centrifuged at 400 g for 5 minutes. The cell pellet was gently re-suspended in 6 mls of 75 mM KCl and incubated at room temperature for 15 minutes. Twelve drops of fixative (methanol, glacial ascetic acid 3:1) were added to the suspension and centrifuged at 400 g for 5 minutes. The supernatant was aspirated and the pellet re-suspended with a further 5 mls of fixative solution and centrifuged at 400 g for 5 minutes. The supernatant was aspirated and the above step repeated. The supernatant was aspirated and the pellet was re-suspended in an appropriate volume of fixative solution (enough to give the suspension a slight cloudy appearance). The suspension was then stored at 4° C for 24 hours. Microscopic slides were washed with methanol and deionised water. The slides were held with one long side held at a 30° angle with the bench top and three evenly spaced drops of the suspension were added to each slide using a Pasteur pipette. Excess fixative was drawn off by tilting the slides and fresh fixative was added to the slides tilted from one long end at a 30° angle. The slides were tilted from the frosted end at a 30° angle and air dried. The slides were incubated at 65° C for 24 hours. The slides were then stained using Giemsa stain (Sigma) and photographs of metaphase chromosomes were taken under 100 x oil immersion objective lens.

2.3.2 Karyotype analysis

Chromosomes from the photographs were arranged with the aid of Smart Type software (Digital Scientific Ltd., http://www.smarttype.biz). The arrangement was carried out according to the International System for Human Cytogenetics Nomenclature scheme (Lindsten *et al.* 1978). The following classifications were used for the arrangement of unbanded chromosomes based on their size and the position of their centromere (Lindsten *et al.* 1978):

Group A: Consists of chromosomes 1-3 which are large metacentric chromosomes that are further distinguished from one another by size and centromere position.

Group B: Consists of chromosomes 4 and 5 which are large submetacentric and are difficult to distinguish from one another.

Group C: Consists of chromosomes 6-12 and the X chromosome. These are medium sized metacentric chromosomes and are difficult to distinguish from one another. The X chromosome is identical to the longer chromosomes of this group.

Group D: Consists of chromosomes 13-15 which are acrocentric with satellites.

Group E: Consists of chromosomes 16-18 which are relatively short. Chromosome 16 is metacentric whereas chromosomes 17 and 18 are submetacentric.

Group F: Consists of chromosomes 19 and 20 which are short metacentric chromosomes.

Group G: Consists of chromosomes 21, 22 and the Y chromosome which are short acrocentric chromosomes. Chromosomes 21 and 22 have satellites whereas the Y chromosome does not consist of satellites.

2.4 Comet assay

Target cells, pelleted at 10^5, were re-suspended in 120 µl serum free media containing 120 µl 1.4% agarose gel. A 50 µl aliquot of the cell suspension was pipetted against a coverslip tilted at a 45° angle on a slide. The coverslip was gently placed down onto its slide and incubated at 4° C for 10 minutes for the gel to set. The coverslips were then removed and one drop of the drug (10 µM camptothecin in DMSO or DMSO only control) was added to the samples, the coverslip was placed back onto the sample area of the slide and incubated at 37° C, in a moist chamber, for one hour. The coverslip was removed and the slide placed in a tray containing lysis buffer (150ml lysis mix, 15ml DMSO, 1.5ml Triton X-100) and incubated for one hour at 4° C. The Slide was then transferred to the electrophoresis chamber containing electrophoresis buffer (18g NaOH, 7.5ml EDTA the volume was made up to 1 litre with distilled water at 15ºC) and incubated for 40 minutes at 4° C.

Electrophoresis was carried out at 1 volt per centimetre for 24 minutes. The slide was then washed and incubated in TRIS buffer for 5 minutes. A second wash in TRIS buffer was carried out. Finally, 35 µl of ethidium bromide was added and the coverslip placed back onto the samples. The slides were viewed using a fluorescent microscope and the data analysed using CASys software (Comet Analysis Synoptics).

2.5 TRAP assay

Detection of telomerase activity was carried out using a Telomere repeat amplification protocol (TRAP) (Kim *et al.* 1994) using the Telo TTAGGG telomerase PCR ELISA kit (Roche) according to the manufactures guidelines. For the assay, the cell extracts (4 x 10^3 cells/ µl) were added to 25 µl PCR reaction mixtures and made to a final volume of 50 µl with RNAse and DNAse free water. Extracts from EK1Br.hTERT cells were used as positive control and extracts from EK1Br cells as negative controls. Additional negative controls were generated for each cell type analysed, by inactivating the telomerase activity by heating the samples at 92° C for 5 minutes prior to adding them to the PCR reaction. PCR was performed using the Techne Genius thermal cycler (model: FGEN 02 TD). The reaction was started with one cycle of primer elongation at 25° C for 30 minutes followed by one cycle of telomerase inactivation at 94° C for 5 minutes. Amplification was carried out with 30 cycles of denaturation (94° C for 30 seconds), annealing (50° C for 30 seconds), and polymerization (72° C for 90 seconds). A final extension step was carried out at 72° C for 10 minutes. The samples were finally held at 4° C prior to transferring them to -20° C for long term storage.

Samples were analysed for the presence of telomerase activity using polyacrylamide gel electrophoresis. The gel was run using a protein II system, with cooling facility. A 12.5 % non-denaturing polyacrylamide gel in 0.5 x TBE was cast. 3.5 µl loading dye (0.03% bromophenol blue, 0.03% xylene cyanol FF, 60% glycerol) was added to 31.5 µl of the PCR product and 20 µl of this was loaded in each well. The tank was filled with 0.5 x TBE running buffer and electrophoresis was carried out at 400 V for approximately 4 hours. The gel was stained with SYBR gold on an orbital shaker for 40 minutes in the dark. The gel was then washed twice in dH_2O for 15 minutes and viewed using a UV imaging instrument with camera (FluorChem, Alpha Innotech).

2.6 Immunodetection assays

2.6.1 Immunofluorescence labelling

Generally the target cells were grown on 13 mm coverslips (VWR International) at the required seeding density and were maintained until they were approximately 60-80% confluent. The cells were washed in PBS prior to fixing. Cells were fixed using different methods, depending on the antigens to be labelled. Dilutions of all primary and secondary antibodies used are listed in table 2.2.

Target protein	Fixative	Permeablising agent	Primary antibody	Secondary antibody
Ki67	methanol, acetone (1:1)	N/A	Polyclonal Rabbit anti-human Ki67 (Santa Cruz); 1:30	Swine anti-rabbit IgG, FITC Conjugated (Dako); 1:30
Involucrin	methanol, acetone (1:1)	N/A	Monoclonal mouse anti-human involucrin (Abcam); 1:100	Donkey anti-mouse IgG, Rhodamine red conjugated (Jackson Immuno Research); 1:200
WRN	4% paraform -aldehyde	0.1% Triton X-100	Polyclonal rabbit anti-human WRN (Abcam); 1:200	Swine anti-rabbit IgG, FITC conjugated (Dako); 1:30
WRN [4H12]	4% paraform -aldehyde	0.1% Triton X-100	Monoclonal mouse anti-human WRN helicase [4H12] (Abcam); 1:200	Rabbit anti-mouse IgG, FITC conjugated (Dako); 1:30
Cytokeratin	methanol, acetone (1:1)	N/A	Monoclonal mouse anti-human cytokeratin 5,6,8,17 and probably 19 (Dako); 1:30	Rabbit anti-mouse IgG, FITC conjugated (Dako); 1:30

Table 2.2 List of antibodies and fixation conditions for immunofluorescence assays Summary of primary and secondary antibodies used in the immunofluorescence labelling of cells including fixative and permeabilising agents used for each protein.

2.6.1.1 Primary antibodies

2.6.1.1.1 Cytokeratin, Ki67 and involucrin

Cells were fixed with a 1:1 methanol:acetone solution for 4 minutes at 4°C. The fixative was aspirated and the cells washed in 3 changes of PBS. The coverslips were transferred to a humid chamber and incubated with the primary antibody. For cytokeratin labelling, a monoclonal mouse anti human cytokeratin against keratins 5, 6, 8, 17 and probably 19 (Dako antibodies) were used at a dilution of 1:30; for labelling Ki67, mouse anti-human Ki67, or rabbit anti human Ki67 (Dako antibodies) were used at a 1:30 dilution; and for involucrin labelling, monoclonal mouse anti-human involucrin (Abcam) was used at a dilution of 1:100. All primary antibodies were diluted in 0.1 % BSA (bovine serum albumin) in PBS for one hour at room temperature or overnight at 4°C.

2.6.1.1.2 WRN

Cells were fixed with 4% paraformaldehyde (w/v) for 4 minutes at room temperature. The fixative was aspirated and the cells washed in 3 changes of PBS. The

cells were permeabilised using 0.1% Triton X-100 for 2 minutes at room temperature. The cells were then washed in 3 changes of PBS. To test WRN expression in WRN knockdown experiments in 1BR.3neo, a polyclonal rabbit anti-human WRN (ABcam) was used at 1:200 dilution in 0.1% BSA (Sigma) and PBS. A monoclonal mouse anti WRN [4H12]-Carboxyterminal end (ABcam) (figure 2.3) diluted 1:200 in 0.1% BSA (Sigma) and PBS was used for keratinocytes (the mouse monoclonal antibody specific to epitope 4H12 was selected for increased specificity because the polyclonal antibody has shown to be non-specific in the keratinocytes). Primary antibodies were added to coverslips containing the cells in a humid chamber and incubated at room temperature for one hour or at 4°C overnight.

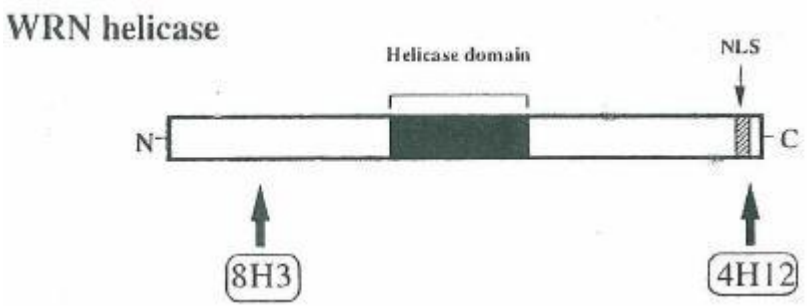

Figure 2.3 WRN helicase Diagram of WRN helicase displaying the helicase domain, nuclear localizing signal region (NLS) and epitope site of 4H12 (Shiratori *et al.* 1999).

2.6.1.2 Secondary antibodies

After incubation with the primary antibody the coverslips were washed in 3 changes of PBS. The coverslips were incubated with a secondary antibody, at specific dilutions (table 2.2), in 0.1 % BSA for 45 minutes at room temperature. Finally, the coverslips were washed in three changes of PBS and mounted in Vectashield mountant, containing 4'6-diamidino-2-phenylindole (DAPI) (Vector labs) as nuclear counter stain. The coverslips were viewed using an inverted fluorescence microscope (Axiovert 25 Carl Zeiss).

2.6.2 Western blot

2.6.2.1 Protein Extraction

Cells for protein extraction were counted, washed in cold PBS and pelleted in an Eppendorf tube. Pellets of 10^6 cells were resuspended in 5 µl of protease inhibitor cocktail (Sigma) and 50µl of Totex buffer (20 mM Hepes pH7.8, 350 mM $NaCl_2$, 20% Glycerol, 1% w/v Igepal 0.006 g $MgCl_2$, 0.5 mM EDTA, 0.1 mM EGTA). For studying phosphorylated proteins, phosphatase inhibitors (1 mM NaV_3O_4, 10 mM NaF) were added to the Totex buffer. Cells were lysed by mixing gently and leaving on ice for 30 minutes. The lysate was then centrifuged at 13,000 g for 5 minutes at 4ºC (Hettich EBA 12 R) and the supernatant was removed for storage at -20ºC.

2.6.2.2 Protein estimation by Bradford assay

Protein concentrations of Totex extracts were estimated using the Bradford assay (Bradford 1976), a standard colorimetric assay for measuring total protein concentration. A standard curve, using BSA (bovine serum albumin) at concentrations of 1.25, 2.5, 10, 15, 20, 25, and 100 µg/ml was generated. Lysates to be analysed were diluted 1:50 in distilled water prior to the assay. Standards were blanked against distilled water and extracts were blanked against a 1 in 50 dilution of Totex buffer in distilled water. Samples (50 µl), standards (50 µl) and blanks (50 µl) were combined with 200 µl of a 1:5 dilution of Bradford concentrate (BioRad) and transferred to a 96-well flat-bottomed microtitre plates. The samples were incubated at room temperature for 15 minutes and the absorbance read at 595 nm, using a Titrek multiscan plus MK2 spectrophotometer. The concentrations of the samples were obtained from the BSA standard curve.

2.6.2.3 SDS-PAGE

Protein extracts were separated by SDS polyacrylamide gel electrophoresis for subsequent blotting and Western hybridisation (Burnette 1981) using a BioRad Protean II system. Separating gels were prepared with different concentrations of acrylamide/bis-acrylamide (29:1) depending on the protein of interest; 6% for WRN; 9% for p53, p63 and involucrin; 12% for phosphorylated p38 and 15% for p16.

The separating gel was composed of the desired concentration of acrylamide/bis-acrylamide (29:1) with 0.375 M Tris-HCl pH 8.8, 0.1% SDS, 0.05% (w/v) ammonium persulphate and 0.05% (v/v) Temed. The stacking gel was composed of 3.98% acrylamide/bis-acrylamide (29:1), 0.125 M Tris-HCl pH 6.8, 0.1% SDS, 0.05 % Ammonium persulphate and 0.1% Temed.

Samples were loaded at 10 µg of protein per well, prepared in 10 µl of TOTEX buffer and 5 µl of Laemmli sample buffer (62.5 mM Tris-HCl pH 6.5, 10% Glycerol, 2% SDS, 0.00125% (w/v) Bromothymol blue, 5% β-mercaptoethanol). The samples were denatured by boiling at 100ºC for five minutes before loading. Gels were run at 120 V in Tris-glycine running buffer (25 mM Tris, 192 mM glycine, 0.1% SDS) for 1 to 1.5hours.

The gels were then transferred to nitrocellulose using a Trans-Blot semi-dry blotting system (Biorad). Gels were pre-soaked in Towbin transfer buffer (25 mM Tris, 192 mM glycine, 20% methanol) for 20 minutes. Nitrocellulose membranes were wetted in distilled water and pre-soaked, together with 2 sheets of blotting paper, in transfer buffer for 10 minutes. The transfer system was then assembled as described in figure 2.4. Transfer was carried out at 20 V for one hour. After transfer the membrane was washed in TBS/T buffer (23.1 mM Tris-HCl, 137 mM NaCl, pH 7.6, 0.1% Tween 20) and stored in blocking solution (TBS/T, 5% milk powder) at 4ºC overnight. The gel was stained in 1% Coomassie Blue (in 40% methanol, 10% acetic acid), followed by destaining in 40% methanol, 10% acetic acid, to check the loading and transfer efficiency.

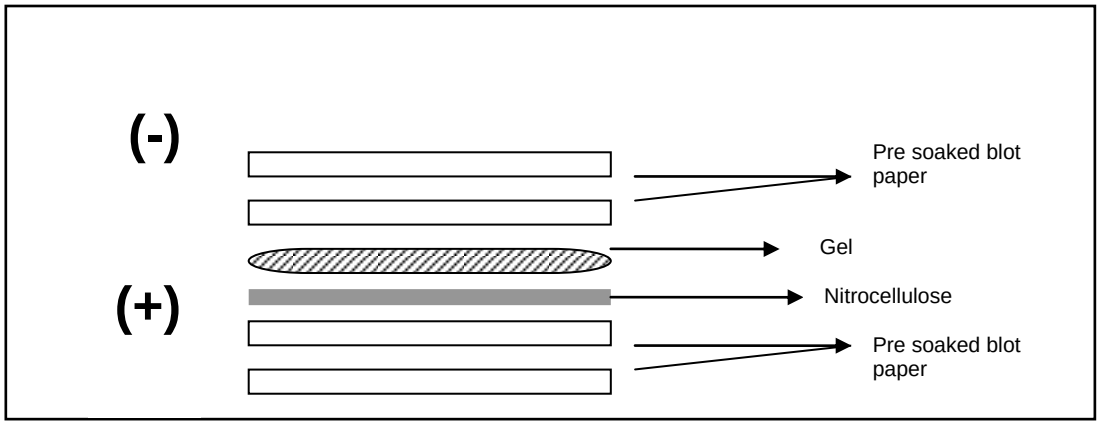

Figure 2.4 Western blot semi dry transfer assembly The diagram shows assembly of the components for semi dry transfer step of a Western blot.

2.6.2.4 Western Blotting

Protein expression was examined by blocking the membrane in 5% milk powder in TBS/T at 4ºC overnight. The membranes were then washed in TBS/T and incubated with the appropriate primary antibody for one hour at room temperature on an orbital shaker. The following primary antibodies and their dilutions were used: mouse monoclonal anti human WRN [4H12] (Abcam); 1:500, mouse monoclonal anti human p53 (Oncogene); 1:80, mouse monoclonal anti human p63 (Abcam); 1:1000, mouse monoclonal anti human involucrin (Abcam);1:1000, rabbit polyclonal anti human p16 (Santa Cruz); 1:200 and rabbit monoclonal anti human phosphorylated p38 (Thr 180/ Tyr 182) (New England Biolabs); 1:1000.

The antibody dilutions were prepared in blocking solution (TBS/T, 5% milk powder). Membranes were then washed in TBS/T three times, for 15 minutes, 10 minutes and 5 minutes. The membranes were then incubated with the secondary antibodies (1:2,000 goat anti mouse IgG horse radish peroxidase conjugate (Dako) or 1:500 goat anti rabbit IgG horse radish peroxidase conjugate (Dako), depending on the primary antibody used) in blocking solution for one hour at room temperature on an orbital shaker. Membranes were washed again in TBS/T for 15 minutes, twice for 10 minutes and three times for five minutes. The membranes were then incubated with ECL detection solution (Amersham) for one minute. Excess solution was drained off, the membrane wrapped in saran wrap and exposed to ECL Hyperfilm (Amersham) for different time durations prior to developing the film.

Chapter 3

3.1 Treatment of Werner's syndrome fibroblasts with SB203580

3.1.1 Introduction

3.1.1.1 Involvement of the mitogen activated protein kinase p38 in cellular senescence

The mitogen activated protein kinase (MAPk) pathway controls signal transduction in cells in response to extracellular stimuli (Zarubin *et al.* 2005). This pathway is involved in many cellular processes including; proliferation, apoptosis and senescence (English *et al.* 1999). The MAPk family is subdivided into four groups which includes: extracellular signal regulated kinases (ERKs), c-jun N-terminal stress activated protein kinases (JNK/SAPK), ERK/ big MAP kinase 1 (BMK1) and the p38 group (Zarubin *et al.* 2005).

Stress induced by oncogenic Ras results in premature senescence of primary human fibroblasts by activating p53 and p16 (Serrano *et al.* 1997). It has been demonstrated that primary human fibroblasts respond to Ras by triggering MEK signalling of p53 and p16. Inhibiting MEK activation, in Ras microinjected primary human fibroblasts, delayed the onset of premature senescence (Lin *et al.* 1998). There are four variants of p38 namely p38α, p38β, p38γ and p38δ (Zarubin *et al.* 2005). The p38 group has been shown to be involved in replicative senescence and induced senescence in response to stress signals including Ras, oxidative stress and shock due to change in culture conditions (Iwasa *et al.* 2003).

An increase in the expression of phosphorylated (active) p38 but not total p38 was observed in normal senescent human fibroblasts at 60 CPD when compared to younger cells at 40 CPD. Furthermore, human fibroblasts induced to express telomerase that had maintained their telomere lengths did not demonstrate increased expression of phosphorylated p38. Senescent fibroblasts that expressed increased levels of phosphorylated p38 had shorter telomeres than younger cells and telomerase expressing cells. These results demonstrate involvement of p38 in telomere dependent replicative senescence (Iwasa *et al.* 2003).

Acute treatment of young human fibroblasts with H_2O_2 results in stress induced premature senescence of the cells. Iwasa *et al* (2003) demonstrated that senescent phenotype (i.e. enlarged slow growing cells) became apparent in cells, treated with 450

μM H_2O_2 for 2 hours, on day 6 post treatment, followed by complete senescence of the culture on day 8.

A pyridinyl imidazole, SB203580 has been shown to specifically inhibit p38 and does not inhibit the Erk or JNK pathways (Lee *et al.* 1994; Cuenda *et al.* 1995). Inhibition of p38 by SB203580 treatment of cells that were stressed by H_2O_2 reduced the rate of growth arrest in these cells. Furthermore, SA-β-galactosidase activity was significantly reduced in the SB203580 treated, H_2O_2 stressed cells. These findings suggest that p38 is involved in stress induced senescence (Iwasa *et al.* 2003).

3.1.1.2 SB203580 treatment increases the growth rate and proliferative lifespan of Werner's syndrome fibroblasts

Previous work by Davis *et al* established that SB203580 treatment of Werner's syndrome (WS) fibroblasts results in an increase in lifespan and growth rate of the cells. Cultured WS fibroblasts (AG05229) senesced at 18.2 CPD and had a growth rate of 0.13 PD/day. The WS fibroblasts growth rates and life spans were significantly lower than normal fibroblast growth rates which are more than 0.4 PD/day and life spans of 30-60 CPD. When treated with SB203580 (10 μM daily supplementation), AG05229 reached a lifespan of 43.7 population doublings and their average growth rate increased to 0.34 population doublings/ day. Treatment of other WS fibroblast strains (AG03141 and AG12795) with SB203580 demonstrated the same effect (Davis *et al.* 2005).

SB203580 treatment had also reduced the rate of exit from the cell cycle. This was demonstrated by measuring BrdU labelling index at consecutive passages. Results showed a -0.57 % and -0.71 % BrdU labelling index / PD in SB203580 as opposed to -1.53 % and -1.31 % in untreated AG05229 and AG03141 strains respectively. SB203580 treatment of fibroblasts from normal individuals however did not have any significant effect on their growth rate or lifespan (Davis *et al.* 2005).

Measurement of telomere erosion using single telomere length analysis (Baird *et al.* 2004) before and after treatment with SB203580 did not yield consistent results between the different WS strains. AG05229 demonstrated high levels of telomere erosion 250 bp / PD and were reduced to 128 bp / PD after SB203580 treatment. AG03141 telomere erosion rates were within normal range before treatment at 99 bp/ PD and were reduced after SB203580 treatment to 85 bp/ PD. However, AG12795 had a rate of 171 bp / PD that had increased with SB203580 treatment to 190 bp / PD (Davis *et al.* 2005).

3.1.2 Aims

The aim of SB203580 treatment of Werner's syndrome fibroblasts is to optimise conditions for the reproduction of the experiment in other cell types, especially keratinocytes.

Primary Werner's syndrome (WS) fibroblasts (AG03141) were cultured and treated with SB203580. Growth curves of the primary WS fibroblasts treated with different doses of SB203580 were established to confirm the optimum dose. Western blot analysis of the cells treated with the optimum dose was carried out to detect the effect of SB203580 on phosphorylated p38 expression. Primary WS fibroblasts treated with the optimum dose of SB203580 and untreated controls were then cultured for an extended period and their growth rates were analysed.

Telomerase immortalised WS fibroblasts (AG03141.hTERT clone 8, referred to as AG03141.hTERT in the text) and telomerase immortalised normal fibroblasts (HCA2.hTERT) were cultured and treated with SB203580 to determine if it had an effect on their growth rates. This was carried out to assess whether SB203580 has an effect on telomerase expressing cells as it did in primary cells.

The effect of SB203580 on DNA damage in telomerase immortalised WS fibroblasts was examined by carrying out Comet analysis of AG03141.hTERT treated and untreated with SB203580.

3.1.3 Results

3.1.3.1 Treatment of primary Werner's syndrome fibroblasts with SB203580

A dose response study was carried out in order to determine the optimum concentration of SB203580 that has an effect on the growth rate of Werner's syndrome fibroblasts (AG03141). Treatments with different concentrations of SB203580 were conducted on AG03141 cells at 12.2 cumulative population doublings (CPD) and were continued for 4 consecutive passages, treatments were carried out in triplicates (figure 3.11). The growth curve demonstrated the highest mean population doubling achieved was by 10 µM treated cells (7.5 CPD) followed by 15 µM (7 CPD), 2 µM (6.9 CPD), 5 µM (6.4 CPD), 20 µM treated (5.6 CPD), DMSO (4.7 CPD) and control cells (4.4 CPD) respectively (figure 3.1.1 and 3.1.2). Analysis of variances (ANOVA) of the mean cumulative population doublings collected at the fourth passage of each treatment demonstrates a significant difference between them ($p=0$). Post Hoc analysis using the Tukey test demonstrated no significant differences between the untreated control and DMSO treated cells ($p=1$). All of the SB203580 treated cells have a significantly higher growth rate than the control and DMSO treated cells ($p<0.05$). The difference between 10 µM, 15 µM and 2 µM is not significant ($p>0.05$). At 20 µM treatment, the cells demonstrated significantly lower population doublings compared to 2 µM , 5 µM and 10 µM treatments ($p<0.05$) but not significantly different from 15 µM treatment ($p=0.013$). From this, it was shown that the 10 µM SB203580 treatment was the optimal concentration to be used for treatments.

The untreated control and 10 µM SB203580 treated AG03141 cultures were continued for up to 89 days. Untreated control cells achieved 18.3 cumulative population doublings whereas the 10 µM SB203580 treated cells achieved 25.3 cumulative population doublings (figure 3.1.3). Univariate analysis of variance demonstrated a significant difference between the slopes ($p=0.009$), asserting that 10 µM SB203580 treated cells have a significantly higher growth rate than the untreated cells (Table 5.1 in appendix I). The untreated Primary Werner's syndrome fibroblasts (AG03141) demonstrated a low rate of population doublings. However, on treatment with 10 µM SB203580, an increase in the rate of population doubling was observed. AG03141 before and after treatment demonstrate a slight difference in morphology that is difficult to demonstrate (figure 3.1.4). Monitoring of cells over time in culture showed that confluent untreated cultures had lower cell counts than confluent 10 µM SB203580 treated cultures.

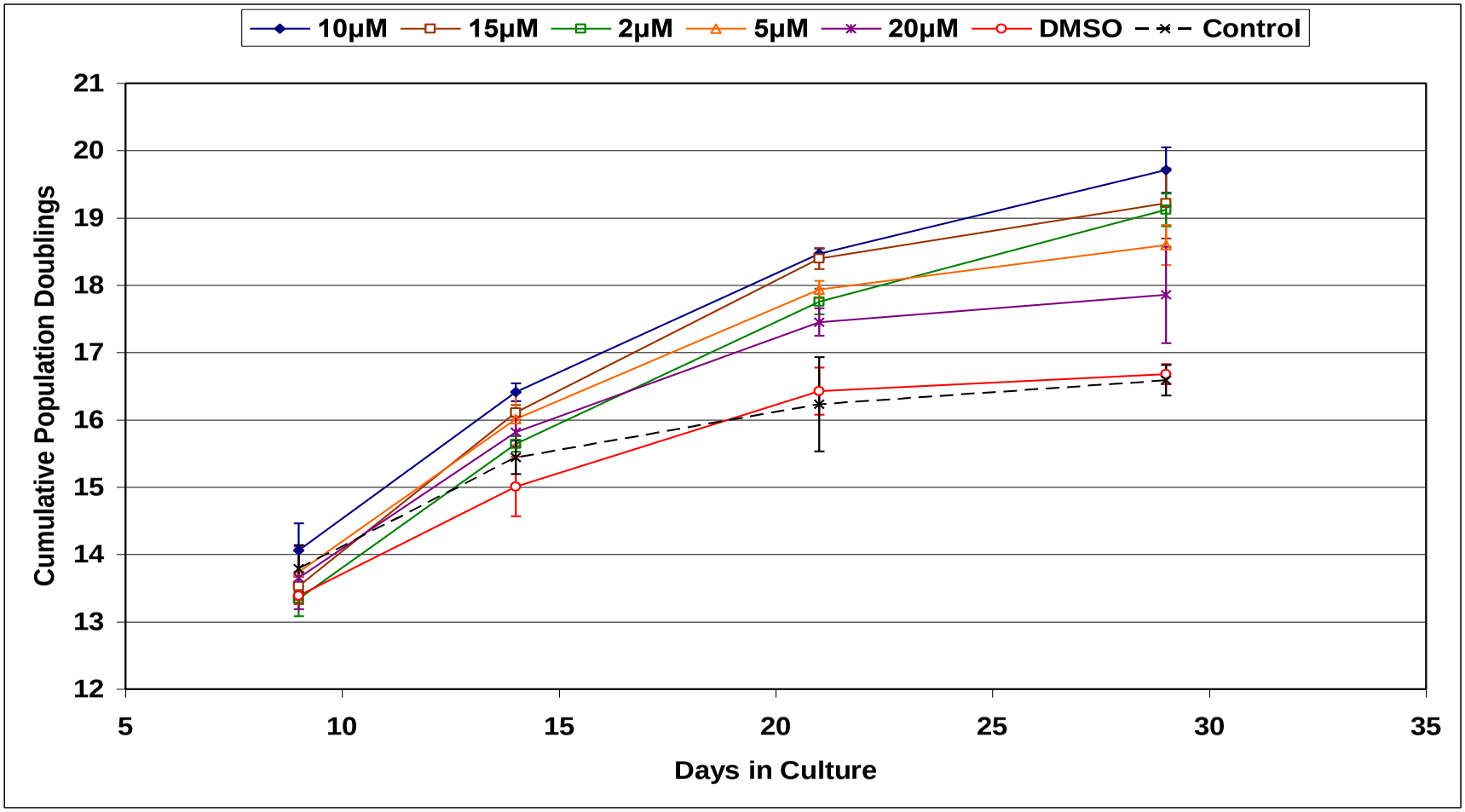

Figure 3.1.1 SB203580 dose response curve in primary Werner's syndrome fibroblasts The growth curve demonstrates cumulative population doublings (CPD) change, in days, for primary Werner's syndrome fibroblasts (AG03141) treated with SB203580 (10 µM, 15 µM, 2 µM, 5 µM and 20 µM), DMSO and untreated control. Treatment was started on the cells at 12.2 CPD and was continued for 4 consecutive passages. N=3, Error bars = ±standard deviation.

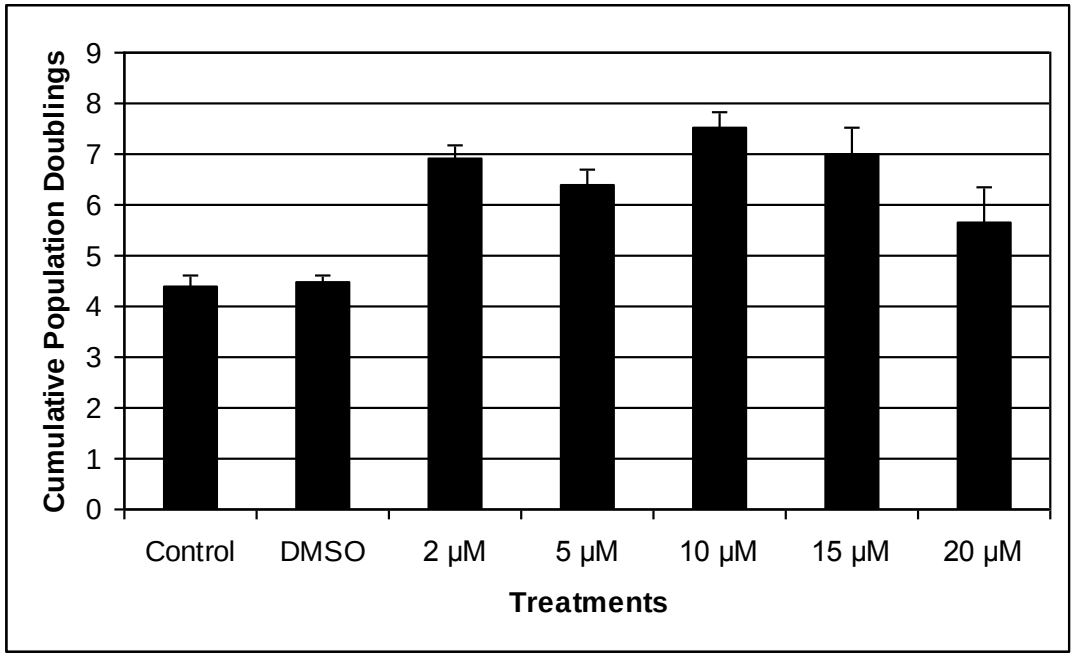

Figure 3.1.2 Cumulative population doublings achieved in Werner's syndrome fibroblasts (AG03141) following treatments with different doses of SB203580. Total CPD after 4 passages from start of treatment at 12.2 CPD. N=3. Error bars= ±standard deviation.

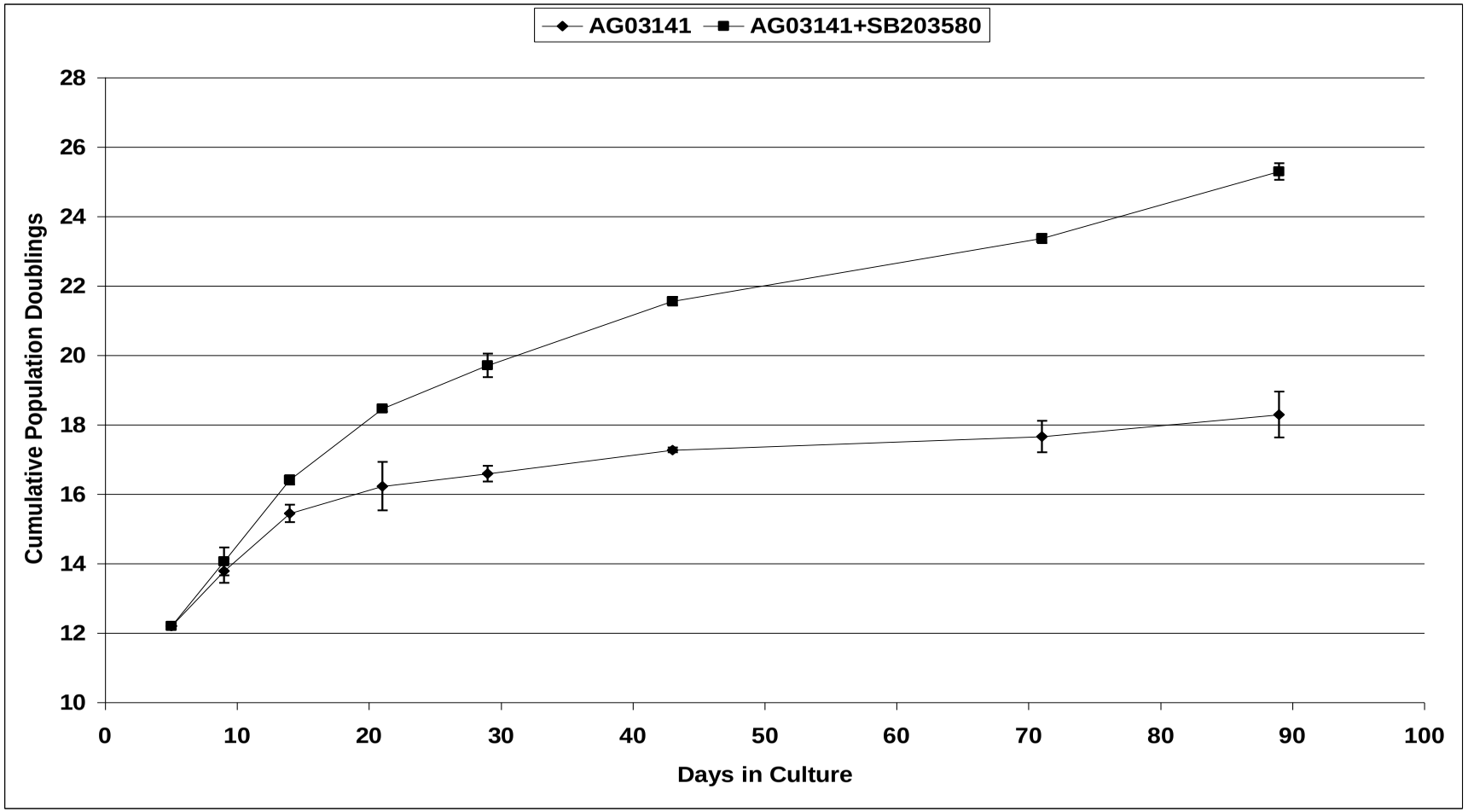

Figure 3.1.3 Growth curve of SB203580-treated and untreated primary WS fibroblasts The growth curve demonstrates primary Werner's syndrome fibroblasts (AG03141) before and after treatment with SB203580. N=3; Error bars= ± standard deviation.

a)

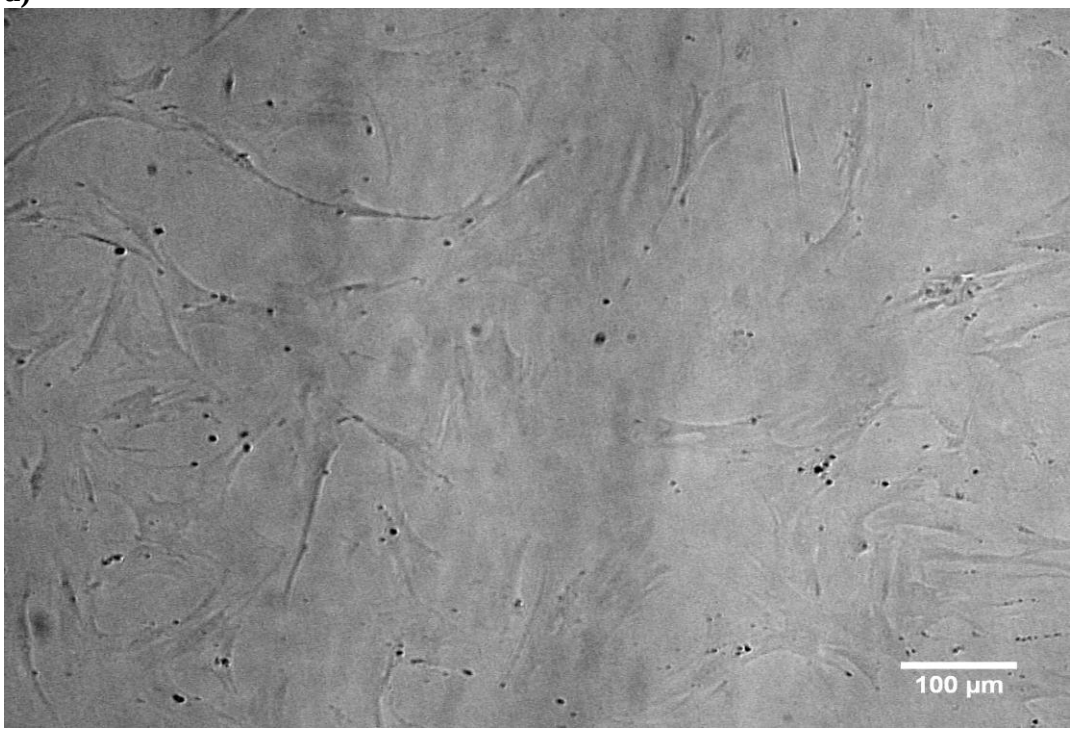

b)

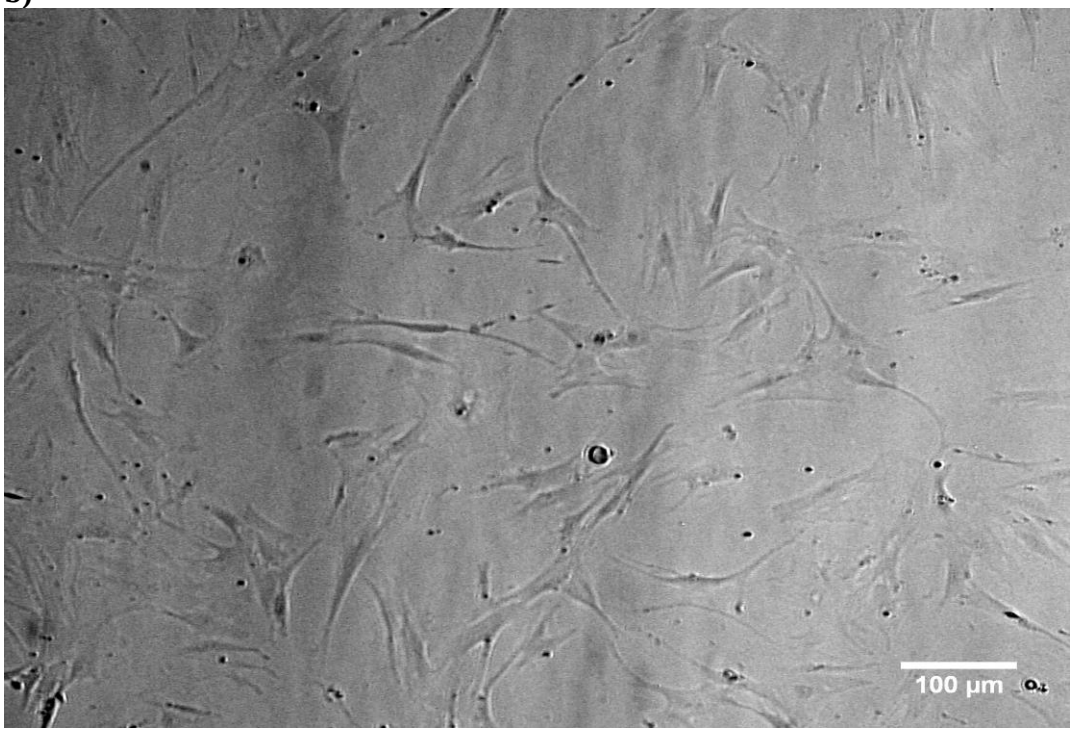

Figure 3.1.4 Photographs of SB203580 treated and untreated primary WS fibroblasts Primary WS fibroblasts (AG03141); a) untreated cells (14.22 CPD) b) cells treated with 10µM of SB203580 (14.86 CPD).

3.1.3.2 The effect of 10 µM SB203580 treatment on activated p38 levels

Western blot analysis was carried out to evaluate whether treatment with 10µM SB203580 had an effect on activated p38 levels in Werner's syndrome fibroblasts (AG03141) (figure 3.1.5). The phosphorylated p38 bands were normalised against bands of GAPDH and compared against each other (figure 3.1.6). The results demonstrated reduced levels of phosphorylated p38 in 10µM SB203580 treated compared to untreated AG03141 fibroblasts. However, a two tailed T-test shows that the reduction due to the treatment is not significant (t=2.731, p=0.088).

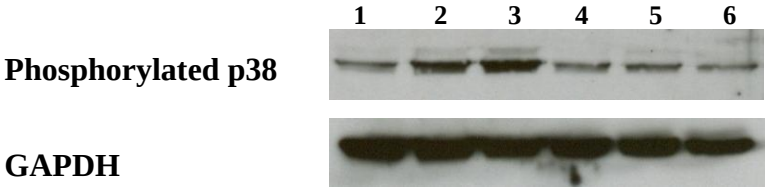

Figure 3.1.5 Western blot assay of phosphorylated p38 Assessment of phosphorylated p38 levels in untreated (1, 2, 3) and 10 µM SB203580 treated (4, 5, 6) Werner's syndrome fibroblasts (AG03141).

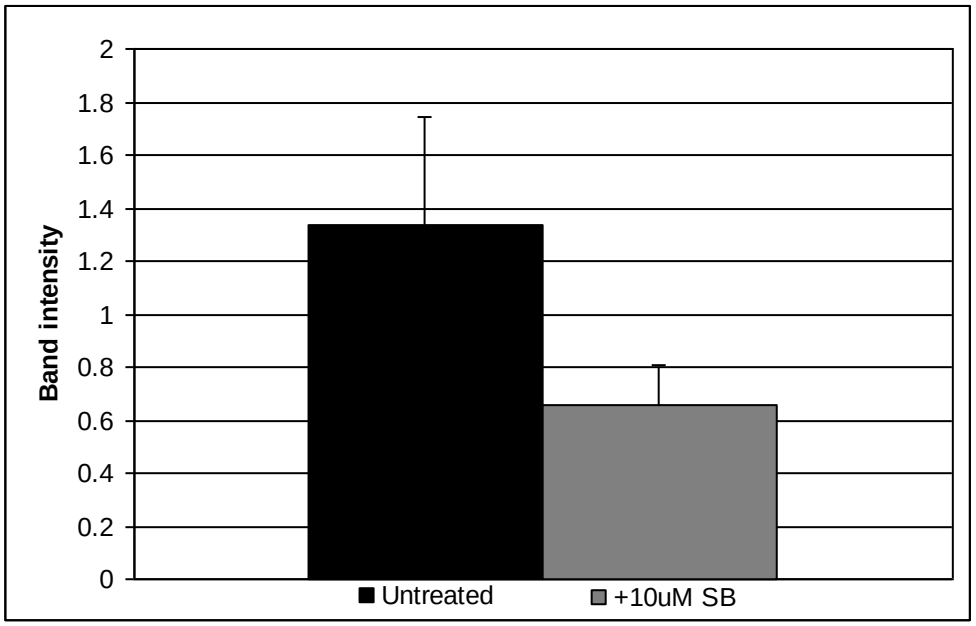

Figure 3.1.6 Intensity of phosphorylated p38 bands in Werner's syndrome fibroblasts Analysis of the phosphorylated p38 bands detected by Western blot in untreated and 10 µM SB203580 treated Werner's syndrome fibroblasts (AG03141). The bands have been normalised against GAPDH. N=3, error bars= standard deviation.

3.1.3.3 Treatment of hTERT immortalised WS cells with SB203580

Telomerase immortalised normal (HCA2.hTERT) and Werner's syndrome fibroblasts (AG03141.hTERT) were cultured and either left untreated or treated with SB203580. AG03141.hTERT cells were morphologically distinguishable from HCA2.hTERT cells by their large size (figure 3.1.7 and 3.1.8). The untreated cells, AG03141.hTERT, had a slower growth rate than HCA2.hTERT as observed in the growth curve (figure 3.1.9). There was a significant difference between the slopes ($p=0$) (tested by univariate analysis of variance).

Treatment of both cell lines with 10 μM SB203580 did not demonstrate any apparent changes in their morphological characteristics (figure 3.1.7 and 3.1.8) and did not have any significant effect on their growth rates (figure 3.1.9). Univariate analysis of variance demonstrated no significant difference between slopes of untreated and treated HCA2.hTERT cells ($p=0.31$) and AG03141.hTERT cells ($p=0.057$) (see table 5.2 and 5.3 in appendix I).

a)

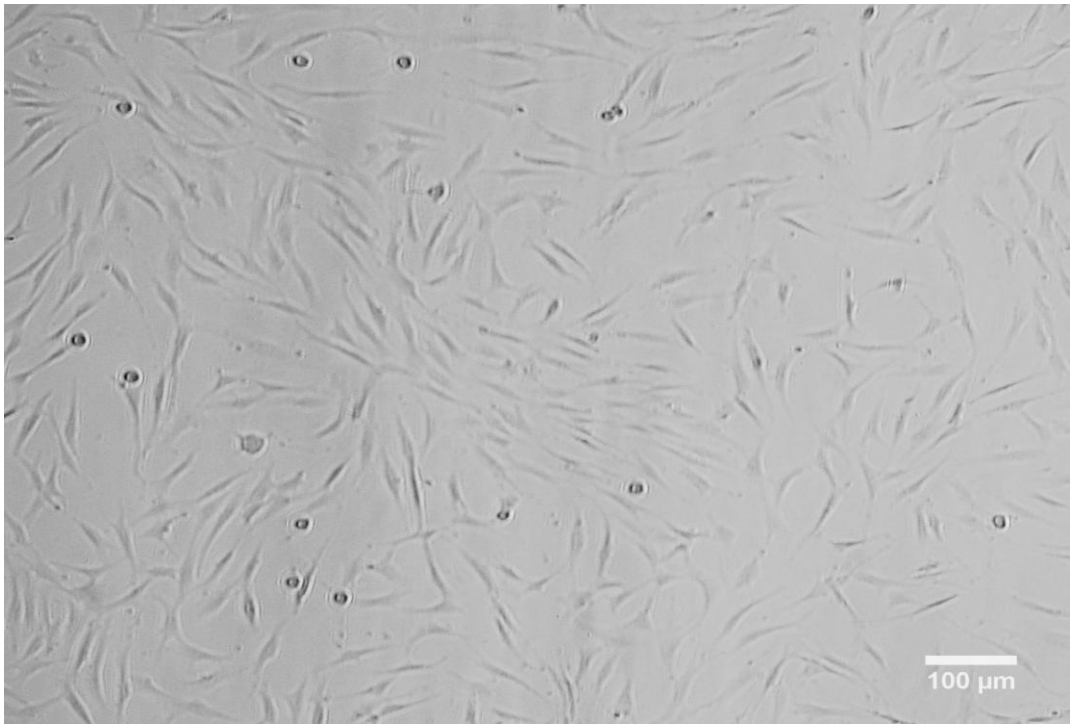

b)

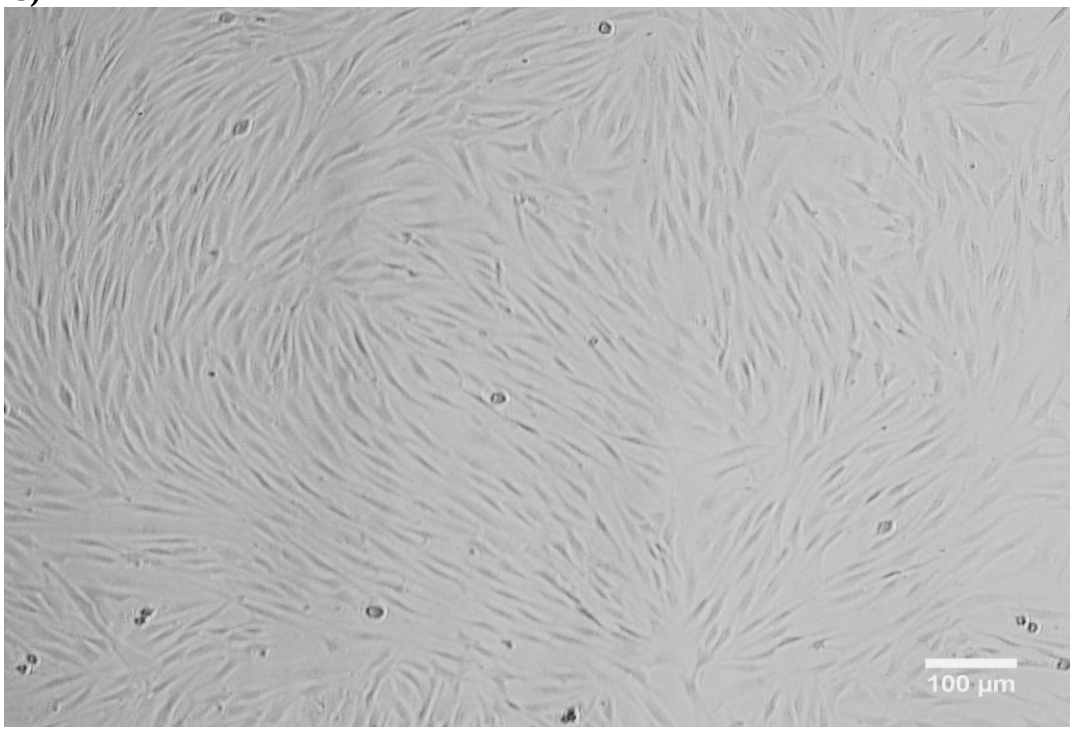

Figure 3.1.7 Photographs of SB203580 treated and untreated telomerase immortalised normal fibroblasts Telomerase immortalised normal fibroblasts (HCA2.hTERT) a) untreated, b) treated with SB203580. Both treated and untreated demonstrate normal fibroblast morphology and do not differ in their rate of growth (the differences between the photographs is in the confluency of the culture).

a)

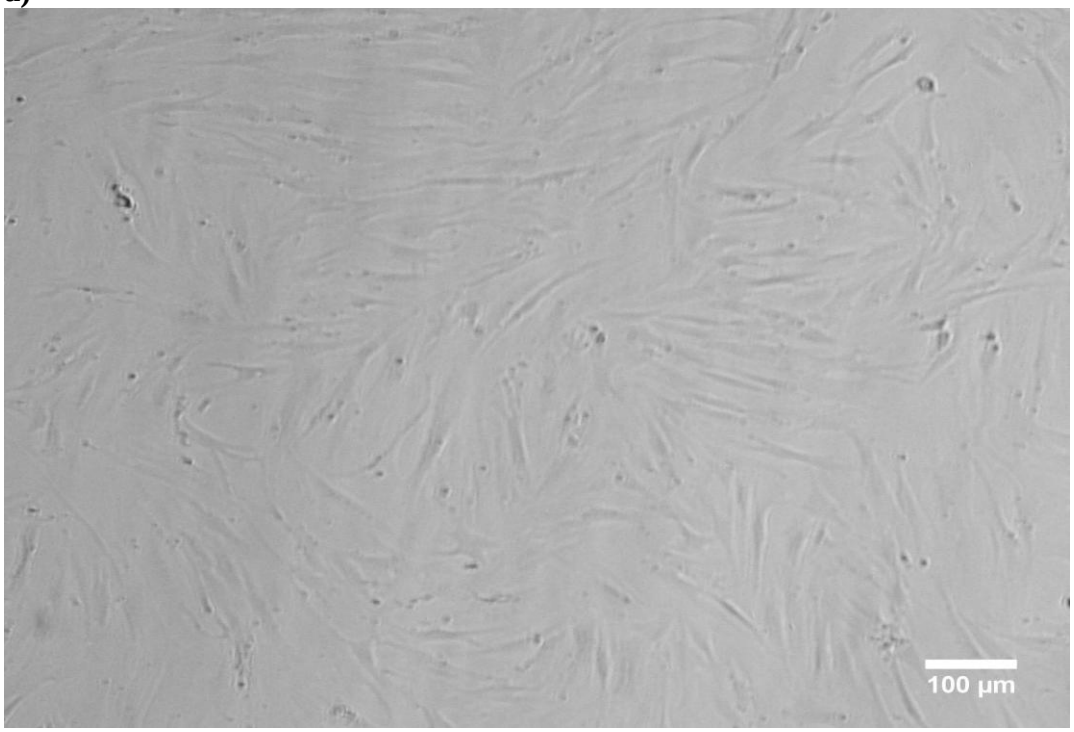

b)

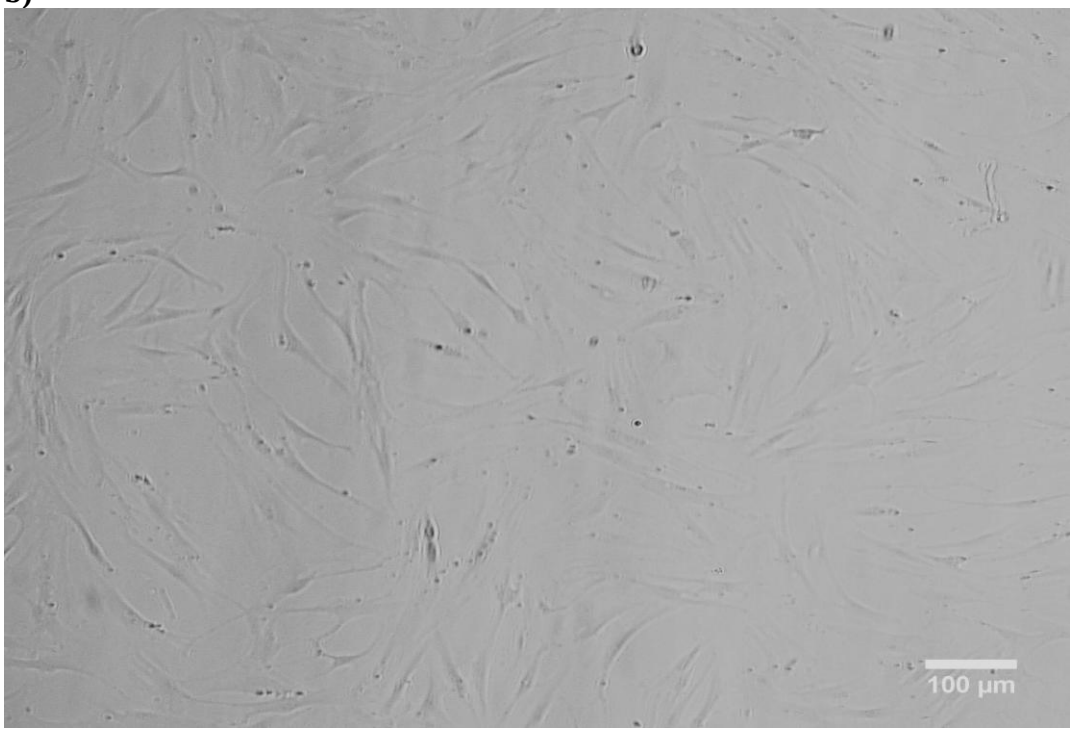

Figure 3.1.8 Photographs of SB203580 treated and untreated telomerase immortalised WS fibroblasts Telomerase immortalised Werner's syndrome fibroblasts (AG03141.hTERT) a) untreated and b) treated with SB203580.

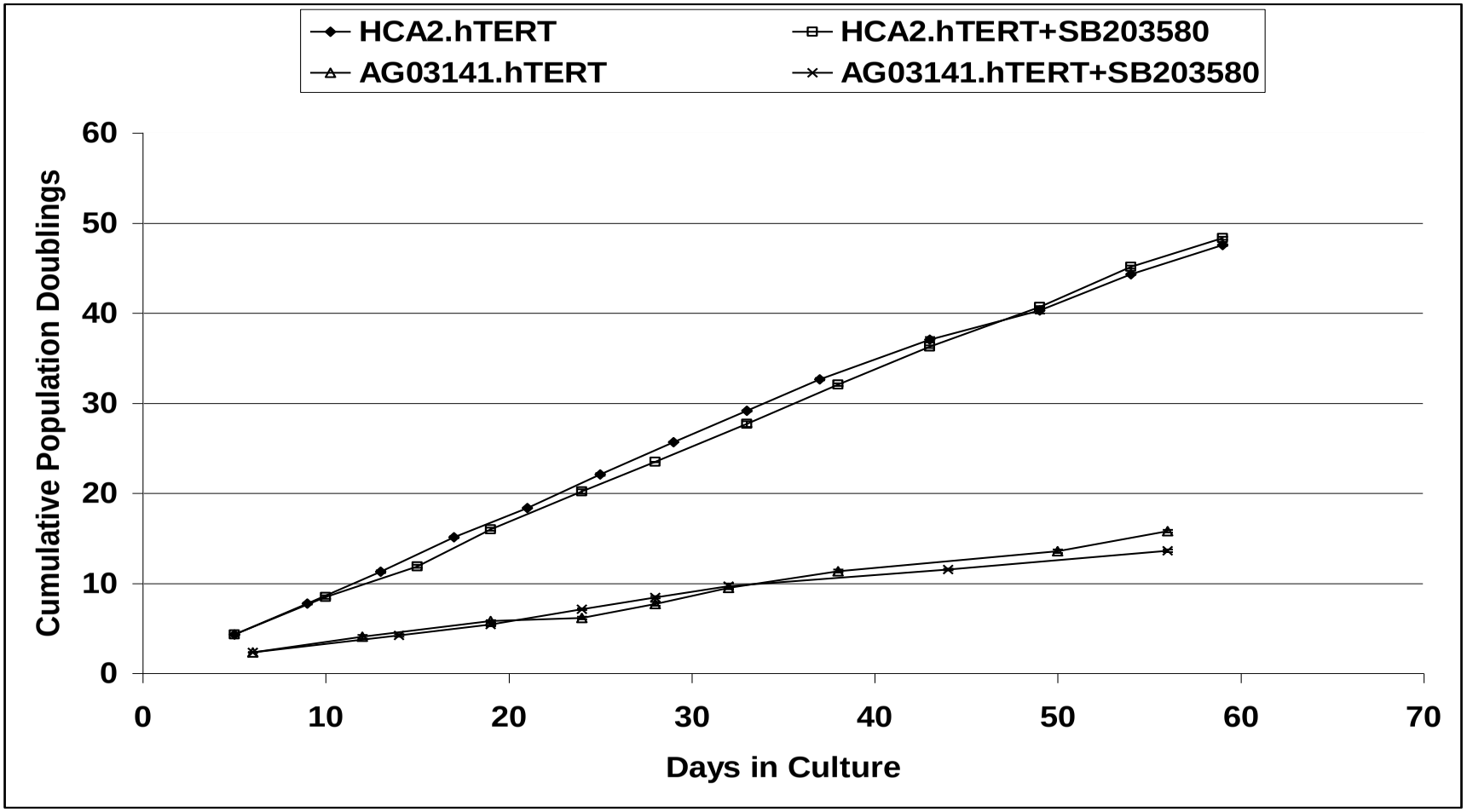

Figure 3.1.9 Growth curve of SB203580 treated and untreated telomerase immortalised normal and WS fibroblasts

The growth curve demonstrates telomerase immortalised normal (HCA2.hTERT) and Werner's syndrome (AG03141.hTERT) fibroblasts treated or untreated with SB203580. N=3; Error bars= ± standard deviation.

3.1.3.4 DNA damage in telomerase immortalised Werner's syndrome fibroblasts treated with SB203580

A Comet assay was carried out to test the DNA damage repair response in hTERT immortalised Werner's syndrome fibroblasts (AG03141.hTERT) treated with SB203580. This is demonstrable by inducing damage to DNA by treatment with agents such as camptothecin. A dose response study carried out by Lowe *et al* (2004) demonstrated that treatment with 10 μM of camptothecin for 1 hour was the optimum dose required for detecting significant differences in DNA damage using Comet assay. Accordingly, acute treatment with 10 μM camptothecin for 1 hour was carried out on SB203580 treated and untreated AG03141.hTERT fibroblasts prior to measuring the tail lengths. The mean, camptothecin generated, Comet tail length was 28.39 μm in WV-1 cells, 11.88 μm in 1Br.3neo, 6.91 μm in AG03141.hTERT and 8.20 μm in SB203580 treated AG03141.hTERT (figure 3.1.10). These results demonstrate, treatment with SB203580 had no significant effect on the camptothecin generated Comet tail lengths in AG03141.hTERT cells (analysed by two tailed t-test, t= -0.645, p =0.58).

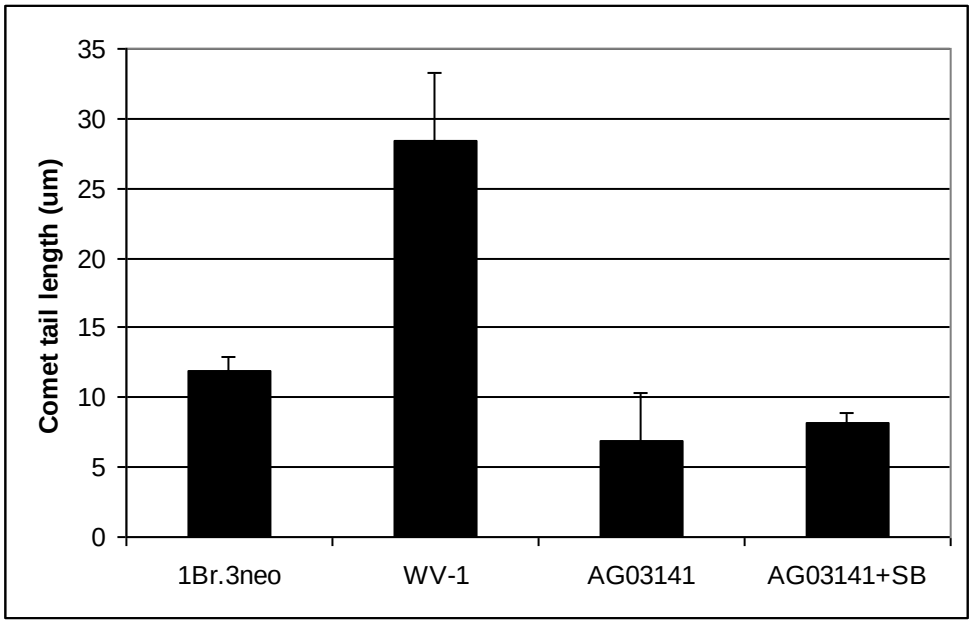

Figure 3.1.10 Comet analysis of telomerase immortalised WS fibroblasts treated, or untreated, with SB203580 Comet tail lengths of telomerase expressing Werner's syndrome fibroblasts (AG03141.hTERT) treated with SB203580 and untreated. SV40 immortalised fibroblasts from normal (1Br.3neo) and Werner's syndrome (WV-1) were tested as control cells. DNA damage was initiated by treatment with 10 μM camptothecin for 1 hour prior to carrying out the Comet assay. N =3; Error bars=standard deviation.

3.1.4 Discussion

An initial dose response (carried out in section 3.1.3.1) assay confirmed that 10 μM SB203580 was the optimum concentration (also used in studies by Davis *et al* (2005). Univariate analysis of variance demonstrated a significant difference between the slopes of untreated and 10 μM SB203580 treated Werner's syndrome fibroblasts. This suggests that treatment with 10 μM SB203580 significantly increases the growth rate of Werner's syndrome fibroblasts. These results are in agreement with previous findings by Davis *et al* (2005).

It has been shown that p38 activation is involved in cellular senescence (Lin *et al.* 1998; Iwasa *et al.* 2003). Treatment of cells with SB203580 has shown to inhibit p38 activity (Lee *et al.* 1994; Cuenda *et al.* 1995). In the study conducted by Davis *et al* (2005), Werner's syndrome fibroblasts treated with 10 μM SB203580 had demonstrated a significant reduction in levels of phosphorylated p38 along with increased growth rates and delayed cellular senescence. However, the reduced levels of phosphorylated p38 were observed in young cells. Phosphorylated p38 in nearly senescent SB203580 treated Werner's syndrome fibroblasts had increased to levels resembling that seen in untreated Werner's syndrome fibroblasts (Davis *et al.* 2005). These findings led to a conclusion that p38 activity is involved in the premature senescence seen in Werner's syndrome fibroblasts. However, the study reproduced in this thesis showed that the reduction in phosphorylated p38 levels following 10 μM SB203580 treatment was not significant. One possibility for this contradictory outcome may be that the Werner's syndrome fibroblast cultures studied were at a 'near senescence' stage when the SB203580 treatment was initiated. In whick case, the culture would contain a large number of cells that have already entered senescence and would lead to the detection of high levels of p38. This coincides with findings by Davis *et al* (2005) with regards to Werner's syndrome fibroblast cultures that are at a 'near senescence' stage. The mechanism by which SB203580 improves growth rates of Werner's syndrome fibroblasts needs further investigation. The effect of SB203580 on p38 in the MAP kinase context needs to be studied in more detail.

Results obtained from the study by Davis *et al* (2005) demonstrated that telomere erosion rates in Werner's syndrome fibroblasts from both SB203580 treated and untreated strains were within normal range. In addition, telomerase immortalised Werner's syndrome fibroblasts demonstrated an increase in growth rate after treatment with SB203580. This suggests that senescence occurred as a result of stress independent of telomere erosion in Werner's syndrome fibroblasts (Davis *et al.* 2005).

In the study carried out in section 3.1.3.3, telomerase immortalised Werner's syndrome fibroblasts (AG03141.hTERT) demonstrated a slow growth rate compared to normal telomerase immortalised fibroblasts (HCA2.hTERT), which complements the findings by Davis *et al* (2005). However, in contrast to the observations by Davis *et al* (2005), SB203580 did not improve growth rates of AG03141.hTERT. Furthermore, Comet analysis demonstrated low levels of DNA damage in SB203580 treated and untreated AG03141.hTERT cells as compared to SV40 immortalised normal (1BR.3neo) and Werner's syndrome (WV-1) fibroblasts. There was also no difference in DNA damage levels between SB203580 treated and untreated cells. These results suggest that DNA damage in AG03141.hTERT was maintained at a low level despite their slow growth rates. The non-responsiveness of the AG03141.hTERT growth rate to SB203580 treatment suggests that these cells may have a different growth repressing signal to p38 MAP kinase.

In conclusion, primary Werner's syndrome (WS) fibroblasts showed improved growth rates when treated with 10 μM SB203580. This data complements the study by Davis *et al* (2005) and provides an optimised method ready for use in other cell types. Implementation of the SB203580 treatment in other cell types and further biochemistry testing would allow better understanding of the mechanisms by which SB203580 improves growth rates and lifespan of Werner's syndrome fibroblasts. A better understanding of these mechanisms could aid in the development of a treatment for Werner's syndrome.

3.2 Attempts to knock down WRN in SV40 immortalised normal human fibroblasts

3.2.1 Introduction

3.2.1.1 Hammerhead ribozymes

Ribozymes are RNA strands capable of catalytic activity that result in the silencing of tRNAs. This occurs by acid / base variation caused by phosphodiester isomerization reactions that break or join the RNA backbone. The hammerhead ribozyme consists of a secondary canonical structure resembling a hammerhead formed by the capping of two of its helices by connecting loops (Scott *et al.* 2009).

3.2.1.2 RNA interference

RNA interference (RNAi) is a process that occurs naturally as a protective mechanism for cell genomes against viruses and transposons. RNAi takes place at the post transcriptional stage targeting specific gene sequences for silencing (Hannon 2002). This process was first discovered in *Caenorhabditis elegans* which demonstrated degradation of mRNA by long double stranded homologous RNA (Fire *et al.* 1998).

The effector RNAi is a short double stranded RNA composed of 21-28 nucleotides called siRNA. A cytoplasmic ribonuclease, Dicer cleaves the siRNA from longer precursor molecules. The cleaved siRNA contains an antisense strand that acts as a template for the RNA-induced silencing complex (RISC). Complementary mRNA is recognised and cleaved by RISC.

Synthetic RNAi molecules are the short interfering RNA (siRNA) composed of 21 to 22 nucleotide long double stranded RNA (dsRNA). The siRNA carries a core 19 bp sequence and two unpaired nucleotides at each 3' end. The synthetic siRNA mimic the product of processed miRNA that naturally take place in the cell. Synthetic siRNA is transiently introduced into cells and needs to be reintroduced at regular bases (Sandy *et al.* 2005).

Short hairpin RNA (shRNA) is the upstream counterpart of siRNA. A shRNA molecule is a 50 to 70 nucleotide single stranded RNA that forms a loop structure *in vivo*. The expression of shRNA in cells is achieved by retroviral introduction of a gene coding for the shRNA. Therefore, the shRNA molecule is stably expressed (Sandy *et al.* 2005).

3.2.1.3 Attempts to knockdown WRN

Previous attempts for the stable knockdown of WRN were carried out by Bird *et al* (2012). The work entailed retroviral introduction of two approaches in separate cell cultures of SV40 immortalised fibroblasts. One approach was a hammerhead ribozyme and the other was shRNA, both directed against different regions of WRN. The hammerhead ribozyme, Rib3 carries a hammerhead core of 24 base pairs between 14 bases at the 5' and 15 bases at the 3' that are complementary sequences to the WRN gene at bases 3297-3327 (constructed by Dr. Katrin Jennert-Burston, School of Pharmaceutical and Biomedical Sciences, University of Brighton, Brighton, UK). The ribozyme was constructed in the pCR2.1-TOPO vector (Invitrogen) and was subcloned into a pU1 snRNA vector (Bird *et al.* 2012). The U1 expression cassette acts as a stabilising stem loop structure for the ribozyme. The U1 was originally excised using *BamHI* digestion and inserted into *BamHI* sites of a modified pZeoSV that lacked the SV40 promoter, polyadenylation site and polylinker (Montgomery *et al.* 1997).

Anti WRN shRNA (WRN4) targeting bases 3724-3742 containing 19 bp inverted repeats separated by a 9 bp spacer was created (constructed by Dr. Seok-Jin Heo, Lawrence Livermore Laboratories, Berkeley, California, USA).

Bird and colleagues (2012) subcloned the U1/ ribozyme hybrid Rib3 and the shRNA WRN4 into pMSCV.puro vectors (plasmid vector containing a puromycin resistance cassette). The pMSCV.puro.Rib3 and the pMSCV.puro.WRN4 constructs were then packaged in the Ψ CRIP amphotropic packaging cell line. The Rib3 and WRN4 constructs were separately introduced into SV40 immortalised normal human fibroblast cell lines (1BR.3neo) by retroviral infection. Neither, shRNA or ribozyme, resulted in WRN silencing as demonstrated by immunocytochemistry and Western blot analysis. However, DNA damage was elevated in Rib3 and WRN4 expressing 1BR.3neo as detected by Comet assay (figure 3.2.1) (Bird *et al.* 2012). This suggests that there might have been a silencing effect of the WRN gene caused by either Rib3 or WRN4.

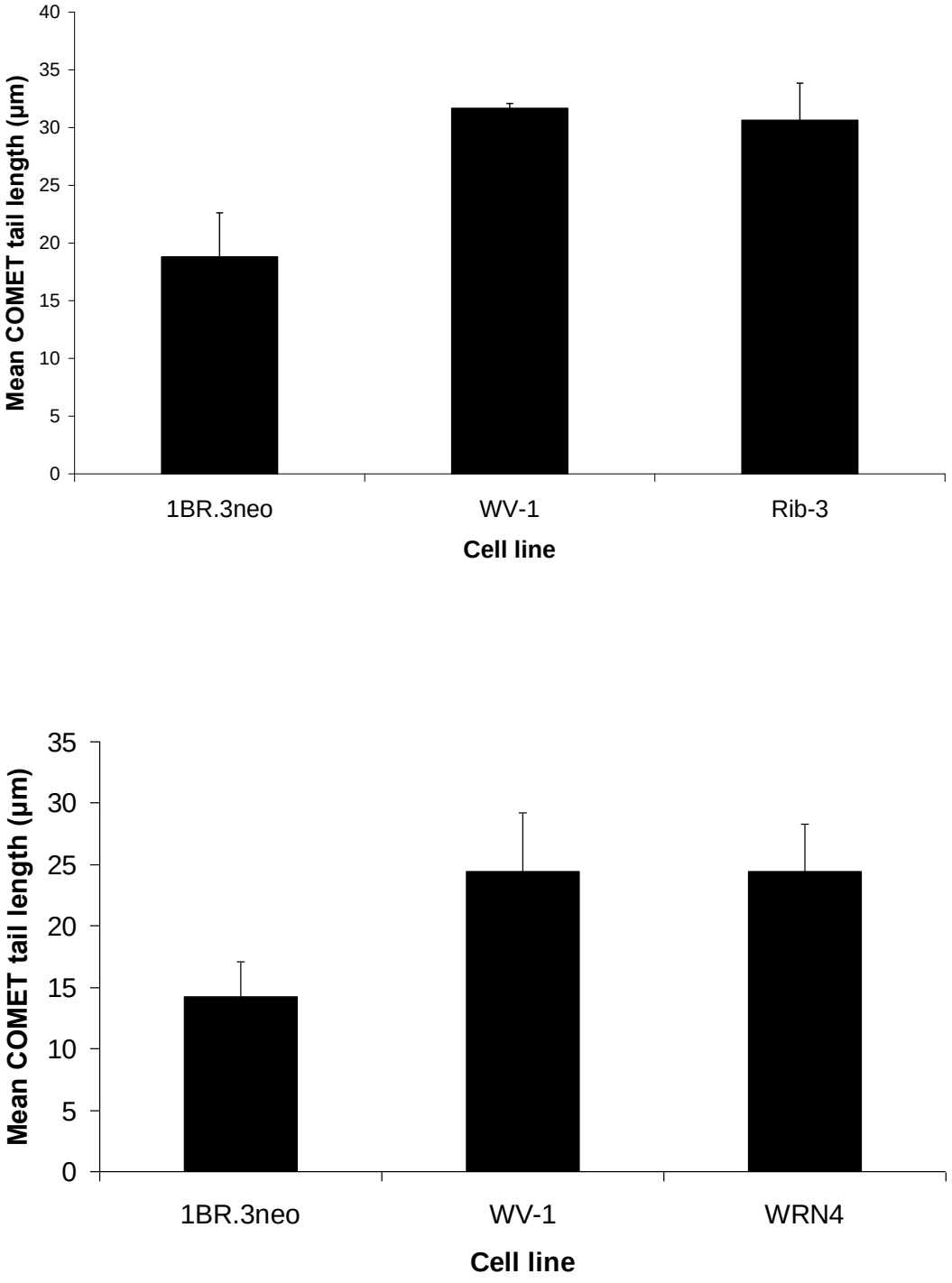

Figure 3.2.1 Comet assay of cells expressing WRN silencing RNA Comet tail lengths of damaged DNA after 1 hour 10 µM camptothecin treatment. N=3, Error bars= standard deviation (Bird *et al.* 2012).

3.2.2 Aims

The aim of the experiment was to knockdown WRN in SV40 immortalised cell lines for the purpose of optimising a workable method for use in primary cells and to generate wild type and $WRN^{-/-}$ cells of isogenic background. Growth dynamics and assessment of WRN expression was carried out to confirm results obtained in the study by Bird *et al* (2012) . Ribozyme (Rib3) was subcloned into a pMSCV.hyg vector and retrovirally introduced into the shRNA expressing cell line (1BR.3neo.WRN4) to produce a combined ribozyme and shRNA expressing cell line (termed 1BR.3neo.WRN4.Rib3). WRN expression in 1BR.3neo.WRN4.Rib3 was assessed by immunocytochemistry and western blot analysis.

3.2.3 Results

3.2.3.1 Generation of pMSCV.hyg.Rib3 recombinants

pMSCV.hyg.Rib3 recombinants were generated as outlined in section 2.2. Recombinant clones were identified by PCR (figure 3.2.2). One recombinant was selected and its plasmid DNA sequenced.

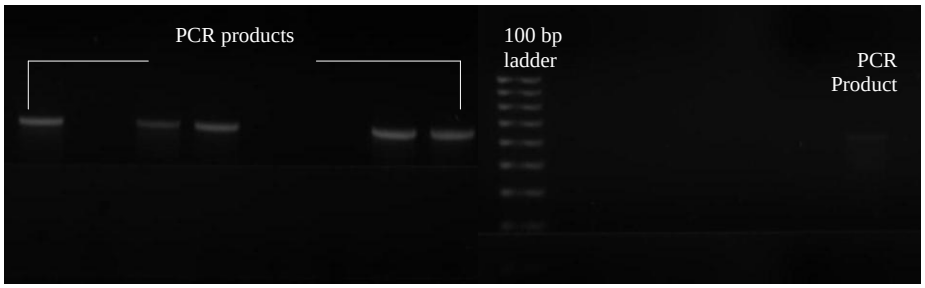

Figure 3.2.2 PCR products of pMSCV.hyg.Rib3 The figure shows the PCR products of pMSCV.hyg-Rib3 recombinants separated on a 1.5% agarose gel. The DNA marker used is a 100 bp ladder. Forward primer: pMSCV 3': 5'-GAGACGTGCTACTTCCATTTGTC-3' and reverse primer: U1 5': 5' ATACTTACCTGGCAGGGGAGAT 3'.

The sequence obtained was compared and matched to sequences of the pMSCV primer and the Rib3 insert using the MACAW software or GENtle V 1.9.4. This was carried out to confirm their origin and that Rib3 had been successfully subcloned into its new vector, pMSCV.hyg. Figure 3.2.3 displays the sequence obtained from the recombinant plasmid pMSCV.hyg.Rib3 and is highlighted in blue.

GCTTTCACTGCGAGCGACTGCGGGGCGGGGGGGACTTCCTGACTAGGGGAGGAGTAGAAGGTGGCGCGA
AGGGGCCACCAAAGAACGGAGCCGGTTGGCGCCTACCGGTGGATGTGGAATGTGTGCGAGGCCAGAGGC
CACTTGTGTAGCGCCAAGTGCCCAGCGGGGCTGCTAAAGCGCATGCTCCAGACTGCCTTGGGAAAAGCGC
CTCCCCTACCCGGTAGAATTCGTTAACCTCGAGAGATCCGCCTCCACTGTAGGATTAACAACTAAGACACAA
ACCAATACGAAAAAAGACATGACCCTTGGCGTACGGTCTGTTTTTGAAACTCCAGAAAGTCAGGGGAAAGC
GCGAACGCAGTCCCCCACTAGTACGAATTCGCCCTTTACAGAGAAGAAGTGTTTCGTCCTCACGGACTCAT
CAGTAACTTGGAGAAGTTAAGGGCGAATTCTGCAGTCGAGTTTCCCACATTTGGGGAAATCGCAGGGGTCA
GCACATCCGGAGTGCAATGGATAAGCCTCGCCCTGGGAAAACCACCTTCGTGATCATGGTATCTCCCCTGC
CAGGTAAGTATGAGATCTTCGGGCTCTGCCCCGACACAGCCTCATACGCCTCACTCTTTACACACACGGTC
ACTTGCCCCGCGCACTCCCGAGCCCTTTCCAGCCCTGACACACAGCTGGGATTCTCACTTCCGATCCGCGG
TCCTGAACCCGCTCCCAGGGCACGGGAACTCCTTCGTGGCGAAGCAGCAAGTGGCGAAGCAGCAGCCTCT
GCGCTGCCTCATCTACATAGAAGTCGCCCTGTCCGTGATGTCACCGACAGTGCCTTGCCCAGTCCCCGTCT
GCCTTTCTGCCACTCAACCGACCAATCTGCTGCCAGAGCCGCCAAGGGGAAGTGACGTCTGCCTCTCCCTT
TTTCCCTCCCGCCCCTGCGTCTGTTCTCTCCCAAAGAAGCTGGTCCTTAGCCTGTGTTAAGGAGCAACCTTT
CGGTGGCGGATCTATTTCCGGCGCCTAGAGAAGGGTGAGGCTGATAAAAAGGAGGATGATC

Ribozyme: 3’ **A**atgtctcttctt**CA**CAAAGCAGGAGTGCCTGAGTAGTCattgaacctcttcaa5’

Antisense: 5’ tacagagaagaa**GT**GTTTCGTCCTCACGGACTCATCAGtaacttggagaagtt**A** 3’

Senserev: 5’ aacttctccaagtta**CTGATGAGTCCGTGAGGACGAAAC**ACttcttctctgta**A** 3’

Motif: 5’ **TACAG**AGAAGAA**GTC**TAACTTGGAGAAGTT 3’

Figure 3.2.3 Sequence of the ribozyme gene containing region of the vector The sequence of the pMSCV.hyg vector region that contains the Rib3 insert. Sequence of the Rib3 ribozyme, its antisense, its reverse sense and the motif are also illustrated in this figure. The sequence highlighted in blue in the vector corresponds to the antisense Rib3.

3.2.3.2 Expression of anti-WRN ribozyme in the newly established 1BR.3neo.WRN4.Rib3 cell strain

After successful transduction of pMSCV.hyg.Rib3 into 1BR.3neo.WRN4 using retroviral infection (see section 2.2), expression of Rib3 was confirmed by RT-PCR. Gel electrophoresis of the PCR products from parent 1BR.3neo and 1BR.3neo.WRN4 expressed the endogenous U1 RNA whereas products from 1BR.3neo.Rib3 and 1BR.3neo.WRN4.Rib3 expressed larger size bands which represent the U1 RNA containing the Rib3 insert (figure 3.2.4).

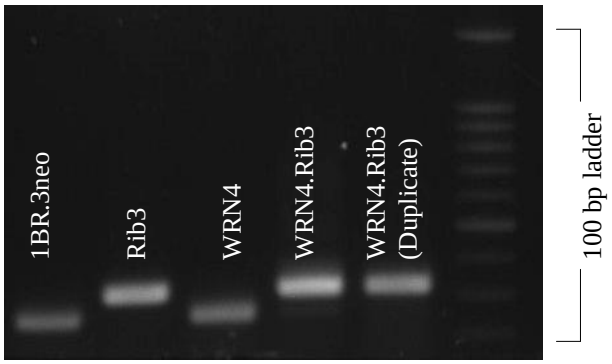

Figure 3.2.4 Agarose gel electrophoresis of reverse transcriptase PCR products containing ribozyme in the U1 cassette Products of reverse transcriptase PCR of Total RNA extracted from 1BR.3neo, Rib3, WRN4 and WRN4.Rib3 cells demonstrating U1 RNA with or without the Rib3 insert. The DNA marker used is a 100bp ladder. Forward primer U1 5': 5'-TCCACTGTAGGATTAACAACTAAG-3' and reverse primer U1 3': 5'-ATACTTACCCTGGCAGGGGAGAT-3'.

3.2.3.3 Immunofluorescence and Western blot detection of WRN in cells expressing ribozyme and shRNA

Immunofluorescence detection of WRN was carried out on SV40 immortalised fibroblasts. Normal (1BR.3neo), ribozyme expressing (1BR.3neo.Rib3), shRNA expressing (1BR.3neo.WRN4) and the dual ribozyme and shRNA expressing (1BR.3neo.WRN4.Rib3) cells demonstrated positive immunofluorescence labelling of WRN. Immunofluorescence was mainly expressed in the nucleoli of these cells (figure 3.2.5: a, b, c, d). The nucleoli of WV-1 cells were not positive but very weak nuclear background fluorescence was observed (figure 3.2.5: e). These results suggest combining the Rib3 ribozyme and WRN4 shRNA is not sufficient to silence WRN.

Western blot analysis further confirmed these results (figure 3.2.6). Total protein was extracted from each cell line (in triplicate) and analysed by western blot for WRN. Bands were present in normal, ribozyme and shRNA expressing SV40 immortalised cell lines but were absent in SV40 immortalised Werner's syndrome cells (WV-1). The intensities of the WRN bands in 1BR.3neo, 1BR.3neo.WRN4, 1BR.3neo.Rib3 and 1BR.3neo.WRN4.Rib3 samples were measured and normalised against bands of GAPDH (figure 3.2.7). Shapiro-Wilk analysis demonstrated that the data acquired by Western blot analysis were normally distributed ($p>0.05$) in each cell line and the homogeneity of variance had not been declined as demonstrated using the Levene test ($p>0.05$). ANOVA analysis demonstrated that there was no significant difference in WRN expression between any of the cell lines ($F(3, 8) = 0.474$, $p = 0.709$).

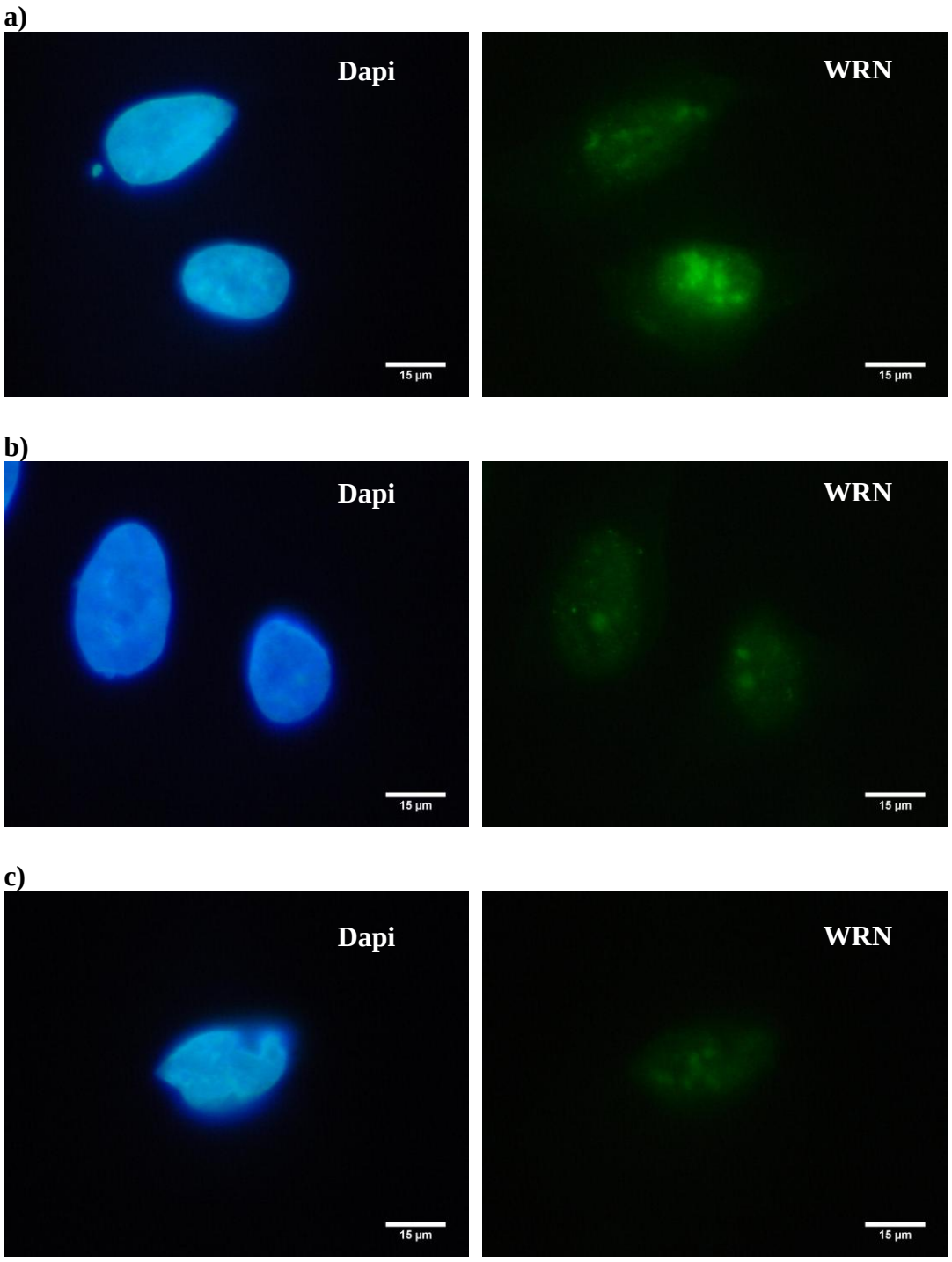

Figure 3.2.5 Immunocytochemical detection of WRN in SV40 immortalised normal, ribozyme expressing, shRNA expressing and WS fibroblasts Dapi (blue) staining and FITC (green) immunofluorescence labelling of WRN (rabbit polyclonal anti human WRN (AbCam)) in a) 1BR.3neo, b) 1Br.3neo.Rib3, c) 1Br.3neo.WRN4 and d) 1BR.3neo.WRN4.Rib3, e) WV-1 fibroblasts, f) primary antibody only (control), g) Secondary antibody only (control). (Size bars = 15 µm).

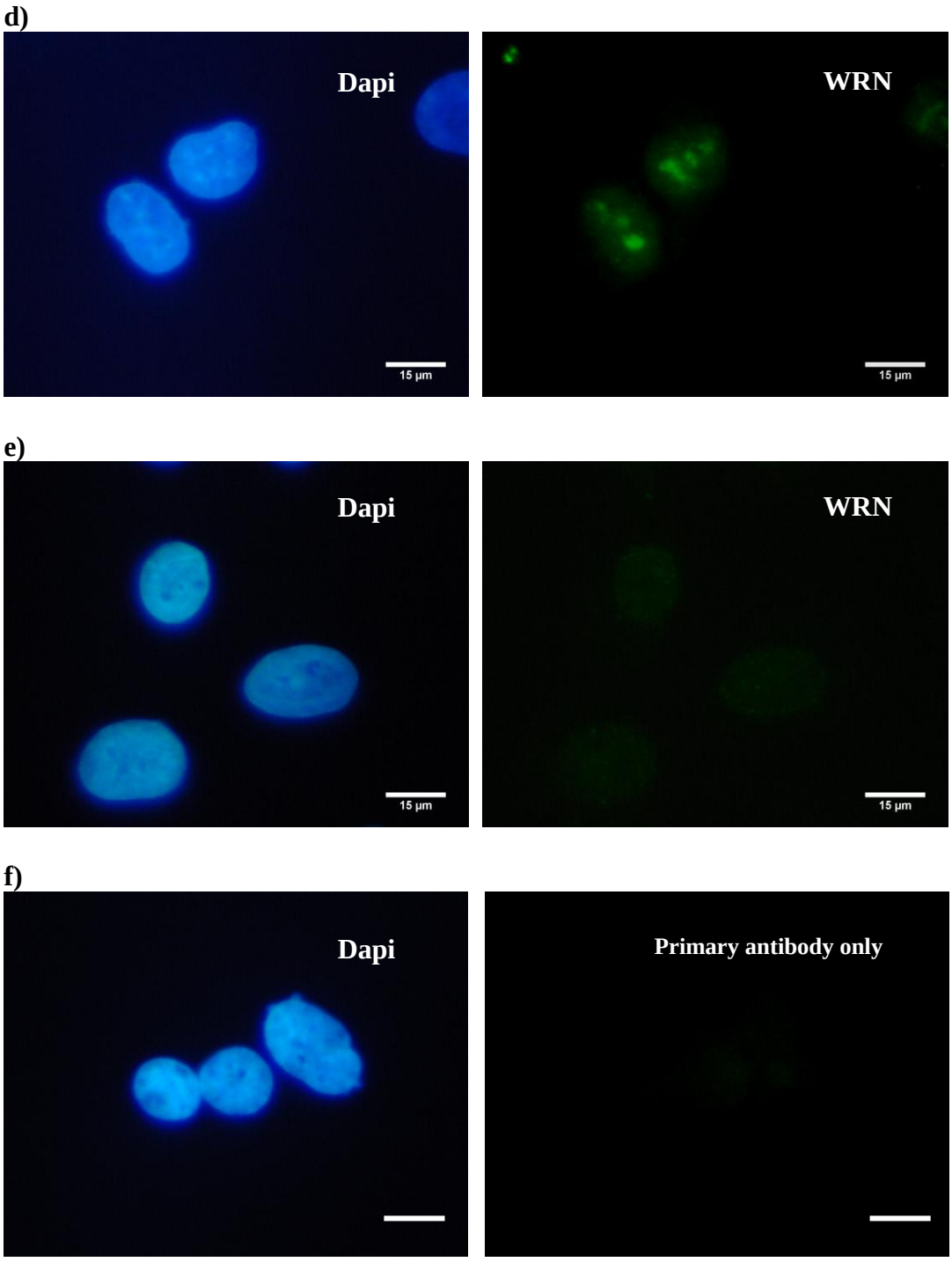

Figure 3.2.5 Immunocytochemical detection of WRN in SV40 immortalised normal, ribozyme expressing, shRNA expressing and WS fibroblasts Dapi (blue) staining and FITC (green) immunofluorescence labelling of WRN (rabbit polyclonal anti human WRN (AbCam)) in a) 1BR.3neo, b) 1Br.3neo.Rib3, c) 1Br.3neo.WRN4 and d) 1BR.3neo.WRN4.Rib3, e) WV-1 fibroblasts, f) primary antibody only (control), g) Secondary antibody only (control). (Size bars = 15 µm).

g)

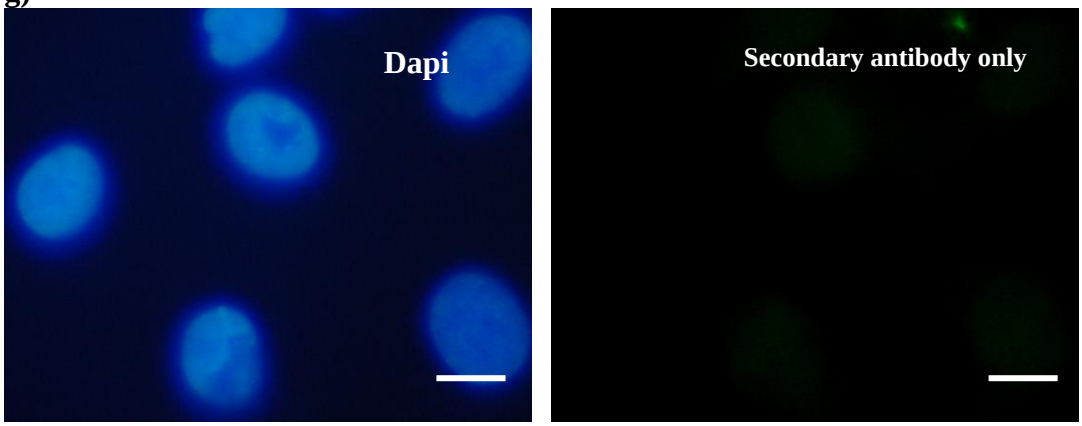

Figure 3.2.5 Immunocytochemical detection of WRN in SV40 immortalised normal, ribozyme expressing, shRNA expressing and WS fibroblasts Dapi (blue) staining and FITC (green) immunofluorescence labelling of WRN (rabbit polyclonal anti human WRN (AbCam)) in a) 1BR.3neo, b) 1Br.3neo.Rib3, c) 1Br.3neo.WRN4 and d) 1BR.3neo.WRN4.Rib3, e) WV-1 fibroblasts, f) primary antibody only (control), g) Secondary antibody only (control). (Size bars = 15 μm).

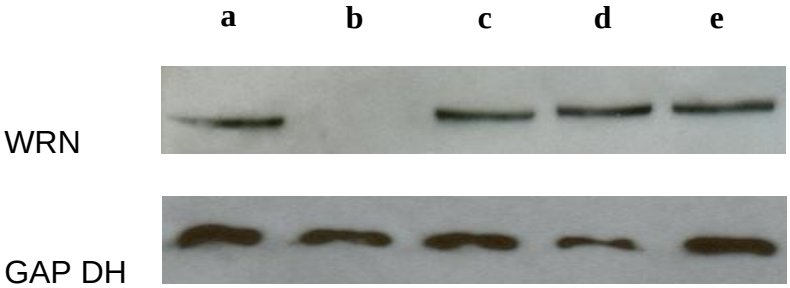

Figure 3.2.6 Western blot detection of WRN in SV40 immortalised normal, ribozyme expressing, shRNA expressing and WS fibroblasts Western blot detection of WRN (mouse monoclonal anti human WRN (AbCam)) of a) 1BR.3neo, b) WV-1 c) 1Br.3neo.Rib3, d) 1Br.3neo.WRN4 and e) 1BR.3neo.WRN4.Rib3.

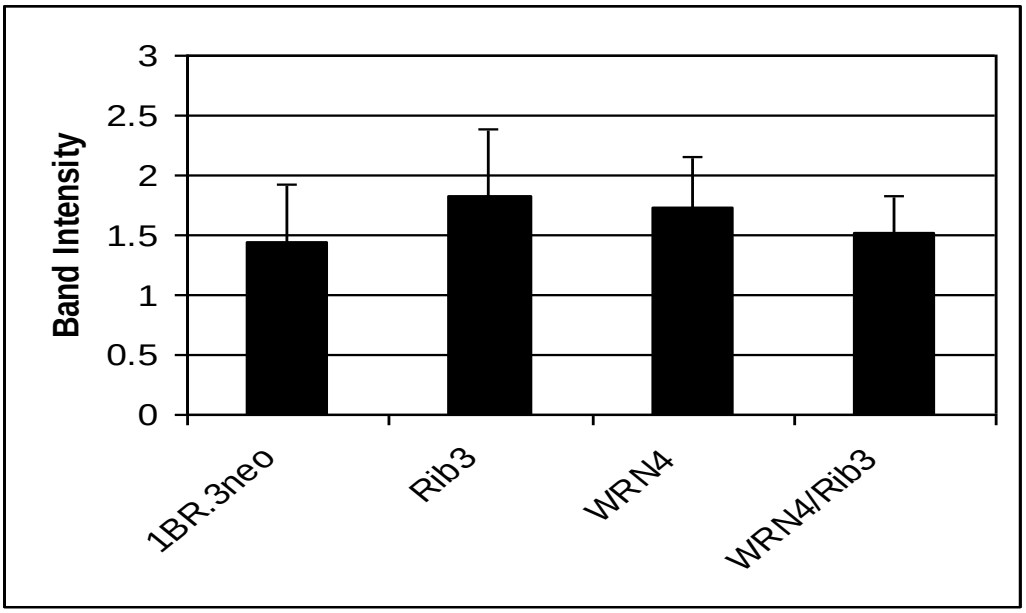

Figure 3.2.7 Densitometry analysis of bands of WRN from western blots Average band intensity of WRN from western blots after normalising against GAP DH. Total protein samples analysed were from 1BR.3neo, 1BR.3neo.Rib3, 1BR.3neo.WRN4 and 1BR.3neo.WRN4.Rib3 cell lines. N=3, error bars=±standard deviation.

3.2.3.4 Growth characteristics

Cultures of 1BR3.neo, WV-1, 1BR3.neo.Rib3, 1BR3.neo.WRN4 and 1BR3.neo.WRN4.Rib3 were monitored for 30 days achieving 5 to 6 passages. Growth curves of 1BR.3neo.Rib3, 1BR.3neo.WRN4 and 1BR.3neo.WRN4.Rib3 were plotted against wild type 1BR.3neo and Werner's syndrome WV-1 cells (figure 3.2.8) (see also table 5.4 in appendix II). The population doublings achieved by the cells after 30 days of culture were compared (figure 3.2.9). Homogeneity of variance using the Levene test indicates there is no difference between the variances in the population ($p=0.29$). The Shapiro-Wilk test demonstrated normality of the data ($p>0.05$) and the ANOVA test demonstrated that there was a significant growth rate differences between the groups ($p=0$). The Tukey Post Hoc analysis demonstrated that there were similar growth rates between 1BR.3neo.WRN4 compared to 1BR.3neo ($p=0.679$). Furthermore, the growth rates of 1BR.3neo.Rib3 and 1BR.3neo.WRN4.Rib3 cultures were not significantly different from each other ($p=0.09$) but were significantly reduced when compared to 1BR3.neo and 1BR.3neo.WRN4 ($p<0.05$). It was seen that WV-1 cells had the highest growth rate and were significantly higher than 1BR.3neo ($p=0$) and all the other cell lines analysed.

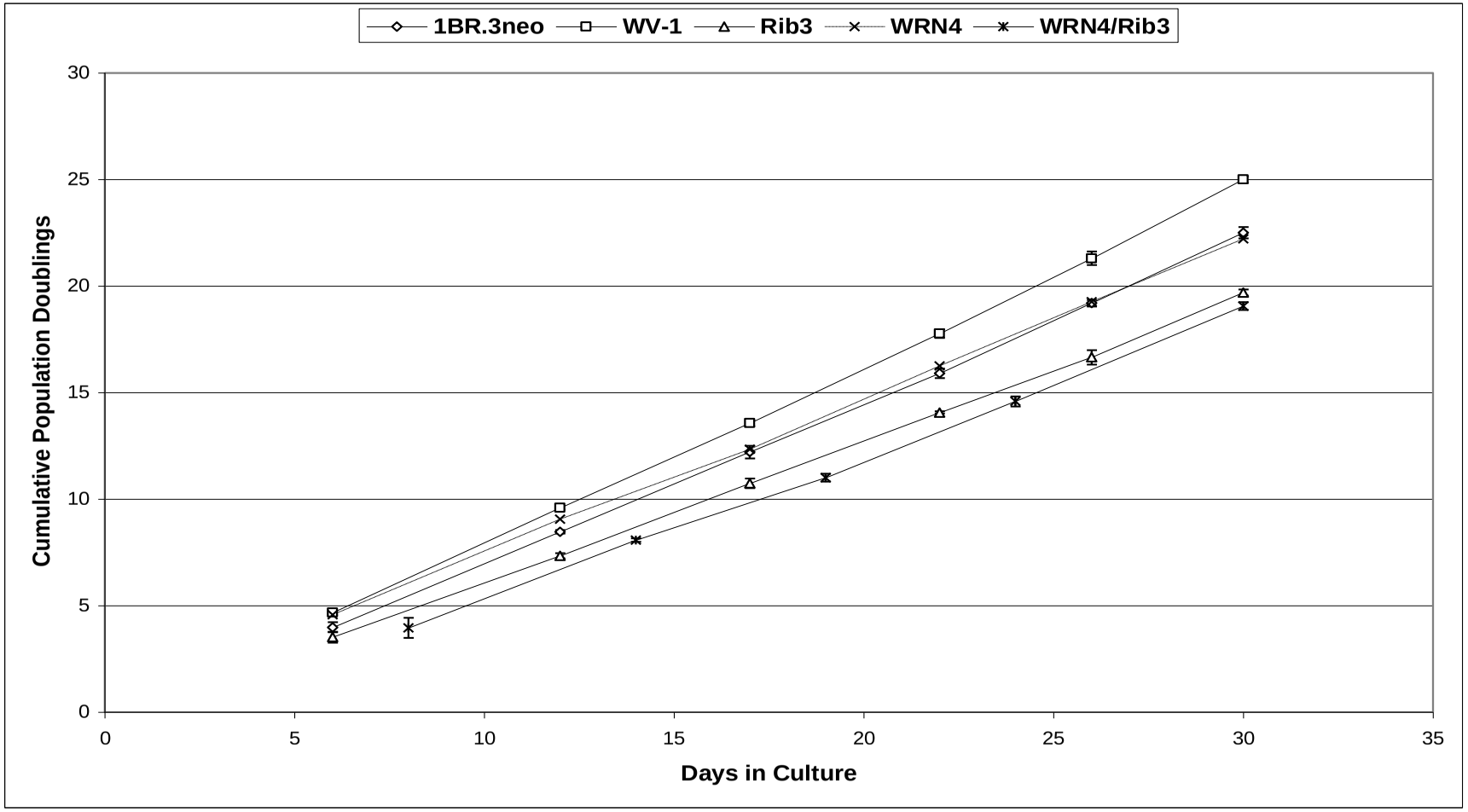

Figure 3.2.8 Growth curves of SV40 immortalised normal, WS, shRNA expressing, ribozyme and both shRNA and ribozyme expressing fibroblasts
Growth curve of the SV40 immortalised fibroblasts from 1Br.3neo (normal), WV-1 (Werner's syndrome), 1BR.3neo.Rib3 (Ribozyme expressing), 1BR.3neo.WRN4 (shRNA), and 1BR.3neo.WRN4.Rib3 (shRNA and Ribozyme expressing) cells. N=3, error bars = ± standard deviation.

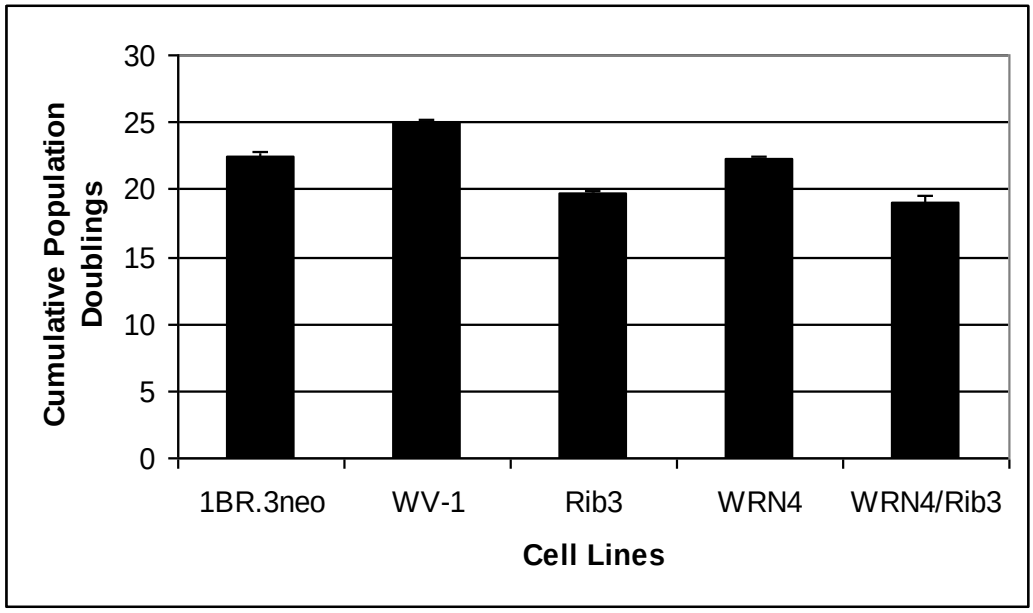

Figure 3.2.9 Population doublings reached over 30 days in SV40 immortalised normal, WS, shRNA expressing, ribozyme and both shRNA and ribozyme expressing fibroblasts SV40 immortalised cell lines 1BR.3neo (wild type), WV-1 (SV40 immortalised Werner's syndrome cell line) 1BR.3neo.Rib3 (ribozyme expressing), 1BR.3neo.WRN4 (shRNA expressing) and 1BR.3neo.WRN4.Rib3 (both ribozyme and shRNA expressing) were grown for 30 days (5 to 6 consecutive passages).
N=3, Error bars= standard deviation.

3.2.4 Discussion

Obtaining samples of tissue from Werner's syndrome patients has proven to be difficult due to the rarity of the disease. Another challenge is that Werner's syndrome cells are currently studied in parallel to non-isogenic wild type control samples. Establishing a WRN knockdown in normal cells would provide valuable research material for the study of Werner's syndrome and ageing. This would generate ample material for research as well as providing isogenic samples for the study of the biochemistry of WRN.

Long term experiments such as growth dynamic studies would require stable regulation of WRN expression. The most recent study involving shRNA for stable knockdown of WRN has been carried out in Chinese hamster ovary cell lines for the study of WRN function in recombination (Rahn *et al.* 2010).

To date there have not been any studies carried out on human cell lines with stable WRN knockdown. Therefore the attempts for WRN knockdown were carried out in this study. The WRN knockdown in Chinese hamster ovary cell lines has been conducted very recently after our attempts were carried out. Therefore, the approach used by Rahn *et al* (2010) was not taken into account.

Attempts for the stable knockdown were initially carried out in SV40 cell lines to optimise the knockdown technique prior to applying it to irreplaceable primary cells that have limited replicative potential. Attempts to knockdown WRN in 1BR.3neo using individual expression of either shRNA or ribozyme was not successful (Bird *et al.* 2012) (figure 3.2.5 and 3.2.7). This was demonstrated by the detection of WRN protein in the nucleoli of 1BR.3neo.Rib3 and 1BR.3neo.WRN4 by immunofluorescence labelling. Moderate reduction in the growth rate of 1BR.3neo.Rib3 was observed, whereas growth rate of 1BR.3neo.WRN4 was not affected. This suggests a possible reduction in WRN expression by the introduction of Rib3. Furthermore, Western blot results detected lower levels of WRN expression in both 1BR.3neo.WRN4 and 1BR.3neo.Rib3. This was followed by Comet analysis which detected high camptothecin generated tail lengths in 1BR.3neo.WRN4 and 1BR.3neo.Rib3 when compared to normal cells (Bird *et al.* 2012).

WRN knockdown in 1BR.3neo was attempted again, in this study, by using a combined approach composed of Rib3 ribozyme and WRN4 shRNA. Rib3 was stably introduced into 1BR.3neoWRN4 by retroviral infection with a hygromycin resistance cassette to yield the dual knock down cell line, 1BR.3neo.WRN4.Rib3. Examination of 1BR.3neo.WRN4.Rib3 cells by indirect immunofluorescence staining demonstrated that WRN protein is being expressed. Western blot analysis further confirmed the expression of WRN in 1BR.3neo.WRN4.Rib3 cells and did not detect any significant reduction in the levels of WRN expression. The 1BR.3neo.WRN4.Rib3 cells however, demonstrated a reduced growth rate compared to the parent 1BR.3neo cell line. These results conclude that introduction of a hammerhead ribozyme (Rib3), shRNA (siWRN4) or both into the SV40 immortalised fibroblasts (1BR.3neo) did not silence the transcription of WRN.

3.3 Replicative senescence in Werner's syndrome keratinocytes

3.3.1 Introduction

3.3.1.1 Brief introduction to skin tissue

The skin is one of the largest organs of the human body and makes up 15-16 % of the total adult body weight (Edward *et al.* 1985; Fossel 2004). The skin is formed of three different layers; the epidermis, dermis and the subcutaneous layer. The epidermis is the outermost layer that is 90-95 % formed of stratified squamous epithelial cells, keratinocytes. Melanocytes (responsible for skin pigmentation), Langerhans cells (immune cells of the skin) and Merkel's cells (sensory receptors) form 5-10 % of the epidermis (Edward *et al.* 1985). The dermis is mainly formed of extracellular matrix proteins, produced by fibroblasts. The dermis provides the skin with its elasticity and holds blood vessels, sensory organs and immune system. The subcutaneous layer is formed of adipose cells and loose collagen that gives the skin its structure (Fossel 2004).

Skin ages by different mechanisms involving intrinsic factors (genetic, metabolic) and extrinsic factors (environmental). Extrinsic factors accelerate skin ageing that has already been affected by endogenous factors and is mainly seen in sun exposed areas. The sun exposed parts can be noticeably different to the sun protected parts of the skin when it comes to the ageing process (i.e. wrinkles) (McCullough *et al.* 2006). In order to learn about the intrinsic causes of ageing, notably pathways that lead to replicative senescence, it is important to distinguish between senescence pathways that are resultant of extrinsic triggers and senescence pathways triggered by intrinsic factors. Therefore, skin samples need to be collected from areas, such as the abdomen, that are protected from long term exposure to the sun.

The different skin layers undergo different functional and structural deteriorations that lead to the aged phenotype of the skin. In the epidermis, the normal turnover time of keratinocytes is two to three weeks or approximately 28 days (Edward *et al.* 1985; Fossel 2004). Furthermore, it has been postulated that epidermal turnover time is longer in older individuals. This was demonstrated by labelling skin surfaces of young and old individuals with a dansyl chloride fluorescence marker. The time required for the fluorescence marker to subside was used as the indicator for skin turnover. The fluorescence marker lasted about 20 days in young individuals whereas in older individuals it took more than 30 days to disappear (Grove *et al.* 1983).

Weinstein *et al* (1984) intradermally incorporated [^{3}H] thymidine into normal skin and collected punch biopsies for examination. Autoradiography was used to measure cell cycle time in proliferative and differentiated states of the cells. The proliferative state had

a cycle time of 13 days, the differentiated cells had 12 days, and the cornified cells lasted 14 days. The mean value for the total turnover time for the epidermis calculated was 39 days (Weinstein *et al.* 1984).

Another observation is the presence of senescent keratinocytes was higher in tissue samples from older individuals than in younger when measured by SA-β-galactosidase (Dimri *et al.* 1995).

3.3.1.2 Keratinocyte culture

Keratinocytes grown *in vitro* for the purpose of studying cellular senescence is mainly carried out using one of two culture methods, the feeder cell system or using serum free media.

The feeder cell system was developed by Rheinwald and Green in 1975 (Rheinwald *et al.* 1975). Keratinocytes in culture require the presence of feeder cells to provide them with the same nourishment that is provided to them *in vivo* by the dermal fibroblasts. The feeder cells, along with other supplements, maintain the keratinocytes in their proliferative state and prevent them from differentiation. These supplements include; hydrocortisone which helps maintain growth rate, colony morphology and differentiation (Parkinson *et al.* 1992); cholera toxin maintains cell size and prevents terminal differentiation by increasing levels of cAMP (Parkinson *et al.* 1992); and epidermal growth factor (EGF) which prevents crowding of cells in the centre of the colony and encourages migration of the cells to the periphery. EGF also reduces terminal differentiation and promotes the expansion of a keratinocyte culture. Addition of EGF to a culture results in an increase in neonatal keratinocyte lifespan from 50 CPD to 150 CPD (Rheinwald *et al.* 1977; Parkinson *et al.* 1992).

Defined media to replace the requirements of feeder cells and serum have been developed and are presently still undergoing modifications. Early attempts by Eisinger *et al* (1979) involved growing keratinocytes without additional supplements, promoted sufficient proliferation to form a confluent flask. Improvements came into place with formulations of the MCDB151 followed by MCDB152 and MCDB153 mediums respectively (Peehl *et al.* 1980; Tenchini *et al.* 1992). The addition of epidermal growth factor, hydrocortisone, insulin, transferrin, monoethanolamine, phosphoethanolamine and bovine pituitary extract composed the final defined culture medium and allowed keratinocyte growth in the absence of serum and feeder cells. Keratinocytes grown in the serum free medium with these supplements can achieve a maximum of 40 CPD (Tenchini *et al.* 1992).

3.3.1.3 Stratification of epidermal keratinocytes

Keratinocytes generate from the dermal-epidermal basement junction, forming four layers. The bottom layer is the first layer, the basal layer (stratum basale), which migrates upwards and differentiates into stratum spinosum, stratum granulosum and stratum corneum respectively (Fuchs 1990). The basal layer is the proliferative layer and consists of epidermal stem cells and transient amplifying cells. The basal keratinocytes have also been classified according to their clonogenicity in culture as holoclones, meroclones and paraclones. The classification was carried out by scoring for the percent of terminal non proliferating colonies. Holoclones consist of 0-5% terminal colonies, paraclones consist of almost 100% terminal colonies, whereas meroclones are intermediate and consist of more than 5% and less than 100% terminal colonies. Holoclones are in fact the epidermal stem cells, meroclones and paraclones are the two stages of transient amplifying cells. Transition of holoclones into meroclones then paraclones occurs in a unidirectional order (Barrandon *et al.* 1987).

The end stage for transient amplifying keratinocytes, that have committed to differentiate, is terminal differentiation. Several changes occur in keratinocytes as they enter their stages of differentiation including changes in expression of keratins and degradation of organelles. The basal keratinocytes, whether or not they have committed to differentiation, mainly express keratin k14, k5 and to a lesser degree k15 (Fuchs 1990). Keratinocytes that have committed to terminally differentiate, move towards the surface of the skin, increase in size and start to express involucrin (Watt *et al.* 1981; Watt 1983). Differentiation into stratum spinosum which starts to express keratins k1 and k10 takes place. The cells then differentiate into stratum granulosum, reduce protein production to a minimum but maintain involucrin expression and low levels of k1 and k10. Filaggrin is amongst the few proteins that are expressed at the granular stage before the cells completely cease production and most organelles degrade. Involucrin becomes incorporated into the cornified envelope formation in the transition stage (Watt 1983; Robinson *et al.* 1996) between spinosum granulosum and the final stage, stratum corneum which has no organelles and the cellular metabolic activity stops. Stratum corneum cells tightly adhere to each other by lipids and assemble a tight barrier that forms the skin surface (Fuchs 1990). Figure 3.3.1 illustrates a schematic diagram of the keratinocyte differentiation process from keratinocyte stem cell to stratum corneum and lists the keratins associated with each stage.

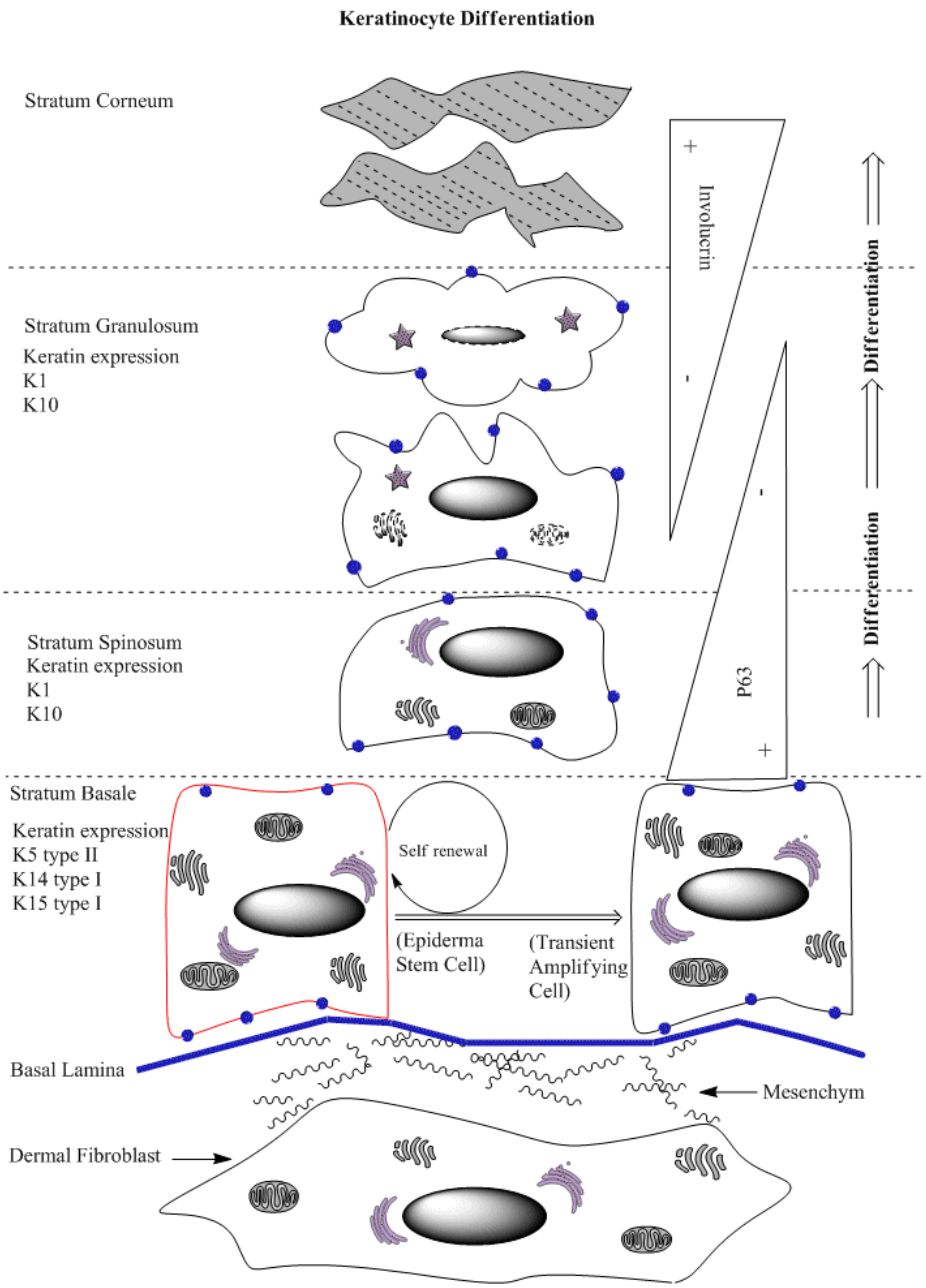

Figure 3.3.1 Diagram of keratinocyte differentiation The schematic diagram shows the differentiation of keratinocytes. Changes in cell composition are accompanied by changes in protein expression. The epidermal stem cell and transient amplifying keratinocytes lie above the dermal fibroblasts on the basal lamina and move towards the top to the final differentiated stage, the stratum corneum. The diagram was constructed using BioDraw Ultra 12.0 software.

3.3.1.4 Clonal evolution of keratinocytes

The transition of keratinocytes from the stem cell stage to transient amplifying cells is a clonal evolution process. Keratinocytes are highly regenerative somatic cells and are capable of expressing telomerase (Taylor *et al.* 1996; Shay *et al.* 1997). While telomerase expression is maintained in the keratinocyte stem cells, it is repressed in the transient amplifying cells (Dellambra *et al.* 2000). It has been proposed that epidermal stem cells have the capacity to proliferate indefinitely whereas transient amplifying cells divide a finite number of times prior to terminally differentiating or entering senescence (Dellambra *et al.* 2000). The epidermal stem cells divide in a stochastic manner and can potentially yield either; two stem cells, a stem cell and a transient amplifying cell or two transient amplifying cells (Houben *et al.* 2007). Epidermal stem cells can be distinguished by surface expression levels of the β1 integrin family, which is two folds higher than in transient amplifying keratinocytes (Jones *et al.* 1995). A more specific marker for keratinocyte stem cells is p63. Levels of p63 is expressed in holoclones by 8 to 10 fold more than in meroclones and up to 200 fold more than in paraclones (Pellegrini *et al.* 2001). Several studies have demonstrated that inhibition of clonal evolution results in the maintenance of keratinocytes in the stem cell compartment. Proteins involved in the clonal evolution include 14-3-3σ and p16 as promoters of clonal evolution (Dellambra *et al.* 2000), and YAP1 as a suppressor (Overholtser *et al.* 2006).

In situ hybridisation of skin biopsies demonstrated low levels of 14-3-3σ mRNA expression in the basal layer keratinocytes that increased significantly in keratinocytes of the suprabasal layers. Protein immunostaining revealed the low levels of 14-3-3σ polypeptide in stratum basale which increased alongside keratin 1 and 10 expressions in stratum spinosum and stratum granulosum layers. Expression of 14-3-3σ disappears in stratum corneum. Levels of 14-3-3σ were very low in proliferating keratinocytes that expressed PCNA and were increased in differentiating cells that expressed involucrin (Dellambra *et al.* 2000). Stable retroviral induction of an antisense 14-3-3σ into keratinocytes was carried out. Antisense induced keratinocytes were maintained in their stem cell compartment and had ceased clonal evolution.

The Yes-associated protein (YAP1) is a 65 kDa transcriptional co-activator protein involved in multiple cellular paths including apoptosis and tumour suppression. YAP1 has also shown to be a candidate oncogene (Overholtser *et al.* 2006). D'Addario *et al* (2010) demonstrated YAP1 involvement in clonal evolution of keratinocytes. The study involved introduction of YAP1 overexpressing gene and vector only control into two normal human keratinocyte strains. Clonogenic proportions were classified in the

vector only control cells as 50% meroclones, 45% paraclones and only 5% holoclones. Whereas the YAP1 overexpressing cells were composed of 58% holoclones 13% meroclones and 29% paraclones. Furthermore, the YAP1 overexpressing keratinocytes when compared to control keratinocytes demonstrated an increase in the expression of p63 and PCNA, a downregulation of 14-3-3 σ and mild reduction in involucrin expression. Growth of the keratinocytes in an organotypic culture system demonstrated normal stratification of the control cells whereas the YAP1 overexpressing cells demonstrated disorganised strata. These results suggest that YAP1 overexpression blocks clonal evolution and maintains keratinocytes in the stem cell compartment but impedes correct differentiation (D'Addario *et al.* 2010).

3.3.1.5 Replicative senescence in keratinocytes

Rheinwald and Green have demonstrated that keratinocytes in culture can achieve over 80 CPD in samples obtained from adults and 150 CPD in samples from neonatal foreskin (Rheinwald *et al.* 1977; Parkinson *et al.* 1992). However, there have been primary cultures of keratinocytes that have exceeded this range. One case has reported normal adult keratinocyte *in vitro* lifespan to reach 188 CPD (Maurelli R 2006). It has been shown that Keratinocytes maintain a steady growth rate in culture until the end of their replicative lifespan when the growth rate declines sharply (Rheinwald *et al.* 1975). However, there is evidence suggesting that keratinocyte stem cells have an indefinite proliferative capacity if maintained in the stem cell compartment (Dellambra *et al.* 2000; D'Addario *et al.* 2010).

Furthermore, the three identified clones of the basal cells have different proliferative capacities. The holoclones which are the keratinocyte stem cells would maintain the highest possible proliferative capacity in a culture and possibly an indefinite lifespan until it clonally evolves into a transient amplifying cell. Meroclones have an intermediate lifespan and achieve 21-38 CPD. The paraclones are committed to differentiate and have a low proliferative capacity of 0-15 CPD (Barrandon *et al.* 1987).

The presence of SA β-galactosidase positive cells has been shown to specifically rise in senescent keratinocytes. Labelling nuclei of cultured keratinocytes with [^{3}H] thymidine was carried out to detect proliferating cells using autoradiography. Keratinocytes that were positively labelled with [^{3}H] thymidine did not stain with SA β-galactosidase and vice versa. SA β-galactosidase stained the basal layer keratinocytes in skin tissue samples but did not stain the upper terminally differentiated layers. Furthermore, young keratinocytes that were induced to terminally differentiate did not

express SA β-galactosidase. This further demonstrates the specificity of SA β-galactosidase staining of senescent cells. In addition, staining of basal epidermis was higher in old donors than in young suggesting an increase with age (Dimri *et al.* 1995).

3.3.1.6 Mechanisms of replicative senescence in keratinocytes

The study of mechanisms of keratinocyte senescence has proven to be challenging for several reasons. One of the reasons is due to the fact that production of keratinocyte daughter cells from stem cells occurs in a stochastic manner (either two daughter stem cells, a stem cell and a transient amplifying cell or two transient amplifying cells) (Houben *et al.* 2007). As a result, cultured keratinocytes exist as a heterogeneous clonal population (holoclones, meroclones and paraclones) (Barrandon *et al.* 1987). The diversity in the culture makes it difficult to monitor changes as there is no pattern. Another challenge arises as a result of the existence of different keratinocyte culture systems. Keratinocyte have shown to undergo different mechanisms of senescence depending on their culture conditions (K-SFM or feeder system) (Fu *et al.* 2003). Studies have been conducted in both culture methods and have produced conflicting results (Dickson *et al.* 2000; Ramirez *et al.* 2001). These conflicting results make it difficult to quote previous work relating to mechanisms of keratinocyte senescence.

Kiyono *et al* (1998) grew human foreskin keratinocytes (HFK) in keratinocyte serum free media (K-SFM) and infected them with either a vector only control or hTERT expressing gene at 4-10 CPD. Clones were isolated from the cultures prior to studying their growth dynamics. HFKs that were $hTERT^{+}$ had the same lifespan as the vector only control of 2 – 10 CPD post cloning. Induction of E7 expression, which inactivates Rb, increased the lifespan HFK cells to 10 - 20 CPD post cloning. Introduction of hTERT in conjunction with E7 increased cell lifespan to over 70 CPD post cloning. These results suggest the requirement of p16 and Rb inactivation for the initial bypass of senescence (Kiyono *et al.* 1998).

Telomerase activity was not detected in primary HFK or HFK-E7 (Kiyono *et al.* 1998). In addition, the cells had a very low lifespan that did not meet the expected normal lifespan range of keratinocytes grown in the feeder system (80-150 CPD (Rheinwald *et al.* 1977; Parkinson *et al.* 1992)). This suggests that the keratinocytes may have clonally evolved into transient amplifying cells prior to senescing or senesced prematurely as a result of stress activation of p16 due to culture conditions in K-SFM.

Oral keratinocytes which are structurally and functionally similar to epidermal keratinocytes were grown in K-SFM and had a replicative lifespan of 40 CPD. The cells

were induced to overexpress cyclin D1, which promotes cell cycle progression by overcoming p16 inhibition. Cyclin D1 overexpression resulted in the extension of their lifespan to 80 CPD. Inactivation of p53 by introducing a mutant form dominant negative p53 gene to the oral keratinocytes led to the extension of their replicative lifespan to 100 CPD. When cyclin D1 overexpression was combined with P53 inactivation it led to the immortalisation of oral keratinocytes (cells grew beyond 160 CPD). Primary oral keratinocyte cultures as well as lifespan extended and immortalised cultures had demonstrated absence of telomerase activity when analysed by TRAP assay (Opitz *et al.* 2001).

Primary keratinocytes that were grown in serum free media demonstrated a significantly reduced replicative capacity of 20-40 CPD (Kiyono *et al.* 1998; Opitz *et al.* 2001) than what has been reported in primary keratinocytes grown in the feeder system which have a lifespan of 80-150 CPD (Rheinwald *et al.* 1977; Parkinson *et al.* 1992). Telomerase activity, which is naturally present in primary keratinocytes (Taylor *et al.* 1996; Shay *et al.* 1997), was absent in primary keratinocytes grown in K-SFM (Kiyono *et al.* 1998; Opitz *et al.* 2001; Fu *et al.* 2003).

Dickson *et al* (2000) ectopically expressed hTERT in keratinocytes by retroviral infection. The keratinocytes were initially grown in the feeder system but were transferred to K-SFM soon after the retroviral infection. Keratinocytes that expressed hTERT continued to divide at a slower rate instead of arresting proliferation when they reached the lifespan limit of the control keratinocytes (35 to 55 CPD). Slow growth rates continued in the keratinocyte culture for three weeks to three months with a constant low population doubling time (0.03-0.29 PD / day). After the period of slow division, rapidly dividing cells appeared and eventually took over the culture (≈ 0.77 PD / day). Rapidly dividing $hTERT^{+}$ keratinocytes were shown to be deficient in p16 expression by western blot and immunocytochemical staining. These cells continued to grow for more than 50 population doublings beyond the lifespan of the control cells achieving more than 85-105 CPD (Dickson *et al.* 2000).

Ramirez *et al* (2001) suggested that the change in culture environment from feeder layer system to serum free media cause hTERT expressing keratinocytes to senesce prematurely. Ectopic introduction of hTERT in keratinocytes that were continuously cultured in a feeder system caused them to resist arrest and achieve more than 160 CPD even with increasing p16 levels. However, when the $hTERT^{+}$ keratinocytes were transferred from a feeder system to a K-SFM at 89 CPD they only achieved a further 9 PD arresting at 98 CPD (Ramirez *et al.* 2001).

Darbro *et al* (2006) demonstrated that ectopic expression of hTERT in primary keratinocytes grown in the feeder system extended their lifespan without an apparent slow growth phase. However, when transferred from the feeder system to K-SFM medium, the $hTERT^{+}$ keratinocytes underwent a slow growth phase followed by immortalisation and rapid growth. Soon after the transfer of $hTERT^{+}$ keratinocytes (48-54 CPD) to K-SFM medium the cells expressed increased levels of p16 during the slow growth phase. Levels of p16 had dropped as the cells entered the rapid growth immortalised phase and became undetectable at later passages. Keratinocytes that were $hTERT^{+}$ were then transferred from feeder system to K-SFM at varying population doublings to test whether time spent in co-culture with feeder cells had any effect. Cells that were transferred at 25, 29 and 35 CPD had ceased proliferation after 7 passages in K-SFM. Cells that were transferred at later CPD of 41 and 51 demonstrated a slow growth phase prior to the emergence of rapid dividing cells (Darbro *et al.* 2006).

DNA methyltransferase inhibitor, 5-aza-2' deoxycytidine treatment of $hTERT^{+}$ keratinocytes that were in their rapid dividing immortal phase in the feeder system and $hTERT^{+}$ keratinocytes that were transferred from feeder to K-SFM was carried out to test whether p16 promoter gene was methylated. An increase in p16 mRNA and protein levels was observed in $hTERT^{+}$ keratinocytes from both the feeder system and K-SFM after treatment with 5-aza-2' deoxycytidine. This indicates that p16 was in a methylated state in both culture systems and treatment with 5-aza-2' deoxycytidine had reintroduced p16 expression. Ectopic retroviral induction of p16 in the cells with methylated p16 resulted in proliferation arrest in both culture systems (Darbro *et al.* 2006).

Fu *et al* (2003) demonstrated that keratinocyte growth conditions modulate natural telomerase expression. Primary keratinocytes cultured using the feeder system demonstrated telomerase activity and a reduced p16 expression. Transfer of primary keratinocytes from the feeder system to K-SFM resulted in telomerase inactivation and p16 upregulation (Fu *et al.* 2003).

Increased p16 levels with increasing generations in culture have been recorded in primary keratinocytes grown in both feeder system and K-SFM (Rheinwald *et al.* 2002). Although primary keratinocytes grown in the feeder system demonstrate a delayed rise in p16 levels when compared with primary keratinocytes grown in K-SFM, levels of p16 in primary keratinocytes grown in the feeder system do eventually increase as they approach senescence (Darbro *et al.* 2005).

Retroviral introduction of antisense $p16^{INK4a}$ cDNA into four strains of primary keratinocytes grown in the feeder system resulted in the immortalisation of these cells. The population doublings achieved by vector only transduced keratinocytes before

senescence were 128, 188, 140 and 121 CPD. Keratinocytes that were transduced with the antisense $p16^{INK4a}$ had a lifespan of 530, 553, 524 and 499 CPD and continued to grow. The keratinocytes with extended lifespans did not demonstrate signs of a slow growth phase in the growth curve (Maurelli *et al.* 2006).

The confliction of results observed between the studies may be due to the differences in the culture conditions as well as heterogeneity of the keratinocyte populations studied by the different groups. More recent studies have demonstrated that clonal evolution dictates the proliferative potential of the cultured keratinocytes.

Transduction of primary keratinocyte cultures with antisense 14-3-3σ resulted in stable downregulation of 14-3-3σ protein and prevention of clonal evolution. The anti-sense 14-3-3σ expressing keratinocytes were maintained in the stem cell compartment and had achieved immortalisation. Transduction with vector only controls caused the cells to senesce at 119.5, 112.1, 54.1 CPD. Whereas transduction with anti-sense 14-3-3σ resulted in the immortalisation of the keratinocytes that have achieved 409.3, 361.4, 385.3 CPD so far and continued to proliferate (Dellambra *et al.* 2000).

Overexpression of YAP1 in keratinocytes prevented clonal evolution and resulted in immortalisation of the cells. YAP1 overexpressing keratinocytes had achieved 291 and 263 CPD and continued to grow as opposed to senescence at 51 and 27 CPD in their control counterparts (D'Addario *et al.* 2010).

Prevention of clonal evolution by the inactivation of 14-3-3σ or overexpression of YAP1 resulted in reduced expression of p16, maintenance of telomerase and consequently immortalisation of the cells (Dellambra *et al.* 2000; D'Addario *et al.* 2010).

Cordisco *et al* (2010) demonstrated that Bmi-1 downregulation takes place in replicative as well as in stress induced senescent keratinocytes followed by an increase in p16 levels. A study of keratinocyte samples collected from patients with varying ages was carried out. The keratinocytes were cultivated and the first passage was examined for clonogenicity and p16 expression. Keratinocytes from young donors did not produce paraclones and demonstrated almost undetectable levels of p16. Older donors that were presented with high percentages of paraclones expressed high levels of p16 (Cordisco *et al.* 2010).

Inactivation of P16 at the stem cell stage has shown to maintain keratinocytes in the stem cell compartment. However, inactivation of p16 in transient amplifying colonies does not prevent cells from entering senescence or terminal differentiation suggesting involvement of other factors in the maintenance of the transient state (Maurelli *et al.* 2006).

From these previous studies, we gather that in natural occurrences, keratinocyte stem cells remain in the stem cell compartment as immortal cells that express telomerase and maintain reduced p16 levels. When keratinocyte stem cells clonally evolve into transient amplifying cells, they lose telomerase activity and upregulate p16 expression. At this point, keratinocytes either terminally differentiate or senesce primarily via a p16 dependant mechanism. Figure 3.3.2 summarizes clonal evolution control in keratinocytes.

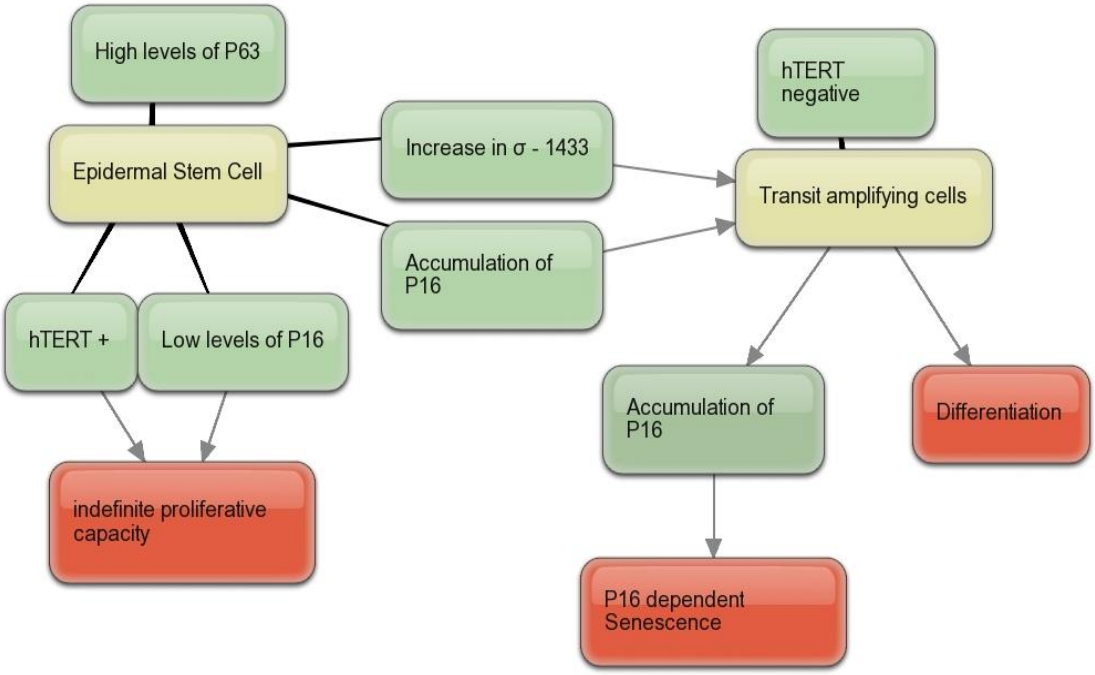

Figure 3.3.2 Clonal evolution control in keratinocytes The diagram describes how keratinocyte clonal evolution is controlled from the epidermal stem cell to the transient amplifying stage. The blue boxes are the features present in a stage or factors promoting transition into the next stage. The red boxes are the final outcomes of the epidermal stem cell or transient amplifying cells.

3.3.1.7 Spontaneous transformation of keratinocytes

Mouse epidermal cells have been known to spontaneously transform in culture whereas spontaneous transformations in cultures of normal human epidermal cells are rare (Boukamp *et al.* 1988), (Fusenig *et al.* 1998). Few cases of spontaneous transformation in human keratinocytes have been reported and each transformed cell line is distinguishable from the other by different characteristics.

Survival and proliferation of keratinocytes in the absence of normal keratinocyte growth requirements, mainly feeder cells, is an indication of transformation. In the absence of feeder cells, keratinocytes would terminally differentiate. Keratinocytes would display a fast rate of terminal differentiation and a reduced lifespan in the absence of epidermal growth factor (Rheinwald *et al.* 1977; 1980). Another important characteristic

of normal and untransformed cells is anchorage dependence. Various transformed cells have been reported to survive and proliferate in suspension and show characteristics of anchorage independence (Stoker *et al.* 1968). The HaCaT cell line, collected from the surroundings of a malignant melanoma (Boukamp *et al.* 1988), is the most extensively characterised spontaneous transformed keratinocyte cell line. The HaCaT cell line is anchorage independent and shows structural and numerical karyotypic abnormalities but was not tumourigenic when transplanted onto immunocompromised mice.

To test anchorage dependence, cells suspended in culture media containing methyl cellulose are spread on a soft agar base. The agar base prevents cells from attaching to the surfaces of the culture dish whilst methyl cellulose gel prevents cells from aggregation. Cells would then be collected from the suspension after a period of time. A significant increase in cell number would signify anchorage independence of the cells in culture. A reduced, constant or slow increase in cell count implies that the cells have retained their anchorage dependency. Anchorage dependency of the cultured cells does not rule out transformation (Stoker *et al.* 1968). Another method for testing transformation in keratinocytes is by altering Ca^{+} levels in the culture media to induce differentiation. While grown in a low Ca^{+} medium normal keratinocytes would proliferate. Increasing Ca^{+} concentrations causes keratinocytes to terminally differentiate. Transformed cells in the instance of increased Ca^{+} concentrations would show signs of slow differentiation but would continue proliferation (Yuspa *et al.* 1980). Keratinocyte cultures that expressed telomerase and maintained diploidy at early passages spontaneously transformed after 400 generations and displayed an abnormal karyotype (Rea *et al.* 2006).

3.3.2 Aims

The aim of this section is to study a cell type that normally senesces by a telomere independent mechanism in the case of Werner's syndrome. Keratinocytes have been reported to senesce via a telomere independent pathway in normal individuals. To date, there have not been any studies on the mechanisms of senescence in keratinocytes from Werner's syndrome patients. Therefore, keratinocytes were selected for this study. Keratinocytes from normal and WS individuals were cultured and their growth kinetics and dynamics were examined. The tests following the study of their growth behaviour were to identify and characterise the cells. These tests include assays for transformation, check point control and exclusion of the possibility of cross contamination.

Growth kinetics were assessed by measuring cell proliferation rates by Ki67 labelling index, cell differentiation by involucrin staining and cell senescence by SA-β-Galactosidase. Growth dynamics were monitored by prolonged cell culture and calculating population doublings. The keratinocytes were characterised by colony morphology, cell behaviour studies, cytokeratin labelling and WRN expression. Karyotype assessment and analysis of cell cycle control proteins were carried out as investigations for cytogenetic and biochemical abnormalities. Furthermore, the keratinocytes were tested for telomerase expression and p63 expression to determine if the culture contains cells that have remained in the stem cell compartment.

3.3.3 Results

3.3.3.1 Characterisation of normal and Werner's syndrome keratinocytes

To confirm the cell types and their origins, a study of their morphology, cytokeratin expression pattern, WRN expression and karyotyping were performed.

3.3.3.1.1 Morphology and culture characteristics

Keratinocytes from normal (SK206AK and SKK372) and Werner's syndrome (WSK368 and WSK369) individuals were isolated from skin samples by Dr. Elizabeth James (University of Brighton) using a technique involving dispase and trypsin treatments. All keratinocyte cell strains displayed typical epithelial morphology when cultured using a feeder system. The cultures contained tightly packed cells that grew in colonies (figures 3.3.3 and 3.3.4). The cultures were initially seeded with a high percent of feeder cells compared to the number of keratinocytes. The cells proliferated by, spreading out from the centre of the colony pushing against the surrounding feeder cells, therefore, compressing them into thick strands. As the keratinocytes proliferated and their colony size increased progressively, the feeder cells were pushed out and detached from the flask leaving higher keratinocyte to feeder cell ratio.

Of the four strains obtained, normal strain SK206AK and WS strain WSK368 were extensively studied. Normal keratinocyte strain, SKK372 was the initial strain to be used as the normal control but had been contaminated with fibroblasts and therefore was replaced by SK206AK and the WS keratinocyte strain, WSK369 was discontinued after the sixth passage, as it was not viable to maintain so many cultures simultanously.

Photographs of SK206AK and WSK368 cultures were taken to illustrate the morphology and growth behaviour of the cells. The photographs were taken at an early stage after seeding when colonies were small, containing few cells (less than 10 % confluent), and at a later stage when cells were at a high confluence (60-80 % confluent) (figures 3.3.3 and 3.3.4 respectively).

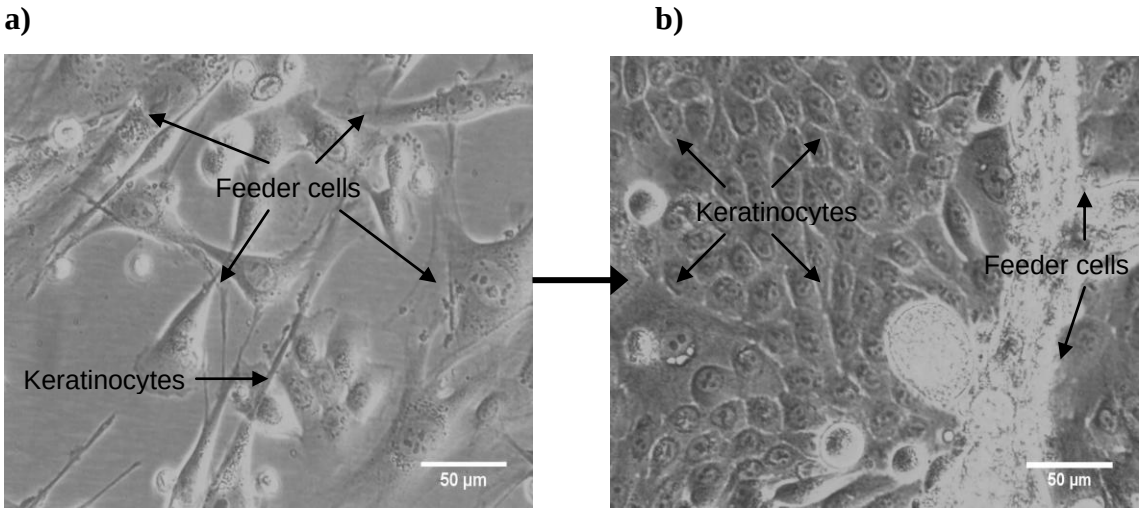

Figure 3.3.3 Photograph of cultured normal keratinocytes Normal keratinocytes SK206AK (passage 24, 60.7 CPD) at **a)** early stage (< 10% confluent) and **b)** late stage (60-80% confluent).

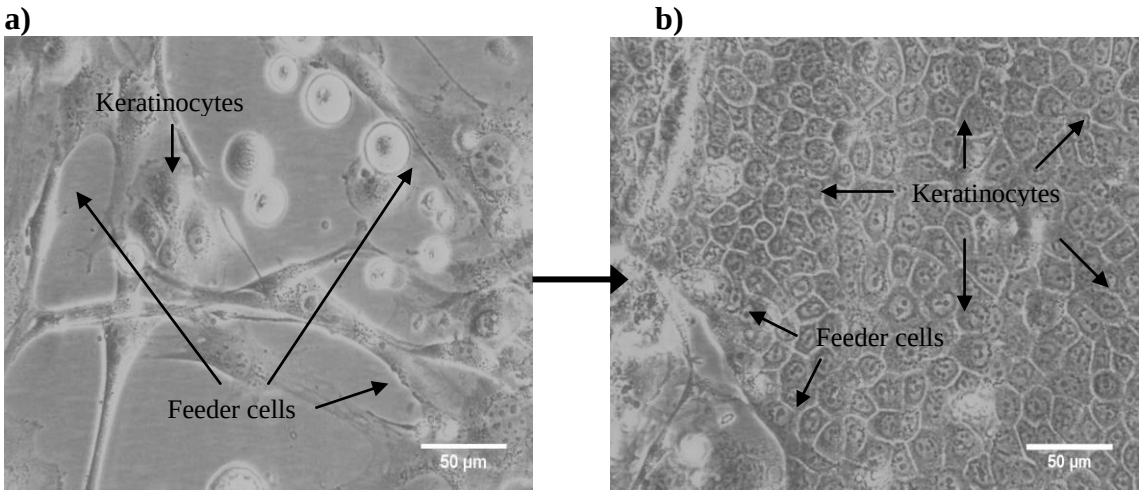

Figure 3.3.4 Photograph of cultured Werner's syndrome keratinocytes Werner's syndrome keratinocytes WSK368 (passage 38, 96.28 CPD) at **a)** early stage (<10% confluent) and **b)** late stage (60-80% confluent).

Cytokeratin staining was carried out as confirmation that SK206AK and WSK368 cultures were epithelial and to ensure that there was no contamination by fibroblasts (cytokeratins are present in epithelial cells but absent in fibroblasts). The cytokeratin markers analysed corresponded to cytokeratins 5, 6, 8, 17 and probably 19 (as described by the manufacturer). This wide spectrum of cytokeratin labelling ensured that the keratinocytes have been targeted at all stages of differentiation. Both keratinocyte cell strains SK206AK (passage 19, 46.79 CPD) and WSK368 (passage 41, 108.81 CPD) demonstrated typical cytoplasmic staining whereas the dermal fibroblast cell strain SKF276 was negative (figure 3.3.5).

a)

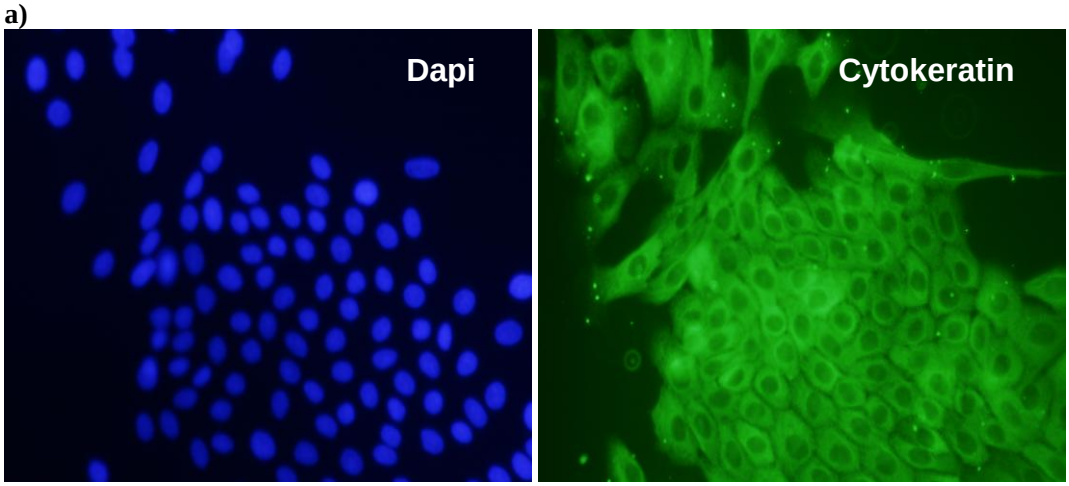

b)

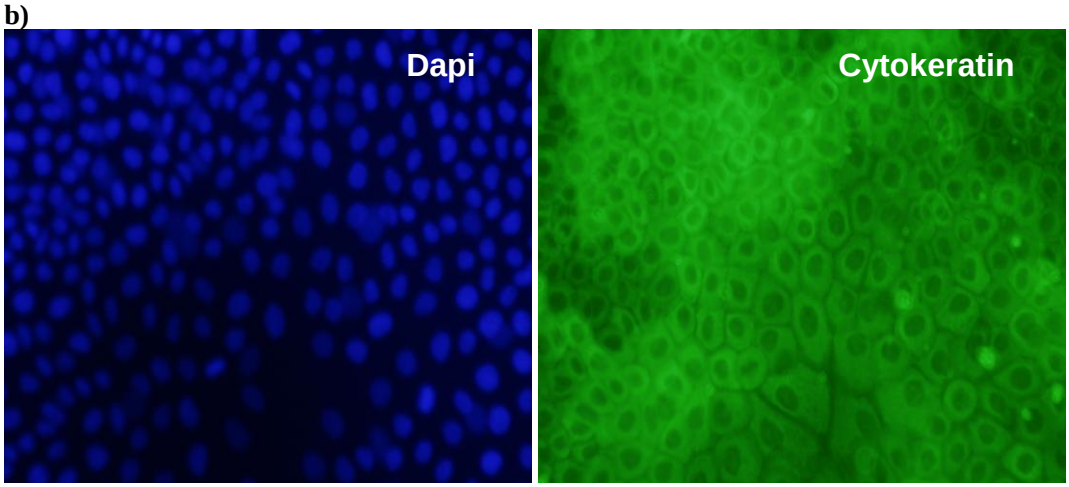

c)

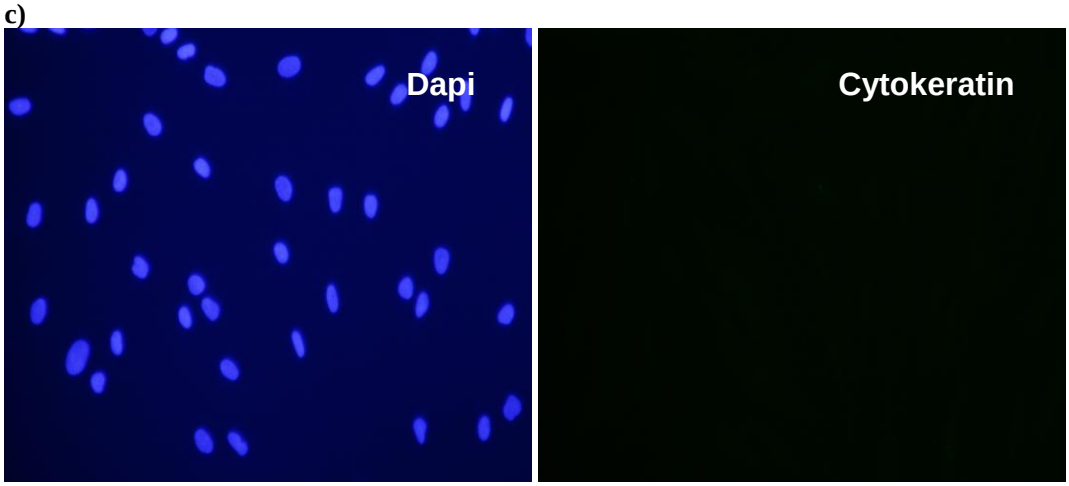

Figure 3.3.5 Immunocytochemical detection of cytokeratin in normal and WS keratinocytes DAPI (nuclear stain, blue) and anti-cytokeratin (cytokeratin 5, 6, 8, 17 and probably 19; cytoplasmic, FITC (green) staining of **a)** normal keratinocytes (SK206AK, 46.79 CPD), **b)** WS keratinocytes (WSK368, 108.81 CPD) and **c)** normal dermal fibroblasts (SKF276) used as negative control.

3.3.3.1.2 Immuno-detection of WRN protein in the keratinocyte samples

Monoclonal mouse antibody to Werner's syndrome helicase, WRN [4H12], was used to assess WRN expression in the keratinocytes. WRN was observed in the nuclei of SK206AK (passage 19, 46.79 CPD) and was also, unexpectedly, present in the nuclei of WSK368 (passage 41,108.81 CPD) (figure 3.3.6).

Western blot analysis was carried out using the WRN [4H12] for higher specificity. A band of approximately 170 kDa (WRN=163 kDa) was detected in SK206AK (8.12 and 56.17 CPD) but absent in WSK368 (7.93 and 122.44 CPD). A non-specific band measuring 100 kDa was present in both SK206AK and WSK368 cells (figure 3.3.7). These results provided confirmation that SK206AK is from a normal individual and WSK368 is from a Werner's syndrome patient.

a)

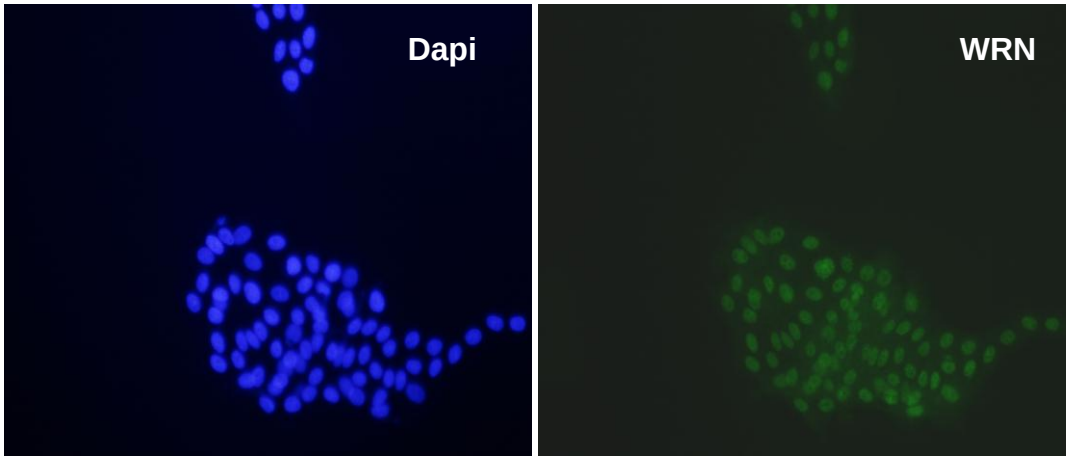

b)

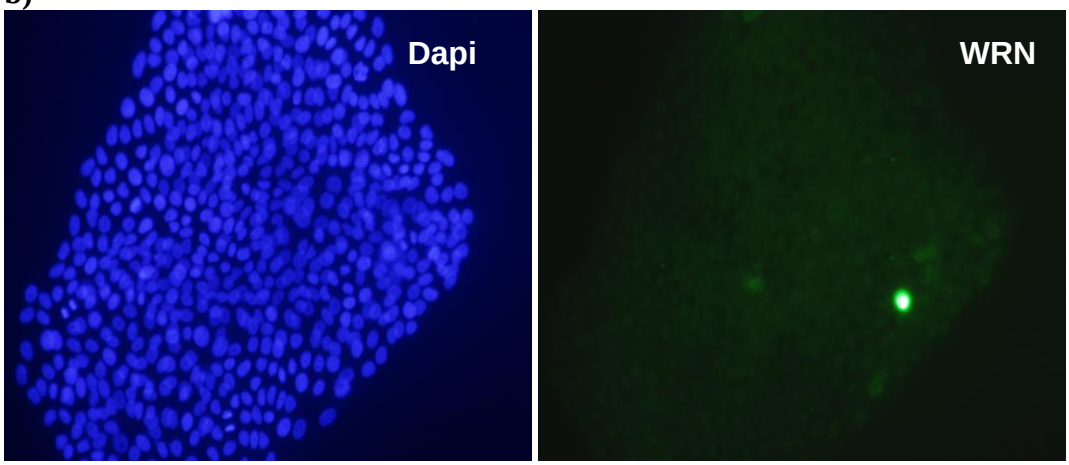

Figure 3.3.6 Immunocytochemical detection of WRN Imunofluorescence staining with DAPI (blue, nuclear) and for WRN [4H12] (FITC (green), nuclear) in **a)** SK206AK (passage 19, 46.79 CPD) and **b)** WSK368 (passage 41,108.81 CPD).

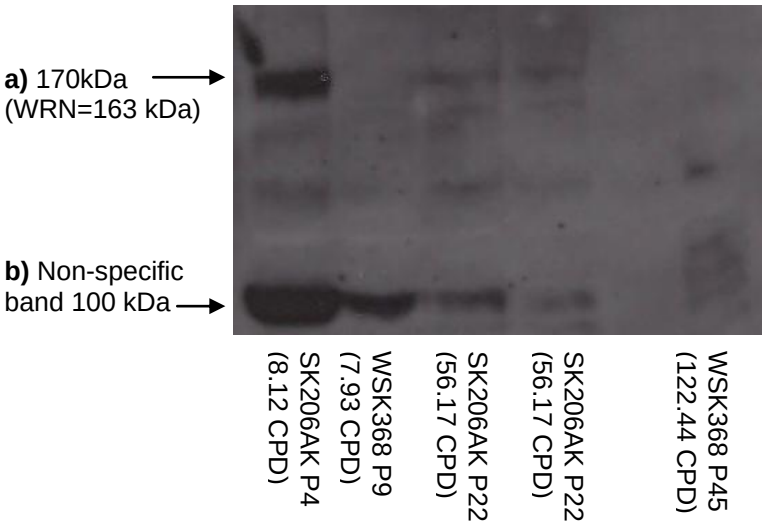

Figure 3.3.7 Western blot detection of WRN in normal and WS keratinocytes Western blot analysis of WRN in SK206AK (8.12 and 56.17 CPD) and WSK368 (7.93 and 122.44 CPD); **a)** band of an approximate size of 170 kDa representative of WRN (163 kDa) in normal keratinocytes that was absent in WS keratinocytes, **b)** second band at 100 kDa is a non-specific band present in both SK206AK and WSK368.

3.3.3.1.3 SK206AK and WSK368 keratinocytes do not express numerical chromosome abnormalities

Karyotype analysis was carried out to investigate numerical chromosome abnormalities in SK206AK and WSK368. Analysis of two cells are considered enough to exclude carriers of a familial rearranged chromosome, thirty cells for excluding a 10-15% or more mosaicism and two hundred are required for the exclusion of a low grade mosaicism. However, analysis of three cells is enough to detect any chromosome disorders if the preparations are of a good quality (Jonasson 1986). Therefore, three unbanded Giemsa stained metaphases from each cell strain were analysed (SK206AK and WSK368). Figure 3.3.8 shows karyotypes of SK206AK (56.17 CPD) and WSK368 (89.61 CPD) (figure 5.1 in appendix III provides adddtional photographs of the metaphases). Chromosomes were arranged automatically, according to size and centromere position, by the aid of chromosome analysis software, Smart Type (Digital Scientific Ltd., http://www.smarttype.biz). Corrections were made by manually arranging misplaced chromosomes in the correct compartments as described by the ISCN for the arrangement of unbanded chromosomes (Lindsten *et al.* 1978). Karyotypes of both SK206AK and WSK368 displayed a total of 46 chromosomes composed of 22 pairs of autosomes and a pair of sex chromosomes (46XY for SK206AK and 46XX for WSK368). The karyotypes do not rule out translocations or chromosomal rearrangements but do rule out aneuploidy of total chromosome numbers and polyploidy. Variegated translocation mosaicsm (VTM) a typical feature of WS fibroblasts and lymphocytes

(Hoehn *et al.* 1975; Scappaticci *et al.* 1982), could not be investigated in the unbanded karyotypes because special band staining is required to detect translocations.

a)

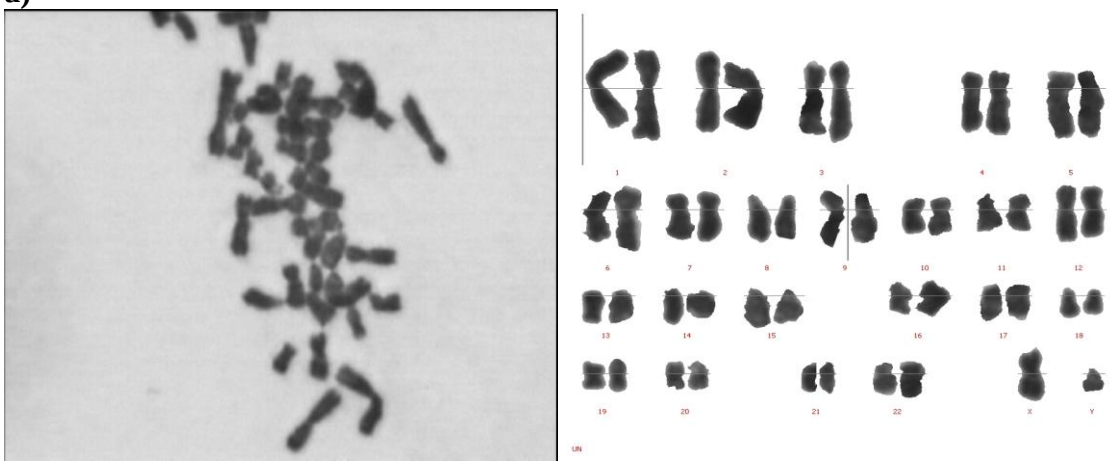

b)

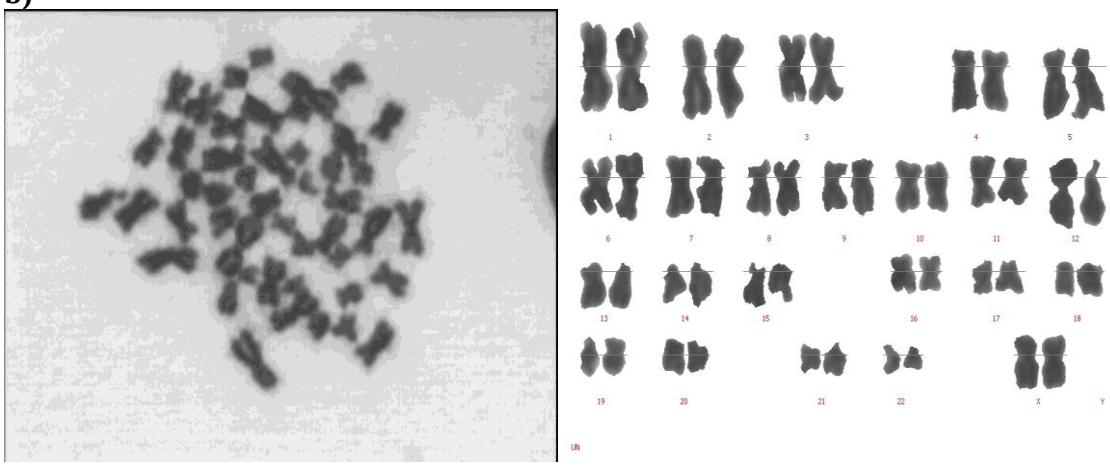

Figure 3.3.8 Karyotype of normal and WS keratinocytes Giemsa stained metaphase and arranged karyotypes of **a)** SK206AK (passage 22, 56.17 CPD) and **b)** WSK368 cells (passage 36, 89.61 CPD). Karyotypes were arranged using Smart Type software (Digital Scientific Ltd., http://www.smarttype.biz).

3.3.3.1.4 Anchorage independence

Methylcellulose/ agar culture systems which prevent cell attachment to the surface of the plate as well as adhesion between cells are used to analyse cells for anchorage independence. Cells that are capable of proliferating in methylcellulose/ agar are considered anchorage independent, which is a feature of transformed cells that are possibly malignant. Normal (SK206AK) and WS (WSK368) keratinocytes were cultured in methylcellulose/ agar to look for the presence of the anchorage independence feature seen in transformation. SK206AK cells were seeded at 3.03 x 10^5 cells and harvested after 18 days with a count of 3 x 10^5 cells (-0.012 PDs). WSK368 were seeded at 2.37 x 10^5 and harvested after 18 days with a count of 2.47 x 10^5 cells (0.062 PDs). Both SK206AK and WSK368 did not demonstrate sufficient proliferation during this time,

which suggests that both SK206AK and WSK368 retain their anchorage dependent phenotype.

3.3.3.2 Growth dynamics and kinetics of keratinocyte cultures

3.3.3.2.1. Growth dynamics of normal and Werner's syndrome keratinocytes

Normal (SK206AK and SKK372) and Werner's syndrome (WSK368 and WSK369) keratinocytes (starting at passage two) were cultured and monitored for five consecutive passages (figure 3.3.9). At passage one, the cells were isolated from tissue and the population doublings were not taken (CPD=0). The growth rates were calculated by dividing the mean population doublings achieved at each passage by the number of days of each passage (growth rates= mean PD per passage / number of days of the passage). Figure 3.3.10 shows a bar chart of the first five consecutive passages, SK206AK achieved an average mean of 0.325 ± 0.159 PD/day, SKK372 achieved an average mean of 0.348 ± 0.0727 PD/day, WSK368 achieved an average mean of 0.4 ± 0.125 PD/day and WSK369 achieved an average mean of 0.28 ± 0.123 PD/day. Shapiro-Wilk analysis demonstrated that the data (in each of the four samples) was normally distributed ($P>0.05$) and the homogeneity of variance had not been rejected, as demonstrated using the Levene test ($P>0.05$). ANOVA analysis demonstrated that there was no significant difference between the growth rates of SK206AK, SKK372, WSK368 and WSK369 ($F(3, 16) = 0.308$, $P = 0.819$). These results suggest that growth rates of early passage Werner's syndrome keratinocytes lie within the growth rate range of normal keratinocytes.

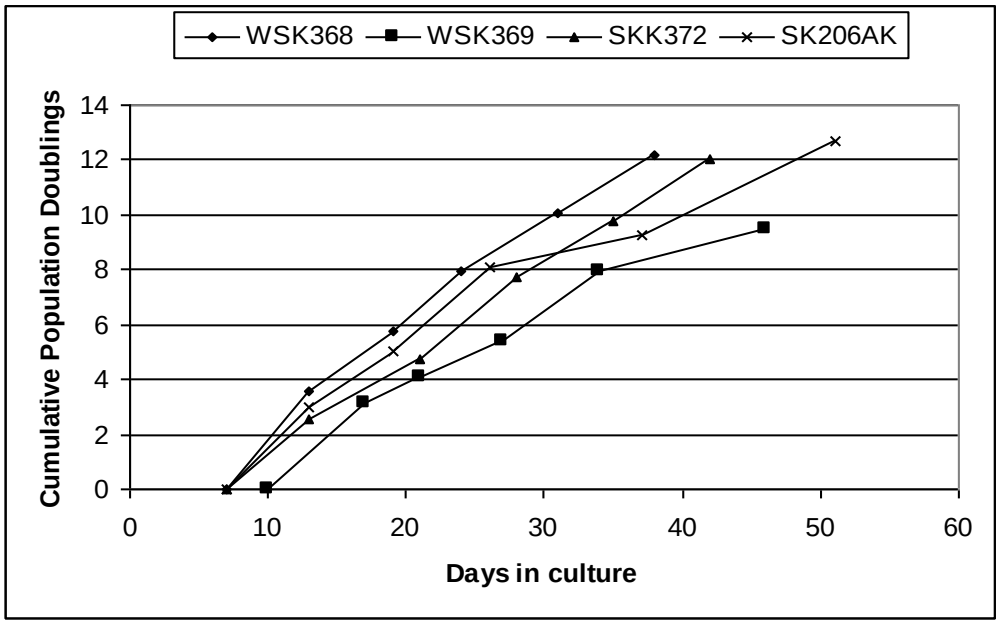

Figure 3.3.9 Growth curve comparing growth rates of two normal and two Werner's syndrome keratinocyte strains The growth curve demonstrates the first five passages of normal keratinocytes (SK206AK and SKK372) and Werner's syndrome keratinocytes (WSK368 and WSK369). Cell counts were not performed at passage 1 and were counted from there after (i.e. passage 2 to 6).

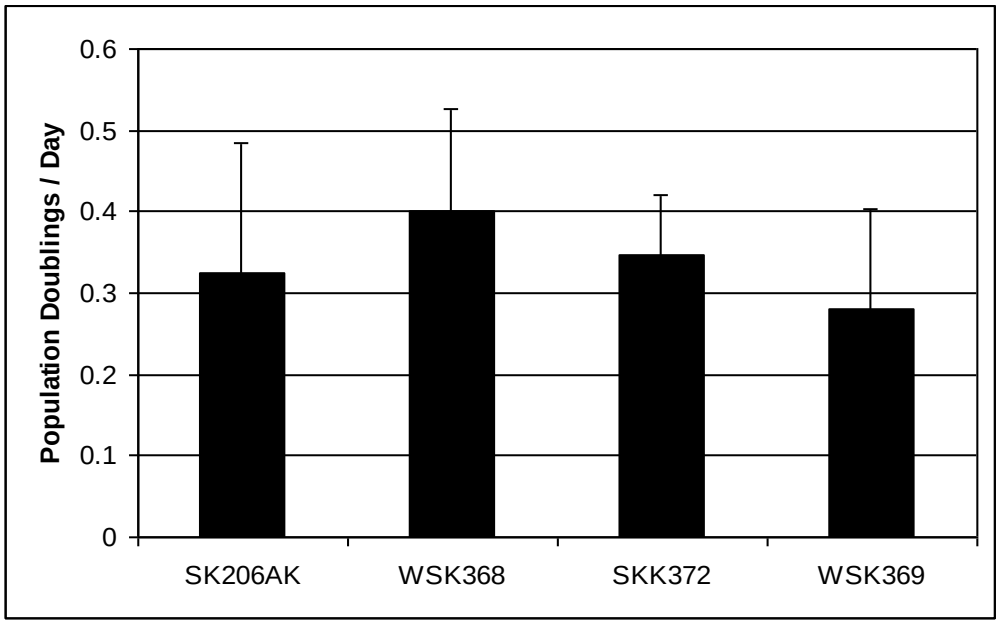

Figure 3.3.10 Growth rate comparison between two normal and two Werner's syndrome keratinocytes Average (mean) of estimated growth rates (PD/Day) of normal (SK206AK and SKK372) and Werner's syndrome (WSK368 and WSK369) keratinocytes over five consecutive passages (n=5). Error bars = standard deviation.

SK206AK and WSK368 were grown in culture with the aim of achieving replicative senescence. However, senescence of both cultures was not achieved due to the unexpectedly long lifespan of the cells. Growth rates of SK206AK and WSK368 were monitored until the cultures were terminated, SK206AK achieved 60.7 CPD in 259 days with a cumulative growth rate of 0.265 ± 0.103 PD/day and WSK368 achieved 66.44 CPD in 263 days with a mean growth rate of 0.26 ± 0.16 PD/day (figure 3.3.11). Univariate analysis of variance demonstrated no significant difference between the slopes ($p=0.966$), suggesting there was no significant difference between the cumulative growth rates of SK206AK and WSK368. The WSK368 keratinocyte culture was continued for a total of 407 days and achieved a total of 130 CPD with a final mean growth rate of 0.331 ± 0.17 PD/day before terminating the culture. Cellular senescence did not occur in any of the cultures studied; both the SK206AK and WSK368 strains continued to divide steadily throughout their time in culture and did not demonstrate signs of proliferative decline (figure 3.3.11).

Preliminary growth rate monitoring of two normal (SKK372 and SK206AK) and two WS (WSK368 and WSK369) demonstrated that there was no difference between the growth rates of normal and WS keratinocytes. Prolonged monitoring of normal (SK206AK) and WS (WSK368) keratinocytes over 60 CPD did not demonstrate any difference in growth rates between the cell strains and did not demonstrate decline in growth rates over their long period of time in culture. Furthermore, continuation of WS keratinocytes (WSK368) growth to 130 CPD, which is within the range of normal keratinocyte maximum proliferative capacity (80-150 CPD), did not demonstrate any decline in growth rates. Table 3.3.1 summarizes the growth dynamics of normal and WS keratinocytes (see also table 5.5 in appendix III).

Cell strains	Total passages achieved	Maximum days In culture	Average growth rate (PD/day)	Maximum CPD achieved before stopping the culture
SK206AK	24	259	0.325 ± 0.15 (in 5 passages) 0.265 ± 0.103 (in 23 passages)	60.7
SKK372	6	42	0.348 ± 0.0727 (in 5 passages)	12.03
WSK368	47	407	0.4 ± 0.125 (in 5 passages) 0.26 ± 0.16 (in 26 passages) 0.331 ± 0.17 (in 46 passages)	130
WSK369	7	74	0.28 ± 0.123 (in 5 passages)	12.97

Table 3.3.1 Summary of growth dynamics of normal and WS keratinocytes at different stages Growth rates of SK206AK, SKK372, WSK368 and WSK369 at different passages and maximum passages, days and cumulative population doublings achieved before the cultures were discontinued.

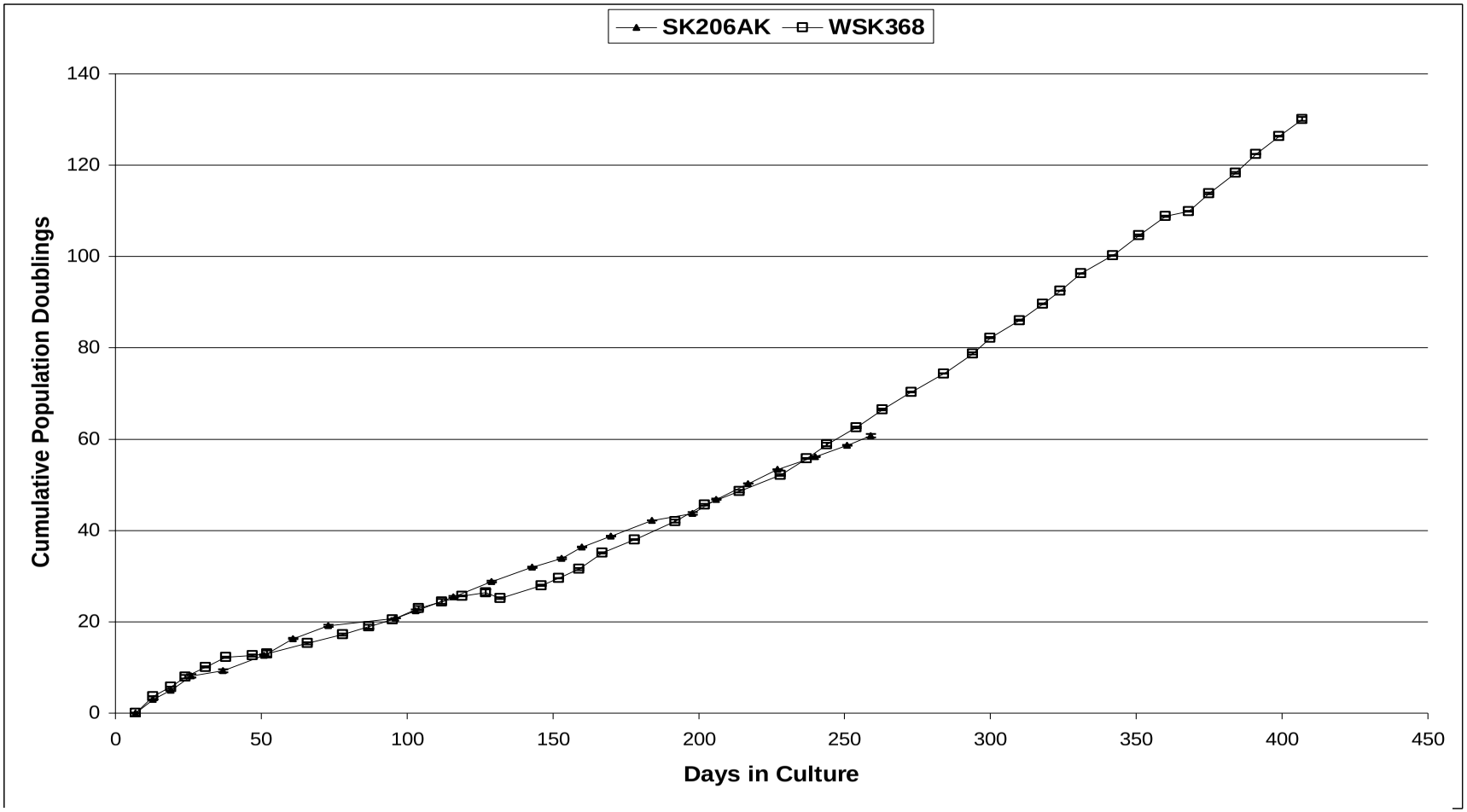

Figure 3.3.11 Comparison of growth curves between normal and Werner's syndrome keratinocyte over an extended period of time Growth curves of normal (SK206AK) and Werner's syndrome (WSK368) keratinocytes. Both strains did not express reduction in growth rates or signs of replicative senescence. The data plotted are cumulative population doublings against the number of days in culture. N=3; Error bars= ± standard deviation.

3.3.3.2.2 Growth kinetics of normal and Werner's syndrome keratinocytes

Normal (SK206AK) and Werner's syndrome (WSK368) keratinocytes were assessed for Ki67 index to monitor changes in percentages of proliferating cells with increased population doublings. Differentiation was also assessed at different population doublings by labelling cells with involucrin (figure 3.3.12 and 3.3.13).

Immunocytochemical staining of Ki67 was carried out in SK206AK and WSK368 at different population doublings. The results show that fluctuating levels of Ki67 labelling index were demonstrated in both SK206AK and WSK368 keratinocyte strains throughout their time in culture. The Ki67 index had a range of 44.7 % to 63.6 % over different population doubling points for SK206AK (n=12). In WSK368 the Ki67 levels were between 23.7 % and 72.9 % (n=38). Despite the fluctuations in Ki67 labelling index, a scatter diagram complemented with statistical analysis demonstrated an unchanged Ki67 index trend with successive population doublings in both SK206AK and WSK368 (figure 3.3.14). Kendall's correlation coefficiency test excludes upward or downward trends in Ki67 index with increased population doublings in SK206AK (τ =0.066, $p > 0.05$) and WSK368 (τ =0.137, $p > 0.05$). The average mean percentage of Ki67 in SK206AK and WSK368 were plotted in figure 3.3.15. Two tailed T-test demonstrates that the difference between percentages of Ki67 index between SK206AK and WSK368 is not significant (t=0.603, p=0.424).

Assessment of involucrin expressing cells was carried out to estimate the fraction of the keratinocyte culture that has committed to differentiate. Immunocytochemical staining of involucrin was carried out in SK206AK and WSK368 cultures at different passages. Difficulty was experienced in obtaining accurate counts of involucrin stained cells due to varying intensities of fluorescence and presence of background. The coexistence of various stages of differentiated keratinocytes that express different levels of involucrin is probably the reason for the varying intensities of fluorescence.

The estimated counts of involucrin-positive cells that were obtained for SK206AK were 9.59 % at passage 5 (5.12 CPD), 2.01 % at passage 15 (36.34 CPD) and 4.83 % at passage 20 (50.23 CPD). The estimated counts of involucrin-positive WSK368 were 14.74 % at passage 6 (12.19 CPD), 2.12 % at passage 34 (82.17 CPD), 4.02 % at passage 42 (109.85 CPD) and 6.65 % at passage 44 (118.28 CPD). The average mean of the percentages of involucrin staining in both SK206AK and WSK368 were plotted in a bar chart (figure 3.3.16). Two tailed T-test demonstrated that the differences between SK206AK and WSK368 percentages of involucrin staining is not significant (t= -0.373, p=0.709). This suggests that the proportions of keratinocytes committed to differentiation are similar in both SK206AK and WSK368.

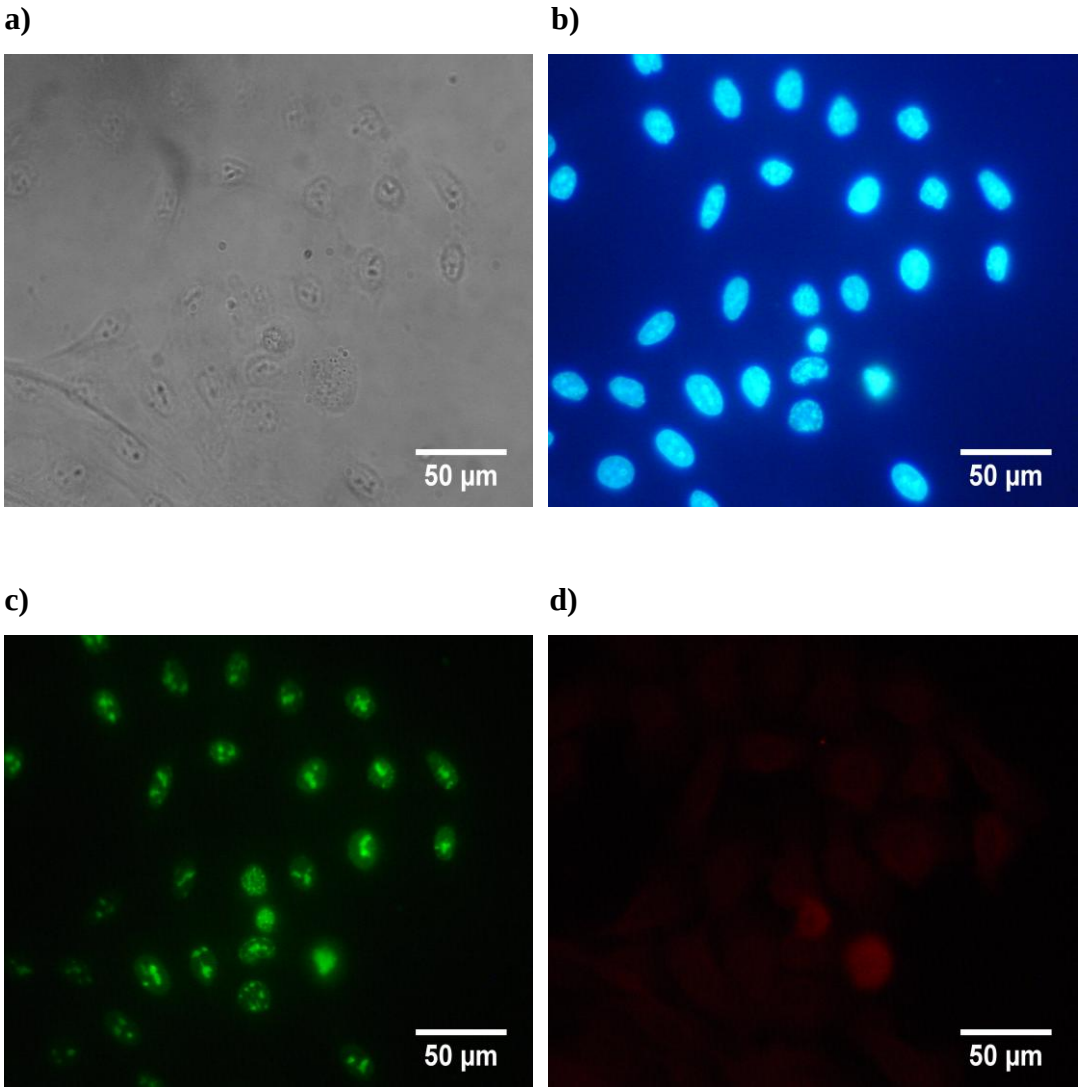

Figure 3.3.12 Photographs of light microscope view of normal keratinocytes, DAPI and fluorescence labelling of Ki67 and involucrin The photographs illustrate a) light microscope view and different fluorescence labels b) DAPI (blue, nuclear), c) Ki67 labelled with FITC (green, nucleolar) and d) involucrin labelled with rhodamine red (red, cytoplasmic) in the same microscopic field of normal keratinocytes (SK206AK).

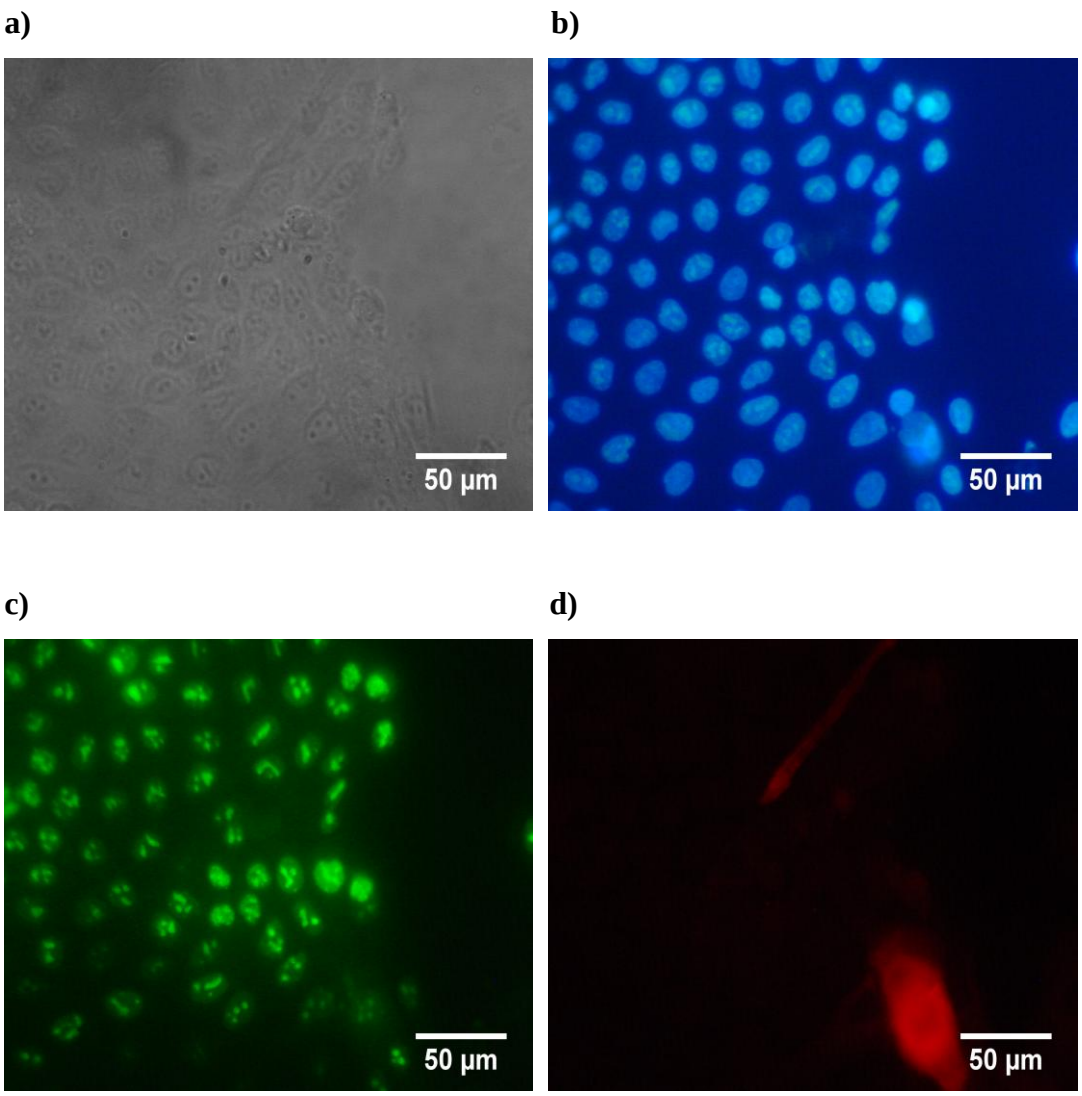

Figure 3.3.13 Photographs of light microscope view of Werner's syndrome keratinocytes, DAPI and fluorescence labelling of Ki67 and involucrin The photographs illustrate a) light microscope view and different fluorescence labels b) DAPI (blue, nuclear), c) Ki67 labelled with FITC (green, nucleolar) and d) involucrin labelled with rhodamine red (red, cytoplasmic) in the same microscopic field of Werner's syndrome keratinocytes (WSK368).

a)

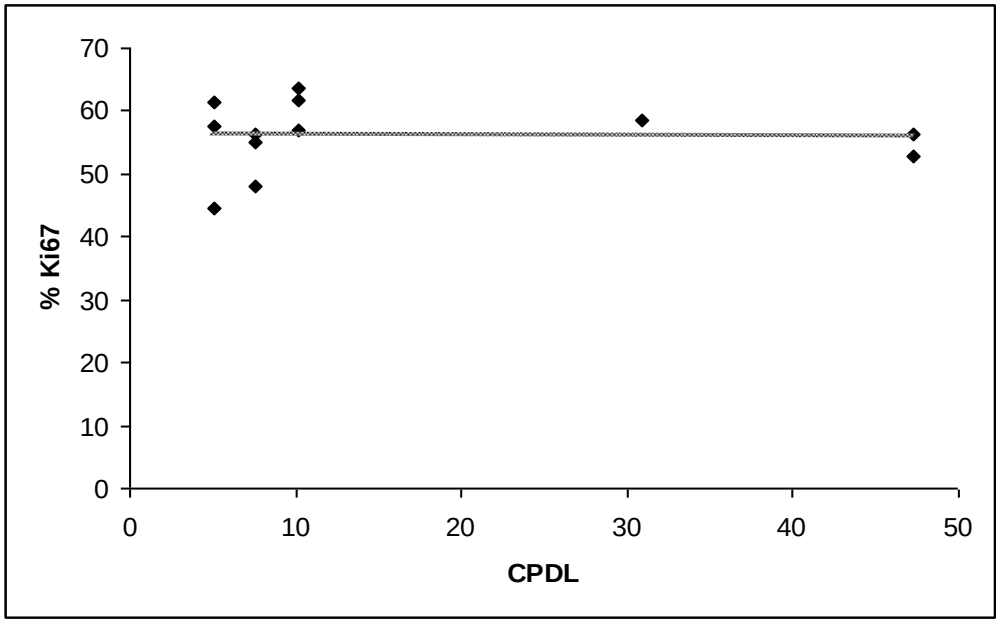

b)

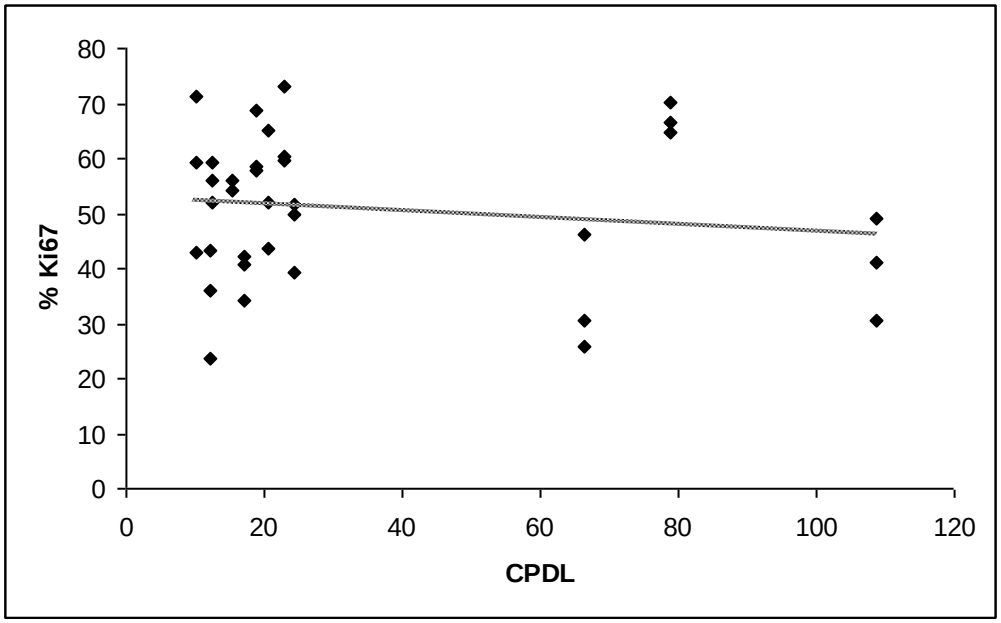

Figure 3.3.14 Trend of Ki67 labelling index in normal and Werner's syndrome keratinocytes with successive population doublings Scatterplot of Ki67 labelling index against cumulative population doublings (CPD) of **a)** normal keratinocytes (SK206AK) and **b)** Werner's syndrome keratinocytes (WSK368).

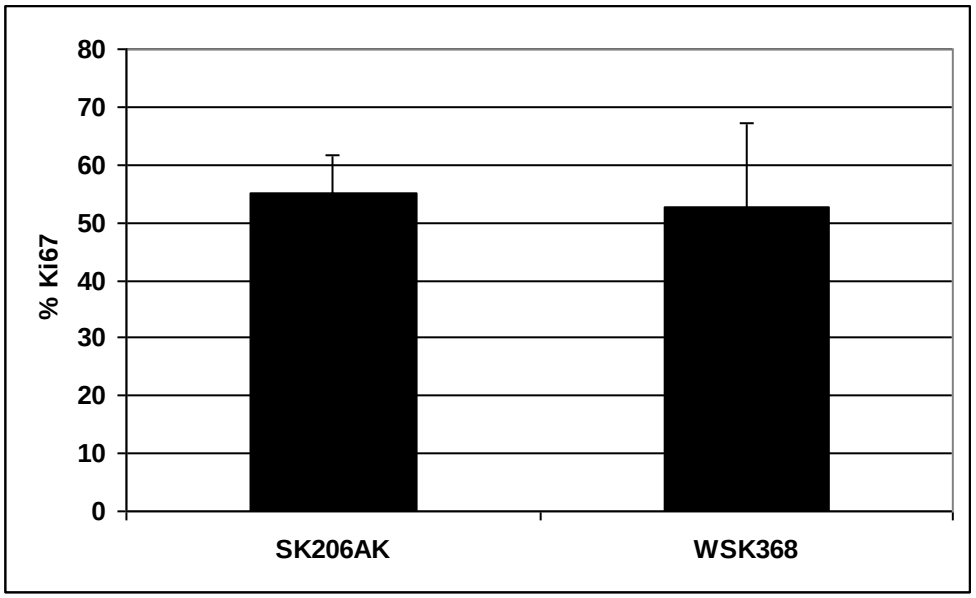

Figure 3.3.15 Ki67 labelling index in normal and Werner's syndrome keratinocytes Mean Ki67 labelling percentages in normal (SK206AK) (n=12) and Werner's syndrome keratinocytes (WSK368) (n=38). Error bars= standard deviation.

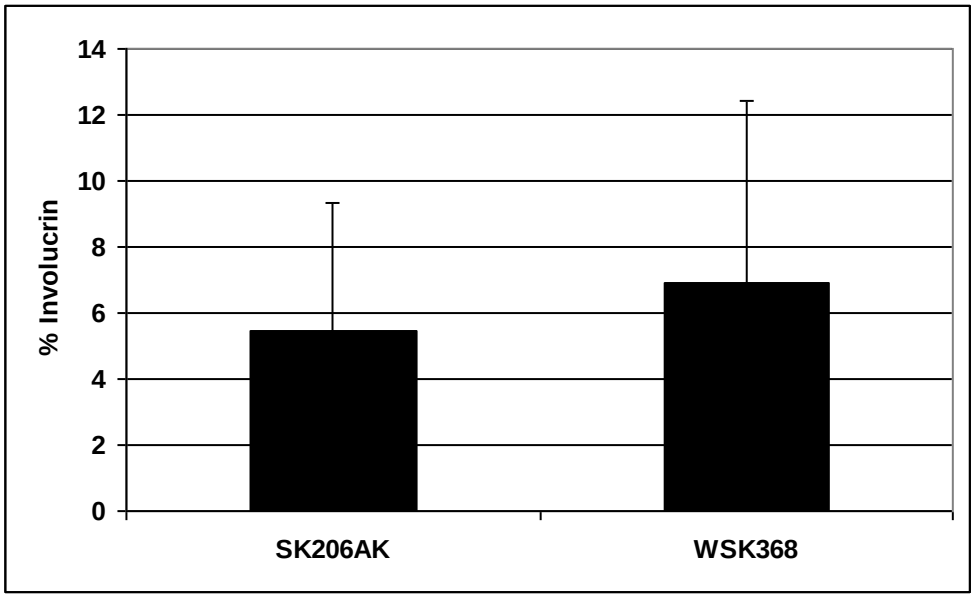

Figure 3.3.16 Involucrin labelling index in normal and Werner's syndrome keratinocytes Mean involucrin labelling percentages in normal (SK206AK) (n=3) and Werner's syndrome keratinocytes (WSK368) (n=4). Error bars= standard deviation.

3.3.3.2.3 Senescence associated β- galactosidase (SA β-gal) activity in normal and WS primary keratinocytes

SA β-galactosidase assay was carried out for the detection of senescent cells in SK206AK and WSK368 keratinocytes. Cells at different population doublings (ranging from early to late) were assessed in triplicates. Table 5.6 in appendix III lists all the cumulative population doublings of SK206AK and WSK368 tested with their corresponding passages. Careful screening was carried out on all the preparation for the presence of SA β–Gal staining. The cells from both SK206AK and WSK368 had tested negative, yielding 0% SA β–Gal staining through all the population doublings assayed (figure 3.3.17: a and b). Photographs were taken to demonstrate the negative SA β –Gal staining in SK206AK and WSK368 keratinocytes (figure 3.3.18: a and b respectively) as compared to positive SA β–Gal staining in late stage normal dermal fibroblasts (SKF276) (figure 3.3.18: c). All test groups were accompanied by a positive control X-Gal staining carried out at pH 4.0 (figure 3.3.18: a, b and c).

a)

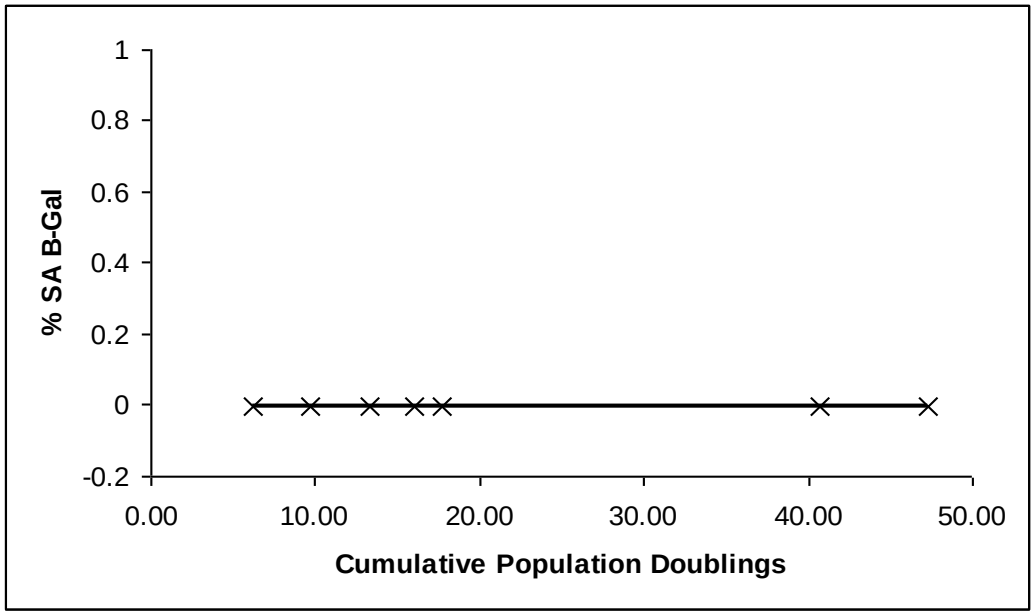

b)

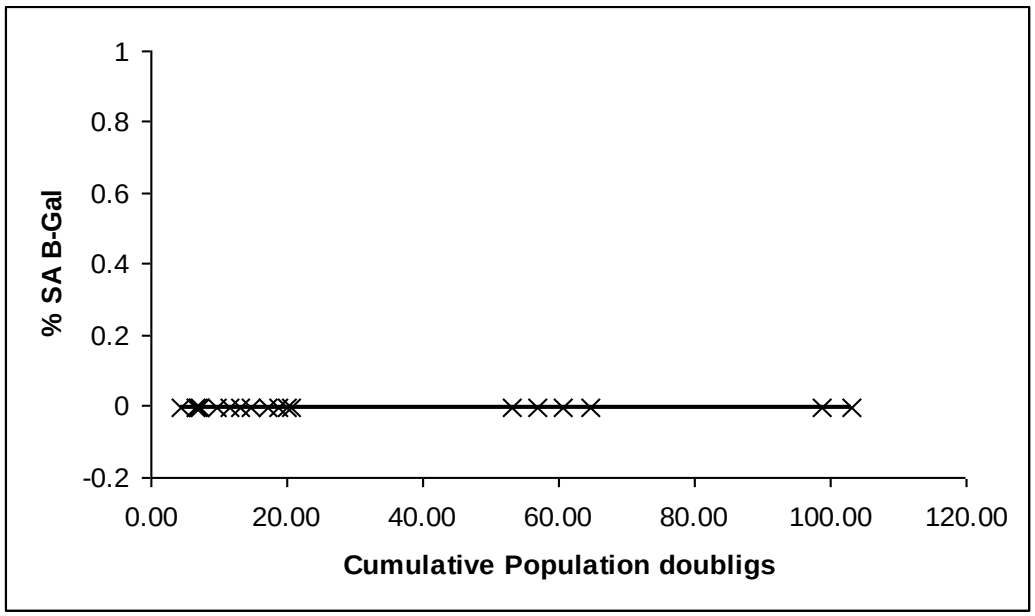

Figure 3.3.17 Percentage of SA β-galactosidase staining at different population doublings in normal and Werner's syndrome keratinocytes The graph demonstrates percentage of SA β-gal staining at a range of cumulative population doublings (CPD) in a) normal (SK206AK) and b) Werner's syndrome (WSK368) keratinocytes. All of the samples were carried out in triplicates and were carefully screened.

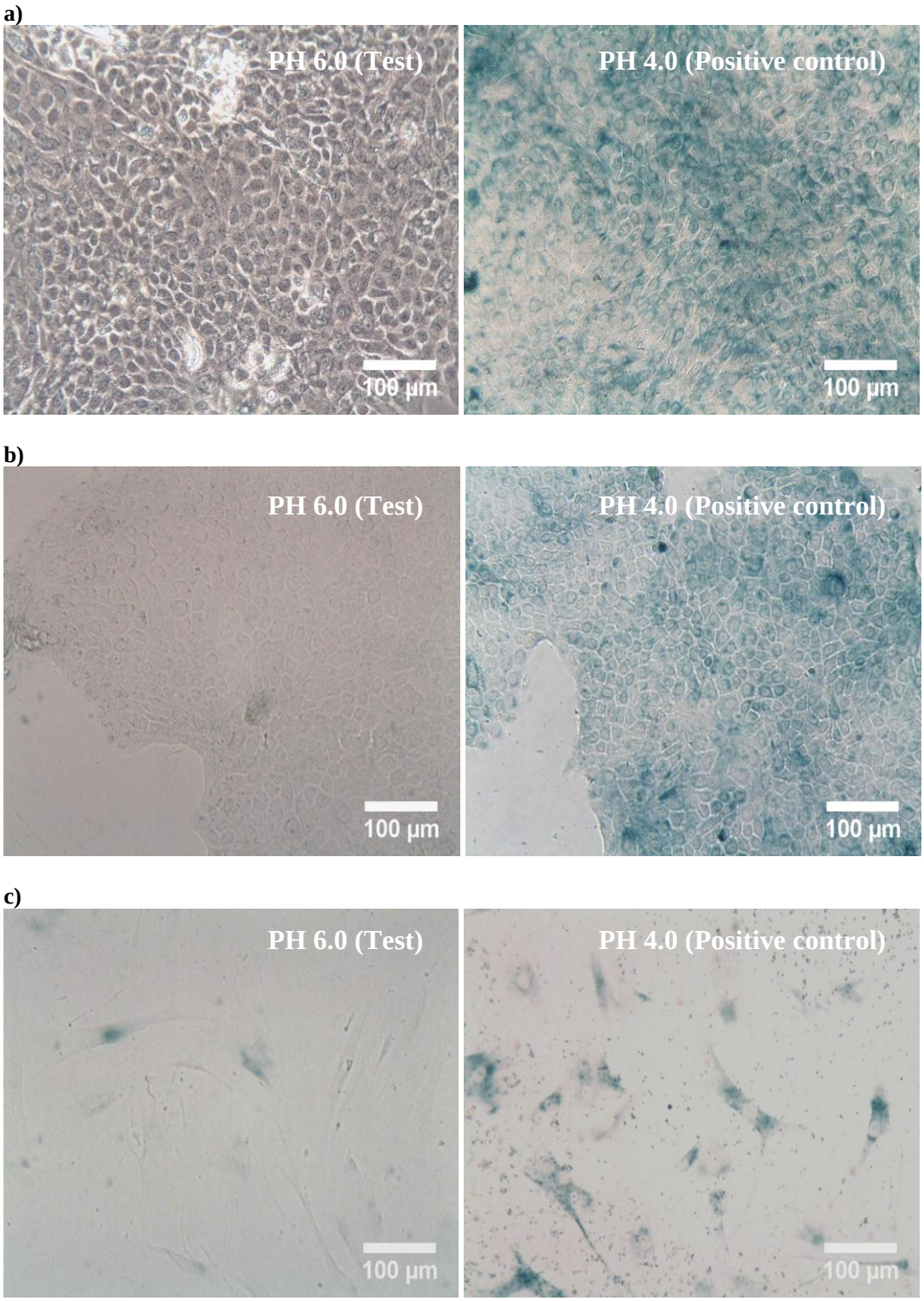

Figure 3.3.18 SA β-gal assay of normal and Werner's syndrome keratinocytes Senescence associated β-galactosidase (pH 6.0) and lysosomal β-galactosidase (pH 4.0) staining of a) normal (SK206AK) keratinocytes (passage 18, 40.71 CPD) b) Werner's syndrome (WSK368) keratinocytes (passage 31, 64.57 CPD) and c) normal dermal fibroblasts (SKF 276).

3.3.3.3 Effects of altered culture conditions on keratinocyte behaviour

Keratinocytes have been shown to grow optimally in the feeder system (Rheinwald *et al.* 1975; Rheinwald *et al.* 1977). Transfer of keratinocytes to a serum free media results in changes in the expression of protein levels, such as p16, and leads to premature senescence (Cordisco *et al.* 2010). However, when grown in Rheinwald and Green media in the absence of feeder cells, keratinocytes terminally differentiate (Rheinwald *et al.* 1980). Other culture supplements such as hydrocortisone, cholera toxin and epidermal growth factor are equally required for optimum growth of primary keratinocytes. Absence of these supplements from the media, even in the presence of feeder cells, results in keratinocyte differentiation (Rheinwald 1980). The effect of these altered culture conditions on normal (SK206AK) and Werner's syndrome (WSK368) keratinocyte cultures are assessed in the following sections.

3.3.3.3.1 Transfer of keratinocytes to serum free media

SK206AK and WSK368 Keratinocytes cultures were transferred from the feeder system to K-SFM, to test their growth behaviour in response to the change of culture condition. Both SK206AK and WSK368 attached to the surface and maintained shape and size of a proliferating epithelial cell soon after their transfer from the feeder system to K-SFM (figure3.3.19). However, a significant decrease in cell proliferation and growth rates in both SK206AK and WSK368 cultures was observed.

SK206AK were transferred to K-SFM at passage 22 (56.17 CPD) with a seeding density of 4.56×10^5 cells. The cells were harvested after 12 days in culture at passage 23 (P1*) with a mean count of 1.4×10^5 (-1.79 PD). The cells were reseeded at density of 1.4×10^5 cells and achieved a count of 1.87×10^5 cells (0.42 PD) after 9 days in culture at passage 24 (P2*). Figure 3.3.20 (a) shows the growth trend of SK206AK in the feeder system from passage 21 to 24 and parallel passages in K-SFM; passage 23 (P1*) and passage 24 (P2*).

WSK368 were transferred to K-SFM at passage 44 (118.28 CPD) with a seeding density of 4.72×10^5 cells. WSK368 harvested from K-SFM after 7 days at passage 45 (P1*) had a mean count of 2.29×10^6 cells (2.27 PD). The cells were reseeded at 4.57×10^5 cells and achieved a mean count of 7.92×10^5 cells (0.77 PD) after 18 days at passage 46 (P2*). Figure 3.3.20 (b) shows the growth trend of WSK368 in the feeder system from passage 43 to 46 and parallel passages in K-SFM; passage 45 (P1*) and passage 46 (P2*). The growth rate decline observed in SK206AK at P1* was sudden and was followed by a very slow rise at P2*. Whereas WSK368 gradually slowed down at P1*

followed by further reduction in growth rate at P2*. Both cell strains did not show further proliferation past P2* and the cultures were discontinued as cell numbers were too low to count.

a) **b)**

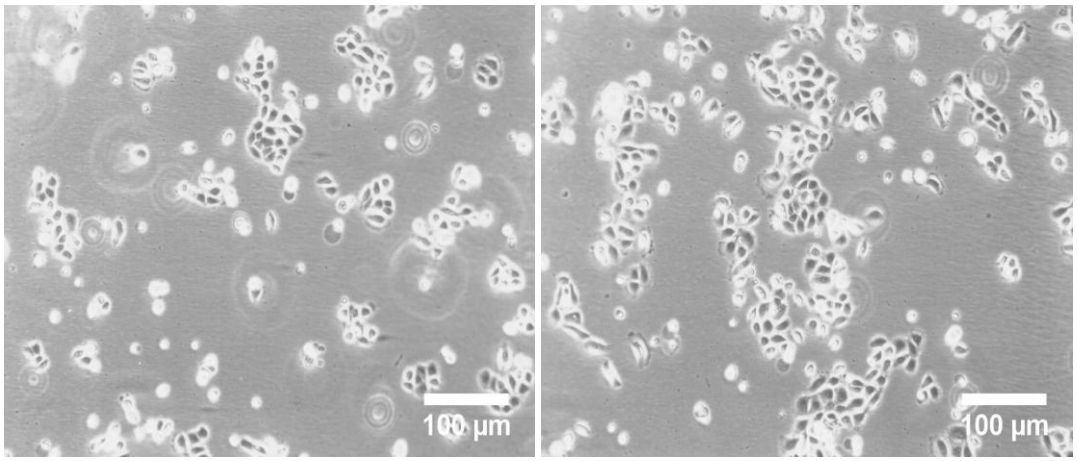

Figure 3.3.19 Photographs of normal and Werner's syndrome keratinocytes after transfer to K-SFM Keratinocytes from a) Normal (SK206AK) (passage 22, 56.17 CPD) and b) WS (WSK368) (passage 44, 118.28 CPD) strains transferred to K-SFM. (Size bar=100µm).

a)

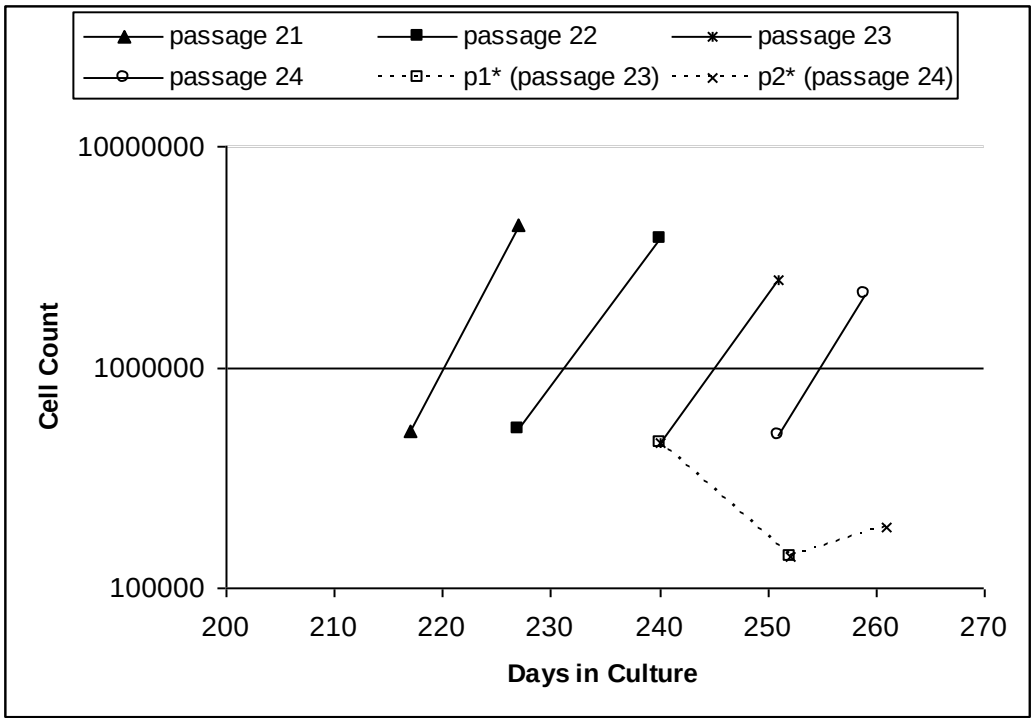

Figure 3.3.20 a) Changes of growth trends after transfer of normal keratinocytes to K-SFM Growth trends of consecutive passages of normal keratinocytes (SK206AK) grown in the feeder system and two passages after their transfer to K-SFM, P1* (passage 23) and P2* (passage 24).

b)

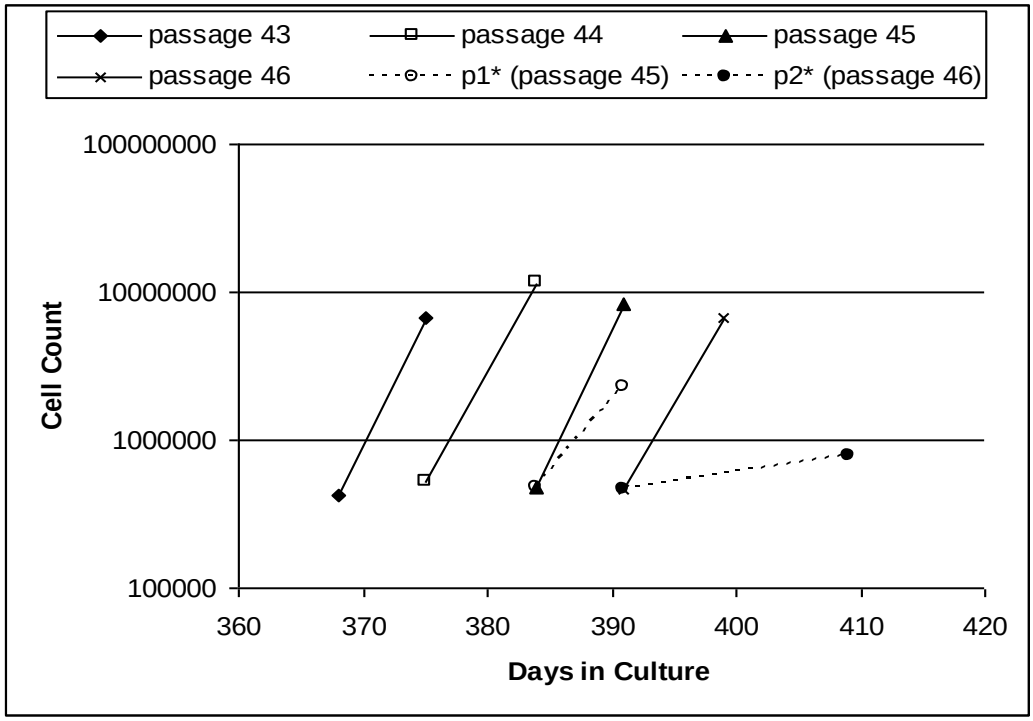

Figure 3.3.20 b) Changes of growth trends after transfer of Werner's syndrome keratinocytes to K-SFM Growth trends of consecutive passages of Werner's syndrome keratinocytes (WSK368) grown in the feeder system and two passages after their transfer to K-SFM, P1* (passage 45) and P2* (passage 46).

3.3.3.3.2 Dependence on feeder cells and growth factors

WSK368 and SK206AK were cultured in Rheinwald and Green (R and G) media in the absence of feeder cells to test if the keratinocytes have transformed and are able to grow independent of a feeder layer. The cell strains demonstrated an increase in cell size when they were transferred to R and G media, without the presence of a feeder layer and appeared to be stretching out for contact to the surrounding cells (figure 3.3.21). Subsequently, an apparent reduction in Ki67 and increase in involucrin labelling was observed in both SK206AK (figure 3.3.22) and WSK368 (figure 3.3.23) cultures when they were grown in R and G media without the feeder layer.

Transformed keratinocytes may acquire independence of essential cell culture supplements (which includes cholera toxin, hydrocortisone and epidermal growth factor). Therefore, keratinocytes were cultured in DMEM media supplemented with 10 % FCS in the presence of feeder cells but lacking cholera toxin, hydrocortisone and epidermal growth factor. As a result, keratinocyte colonies did not expend and had differentiated in a cluster in the middle of feeder cells (figure 3.3.24). This indicates that the supplements in the Rheinwald and Green medium and the feeder cells are equally required for normal proliferation of both normal (SK206AK) and WS (WSK368) keratinocyte strains.

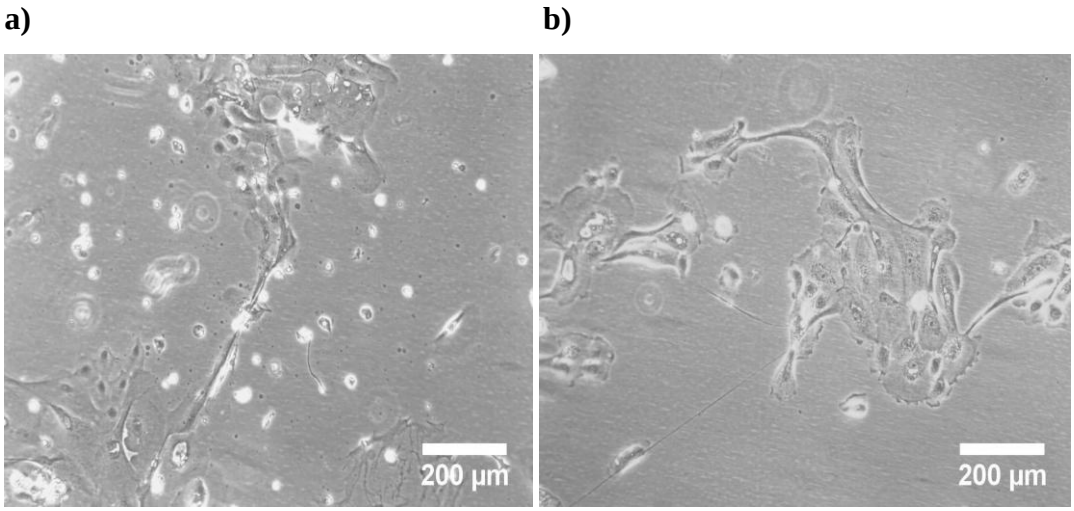

Figure 3.3.21 Exclusion of feeder layer from normal and Werner's syndrome keratinocyte cultures Normal **a)** SK206AK (passage 18, 43.7 CPD) and Werner's syndrome **b)** WSK368 (passage39, 100.23 CPD) keratinocytes transferred to Rheinwald and Green media without feeder cells.

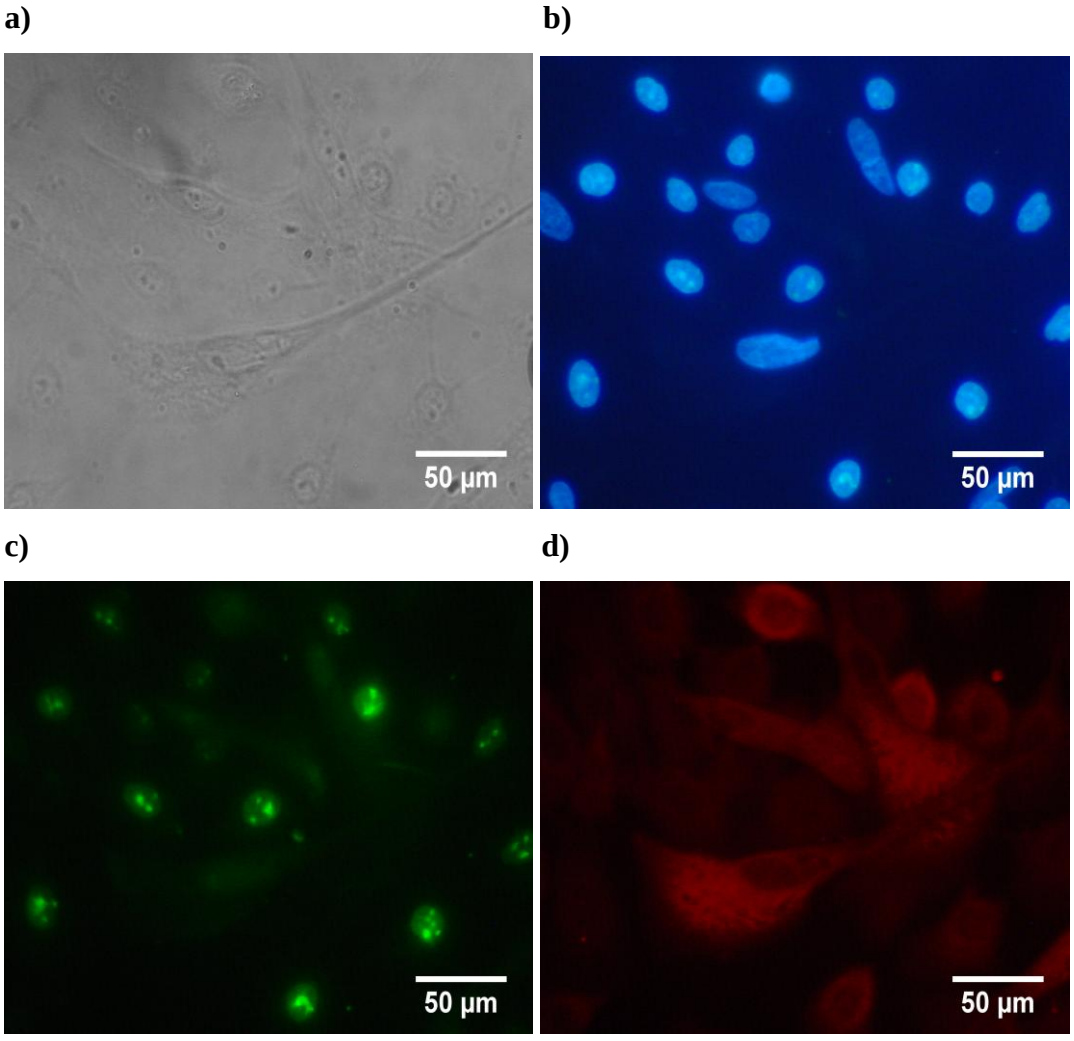

Figure 3.3.22 Photographs of light microscope view of normal keratinocytes, DAPI and fluorescence labelling of Ki67 and involucrin after exclusion of feeder cells a) light microscope, b) DAPI staining and fluorescence labelling of c) Ki67 and d) involucrin in SK206AK (passage 18, 43.7 CPD) that were transferred to R and G media without feeder cells.

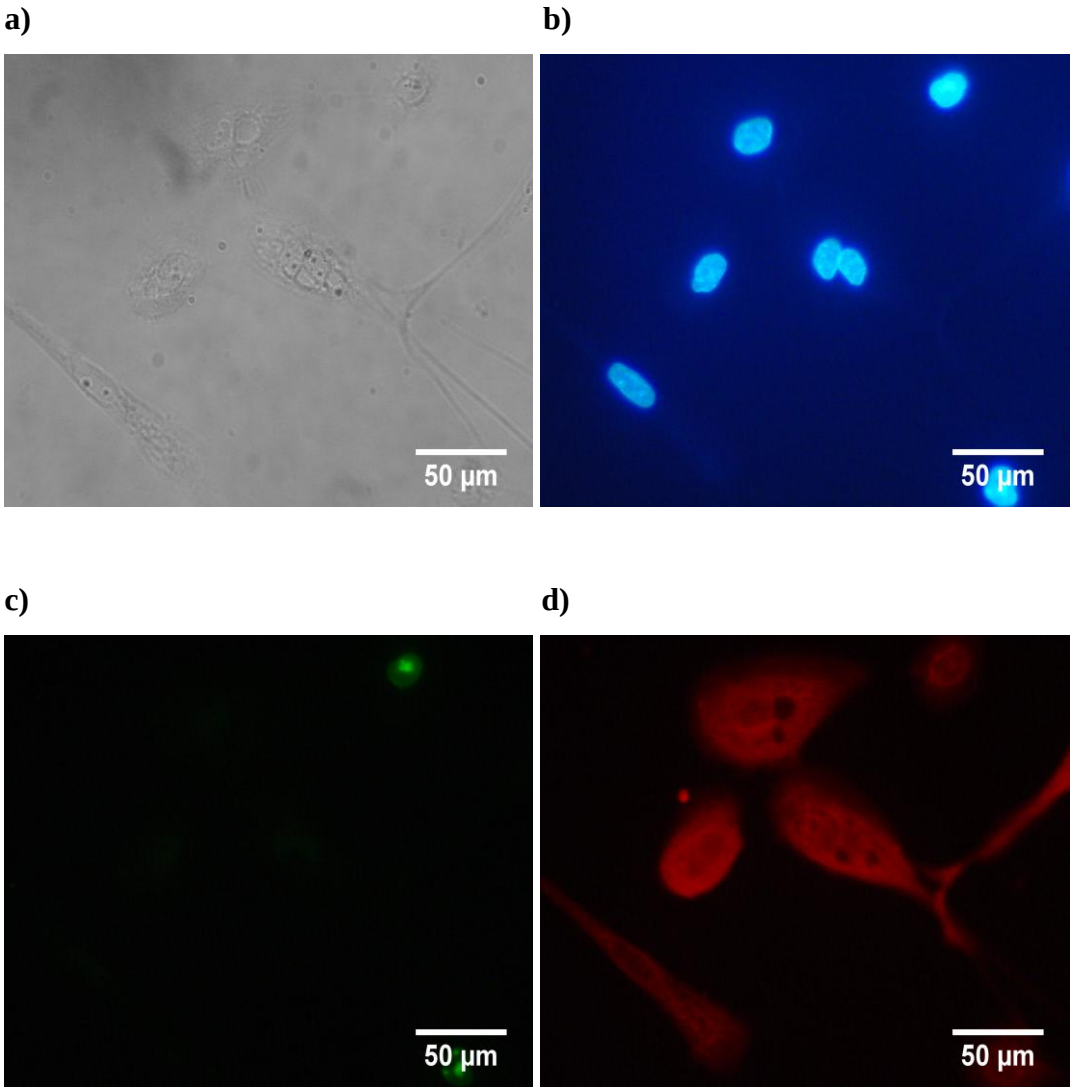

Figure 3.3.23 Photographs of light microscope view of Werner's syndrome keratinocytes, DAPI and fluorescence labelling of ki67 and involucrin after exclusion of feeder cells a) light microscope, b) DAPI staining and fluorescence labelling of c) Ki67 and d) involucrin in WSK368 (passage 39, 100.23 CPD) that were transferred to R and G media without feeder layer.

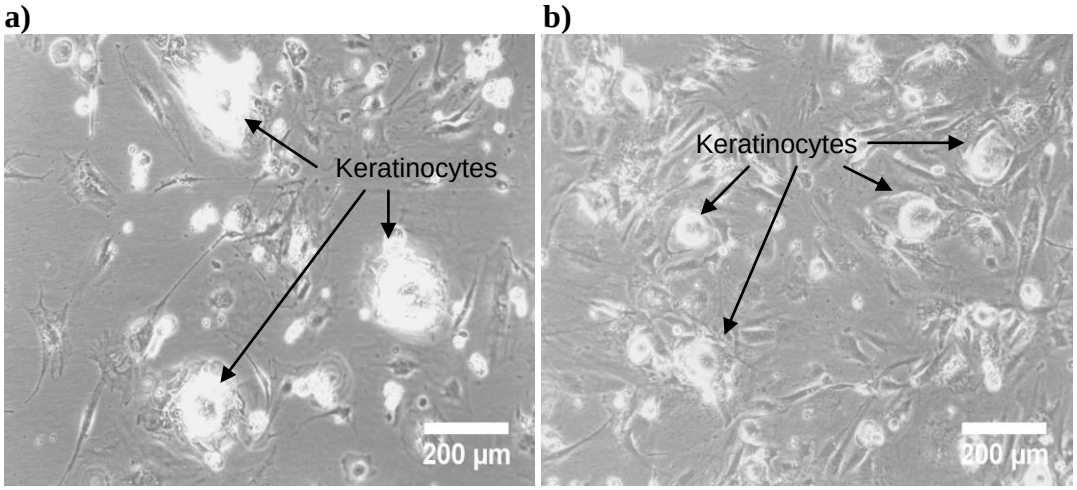

Figure 3.3.24 Photographs of normal and Werner's syndrome keratinocytes transferred to media without keratinocyte essential growth supplements in the presence of feeder cells Normal **a)** SK206AK (passage 18, 43.7 CPD) and Werner's syndrome **b)** WSK368 (passage39, 100.23 CPD) keratinocytes transferred to DMEM media with 10% FCS without keratinocyte essential growth supplements in the presence of feeder cells. Keratinocytes are marked by the arrows, all other cells are mostly feeder cells.

3.3.3.4 Cell cycle check point proteins p16 and p53 expression in Werner's syndrome keratinocytes

Cellular senescence through its various mechanisms is activated by two main cell cycle inhibitor proteins, p53 and p16 (Campisi 2005). Mutation of either can result in the transformation of cells. Therefore, investigation of p53 and p16 cell cycle inhibitors in SK206AK and WSK368 was carried out. Western blot analysis demonstrated that p16 and p53 were present at different population doublings in both SK206AK and WSK368 (figure 3.3.25).

The p16 expression trends in SK206AK were observed as high expression at passage 4 that dropped at passage 12 and increased again in passage 22. WSK368 expressed high levels of p16 at passage 6 which was decreased at passage 22 and slightly increased again at passage 45. Trends of p53 expression in SK206AK demonstrated a slight decrease in passage 12 compared to passage 4 followed by a two fold increase in passage 22. WSK368 trends of p53 demonstrated a slight increase in passage 22 compared to passage 6 followed by a slight decrease in passage 45 (figure 3.3.26 and 3.3.27). The trends of p53 and p16 expression in both SK206AK and WSK368 did not display a clear pattern. Therefore, examination of changes with age in culture is not possible with the current data.

Levels of p16 and p53 increased following one passage after transfer from the feeder system to K-SFM in both SK206AK (passage 23, P1*) and WSK368 (passage 46, P1*). The increase in p16 levels was by two fold in SK206AK (passage 23, P1*) and six fold in WSK368 (passage 46, P1*) (figure 3.3.26). Levels of p53 increased slightly in SK206AK (passage 23, P1*) whereas levels in WSK368 (passage 46, p1*) increased by four folds (figure 3.3.27). Furthermore, a second band of reduced molecular size was observed in the p53 Western blots characteristic of both SK206AK (passage 23, P1*) and WSK368 (passage 46, p1*) transferred to K-SFM (figure 3.3.25 and 3.3.28). The changes in p16 and p53 expression due to transfer of cells to K-SFM were accompanied by growth rate deterioration and eventually growth arrest.

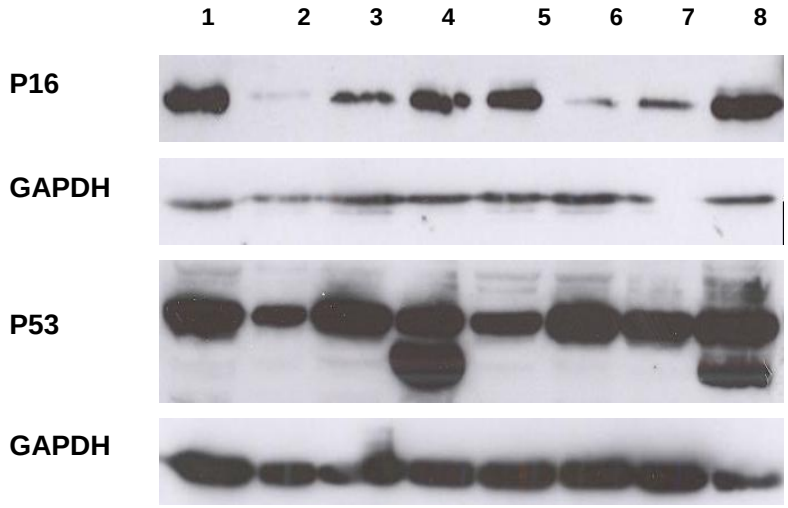

Figure 3.3.25 Western blot detection of p16 and p53 in normal and Werner's syndrome keratinocytes Western blots of p16 and p53 in normal (SK206AK; 1) passage 4, 2) passage 12, 3) passage 22, 4) passage 1* in K-SFM) and Werner's syndrome (WSK368; 5) passage 6, 6) passage 22, 7) passage 45 and 8) passage 1* in K-SFM) keratinocytes demonstrating bands at various passages grown in the feeder system and one passage after they were transferred to K-SFM (P1*). The bands were normalised against GAPDH.

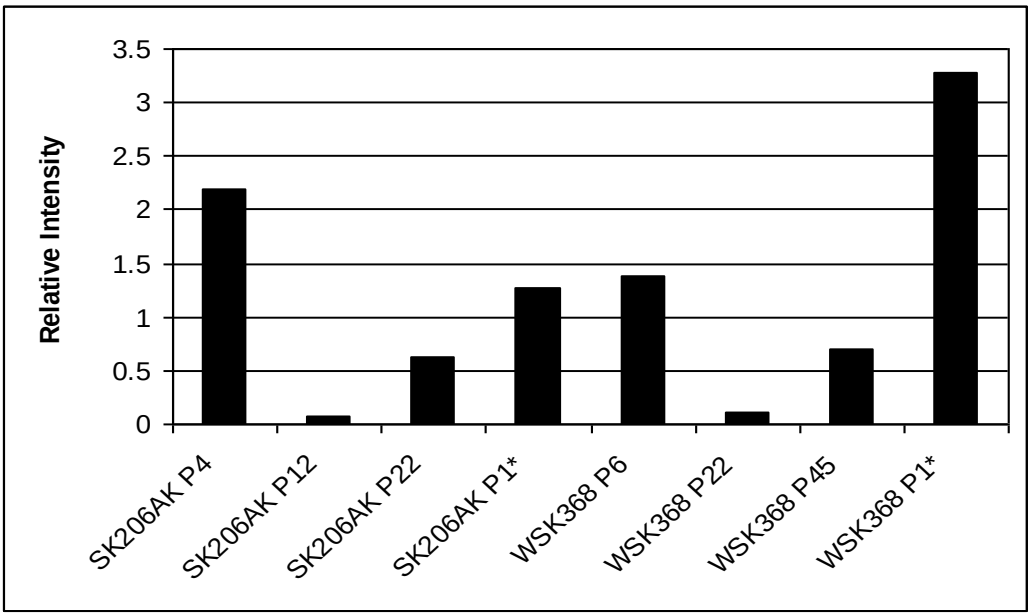

Figure 3.3.26 Analysis of p16 protein levels in normal and Werner's syndrome keratinocytes Analysis of western blot bands of p16 normalised against GAPDH of various passages of SK206AK (p4, p12, p22 and p1* transferred to K-SFM) and WSK368 (p6, p22, p45 and p1* transferred to K-SFM).

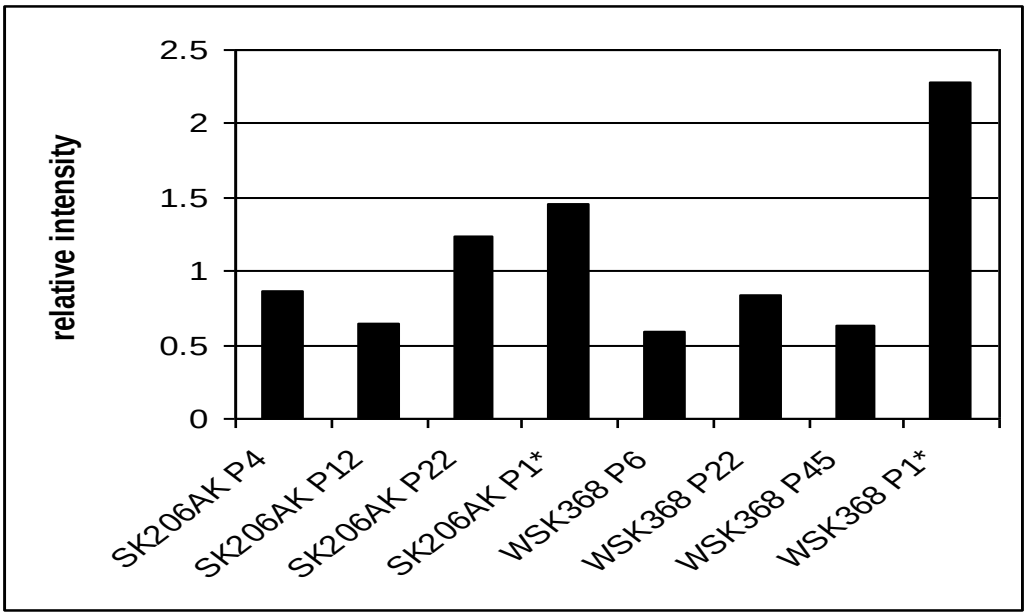

Figure 3.3.27 Analysis of p53 protein levels in normal and Werner's syndrome keratinocytes Analysis of western blot bands of p53 normalised against GAPDH of various passages of SK206AK (p4, p12, p22 and p1* transferred to K-SFM) and WSK368 (p6, p22, p45 and p1* transferred to K-SFM).

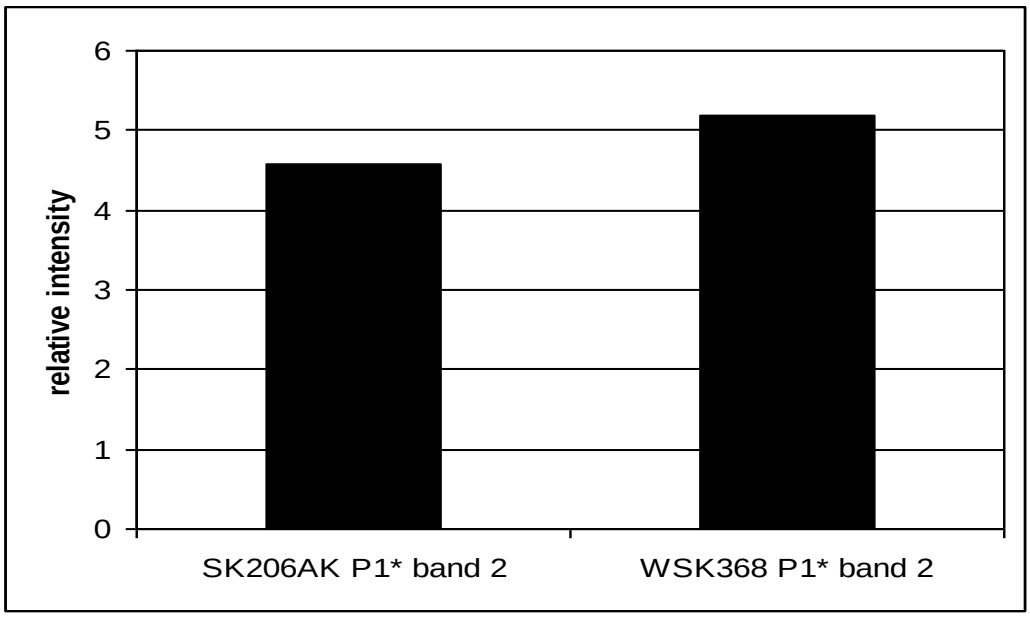

Figure 3.3.28 Analysis of second band detected in p53 western blots of normal and Werner's syndrome keratinocytes transferred to K-SFM Analysis of the second bands in the P53 western blots (expressed when cells were transferred to K-SFM) after normalising against GAPDH in SK206AK and WSK368 grown in K-SFM.

3.3.3.5 Treatment of keratinocytes with adriamycin

Acute treatment of epithelial cells with adriamycin causes cells to senesce and express SA β- galactosidase. However, in the absence of p53, adriamycin does not trigger SA β- galactosidase activity but results in delayed apoptosis (Elmore *et al.* 2002). In order to assess functionality of p53, SK206AK and WSK368 keratinocytes were treated with adriamycin and assayed for SA β- galactosidase activity. Acute treatment of keratinocytes with 1 μM adriamycin (doxorubicin) for 2 hour caused the cells to expand in size. This altered morphology became more evident after 2-3 days after treatment in both SK206AK and WSK368. SA β- galactosidase was carried out 3 days post treatment with adriamycin. Staining of cells with β- galactosidase at pH 6.0 was positive in 29.93 % of SK206AK and 60.65 % of WSK368 adriamycin treated cells (figure 3.3.29) but negative in untreated cells (figure3.3.18).

a)

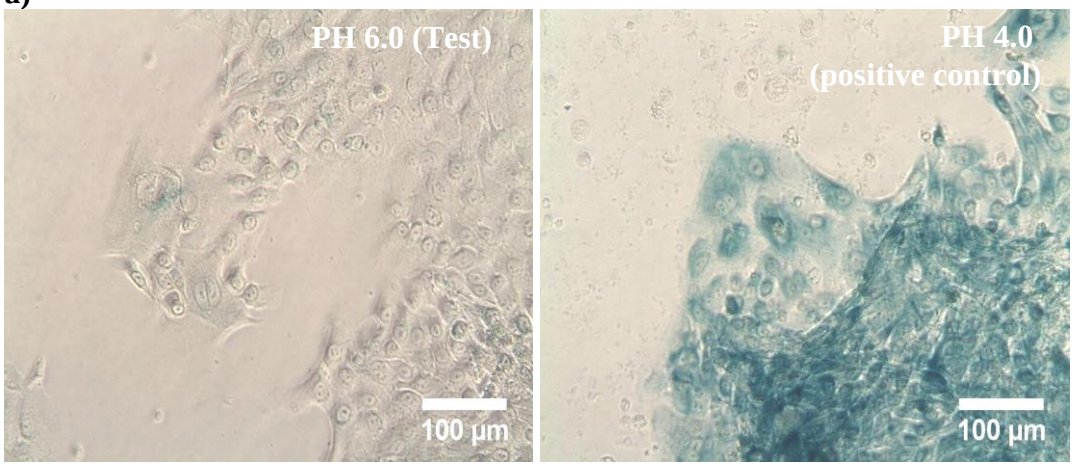

b)

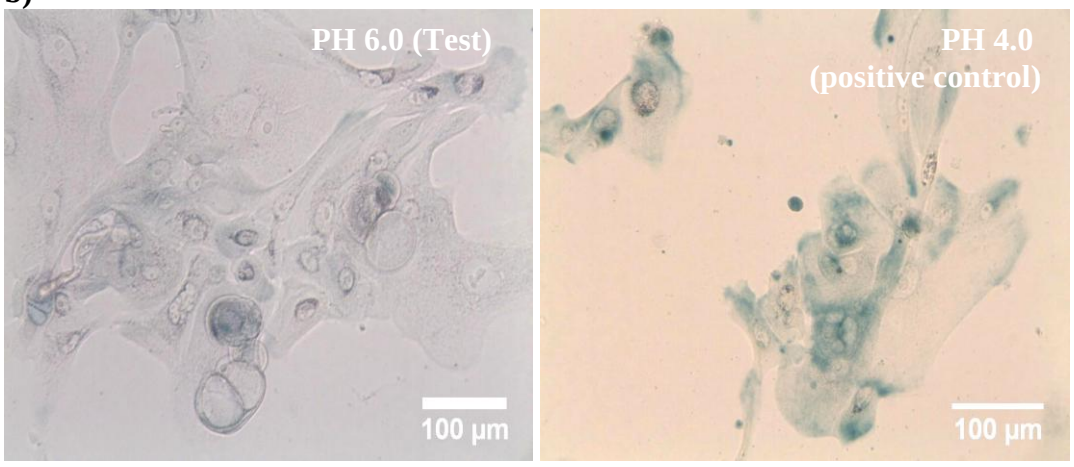

Figure 3.3.29 SA β Galactosidase assay of normal and Werner's syndrome keratinocytes keratinocytes treated with adriamycin Photographs of SA β Galactosidase assay of adriamycin treated a) normal keratinocytes (SK206AK), b) Werner's syndrome keratinocytes (WSK368). Left side photograph demonstrates senescence associated labelling of β-Galactosidase (pH 6.0) and right photograph displays the lysosomal β-Galactosidase control (pH 4.0).

3.3.3.6 Normal and Werner's syndrome keratinocyte cultures are composed of a heterogeneous clonal population

The basal layer of the epidermis contains Keratinocyte stem cells that divide to yield either stem or transient amplifying daughter cells in a stochastic manner (Houben *et al.* 2007). Basal cells, isolated from tissue and cultured in the feeder system have shown to maintain the keratinocytes in the stem cell compartment for long periods before they clonally evolve into transient amplifying cells. Keratinocyte stem cells express telomerase and p63, but do not differentiate. Transient amplifying keratinocytes on the other hand do not express telomerase, express low or undetectable levels of p63 and have a finite replicative lifespan after which they either senesce or terminally differentiate (Dellambra *et al.* 2000; Pellegrini *et al.* 2001). Keratinocytes that have committed to terminally differentiate are characterised by involucrin expression (Watt 1983; Robinson *et al.* 1996). Assessment of telomerase, p63 and involucrin would depict the heterogeneity of normal (SK206AK) and Werner's syndrome (WSK368) keratinocytes.

3.3.3.6.1 Detection of telomerase activity in normal and Werner's syndrome keratinocytes

Keratinocytes are amongst the highly regenerative cells and are known to naturally express telomerase. Telomerase expression however, takes place in keratinocyte stem cells but is repressed in the transient amplifying cells (Dellambra *et al.* 2000). Keratinocytes from different passages of SK206AK (P3, P11, P23) and WSK368 (P5, P11, P21, P46) cultured using the feeder system, were analysed for presence of telomerase activity using TRAP assay (Kim *et al.* 1994). Samples from SK206AK and WSK368 one passage after the transfer to K-SFM, primary fibroblasts Ek1Br (as a negative control) and fibroblasts that were ectopically induced to express telomerase (Ek1Br.hTERT as a positive control) were also assayed. Each sample tested was paralleled by a heat treated sample to inactivate telomerase as a negative control.

Figure 3.3.30 is a photograph of the TRAP assay containing all the samples mentioned. The samples presented with a ladder were positive for telomerase whereas samples that did not display a visible ladder were considered negative. Results of the assay demonstrate presence of telomerase activity in all passages of both SK206AK and WSK368 strains. Cells transferred to K-SFM were also positive for telomerase in both SK206AK and WSK368. Ek1Br.hTERT was strongly positive whereas the heat inactivated samples and the Ek1Br were equally negative.

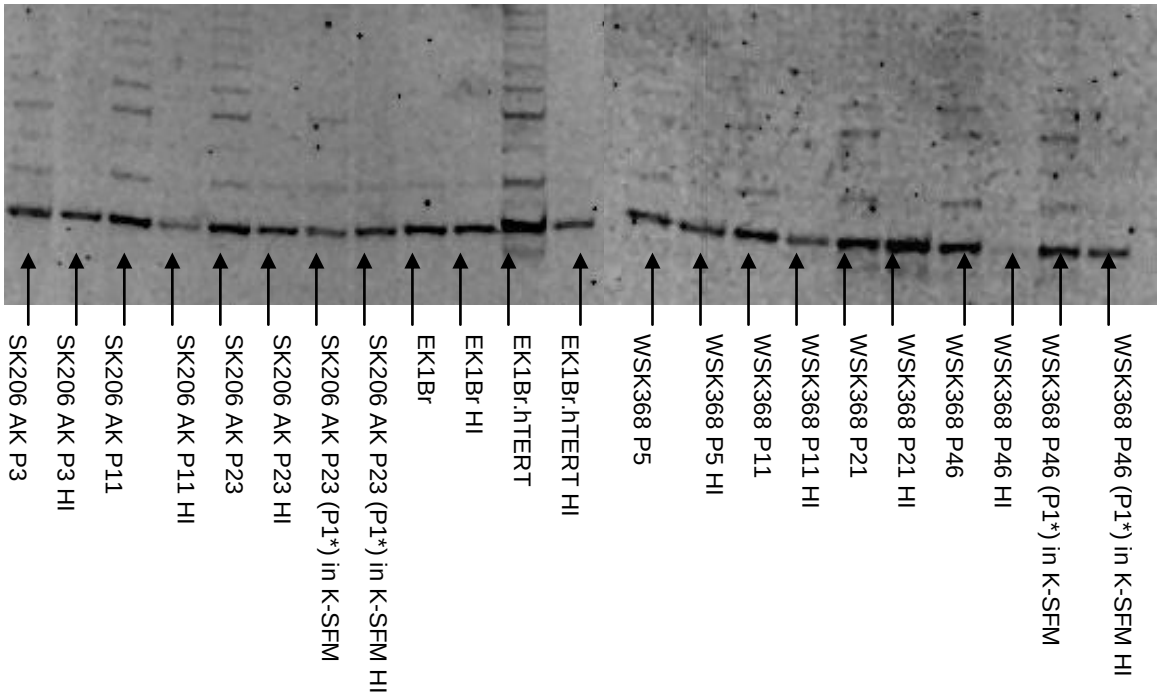

Figure 3.3.30 TRAP assay of normal and Werner's syndrome keratinocytes TRAP assay of SK206AK (passages 3, 11 and 23 in the feeder system and passage 1* in K-SFM) and WSK368 (passages 5, 11, 21 and 46 in the feeder system and p1* in K-SFM) at different passages. Primary fibroblast cell strain EK1Br and immortalised EK1Br.hTERT were used as negative and positive controls respectively. Each sample was paralleled by a heat inactivated (HI) counterpart as negative control.

3.3.3.6.2 Expression of p63 and involucrin in normal and Werner's syndrome keratinocytes

Total protein from SK206AK and WSK368 cells at different passages were collected and assayed for p63 expression (a marker of keratinocyte stem cell, holoclones) by western blot. All the samples analysed from both SK206AK and WSK368 expressed p63 (figure 3.3.31). The p63 bands detected were analysed by densitometry. The density readings obtained were normalised against GAPDH (figure 3.3.32). Levels of p63 were very high at passage 4 of SK206AK and had dropped dramatically at passage 12 and increased at passage 22. In WSK368 the levels of p63 were at its lowest at passage 6 and had substantially increased at passage 22 and dropped again at passage 45. The levels of p63 expression did not follow an age specific pattern and fluctuated between the different passages of SK206AK and WSK368.

SK206AK at very early passage P4 expressed very high levels of involucrin which had dropped in later passages. In WSK368, involucrin was slightly elevated at P6 and had dropped at P22 and rose again at P45 (figure 3.3.33).

Transfer of both SK206AK and WSK368 to K-SFM demonstrated low levels of involucrin expression (figure 3.3.33). The transfer of both SK206AK and WSK368 to K-SFM, where the cultures had reduced proliferation and expressed elevated levels of p16, maintained p63 expression and expressed low levels of involucrin.

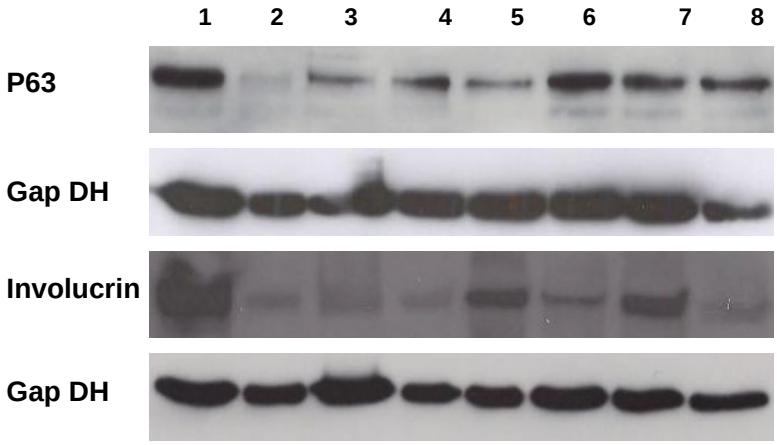

Figure 3.3.31 Western blot detection of p63 and involucrin in normal and Werner's syndrome keratinocytes Western blots of P63 and involucrin in normal (SK206AK; 1) passage 4, 2) passage 12, 3) passage 22, 4) passage 1* in K-SFM), and Werner's syndrome (WSK368); 5) passage 6, 6) passage 22, 7) passage 45 and 8) passage 1* in K-SFM) keratinocytes demonstrating are displayed in the photograph. The bands were normalised against GAPDH to ensure equal loading.

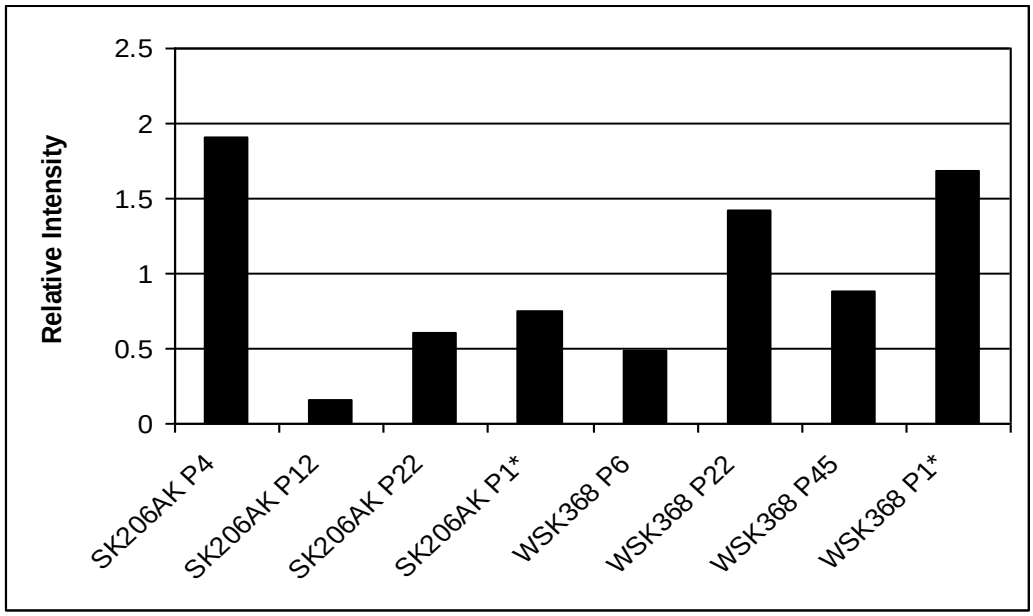

Figure 3.3.32 Densitometric measurement of p63 protein levels detected in western blots of normal and Werner's syndrome keratinocytes Levels of p63 expression at different passages in normal (SK206AK) and Werner's syndrome (WSK368) keratinocytes measured by densitometry analysis of the western blot bands normalised against bands of GAPDH. All samples were grown in the feeder system except SK206AK P1* and WSK368 P1* which were transferred to K-SFM and had been passaged once after their transfer.

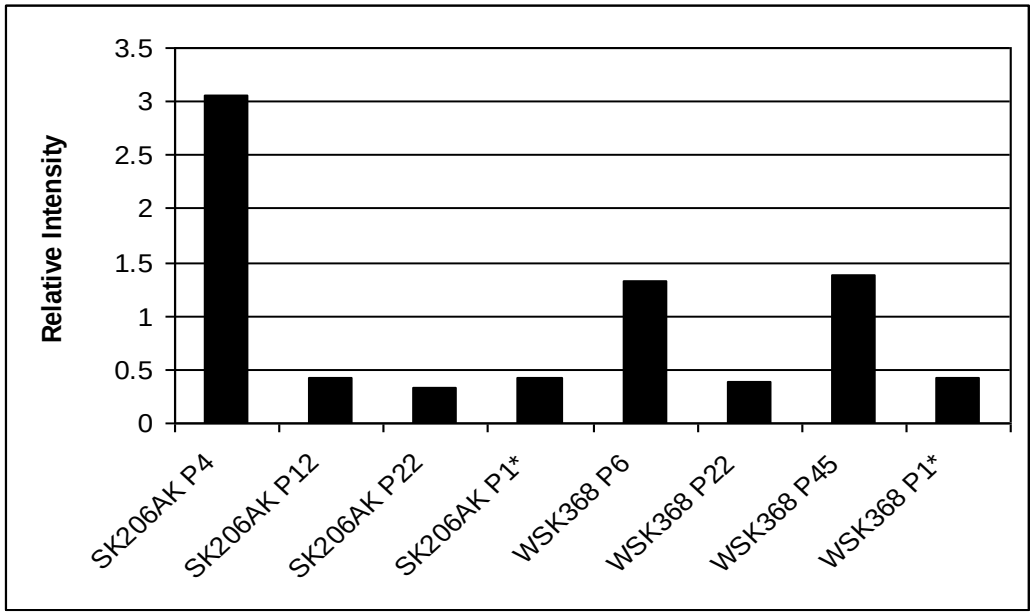

Figure 3.3.33 Densitometric measurement of involucrin protein levels detected in western blots of normal and Werner's syndrome keratinocytes Levels of involucrin expression in normal (SK206AK) and Werner's syndrome (WSK368) keratinocytes measured by densitometry analysis of the western blot bands normalised against GAPDH. All samples were grown in the feeder system except SK206AK P1* and WSK368 P1* which were transferred to K-SFM and had been passaged once after their transfer.

3.3.4 Discussion

3.3.4.1 Characterisation of the cell strains

It is important to confirm that the cells have maintained their identities and ensure that over the long term cultivation they have not been overcome by a contaminant cell type. This was carried out by monitoring cell morphology, examining surface markers, evaluating WRN expression and karyotyping.

Since the start of the study, normal (SK206AK and SKK372) and Werner's syndrome (WSK368 and WSK369) strains displayed typical keratinocyte morphology. Keratinocytes grew from single cells to macroscopic colonies as described by Rheinwald and Green (Rheinwald *et al.* 1977; Rheinwald 1980). All four cell strains were grown in the conditions set by Rheinwald and Green which favour the growth of normal primary keratinocytes and prevent the growth of fibroblasts (Rheinwald *et al.* 1977; Rheinwald 1980; Parkinson *et al.* 1992) and squamous carcinoma cells (Parkinson *et al.* 1992).

Two cell strains were studied intensively (normal (SK206AK) and Werner's syndrome (WSK368)). They were maintained in culture for a long period of time and were confirmed to be keratinocytes by imunofluorescence labelling of a wide spectrum of cytokeratins (cytokeratins 5, 6, 8, 17 and probably 19 as described by the supplier). Cytokeratins are specific markers of epithelial cells and are not expressed in fibroblasts (Fuchs 1990). Dermal fibroblasts (SKF276) were used as control and were negative for cytokeratin markers. Therefore, cytokeratin labelling had also excluded occurrence of fibroblast contamination in the keratinocyte cultures, which is known to take place in some long term cultures when opportunity arises (Parkinson *et al.* 1992).

WRN was detected in both the SK206AK and WSK368 cells by immunocytochemistry. Western blot analysis clearly showed the distinction between the two strains by identifying a band of ≈ 163 kDa in SK206AK which represents the WRN protein that was absent in WSK368. However, a band of 100 kDa was present in both cell strains (SK206AK and WSK368). This is possibly a non-specific band or degraded protein. The WRN western blots carried out on the keratinocytes had demonstrated that SK206AK expressed WRN at early and late cultures (passage 4 (8.12 CPD) and 22 (56.17 CPD)) and that WSK368 were negative for WRN at early and late cultures (passage 9 (15.28 CPD) and 45 (122.43 CPD)).

Three karyotypes from each of the two cultures were performed. SK206AK cells displayed 22 and male (X, Y) chromosomes and WSK368 cells displayed 22 and female (X, X) chromosomes. Western blot analyses confirmed that WRN is present in SK206AK and absent in WSK368. These results confirm that SK206AK and WSK368 have

maintained their identities and rule out the possibilities of cross contamination between the cultures.

3.3.4.2 Werner's syndrome keratinocyte exhibited normal growth rates and replicative lifespan

Keratinocytes from Werner's syndrome patients demonstrated normal growth rates compared to normal keratinocytes at early passages in culture immediately after isolation from tissue. Comparisons were carried out between keratinocytes from 2 normal (SK206AK and SKK372) and 2 Werner's syndrome patients (WSK368 and WSK369) in their first 5 passages after isolation from skin tissue (passage 2 to 6). The cell population doublings per day were obtained at each passage and the mean averages were plotted and compared in a bar chart. Analysis of variance between the four cultures did not detect any significant changes using ANOVA. These results demonstrate two different samples of Werner's syndrome keratinocytes (WSK368 and WSK369) that do not display features of slow growth rate in early cultures as opposed to that seen in Werner's syndrome fibroblasts (Kill *et al.* 1994).

Keratinocytes of the WSK368 were continued in culture for over 407 days and had achieved 130 CPD and continued to divide. At the time of writing, no decline in cell proliferation had been observed. The normal keratinocyte lifespan has a range of 80-150 CPD. The results in this study suggest that keratinocytes from a Werner's syndrome have maintained a normal life span. The observation of a normal growth rate in conjunction with the achievement of normal lifespan suggests that Werner's syndrome keratinocytes do not display the premature senescent phenotype demonstrated by Werner's syndrome fibroblasts (Holliday *et al.* 1985).

The cell kinetics of Werner's syndrome keratinocytes was similar to that seen with normal keratinocytes. The proliferation marker, Ki67, used to label both normal and Werner's syndrome keratinocytes, demonstrated a straight line. The ratio between Ki67 and increasing cumulative population doubling remained constant. The data were statistically interpreted using Kendall's test for correlation coefficiency, SK206AK ($\tau = 0.066$, $p > 0.05$) and WSK368 ($\tau = 0.137$, $p > 0.05$). These tests rule out upward or downward trends of Ki67 with increasing cumulative population doublings in both normal and Werner's syndrome keratinocytes. Furthermore, the percentages of Ki67 positive cells were not significantly different between SK206AK and WSK368. These results suggest that the fraction of proliferative cells do not vary between normal and Werner's syndrome keratinocytes.

The fraction of differentiating keratinocytes was estimated in both normal and Werner's syndrome keratinocytes at different passages by immunofluorescence labelling of involucrin. The exact counts could not be achieved without ruling out the possibility of errors. This was due to variations in levels of involucrin expressed by each cell (Robinson *et al.* 1996) and therefore variations in the intensity of fluorescence between cells. Nevertheless, all suspected involucrin positive cells were counted. Observations including the highest counts indicate that involucrin staining was maintained at below 15% in both normal and Werner's syndrome cell populations. This suggests that majority of the cells were not differentiated. Involucrin levels were noticeably highest in the earliest passages of both SK206AK (passage 4) and WSK368 (passage 6). This may be due to a high number of differentiated cells that were present in early stages after isolation of cells from the tissue. Because the culture conditions favour proliferation, later passages would contain more proliferating basal cells and fewer involucrin positive (differentiating) cells.

Expression of involucrin was confirmed in SK206AK and WSK368 using Western blot. In SK206AK involucrin protein levels were at the highest density at passage 4, the levels decreased by six folds at passages 12 and slightly decreased again at passage 22. In WSK368 involucrin protein levels decreased by three fold at passage 22 from passage 6 and rose by three fold again at passage 45. The pattern of involucrin expression analysed by Western blot did not match the pattern of involucrin positive cells detected by immunocytochemistry but do share the high level seen in the earliest passage. This means that the involucrin protein levels were not proportionate to the number of involucrin positive cells except in the earliest passage. This is again due to variations between cells in levels of protein expressed (i.e. some involucrin positive cells may have higher levels of involucrin expression than other involucrin positive cells). This is attributed to the variation in the number of differentiating cells as well as stages of differentiation in each passage.

Screening for senescent keratinocytes was carried out by senescence associated β-galactosidase staining (SA β-gal). SA β-gal staining is the X-gal staining of β-galactosidase in cells at pH 6.0. Staining at pH 4.0 is lysosomal β-galactosidase which is always positive and is used as control alongside SA β-gal (Dimri *et al.* 1995). It has however been demonstrated that SA β-gal is in fact lysosomal β-galactosidase that most probably does not have a role in cellular senescence (Lee *et al.* 2006). Nevertheless, the rise in β-galactosidase at pH 6.0 that is detected as a consequence of cells entering senescence can be useful for monitoring and screening for senescence in culture. Furthermore, it has been demonstrated that proliferating, quiescent and differentiated

cells do not stain for SA β-gal (Dimri *et al.* 1995) making it a reliable indicator of senescence.

SA β-gal staining of keratinocytes from both SK206AK and WSK368 at several passages was negative. The negative SA β-gal staining alongside stable growth rates and positive Ki67 expression throughout the lifespan of the cultures confirms that replicative senescence did not occur in either SK206AK or WSK368 strains. Positive β-galactosidase staining was detected in keratinocytes that were stained at pH 4.0 in all the passages. Furthermore, SK206AK and WSK368 were treated with adriamycin, an anthracyclin drug that has shown to induce DNA damage resulting in p53 activated senescence (Elmore *et al.* 2002), and assayed for SA β-gal staining. The treatment resulted in enlargement of cells and SA β-gal positive staining, suggesting that cells from both SK206AK and WSK368 strains entered senescence. Percentage of SA β-gal staining in WSK368 was higher than that seen in SK206AK. The percentage estimations imply that increased sensitivity of Werner's syndrome keratinocytes is observed. These results however need further confirmation by increasing the number of experiments and carrying out additional assays such as Comet analysis.

3.3.4.3 Werner's syndrome keratinocytes exhibit properties of stem cells

The long lifespan of WSK368 in culture and the absence of cellular senescence, or decline in their proliferative capacity, prompted the investigation of the cause of this phenotype. Telomerase activity is a feature of immortalised cell lines, cancer cells, germ cells and highly regenerative cells. Keratinocytes are amongst the highly regenerative cells that naturally express telomerase (Taylor *et al.* 1996; Shay *et al.* 1997). However, telomerase expression is maintained in keratinocytes that are in the stem cell compartment. Keratinocytes that have clonally evolved into transient amplifying cells discontinue expressing telomerase (Dellambra *et al*. 2000; Fu *et al*. 2003; D'Addario *et al*. 2010).

Therefore, detection of telomerase expression was carried out in SK206AK and WSK368 at various passages using the TRAP assay (Kim *et al.* 1994). Both SK206AK and WSK368 strains were positive for telomerase expression at all passages. This suggests that the SK206AK and WSK368 keratinocytes are, possibly, still retained in the stem cell compartment or have spontaneously transformed.

Keratinocytes in the stem cell compartment have shown to specifically express high and detectable levels of p63. Pellegrini *et al* (2001) demonstrated that p63 detected by western blot is highly expressed in holoclones (keratinocyte stem cells). The transient

amplifying keratinocytes; meroclones demonstrated hardly any detectable levels of p63 and paraclones were negative for p63 expression (Pellegrini *et al.* 2001). SK206AK and WSK368 were examined for the characteristics of populations containing stem cells by carrying out a western blot for the detection of p63. Expression of p63 was present at all passages of both WSK368 and SK206AK cultures confirming the presence of holoclones.

Clonal evolution is required to take place in keratinocytes prior to their entry into cellular senescence, this was demonstrated by studies that have shown that forced inhibition of clonal evolution by silencing 14-3-3 σ (Dellambra *et al.* 2000), p16 (Maurelli *et al.* 2006; Cordisco *et al.* 2010) or overexpressing YAP-1 (D'Addario *et al.* 2010) cause the keratinocytes to remain in the stem cell compartment as holoclones. Keratinocytes in the stem cell compartment are considered immortal until stimulated to clonally evolve (Dellambra *et al.* 2000; Maurelli *et al.* 2006; Cordisco *et al.* 2010; D'Addario *et al.* 2010).

Growth dynamics show that SK206AK and WSK368 have prolonged lifespans, maintain a proliferative state and do not demonstrate decline in growth rates. Endogenous expression of telomerase and detectable levels of p63 suggest that both SK206AK and WSK368 are composed of a population of holoclones that did not clonally evolve. Therefore, the upward growth dynamics demonstrated in the WSK368 strain is due to the presence of keratinocytes that have remained in the stem cell compartment as holoclones. This explains the long lifespan of over 130 CPD observed in WSK368 keratinocytes. This long lifespan would probably be evident in SK206AK if the cells were continued in culture after their last passage (P24) at which they achieved 60.7 CPD.

3.3.4.4 Werner's syndrome keratinocytes preserve normal culture requirements

It has been established that normal keratinocytes would terminally differentiate in the absence of feeder cells (Rheinwald *et al.* 1980). Both SK206AK and WSK368 demonstrated typical keratinocyte colony forming phenotype surrounded by irradiated 3T3 feeder cells. When SK206AK and WSK368 were transferred to cultures in the absence of feeder cells, they suddenly slowed down their rates of proliferation and mostly ceased to divide. The slow growing keratinocytes had enlarged in size and the peripheral cells migrating away from the colony are probably in search of fibroblasts. Keratinocytes in the centre of the colony maintained normal proliferating cell morphology for a slightly longer period before they started to behave like the peripheral cells. Increased differentiation in SK206AK and WSK368 grown in the absence of feeder cells was

confirmed by increased levels of involucrin demonstrated by immunofluorescence staining.

It has been reported that keratinocytes in their senescent state are positive for SA β-galactosidase but are negative in their differentiated state (Dimri *et al.* 1995). SA β-galactosidase staining was not present in SK206AK and WSK368 cultures without feeder cells, confirming that the cells had terminally differentiated and had not entered senescence.

Cholera toxin, hydrocortisone and epidermal growth factor are essential supplements for the proliferation of both SK206AK and WSK368. Transfer of SK206AK and WSK368 to a culture media of DMEM with 10% FCS without the supplements caused the cells to enlarge in size and display characteristics of differentiation even in the presence of feeder cells. This indicates that the keratinocytes maintained their dependence on supplements which include hydrocortisone, cholera toxin and epidermal growth factor in addition to their requirement for feeder cells.

Keratinocytes that were transferred to K-SFM at passage 1* were analysed for the presence of telomerase activity by TRAP assay and the presence of p53 and p16 expression by western blot. Passage 1* in K-SFM of both SK206AK and WSK368 strains had maintained telomerase expression. This suggests that keratinocytes from normal and Werner's syndrome exit the cell cycle when transferred to K-SFM even in the presence of telomerase activity. However, bands of SK206AK passage 1* demonstrated in the TRAP assay were fainter than bands of passage 23 in the feeder system suggesting a reduction in telomerase upon transfer to K-SFM. Later passages in K-SFM may demonstrate decline of telomerase activity with time if maintained in culture as keratinocytes grown in K-SFM are known to inactivate telomerase expression (Fu *et al.* 2003).

Levels of p16 increased substantially by more than 2 fold in SK206AK and dramatically by more than six fold in WSK368 in the first passage after transfer to K-SFM. This observation was demonstrated in other studies by Cordisco *et al* (2010) which showed that downregulation of Bmi-1 correlated with the immediate increase in p16 levels in keratinocytes transferred from the feeder system to K-SFM. Western blot analysis demonstrated that levels of p53 increased slightly in SK206AK and by two fold in WSK368 and had demonstrated an additional band of a smaller molecular size. The cells proliferative potential dropped in both SK206AK and WSK368 at passage 1*. This suggests that changes in p16 and p53 expression were involved with growth regulation of both SK206AK and WSK368 transferred to K-SFM. The increase in p53 and p16 following transfer to K-SFM was higher in WSK368 than in SK206AK suggesting

possible increased sensitivity of Werner's syndrome keratinocytes to stress and DNA damage. This coincides with the results observed in the SA β-Gal assay of adriamycin treated cells (which showed higher SA β-Gal staining in Werner's syndrome keratinocytes than in normal). However, Werner's syndrome keratinocytes transferred to K-SFM had a less pronounced growth rate decline than that seen in normal keratinocytes, which contradicts the evidence for hypersensitivity. Further studies are needed to assess the extent of sensitivity of Werner's syndrome keratinocytes to stress and DNA damage.

Immediate decline in cell proliferation upon transfer to K-SFM in the presence of telomerase activity and sudden upregulation of p16 and p53 suggests that the mechanism of induced senescence demonstrated in SK206AK and WSK368 were p16 and p53 regulated but independent of telomere. These findings suggest that the mechanism of induced senescence in normal and Werner's syndrome keratinocytes are the same.

3.3.4.5 Cell cycle inhibitor proteins p53 and p16 expression in Werner's syndrome keratinocytes

Western blot analysis confirmed that p53 and p16 were being expressed in both the normal SK206AK and WSK368 cell strains. P53 is the most common mutated tumour inhibitor in most cancers (Levine 1997). Presence of p53 in SK206AK and WSK368 demonstrates that they have not lost p53 expression. Elmore *et al* (2002) demonstrated that cells treated with adriamycin enter senescence but enter apoptosis when p53 is inactivated by E6. This suggests that adriamycin induced senescence requires functional p53. SK206AK and WSK368 entered senescence following adriamycin treatment as confirmed by SA-β Gal staining. These results confirm that p53 is present and functional in SK206AK and WSK368 cells

Studies have demonstrated that p16 expression is higher in transient amplifying cells than in keratinocyte stem cells (Cordisco *et al.* 2010). Western blot analysis demonstrated presence of p16 and involucrin expression in both SK206AK and WSK368 at early and late population doublings. These findings suggest that clonal evolution and differentiation occurs in all ages of SK206AK and WSK368 cultures.

3.3.4.6 Screening normal and Werner's syndrome keratinocytes for transformation

Spontaneous transformation is a common feature of mouse cells but is rare in human epithelial cells. Nevertheless, spontaneous transformation of human keratinocytes has been reported (Rea *et al.* 2006).

Due to the long lifespan and presence of telomerase activity in the Werner's syndrome keratinocytes, the possibility of spontaneous transformation of these cells cannot be disregarded without screening. Reliance on normal growth conditions including feeder cells and keratinocyte media supplements suggests normal culture characteristics of both normal (SK206AK) and Werner's syndrome (WSK368) keratinocyte strains. Ability to differentiate and yield a heterogeneous population in culture is also a feature of normal untransformed cells (Rheinwald *et al.* 1980) which was demonstrated by the expression of both involucrin and p63 in SK206AK and WSK368 cultures.

Cell cycle inhibitors p53 and p16 were both expressed as detected by western blots. Detection by western blot confirms the expression of these important checkpoint proteins but does not demonstrate that they are active. Therefore, cell cycle arrest was induced in the keratinocytes by different treatments to test that both p53 and p16 were functional.

Reaction to adriamycin treatment with enlarged cell size and positive staining for SA-β-galactosidase suggests that p53 is functional (Elmore *et al.* 2002). Culture of keratinocyte in K-SFM results in p16 mediated premature senescence (Kiyono *et al.* 1998; Opitz *et al.* 2001; Fu *et al.* 2003). SK206AK and WSK368 cells enter senescence when treated with adriamycin or transferred to K-SFM. These results confirm that p53 and p16 and present and functional in SK206AK and WSK368. These results suggest that the both keratinocyte strains have maintained expression and function of the most important cell cycle check points involved in senescence throughout their long term culture.

Diploid chromosomes were demonstrated in both SK206AK and WSK368 at late passage cultures. Most of the reported cases of spontaneous transformed keratinocytes have demonstrated chromosomal aberrations in early passages (Boukamp *et al.* 1988; Allen-Hoffmann *et al.* 2000).

Further tests are required for completely ruling out spontaneous transformations in Werner's syndrome keratinocytes. These tests include long term culture of keratinocytes from other Werner's syndrome patients to complement the results obtained from the WSK368 strain. Furthermore, detailed cytogenetic analysis carried out on banded chromosomes for the detection of translocations would provide more comprehensive analysis for chromosomal abnormalities that may result in spontaneous transformation of the keratinocytes.

3.3.4.7 Properties of Werner's syndrome keratinocytes

Collection of the results obtained reveals the properties of Werner's syndrome keratinocytes in vitro. These results are summarised and concluded in this section. Population doubling rates and Ki67 index of Werner's syndrome keratinocytes (WSK368) are within the range of the normal keratinocyte culture (SK206AK). Both normal and Werner's syndrome keratinocytes have continued to proliferate and have entered the normal range of replicative lifespan for keratinocytes. The Werner's syndrome keratinocytes express p63 and telomerase which suggests presence of a population of stem cells in the culture. Furthermore, telomerase activity and prolonged replicative lifespan suggests that the Werner's syndrome keratinocyte culture may be immortal which is a proposed characteristic of normal keratinocytes grown in optimal culture conditions (Dellambra *et al.* 2000; D'Addario *et al.* 2010).

The proportion of arrested cells in normal (SK206AK) and Werner's syndrome (WSK368) keratinocyte cultures were terminally differentiated cells and not senescent. This was demonstrated by presence of involucrin expression (differentiation marker) and absence of SA-β Gal staining (indicator of senescent cells).

Presence of p63 and involucrin in all the passages tested from both SK206AK and WSK368 suggests that the keratinocytes divide in a stochastic manner giving yield to a heterogeneous population of stem cells and transient amplifying cells. Expression of p53 and p16 in both SK206AK and WSK368 was intact. The keratinocytes have demonstrated that their ability to differentiate and senesce is preserved. Differentiation was induced in the keratinocytes by transferring them to below optimal conditions such as media without supplements or feeder cells. Senescence was induced by treating the cells with adriamycin (doxorubicin). These results demonstrate that important regulatory and check point proteins are intact and functional.

There has been evidence of increased sensitivity of Werner's syndrome compared to normal keratinocytes. Transfer of Werner's syndrome keratinocytes to K-SFM demonstrated more dramatic increases in p53 and p16 expression than that seen in normal keratinocytes. However, decline of growth rates of Werner's syndrome keratinocytes transferred to K-SFM was lower than normal. In addition, senescence induced by adriamycin treatment was accompanied by higher percentages of SA-β Gal positive cells than that seen in normal keratinocytes. These findings suggest that induced senescence in response to stress or DNA damage is received with higher sensitivity in Werner's syndrome keratinocytes. However, these findings are preliminary and require further investigation.

In conclusion, Werner's syndrome keratinocytes maintain properties of a heterogeneous culture with normal growth rates and lifespan, and preserve the ability to differentiate.

Chapter 4

General Discussion

4.1 Werner's syndrome as a model for normal ageing

Although Werner's syndrome has been considered to be a rare disease (Goto 1997), its close resemblance to normal ageing makes it a valuable model for studying ageing and age related diseases (Kipling *et al.* 1997; Kipling *et al.* 2004). As opposed to the hundreds to thousands of candidate genes that are involved in normal ageing, the premature ageing features demonstrated in Werner's syndrome are caused by mutation of a single gene, WRN. However, Werner's syndrome patients display other pathological features in addition to abnormal predisposition to cancers that do not necessarily occur with age in the normal population. Additionally, symptoms that are frequent age related problems such as dementia are not characteristic of Werner's syndrome. Therefore, Werner's syndrome has been classified as a segmental progeroid syndrome. Nevertheless, the segmental resemblance of Werner's syndrome to ageing has raised enough interest for using it as a model for ageing (Kipling *et al.* 1997).

4.2 Mechanisms of premature senescence in Werner's syndrome fibroblasts

Accumulation of cellular senescence has been described as a cause of tissue ageing (Martin *et al.* 1970). It has been demonstrated that senescence occurs at an accelerated rate in Werner's syndrome fibroblasts (Faragher *et al.* 1993; Kill *et al.* 1994). This is reminiscent of the premature ageing feature of Werner's syndrome (Werner 1904; Epstein *et al.* 1966; Goto 1997). Premature senescence in Werner's syndrome fibroblasts has been extensively studied. The mechanism of the premature senescence however is not completely understood.

Ectopic expression of telomerase resulted in immortalisation of cultured Werner's syndrome fibroblasts (Wyllie *et al.* 2000). Furthermore, Knockout of WRN alone did not express premature ageing phenotype in mice. When TERC knockouts were introduced in conjunction with WRN-/-, the mice developed most of the premature ageing symptoms

featured in Werner's syndrome patients (Chang *et al.* 2004). These studies support telomere erosion as the principle cause of senescence in Werner's syndrome cells.

Telomere erosion in Werner's syndrome fibroblasts has been shown to occur at an increased rate to normal fibroblasts. However, the overall telomere lengths were not significantly different between normal and Werner's syndrome fibroblasts (Schulz *et al.* 1996).

Furthermore, single cell division measurements of telomere erosion using the STELA (single telomere length analysis) method demonstrated that telomere erosion does not occur at an increased rate in Werner's syndrome fibroblasts (Baird *et al.* 2004). These results suggest that even though WRN is involved in the repair of telomeres, absence of WRN does not necessarily increase telomere erosion rates.

Even though introduction of telomerase resulted in immortalisation of Werner's syndrome fibroblasts, the cells retain their slow growth rates (Davis *et al.* 2005). These results were reproduced in the growth curve in section 3.1 demonstrating telomerase immortalised Werner's syndrome fibroblasts (AG03141.hTERT) with a slower growth rate than telomerase immortalised normal fibroblasts (HCA2.hTERT). This suggests that the premature senescence in Werner's syndrome fibroblasts is not primarily caused by telomere erosion. Stalling of cells that cannot efficiently repair damaged DNA or stabilise the DNA fork during synthesis are most probably stressed. The stress activation signals the senescence pathway prior to the event of telomere shortening.

Inhibition of p38 MAPK results in the prolongation of lifespan and increased growth rate of Werner's syndrome fibroblasts as demonstrated by Davis *et al* (2005) and reproduced in section 3.1. Therefore, premature senescence in Werner's syndrome fibroblasts is stress induced, SIPS.

Telomerase immortalised Werner's syndrome fibroblasts (AG03141.hTERT) treated with SB203580 had demonstrated an increase in growth rates as demonstrated by Davis *et al* (Davis *et al.* 2005). However when reproduced in section 3.1, there was no difference in the growth rate between SB203580 treated and untreated AG03141.hTERT. Comet analysis of AG03141.hTERT treated with SB203580 and untreated did not demonstrate any differences in DNA damage and did not demonstrate any increase in DNA damage compared to SV40 immortalised normal fibroblasts (1BR.3neo) (section 3.1). These results suggest that telomerase has a protective property that compensates for the absence of WRN in response to DNA damage. This correlates with the findings in the mouse model that carries WRN-/- in conjunction with TERC-/-. This feature needs further investigation perhaps between cells with silenced WRN and isogenic controls to

reduce variations. Figure 4.1 describes a simplified suggested pathway for senescence in Werner's syndrome fibroblasts.

The work carried out in SB203580 treatment of Werner's syndrome fibroblasts in section 3.1 provide an optimised method ready for use on other cell types. The proposed plan to carry out SB203580 treatment in Werner's syndrome keratinocytes and study the effects it would have on senescence and growth rates of these cells. However, Werner's syndrome keratinocytes demonstrated normal growth rates and did not approach senescence during their time in culture (section 3.3). Therefore these experiments were not carried out.

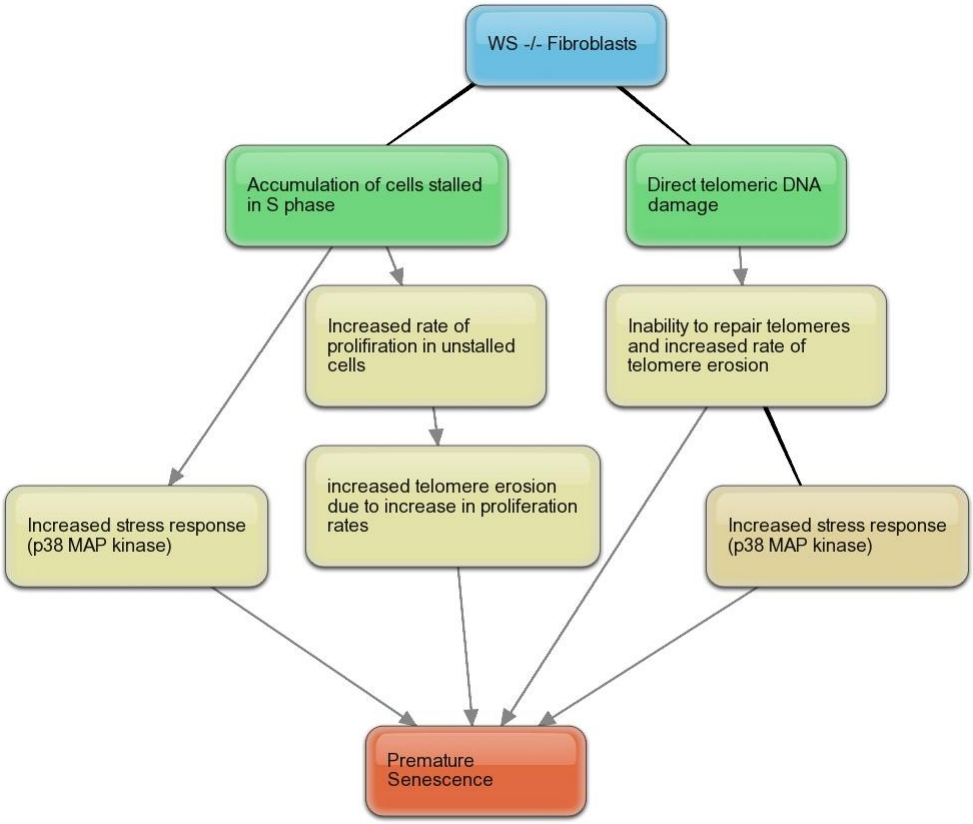

Figure 4.1 Suggested pathways for senescence in Werner's syndrome fibroblasts.

4.3 Mechanisms of senescence in Werner's syndrome keratinocytes

The studies carried out in section 3.3 demonstrate that Werner's syndrome keratinocytes cultured in the feeder system are telomerase positive and express detectable levels of p63 (marker of keratinocyte stem cells), involucrin (differentiation marker), p53

(tumour suppressor) and p16 (cyclin dependant kinase inhibitor). Response to DNA damage and stress has shown to be normal in Werner's syndrome keratinocytes. There is a possibility that Werner's syndrome keratinocytes are hypersensitive to DNA damage and stress, but this requires confirmation. The sum of these results suggest that Werner's syndrome keratinocyte cultures in the feeder system are a heterogeneous population composed of stem and transient amplifying cells.

James et al demonstrated that T lymphocytes from Werner's syndrome patients maintain normal regulation of telomerase activity and have a normal proliferative lifespan (James *et al.* 2000). Keratinocytes at the stem cell stage naturally express telomerase and continue to self renew until they clonally evolve into transient amplifying cells. Telomerase activity is repressed in transient amplifying cells and proliferation is limited. The Keratinocytes in this study were cultured under conditions that maintained optimal proliferation of the cells. TRAP assay demonstrated that telomerase activity was presumed under these culture conditions in both the normal (SK206AK) and Werner's syndrome (WSK368) keratinocytes. Werner's syndrome keratinocytes demonstrated normal population doubling rates and a prolonged replicative lifespan. These studies suggest that natural selective expression of telomerase acts as a protective mechanism against premature senescence in Werner's syndrome in Werner's syndrome keratinocytes.

The skin abnormalities featured in Werner's syndrome patients are very likely a result of connective tissue dysfunction which involves the dermis rather than the epithelial cells of the epidermis. Scleroderma like skin, that is the hallmark of WS, is of connective tissue origin and not epithelium. Although, Werner's syndrome patients are predisposed to cancers, the incidents of skin cancers of epithelial origin have a lower ratio in Werner's syndrome than the normal population. Epithelial to non-epithelial sarcoma has a ratio of 10:1 in normal individuals whereas in WS patients the ratio is reduced to 1:1 (Goto M 1996)**.**

Cells that naturally express telomerase including T lymphocytes, keratinocytes and the mouse model have all demonstrated that WRN mutation did not result in growth deficit or premature senescence. These findings conclude that cells with natural telomerase activity or selective telomerase activity maintain a normal replicative lifespan in Werner's syndrome (figure 4.2).

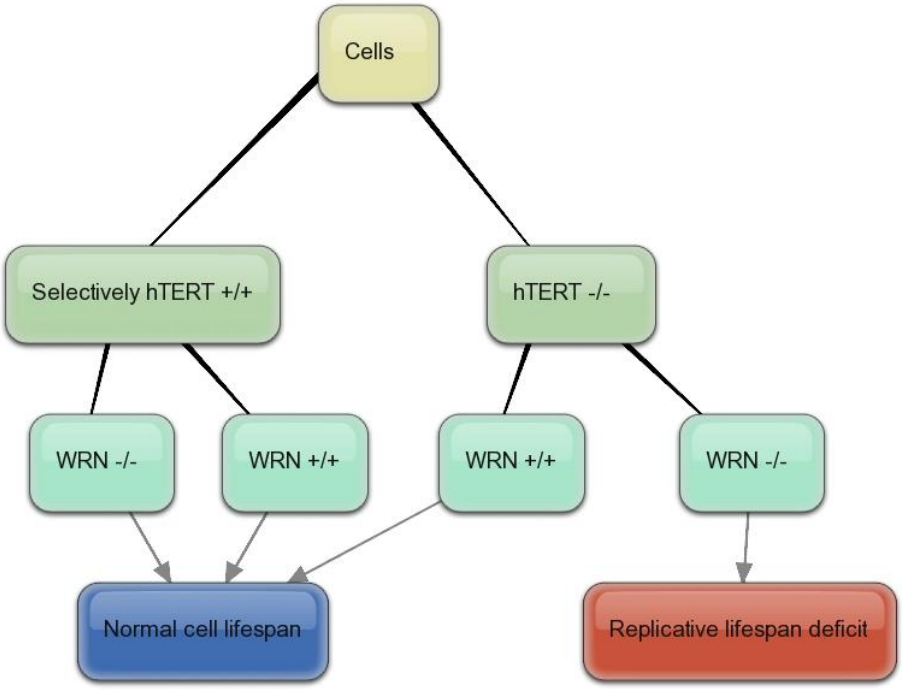

Figure 4.2 Flow chart demonstrating the replicative lifespan in naturally telomerase expressing cells and non telomerase expressing cells in the presence and absence of WRN.

4.4 Future work

WS keratinocytes have behaved in a similar manner to normal keratinocytes when transferred from feeder system to K-SFM. They both ceased proliferation after one or two passages and displayed a second band in the western blot for p53. Therefore, a more detailed analysis of growth arrested cells cultured in K-SFM would be a useful experiment. A study of apoptosis, senescence and differentiation would give us an insight to what is happening to the arrested cells. In addition, analysis of p53 in early stages of culture needs to be carried out.

Adriamycin treatment of cells results in a p53 dependent senescence. Absence of p53 would cause apoptosis of the cells (Elmore *et al.* 2002). These cellular characteristics lead us to use adriamycin treatment for the assessment of p53 functionality (section 3.3). The positive SA-β Gal staining indicated that both normal and Werner's syndrome keratinocytes that were tested have entered senescence suggesting normal p53 activity. However, p53 sequencing would be more conclusive for the confirmation of functional competence of p53 in the keratinocytes and would therefore be a suggestion for future studies.

The study of keratinocytes from Werner's syndrome compared to normal have demonstrated fluctuations in levels of p16, p53, p63 and involucrin protein expression (section 3.3). However, studying the relevant changes is difficult due to patient to patient

variations. WRN knockdown in normal keratinocytes, for the production of isogenic material, would provide more reliable results by significantly reducing variations between samples. Elimination of WRN would also introduce material for the study of other DNA repair pathways that do not require WRN.

Transfer of Werner's syndrome keratinocytes to K-SFM and treatment with adriamycin has shown high sensitivity compared to normal keratinocytes. COMET analysis is required to assess hypersensitivity of Werner's syndrome keratinocytes to DNA damaging agents.

Cultured T lymphocytes selectively express telomerase and have shown to have normal replicative lifespan in the absence of WRN (James *et al*. 2000). This is due to the selective expression of telomerase in T lymphocytes. Werner's syndrome T lymphocytes express variegated translocation mosaicsm (Scappaticci *et al.* 1990) despite their normal *in vitro* replicative lifespan. This evidence suggests that the premature ageing symptoms of Werner's syndrome are not due to the mutator phenotype. It has been demonstrated in the results of this thesis, that keratinocytes from Werner's syndrome displayed diploidy by unbanded karyotyping. Analysis of banded karyotype to determine whether Werner's syndrome keratinocytes display VTM would prove valuable and would add to the conclusion that premature ageing in Werner's syndrome is a result of increased rate of replicative senescence.

Studies of cells from systems that do not exhibit symptoms in Werner's syndrome patients would improve understandings of the causes of the disease. For example, analysis of cells from the nervous system of Werner's syndrome patients such as astrocytes may provide answers to why the nervous system of Werner's syndrome patients is not affected.

5.0 References

Allen-Hoffmann B L, Schlosser S J, Ivarie C A R, Sattler C A, Meisner L F and O'Connor S L (2000). "Normal Growth and Differentiation in a Spontaneoulsly Immortalized Near-Diploid Human Keratinocyte Cell Line, NIKS." The Journal of Investigative Dermatology **114**: 444-55.

Allsop R C and Harley C B (1995). "Evidence for a Critical Telomere Length in Senescent Human Fibroblasts." Experimental Cell Research **219**: 130-136.

Allsop R C, Vaziri H, Patterson C, Goldstein S, Younglai E V, Futcher B A, Greider C W and Harley C B (1992). "Telomere length predicts replicative capacity of human fibroblasts." Proceedings of the National Academy of Sciences of the United States of America **89**: 10114- 10118.

Ariyoshi K, Suzuki K, Goto M, Oshimura M, Ishizaki K, Watanabe M and Kodama S (2009). "Introduction of a Normal Human Chromosome 8 Corrects Abnormal Phenotypes of Werner Syndrome Cells Immortalized by Expressing an hTERT Gene." Journal of Radiation Research **50**: 253-9.

Baird D M, Davis T, Rowson J, Jones C J and Kipling D (2004). "Normal telomere erosion rates at the single cell level in Werner syndrome fibroblast cells." Human Molecular Genetics **13**: 1515-24.

Barrandon Y and Green H (1987). "Three clonal types of keratinocyte with different capacities for multiplication." Proceedings of the National Academy of Sciences of the United States of America **84**: 2302-6.

Baynton K, Otterlei M, Bjoras M, Kobbe C v, Bohr V and Seeberg E (2003). "WRN interacts physically and functionally with the recombination mediator protein RAD52." Journal of Biological Chemistry **278**: 36476-86.

Ben-Porath I and Weinberg R A (2005). "The signals and pathways activating cellular senescence." The International Journal of Biochemistry and Cell Biology **37**: 961-76.

Bird J, Jennert-Burston K, Bachler M, Mason P, Lowe J, Heo S, Campisi J, Faragher R and Cox L (2012). "Recapitulation of Werner syndrome sensitivity to camptothecin by limited knockdown of the WRN helicase/exonuclease." Biogerontology **13**: 49-62.

Blomen V A and Boonstra J (2007). "Cell fate determination during G1 phase progression." Cellular and Molecular Life Sciences **64**: 3084-104.

Bodnar A G, Ouellette M, Frolkis M, Holt S E, Chiu C P, Morin G B, Harley C B, Shay J W, Lichtsteiner S and Wright W E (1998). "Extension of life-span by introduction of telomerase into normal human cells." Science **279**: 334-335.

Bond J A, FHaughton M, Rowson J M, Smith P J, Gire V, Wynford-Thomas D and Wylie F S (1999). "Control of replicative life span in human cells: barriers to clonal expansion intermediate between M1 senescence and M2 crisis." Molecular and Cellular Biology **19**: 3103-14.

Boukamp P, Petrussevska R T, Breitkreutz D, Hornung J, Markham A and Fusenig N E (1988). "Normal keratinization in a spontaneously immortalized

aneuploid human keratinocyte cell line." Journal of Cell Biology **106**: 761-71.

Boukamp P, Petrussevska R T, Breitkreutz D, Hornung J, Markham A and Fusenig N E (1988). "
Normal keratinization in a spontaneously immortalized aneuploid human keratinocyte cell line." Journal of Cell Biology **106**: 761-71.

Bradford M M (1976). "A rapid and sensitive method for the quantitation of microgram quantities of protein utilizing the principle of protein-dye binding." Analytical Biochemistry **7**: 248-54.

Brenner A J, Stampfer M R and Aldaz C M (1998). "Increased p16 expression with first senescence arrest in human mammary epithelial cells and extended growth capacity with p16 inactivation." Oncogene **17**: 199-205.

BroshJr R M, Orren D K, Nehlin J O, Ravn P H, Kenny M K, Machwe A and Bohr V A (1999). "Functional and Physical Interaction between WRN Helicase and Human Replication Protein A." The Journal of Biological Chemistry **274**: 18341-18350.

BroshJr R M, vonKobbe C, Sommers J A, Karmakar P, Opresko P L, Piotrowski J, Dianova I, Dianova G L and Bohr V A (2001). "Werner syndrome protein interacts with human flap endonuclease 1 and stimulates its cleavage activity." The EMBO Journal **20**: 5791-801.

Burnette W N (1981). ""Western blotting": electrophoretic transfer of proteins from sodium dodecyl sulfate-polyacrylamide gels to unmodified nitrocellulose and radiographic detection with antibody and radioiodinated protein A." Analytical Biochemistry **112**: 195-203.

Campisi J (2005). "Senescent Cells, Tumor Suppression, and Organismal Aging: Good Citizens, Bad Neighbors." Cell **120**: 513-22.

Carrel A (1912). "On the permanent life of tissue outside of the organism." Journal of Experimental Medicine **15**: 516-528.

Cerimele D, F F C, Scappaticci S, Rabbiosi G, Borroni G, Sanna E, Zei G and Fraccaro M (1982). "High prevalence of Werner's syndrome in Sardinia. Description of six patients and estimate of the gene frequency." Human Genetics **62**: 25-30.

Chakraverty R and Hickson I (1999). "Defending genome integrity during DNA replication: a proposed role for RecQ family helicases." Bioessays **21**: 286-94.

Chang S, Multani A, Cabrera N, Naylor M, Laud P, Lombard D, Pathak S, Guarente L and DePinho R (2004). "Essential role of limiting telomeres in the pathogenesis of Werner syndrome." Nature Genetics **36**: 877-82.

Chen L and Oshima J (2002). "Werner Syndrome." Journal of Biomedicine and Biotechnology **2**: 46-54.

Cong Y-S, Wright W E and Shay J W (2002). "Human Telomerase and Its Regulation." Microbiology and Molecular Biology Reviews **66**: 407-25.

Constantinou A, Tarsounas M, Karow J K, Brosh R M, Bohr V A, Hickson I D and West S C (2000). "Werner's syndrome protein (WRN) migrates Holliday junctions and co-localizes with RPA upon replication arrest." EMBO Reports **1**: 80-4.

Cordisco S, Maurelli R, Bondanza S, Stefanini M, Zambruno G, Guerra L and Dellambra E (2010). "Bmi-1 Reduction Plays a Key Role in Physiological and Premature Aging of Primary Human Keratinocytes." Journal of Investigative Dermatology **130**: 1048-62.

Crabbe L, Verdun R E, Haggblom C I and Karlseder J (2004). "Defective telomere lagging strand synthesis in cells lacking WRN helicase activity." Science **306**: 1951-3.

Cuenda A, Rouse J, Doza Y N, Meier R, Cohen P, Gallagher T F, Young P R and Lee J C (1995). "SB 203580 is a specific inhibitor of a MAP kinase homologue which is stimulated by cellular stresses and interleukin-1." FEBS Letters **364**: 229-33.

D'Adda F, Faganga D, Reaper P M, Clay-Farrace L, Fiegler H, Carr P, vonZglinicki T, Saretzki G, Carter N P and Jackson S P (2003). "A DNA damage checkpoint response in telomere-initiated senescence." Nature **426**: 194-198.

D'Addario I, Abbruzzese C, Iacono M L, Teson M, Golisano O and Barone V (2010). "Overexpression of YAP1 induces immortalization of normal human keratinocytes by blocking clonal evolution." Histochemistry and Cell Biology **134**: 265-76.

Darbro B W, Lee K M, Nguyen N K, Domann F E and Klingelhutz A J (2006). "Methylation of the p16(INK4a) promoter region in telomerase immortalized human keratinocytes co-cultured with feeder cells." Oncogene **25**: 7421-33.

Darbro B W, Schneider G B and Klingelhutz A J (2005). "Co-regulation of p16INK4A and migratory genes in culture conditions that lead to premature senescence in human keratinocytes." The Journal of Investigative Dermatology **125**: 499-509.

Davis T, Baird D M, Haughton M F, Jones C J and Kipling D (2005). "Prevention of accelerated cell aging in Werner syndrome using a p38 mitogen-activated protein kinase inhibitor." The Journals of Gerontology Series A: Biological Sciences and Medical Sciences **60**: 1386-93.

Davis T, Faragher R G, Jones C J and Kipling D (2004). "Investigation of the signaling pathways involved in the proliferative life span barriers in werner syndrome fibroblasts." Annals of the New York Academy of Sciences **1019**: 274-7.

Davis T, Singhrao S K, Wyllie F S, Haughton M F, Smith P J, Wiltshire M, Wynford-Thomas D, Jones C J, Faragher R G and Kipling D (2003). "Telomere-based proliferative lifespan barriers in Werner-syndrome fibroblasts involve both p53-dependent and p53-independent mechanisms." Journal of Cell Science **116**: 1349-57.

Dellambra E, Golisano O, Bondanza S, Siviero E, Lacal P, Molinari M, D'Atri S and Luca M D (2000). "Downregulation of 14-3-3 Prevents Clonal Evolution and

Leads to Immortalization of Primary Human Keratinocytes." The Journal of Cell Biology **149**: 1117-30.

Dickson M A, Ino W C H Y, Ronfard V, Wu J Y, Weinberg R A, Louis D N, Li F P and Rheinwald J G (2000). "Human keratinocytes that express hTERT and also bypass a p16(INK4a)-enforced mechanism that limits life span become immortal yet retain normal growth and differentiation characteristics." Molecular and Cellular Biology **20**: 1436-47.

Dimri G P, Lee X, Basile G, Acosta M, Scott G, Roskelley C, Medrano E E, Linskens M, Rubel I, Pereira-Smith O, Peacocke M and Campisi J (1995). "A biomarker that identifies senescent human cells in culture and in aging skin *in vivo*." Proceedings of the National Academy of Sciences of the United States of America **92**: 9363-67.

Doherty K M, Sommers J A, Gray M D, Lee J W, vonKobbe C, Thoma N H, Kureekattil R P, Kenny M K and BroshJr R M (2005). "Physical and functional mapping of the replication protein a interaction domain of the werner and bloom syndrome helicases." Journal of Biological Chemistry **280**: 29494-505.

Edward J W and Bladon P T (1985). The Human Skin, Edward Arnold Ltd.

Eisinger M, Lee J S, Hefton J M, Darzynkewicz Z, Chiao J W and DeHarven E (1979). "Human epidermal cell cultures: Growth and differentiation in the absence of dermal components or medium supplements." Proceedings of the National Academy of Sciences of the United States of America **76**: 5340-44.

Elmore L W, Rehder C W, Di X, McChesney P A, Jackson-Cook C K, Gewirtz D A and Holt S E (2002). "Adriamycin-induced senescence in breast tumor cells involves functional p53 and telomere dysfunction." Journal of Biological Chemistry **277**: 35509-35515.

English J, Pearson G, Wilsbacher J, Swantek J, Karandikar M, Xu S and Cobb M H (1999). "New Insights into the Control of MAP Kinase Pathways." Experimental Cell Research **253**: 255-270.

Epstein C J, Martin G M, Schultz A L and Motulsky A G (1966). "Werner's syndrome a review of its symptomatology, natural history, pathologic features, genetics and relationship to the natural aging process." Medicine (Baltimore) **45**: 177-221.

Evans R J, Wyllie F S, Wynford-Thomas D, Kipling D and Jones C J (2003). "A P53-dependent, Telomere-independent Proliferative Life Span Barrier in Human Astrocytes Consistent with the Molecular Genetics of Glioma Development." Cancer Research **63**: 4854-4861.

Faragher R G A (2003). The Relationship Between Cell Turnover and Tissue Aging. Aging of Organs and Systems. Aspinall R. Dordrecht, Kluer Academic Publishers. **3:** 1-28.

Faragher R G A, Kill I R, Hunter J A, Pope F M, Tannock C and Shall S (1993). "The Gene Responsible for Werner Syndrome May be a Cell Division "Counting" Gene." The National Academy of Sciences **90**: 12030-12034.

Faragher R G A and Kipling D (1998). "How might replicative senescence contribute to human ageing?" BioEssays **20**: 985-991.

Fire A, XU S, Montgomery M K, Kostas S A, Driver S E and Mello C C (1998). "Potent and specific genetic interferences by double-stranded RNA in *Caenorhabditis elegans*." Nature **391**: 806-811.

Fornari F, Randolph J, Yalowich J, Ritke M and Gewirtz D (1994). "Interference by doxorubicin with DNA unwinding in MCF-7 breast tumor cells." Molecular Pharmacology **45**: 649-56.

Fossel M B (2004). The Skin. Cells, Aging, and Human Disease. New York, Oxford University Press**:** 140-60.

Franchitto A, Oshima J and Pichierri P (2003). "The G2-phase decatenation checkpoint is defective in Werner syndrome cells." Cancer Research **63**: 3289-95.

Franchitto A and Pichierri P (2004). "Werner syndrome protein and the MRE11 complex are involved in a common pathway of replication fork recovery." Cell Cycle. **3**: 1331-9.

Fry M and Loeb L A (1999). "Human Werner Syndrome DNA Helicase Unwinds Tetrahelical Structures of the Fragile X Syndrome Repeat Sequence d(CGG)n." Journal of Biological Chemistry **274**: 12797-12802.

Fu B, Quintero J and Baker C C (2003). "Keratinocyte Growth Conditions Modulate Telomerase Expression, Senescence, and Immortalization by Human Papillomavirus Type 16 E6 and E7 Oncogenes." Cancer Research **63**: 7815-24.

Fuchs E (1990). "Epidermal Differentiation: The Bare Essentials." The Journal of Cell Biology **111**: 2807-14.

Fusenig N E and Boukamp P (1998). "Multiple Stages and Genetic Alterations in Immortalization, Mlignant Transformation, and Tumor Progression of Human Skin Keratinocytes." Molecular Carcinogenesis **23**: 144-58.

Gebhart E, Schinzel M and Ruprecht K W (1985). "Cytogenetic studies using various clastogens in two patients with Werner syndrome and control individuals." Human Genetics **70**: 324-7.

Gewirtz D A (1999). "A critical evaluation of the mechanisms of action proposed for the antitumour effects of the anthracycline antibiotics adriamycin and daunorubicin." Biochemical Pharmacology **57**: 727-41.

Goto M (1997). "Hierarchical deterioration of body systems in Werner's syndrome: Implications for normal ageing." Mechanisms of Ageing and Development **98**: 239-254.

Goto M (1997). "Hierarchical deterioration of body systems in Werner's syndrome: implications for normal ageing." Mechanisms of Ageing and Development **98**: 239-54.

Goto M, Miller R W, Ishikawa Y and Sugano H (1996). "Excess of rare cancers in Werner syndrome (adult progeria)." Cancer Epidemiology, Biomarkers and Prevention **5**: 239-46.

Goto M M R, Ishikawa Y, Sugano H (1996). "Excess of rare cancers in Werner syndrome (adult progeria)." Cancer Epidemiol Biomarkers Prev. **5**: 239-46.

Goto M and Murata K (1978). "Urinary excretion of macromolecular acidic glycosaminoglycans in Werner's syndrome." Clinica Chimica Acta **85**: 101-6.

Goto M, Tanimoto K, Aotsuka S, Okawa M and Yokohari R (1982). "Age-related changes in auto-and natural antibody in the Werner syndrome." The American Journal of Medicine **72**: 607-14.

Goto M, Tanimoto K, Horiuchi Y and Kuwata T (1982). "Reduced natural killer cell activity of lymphocytes from patients with Werner's syndrome and recovery of its activity by purified human leucocyte interferon." Scandinavian Journal of Immunology **15**: 389-97.

Goto M, Tanimoto K, Horiuchi Y and Sasazuki T (1981). "Family analysis of Werner's syndrome: a survey of 42 Japanese families with a review of the literature." Clinical Genetics **19**: 8-15.

Gray M D, Shen J C, Kamath-Loeb A S, A B, Sopher B L, Martin G M, Oshima J and Loeb L A (1997). "The Werner syndrome protein is a DNA helicase." Nature Genetics **17**: 100-3.

Greider C W (1998). "Telomeres and senescence: The history, the experiment, the future." Current Biology **8**: R178-81.

Greider C W (1999). "Telomeres Do D-Loop-T-Loop." Cell **97**: 419-422.

Grove G L and Kligman A M (1983). "Age-associated changes in human epidermal cell renewal." Journal of Gerontology **38**: 137-42.

Hannon G J (2002). "RNA interference." Nature **418**.

Hansen J (1998). "Common cancers in the elderly." Drugs and Aging **13**: 467-78.

Harbour J W (2006). "Eye cancer: unique insights into oncogenesis: the Cogan Lecture." Investigative Ophthalmology and Visual Science **47**: 1736-45.

Harley C B, Futcher B A and Greider C W (1990). "Telomeres shorten during ageing of human fibroblasts." Nature **345**: 458-60.

Harmon F and Kowalczykowski S (1998). "RecQ helicase, in concert with RecA and SSB proteins, initiates and disrupts DNA recombination." Genes and Development **12**: 1134-44.

Harrison R G, Greenman M J, Mall F P and Jackson C M (1907). "Observations of the living developing nerve fiber." The Anatomical Record **1**: 116-28.

Hayflick L (1965). "The limited in vitro lifetime of human diploid cell strains." Experimental Cell Research **37**: 614-36.

Hayflick L (2003). "Living forever and dying in the attempt." Experimental Gerontology **38**: 1231-1241.

Hayflick L and Moorhead P S (1961). "The serial cultivation of human diploid cell strains." Experimental Cell Research **25**: 585-621.

Herbig U, Jobling W A, Chen B P, Chen D J and Sedivy J M (2004). "Telomere shortening triggers senescence of human cells through a pathway involving ATM, p53, and p21 (CIP1), but not p16 (INK4a)." Molecular Cell **14**: 501-13.

Hoehn H, Bryant E M, Au K, Norwood T H, Boman H and Martin G M (1975). "Variegated translocation mosaicism in human skin fibroblast cultures." Cytogenetics and Cell Genetics **15**: 282-98.

Holliday R, Thompson K V, Huschtscha L I, Rattan S I, SG S G S and Spanos A (1985). "Experimental studies on Werner's syndrome fibroblasts." Advances in Experimental Medicine and Biology **190**: 331-9.

Houben E, Paepe K D and Rogiers V (2007). "A Keratinocyte's Course of Life." Skin Pharmacology and Physiology **20**: 122-32.

Howard A and Pelc S P (1953). "Synthesis of deoxyribonucleic acid in normal and irradiated cells and its relation to chromosome breakage." Heredity **6**: 261-273.

Hu J S, Feng H, Zeng W, Lin G X and Xi X G (2005). "Solution structure of a multifunctional DNA- and protein-binding motif of human Werner syndrome protein." Proceedings of the National Academy of Sciences of the United States of America **102**: 18379-84.

Huang S, Li B, Gray M D, Oshima J, Mian I S and Campisi J (1998). "The premature ageing syndrome protein, WRN, is a 3'-->5' exonuclease." Nature Genetics **20**: 114-6.

Huschtscha L I, Noble J R, Neumann A A, Moy E L, Barry P, Melki J R, Clark S J and Reddel R R (1998). "Loss of p16INK4a Expression by Methylation Is Associated with Lifespan Extension of Human Mammary Epithelial Cells." Cancer Research **58**: 3508-12.

Imamura O, Fujita K, Itoh C, Takeda S, Furuichi Y and Matsumoto T (2002). "Werner and Bloom helicases are involved in DNA repair in a complementary fashion." Oncogene **21**: 954-63.

Itahana K, Zou Y, Itahana Y, Martinez J-L, Beausejour C, Jacobs J J L, vanLohuizen M, Band V, Campisi J and Dimri G P (2003). "Control of the Replicative Life Span of Human Fibroblasts by p16 and the Polycomb Protein Bmi-1." Mol. Cell. Biol. **23**: 389-401.

Iwasa H, Han J and Ishikawa F (2003). "Mitogen-activated protein kinase p38 defines the common senescence-signalling pathway." Genes to Cells **8**: 131-144.

Jabionska S and Blaszczyk M (1998). "Scleroderma-Like Disorders." Seminars in Cutaneous Medicine and Surgery **17**: 65-76.

James S E, Faragher R G A, Burke J F, Shall S and Mayne L V (2000). "Werner's syndrome T lymphocytes display a normal in vitro life-span." Mechanisms of Ageing and Development **121**: 139-49.

Jarrard D F, Sarkar S, Shi Y, Yeager T R, Magrane G, Kinoshita H, Nassif N, Meisner L, Newton M A, Waldman F M and Reznikoff C A (1999). "p16/pRb pathway alterations are required for bypassing senescence in human prostate epithelial cells." Cancer Research **59**: 2957-64.

Johnson D G and Schneider-Broussard R (1998). "Role of E2F in cell cycle control and cancer." Frontiers in Bioscience: a journal and virtual library **3**: 447-8.

Johnson D G and Walker C L (1999). "Cyclins and Cell Cycle Checkpoints." Annual Review of Pharmacology **39**: 295-312.

Jonasson J A (1986). Analysis and Interpretation of Human Chromosome Preparations. Human cytogenetics: a practical approach. Rooney D E and Czepulkowski B H.

Jones P H, Harper S and Watt F M (1995). "Stem cell patterning and fate in human epidermis." Cell **80**: 83-93.

Kamath-Loeb A S, Johansson E, Burgers P M and Loeb L A (2000). "Functional interaction between the Werner Syndrome protein and DNA polymerase delta." Proceedings of the National Academy of Sciences of the United States of America **97**: 4603-8.

Kaszubowska L (2008). "Telomere Shortening and Ageing of the Immune System." Journal of Physiology and Pharmacology **59**: 169-86.

Kawabe Y, Branzei D, Hayashi T, Suzuki H, Masuko T, Onoda F, Heo S, Ikeda H, Shimamoto A, Furuichi Y, Seki M and Enomoto T (2001). "A novel protein interacts with the Werner's syndrome gene product physically and functionally." Journal of Biological Chemistry **276**: 20364-9.

Kill I R, Faragher R G A, Lawrence K and Shall S (1994). "The expression of proliferation-dependent antigens during the lifespan of normal and progeroid human fibroblasts in culture." Journal of Cell Science **107**: 571-79.

Kim N W, Piatyszek M A, Prowse K R, Harley C B, West M D, Ho P L, Coviello G M, Wright W E, Weinrich S L and Shay J W (1994). "Specific association of human telomerase activity with immortal cells and cancer." Science **266**: 2011-5.

Kipling D (2001). "Telomeres, replicative senescence and human ageing." Maturitas **38**: 25- 38.

Kipling D, Davis T, Ostler E L and Faragher R G A (2004). "What can progeroid syndromes tell us about human aging?" Science **305**: 1426-31.

Kipling D and Faragher R G (1997). "Progeroid syndromes: probing the molecular basis of aging?" Molecular Pathology **50**: 234-41.

Kitano K, Yoshihara N and Hakoshima T (2006). "Crystal structure of the HRDC domain of human Werner syndrome protein, WRN." Journal of Biological Chemistry **282**: 2717-28.

Kiyono T, Foster S A, Koop J I, McDougall J K, Galloway D A and Klingelhutz A J (1998). "Both Rb/p16INK4a inactivation and telomerase activity are required to immortalize human epithelial cells." Nature **396**: 84-8.

Ko L J and Prives C (1996). "p53: Puzzle and Paradigm." Genes and Development **10**: 1054-1072.

Kodama S, Kashino G, Suzuki K, Takatsuji T, Okumura Y, M Oshimura, M Watanabe and Barrett J (1998). "Failure to Complement Abnormal Phenotypes of Simian Virus 40-transformed
Werner Syndrome Cells by Introduction of a Normal Human Chromosome 8." Cancer Research **58**: 5188-95.

Lebel M and Leder P (1998). "A deletion within the murine Werner syndrome helicase induces sensitivity to inhibitors of topoisomerase and loss of cellular proliferative capacity." Proceedings of the National Academy of Sciences of the United States of America **95**: 13097-13102.

Lebel M, Spillare E A, Harris C C and Leder P (1999). "The Werner syndrome gene product co-purifies with the DNA replication complex and interacts with PCNA and topoisomerase I." Journal of Biological Chemistry **274**: 37795-9.

Lee A C, Fenster B E, Ito H, Takeda K, Bae N S, Hirai T, Yu Z-X, Ferrans V J, Howard B H and Finkel T (1999). "Ras Proteins Induce Senescence by Altering the Intracellular Levels of Reactive Oxygen Species." Journal of Biological Chemistry **274**: 7936-7940.

Lee B Y, Han J A, Im J S, Morrone A, Johung K, Goodwin E J, Kleijer W J, DiMaio D and Hwang E S (2006). "Senescence-associated β-galactosidase is lysosomal β-galactosidase." Aging Cell **5**: 187-95.

Lee J C, Laydon J T, McDonnell P C, Gallagher T F, Kumar S, Green D, McNulty D, Blumenthal M J, Heys J R, Landvatter S W, Strickler J E, McLaughlin M M, Siemens I R, Fisher S M, Livi G P, White J R, Adams J L and Young P R (1994). "A protein kinase involved in the regulation of inflammatory cytokine biosynthesis." Nature **372**: 739-46.

Lee J W, Harrigan J, Opresko P L and Bohr V A (2005). "Pathways and functions of the Werner syndrome protein." Mechanisms of Ageing and Development **126**: 79-86.

Lee J W, Kusumoto R, Doherty K M, Lin G X, Zeng W, Cheng W H, vonKobbe C, BroshJr R M, Hu J S and Bohr V A (2005). "Modulation of Werner syndrome protein function by a single mutation in the conserved RecQ domain." The Journal of Biological Chemistry **280**: 39627-36.

Levine A J (1997). "p53, the Cellular Gatekeeper for Growth and Division." Cell **88**: 323-31.

Levy M Z, Allsopp R C, Futcher A B, Greider C W and Harley C B (1992). "Telomere end-replication problem and cell aging." Journal of Molecular Biology **225**: 951- 60.

Lewin B (2000). Genes VII. New York, Oxford University Press Inc.

Li B and Comai L (2000). "Functional Interaction between Ku and the Werner Syndrome Protein in DNA End Processing." Journal of Biological Chemistry **275**: 28349-28352.

Li Y J C, Nichols MA, Xiong Y. (1994). "Cell cycle expression and p53 regulation of the cyclin-dependent kinase inhibitor p21." Oncogene **9**: 2261-2268.

Lin A W, Barradas M, Stone J C, Aelst L V, Serrano M and Lowe S W (1998). "Premature senescence involving p53 and p16 is activated in response to constitutive MEK/MAPK mitogenic signaling." Genes and Development **12**: 3008-19.

Lindsten J E, Kinger H P and Hamerton J L, Eds. (1978). An International System for Human Cytogenetic Nomenclature (ISCN). Birth Defects: Original Article Series.

Lowe J, Sheerin A, Jennert-Burston K, Burton D, Ostler E L, Bird J, Green M H L and Faragher R G A (2004). "Camptothecin Sensitivity in Werner Syndrome Fibroblasts as Assessed by the COMET Technique." Annals of the New York Academy of Sciences **1019**: 256-9.

Martens U M, Chavez E A, Poon S S S, Schmoor C and Lansdorp P M (2000). "Accumulation of Short Telomeres in Human Fibroblasts Prior to Replicative Senescence." Experimental Cell Research **256**: 291-9.

Martin G M, Sprague C A and Epstein C J (1970). "Replicative lifespan of cultivated human cells. Effects of donor's age, tissue and genotype." Laboratory Investigation **23**: 86-92.

Matsumoto T, Imamura O, Yamabe Y, Kuromitsu J, Tokutake Y, Shimamoto A, Suzuki N, Satoh M, Kitao S, Ichikawa K, Hiroshi Kataoka, Sugawara K, Thomas W, Mason B, Tsuchihashi Z, Drayna D, Sugawara M, Sugimoto M, Furuichi Y and Goto M (1997). "Mutation and haplotype analyses of the Werner's syndrome gene
based on its genomic structure:
genetic epidemiology in the Japanese population." Human Genetics **100**: 123-30.

Matsumoto T, Shimamoto A, Goto M and Furuichi Y (1997). "Impaired nuclear localization of defective DNA helicases in Werner's syndrome." Nature Genetics **16**: 335-6.

Maurelli R, Zambruno G, Guerra L, Abbruzzese C, Dimri G, Gellini M, Bondanza S and Dellambra E (2006). "Inactivation of $p16^{INK4a}$ (inhibitor of cyclin-dependent kinase 4A) immortalizes primary human keratinocytes by maintaining cells in the stem cell compartment." The FASEB Journal **20**: 1516-8.

Maurelli R Z G, Guerra L, Abbruzzese C, Dimri G, Gellini M, Bondanza S, Dellambra E (2006). "Inactivation of p16INK4a (inhibitor of cyclin-

dependent kinase 4A) immortalizes primary human keratinocytes by maintaining cells in the stem cell compartment." The FASEB Journal **20**: 1516-8.

McCullough J L and Kelly K M (2006). "Prevention and Treatment of Skin Aging." Annals of the New York Academy of Sciences **1067**: 323-31.

McElligott R and Wellinger R J (1997). "The terminal DNA structure of mammalian chromosomes." The EMBO Journal **16**: 3705-3714.

Montgomery R A and Dietz H C (1997). "Inhibition of fibrillin 1 expression using U1 snRNA as a vhicle for the presentation of antisense targeting sequence." Human Molecular Genetics **6**: 519-25.

Moser M J, Oshima J and Monnat R J J (1999). "WRN mutations in Werner syndrome." Human Mutation **13**: 271-9.

Moyzis R K, Buckingham J M, Cram L S, Dani M, Deaven L L, Jones M D, Meyne J, Ratliff R L and Wu J R (1988). "A highly conserved repetitive DNA sequence, (TTAGGG)n, present at the telomeres of human chromosomes." Proceedings of the National Academy of Sciences of the United States of America **85**: 6622- 6626.

Oeseburg H, DeBoer R A, VanGilst W H and VanDerHarst P (2010). "Telomere biology in healthy aging and disease." Pfulgers archiv: European Journal of Physiology **459**: 259-68.

Olovnikov A M (1971). "Principles of marginotomy in template synthesis of polynucleotides." Doklady Akad. Nauk SSSR **201**: 1496-1499.

Olovnikov A M (1996). "TELOMERES, TELOMERASE, AND AGING: ORIGIN OF THE THEORY." Experimental Gerontology **31**: 443-448.

Opitz O G, Suliman Y, Hahn W C, Harada H, Blum H E and Rustgi A K (2001). "Cyclin D1 overexpression and p53 inactivation immortalize primary oral keratinocytes by a telomerase-independent mechanism." The Journal of Clinical Investigation **108**: 725-32.

Oppenheimer B S and Kugel V H (1934). "Werner's syndrome: A heredofamilial disorder with scleroderma, bilateral juvenile cataract, precocious graying of hair and endocrine stigmatization." Transactions of the Associations of American Physicians **49**: 358-70.

Overholtser M, Zhang J, Smolen G A, Muir B, Li W, Sgroi D C, Deng C X, Brugge J S and Harber D A (2006). "Transforming properties of YAP, a candidate oncogene on the chromosome 11q22 amplicon." Proceedings of the National Academy of Sciences of the United States of America **103**: 12405-410.

Pardee A (1974). "A restriction point for control of normal animal cell proliferation." Proc. Natl. Acad. Sci. USA **71**: 1286-1290.

Parkinson E K and Yeudall W A (1992). The Epidermis. Culture of Specialized Cells: Culture of Epithelial Cells. Freshney I**:** 59-80.

Patt H M and Quastler H (1963). "Radiation effects on cell renewal and related systems." Physiological Reviews **43**: 357-96.

Peehl D M and Ham R G (1980). "Clonal growth of human keratinocytes with small amounts of dialyzed serum." In Vitro **16**: 526-40.

Pellegrini G, Dellambra E, Golisano O, Martinelli E, Fantozzi I, Bondanza S, Ponzin D, McKeon F and Luca M D (2001). "p63 identifies keratinocyte stem cells." Proceedings of the National Academy of Sciences of the United States of America **98**: 3156-61.

Poot M, Hoehn H, Runger T M and Martin G M (1992). "Impaired S-phase transit of Werner syndrome cells expressed in lymphoblastoid cell lines." Experimental Cell Research **202**: 267-73.

Postiglione A, Soricelli A, Covelli E M, Iazzetta N, Ruocco A, Milan G, Santoro L, Alfano B and Brunetti A (1994). "Premature Aging in Werener's Syndrome Spares the Centreal Nervous System." Neurobiology of Aging **17**: 325-30.

Prescott D M (1968). "Regulation of Cell Reproductioin." Cancer Research **28**: 1815-20.

Prince P R, Emond M J and MonnatJr R J (2001). "Loss of Werner syndrome protein function promotes aberrant mitotic recombination." Genes and Development **15**: 933-938.

Puri P L, Maclachlan T K, Levrero M and Giordano A (1999). The Intrinsic Cell Cylce: From Yeast to Mammals. The molecular basis of cell cycle and growth control. G.S. Stein R B, A. Giordano and D.T. Denhardt. New York, Wiley-Liss, Inc**:** 15-79.

Puthenveettil J A, Burger M S and Reznikoff C A (1999). "Replicative senescence in human uroepithelial cells." Advances in Experimental Medicine and Biology **462**: 83-91.

Rahn J J, Lowery M P, Della-Colletta L, Adair G M and Nairn R S (2010). "Depletion of Werner helicase results in mitotic hyperrecombination and pleiotropic homologous and nonhomologous recombination phenotypes." Mechanisms of Ageing and Development.

Ramesh H S, Pope D, Gennari R and Audisio R A (2005). "Optimising surgical management of elderly cancer patients." World J Surg Oncol. **3**: 17.

Ramirez R D, Herbert B-S, Vaughan M B, Zou Y, Gandia K, Morales C P, Wright W E and Shay J W (2003). "Bypass of telomere-dependent replicative senescecence (M1) upon overexpression of Cdk4 in normal human epithelial cells." Oncogene **22**: 433-444.

Ramirez R D, Morales C P, Herbert B S, Rohde J M, Passons C, Shay J W and Wright W E (2001). "Putative telomere-independent mechanisms of replicative aging reflect inadequate growth conditions." Genes and Development **15**: 398-403.

Randall W, King R, Deshaies J, Peters J-M and Kirschner M W (1996). "How Proteolysis Drives the Cell Cycle." Science **274**: 1652-1659.

Rao P N and Jhonson R T (1970). "Mammalian cell fusion: Studies on the regulation of DNA synthesis and mitosis." Nature **225**: 159-164.

Rea M A, Zhou L, Qin Q, Barrandon Y, Easley K W, Gungner S F, Phillips M A, Holland W S, Gumerlock P H, Rocke D M and Rice R H (2006). "Spontaneous Immortalization of Human Epidermal Cells with Naturally Elevated Telomerase." Journal of Investigative Dermatology **126**: 2507-15.

Resnitzky D, Gossen M, Bujard H and Reed S I (1994). "Acceleration of the G1/S phase transition by expression of cyclins D1 and E with an inducible system." Molecular and Cellular Biology **14**: 1669-1679.

Rheinwald J G (1980). "Serial cultivation of normal human epidermal keratinocytes." Methods Cell Biol **21A**: 229-54.

Rheinwald J G and Beckett M A (1980). "Defective Terminal Differentiation in Culture as a Consistent and Selectable Character of Malignant Human Keratinocytes." Cell **22**: 629-32.

Rheinwald J G and Green H (1975). "Serial Cultivation of Strains of Human Epidermal Keratinocytes: The Formation of Keratinizing Colonies from Single Cells." Cell **6**: 331-344.

Rheinwald J G and Green H (1977). "Epidermal growth factor and the multiplication of cultured human epidermal keratinocytes." Nature **265**: 421-4.

Rheinwald J G, Hahn W C, Ramsey M R, Wu J Y, Guo Z, Tsao H, DeLuca M, Catricala C and O'Toole K M (2002). "A Two-Stage, p16INK4A- and p53-Dependent Keratinocyte Senescence Mechanism That Limits Replicative Potential Independent of Telomere Status." Molecular and Cellular Biology **22**: 5157-5172.

Rheinwald J G, Hahn W C, Ramsey M R, Wu J Y, Guo Z, Tsao H, Luca M D, Catricalà C and O'Toole K M (2002). "A two-stage, p16(INK4A)- and p53-dependent keratinocyte senescence mechanism that limits replicative potential independent of telomere status." Molecular and Cellular Biology **22**: 5157-72.

Robinson M J, LaCelle P T and Eckert R L (1996). "Involucrin is a covalently crosslinked constituent of highly purified epidermal corneocytes: Evidence for a common pattern of involucrin crosslinking *in vivo* and *in vitro*." Journal of Investigative Dermatology **107**: 101-7.

Rodriguez-Lopez A M, Jackson D A, Nehlin J O, Iborra F, Warren A V and Cox L S (2003). "Characterisation of the interaction between WRN, the helicase/exonuclease defective in progeroid Werner's syndrome, and an essential replication factor, PCNA." Mechanisms of Ageing and Development **124**: 167-74.

Rodriguez-Lopez A M, Whitby M C, Borer C M, Bachler M A and Cox L S (2007). "Correction of Proliferation and Drug Sensitivity Defects in the Progeroid Werner's Syndrome by Holliday Junction Resolution." Rejuvenation Research **10**: 27-40.

Saintigny Y, Makienko K, Swanson C, Emond M J and MonnatJr R J (2002). "Homologous recombination resolution defect in werner syndrome." Molecular and Cellular Biology **22**: 6971-8.

Sakamoto S, Nishikawa K, Heo S J, Goto M, Furuichi Y and Shimamoto A (2001). "Werner helicase relocates into nuclear foci in response to DNA damaging agents and co-localizes with RPA and Rad51." genes Cells. **6**: 421-30.

Salk D (1982). "Werner's syndrome: a review of recent research with an analysis of connective tissue metabolism, growth control of cultured cells, and chromosomal aberrations." Human Genetics **62**: 1-15.

Salk D, Au K, Hoehn H and Martin G M (1981b). "Cytogenetics of Werner's syndrome cultured skin fibroblasts: variegated translocation mosaicism." Cytogenetics and Cell Genetics **30**: 92-107.

Salk D, Au K, Hoehn H, Stenchever M R and Martin G M (1981c). "Evidence of clonal attenuation, clonal succession, and clonal expansion in mass cultures of aging Werner's syndrome skin fibroblasts." Cytogenetics and Cell Genetics **30**: 108-17.

Salk D, Bryant E, Au K, Hoehn H and Martin G M (1981). "Systematic growth studies, cocultivation, and cell hybridization studies of Werner syndrome cultured skin fibroblasts." Hum Genet **58**: 310-6.

Salk D, Bryant E, Hoehn H, Johnston P and Martin G M (1985). "Growth characteristics of Werner syndrome cells in vitro." Advances in Experimental Medicine and Biology **190**: 305-11.

Sandy P, Ventura A and Jacks T (2005). "Mammalian RNAi: a practical guide." Bio Techniques **39**: 215-24.

Scappaticci S, Cerimele D and Fraccaro M (1982). "Clonal structural chromosomal rearrangements in primary fibroblast cultures and in lymphocytes of patients with Werner's Syndrome." Human Genetics **62**: 16-24.

Scappaticci S, Forabosco A, Borroni G, Orecchia G and Fraccaro M (1990). "Clonal structural chromosomal rearrangements in lymphocytes of four patients with Werner's syndrome." Ann Genet **33**: 5-8.

Schuler G D, Altschul S F and Lipman D J (1991). "A Workbench for Multiple Alignment Construction and Analysis." Protiens **9**: 180-90.

Schulz V P, Zakian V A, Ogburn C E, McKay J, Jarzebowicz A A, Edland S D and Martin G M (1996). "Accelerated loss of telomeric repeats may not explain accelerated replicative decline of Werner syndrome cells." Human Genetics **97**: 750-4.

Scott W G, Martick M and Chi Y (2009). "Structure and function of regulatory RNA elements: Ribozymes that regulate gene expression." Biochimica et Biophysica Acta (BBA)-Gene Regulatory Mechanisms **1789**: 634-41.

Serrano M, Hannon G J and Beach D (1993). "A new regulatory motif in cell cycle control causing specific inhibition of cyclin D/ CDK4." Nature **366**: 704-7.

Serrano M, Lin A W, McCurrach M E, Beach D and Lowe S W (1997). "Oncogenic ras Provokes Premature Cell Senescence Associated with Accumulation of p53 and p16INK4a." Cell **88**: 593-602.

Sharma S, Sommers J A, Driscoll H C, Uzdilla L, Wilson T M and BroshJr R M (2003). "The exonucleolytic and endonucleolytic cleavage activities of human exonuclease 1 are stimulated by an interaction with the carboxyl-terminal region of the Werner syndrome protein." J Biol Chem **278**: 23487-96.

Shay J W and Bacchetti S (1997). "A Survey of Telomerase Activity in Human Cancer." European Journal of Cancer **33**: 787-91.

Shen J C, Gray M D, Oshima J and Loeb L A (1998). "Characterization of Werner syndrome protein DNA helicase activity: directionality, substrate dependence and stimulation by replication protein A." Nucl. Acids Res. **26**: 2879-2885.

Sherr C J (1996). "Cancer Cell Cycles." Science **274**: 1672-77.

Shiratori M, Sakamoto S, Suzuki N, Tokutake Y, Kawabe Y, Enomoto T, Sugimoto M, Goto M, Matsumoto T and Furuichi Y (1999). "Detection by epitope-defined monoclonal antibodies of Werner DNA helicases in the nucleoplasm and their upregulation by cell transformation and immortalization." The Journal of Cell Biology **144**: 1-9.

Skladanowski A and Konopa J (1993). "Adriamycin and daunomycin induce programmed cell death (apoptosis) in tumour cells." Biochemical Pharmacology **46**: 375-82.

Sommers J A, Sharma S, Doherty K M, Karmakar P, Yang Q, Kenny M K, Harris C C and BroshJr R M (2005). "p53 modulates RPA-dependent and RPA-independent WRN helicase activity." Cancer Res. **65**: 1223-33.

Stoker M, O'Neill C, Berryman S and Waxman V (1968). "Anchorage and Growth Regulation in Normal and Virus-Transformed Cells." International Journal of Cancer **3**: 683-93.

Suzuki N, Shimamoto A, Imamura O, Kuromitsu J, Kitao S, Goto M and Furuichi Y (1997). "DNA helicase activity in Werner's syndrome gene product synthesized in a baculovirus system." Nucl. Acids Res. **25**: 2973-78.

Taylor R S, Ramirez R D, Ogoshi M, Chaffins M, Piatyszek M A and Shay J W (1996). "Detection of Telomerase Activity in Malignant and Nonmalignant Skin Conditions." Journal of Investigative Dermatology **106**: 759-65.

Tenchini M L, Ranzati C and Malcovati M (1992). "Culture techniques for human keratinocytes." Burns **18**: S11-S15.

vonKobbe C and Bohr V A (2002). "A nucleolar targeting sequence in the Werner syndrome protein resides within residues 949-1092." J Cell Sci. **115**: 3901-7.

Voorhees J J, Duell E A, Chambers D A and Marcelo C L (1976). "Regulation of Cell Cycles." The Journal of Investigative Dermatology **67**: 15-9.

Watt F (1983). "Involucrin and other markers of keratinocyte terminal differentiation." Journal of Investigative Dermatology **81**: 100s-3s.

Watt F M and Green H (1981). "Involucrin synthesis is correlated with cell size in human epidermal cultures." Journal of Cell Biology **90**: 738-42.

Weinstein G D, McCullough J L and Ross P (1984). "Cell proliferation in normal epidermis." The Journal of Investigative Dermatology **82**: 623-8.

Werner O (1904). On cataract in conjunction with scleroderma. Royal Ophthalmology Clinic, Royal Christian Albrecht. Kiel, University of Kiel. **doctoral dissertation**.

Wright W E and Shay J W (1992). "The Two-Stage Mechanism Controlling Cellular Senescence and Immortalization." Experimental Gerontology **27**: 383-9.

Wyllie F S, Jones C J, Skinner J W, Haughton M F, Wallis C, Wynford-Thomas D, Faragher R G and Kipling D (2000). "Telomerase prevents the accelerated cell ageing of Werner syndrome fibroblasts." Nat Genet **24**: 16-17.

Xiong Y, Hannon G J, Zhang H, Casso D, Kobayashi R and Beach D (1993). "p21 is a universal inhibitor of cyclin kinases." Nature **366**: 701-4.

Yamagata K, Kato J, Shimamoto A, Goto M, Furuichi Y and Ikeda H (1998). "Bloom's and Werner's syndrome genes suppress hyperrecombination in yeast sgs1 mutant: implication for genomic instability in human diseases." Proceedings of the National Academy of Sciences of the United States of America **95**: 8733-8.

Yamamoto K, Imakiire A, Miyagawa N and Kasahara T (2003). "A report of two cases of Werner's syndrome and review of the literature." J Orthop Surg (Hong Kong) **11**: 224-33.

Yang J, Chang E, Cherry A M, Bangs C D, Oei Y, Bodnar A, Bronstein A, Chiu C-P and Herron G S (1999). "Human Endothelial Cell Life Extension by Telomerase Expression." The Journal of Biological Chemistry **274, No.37**: 26141-26148.

Yannone S M, Roy S, Chan D W, Murphy M B, Huang S, Campisi J and Chen D J (2001). "Werner syndrome protein is regulated and phosphorylated by DNA-dependent protein kinase." J Biol Chem **276**: 38242-8.

Yokote K and Saito Y (2008). "Extension of the life span in patients with Werner syndrome." Journal of the American Geriatrics Society **56**: 1770-1.

Yu C E, Oshima J, Fu Y H, Wijsman E M, Hisama F, R R A, Matthews S, Nakura J, Miki T, Ouais S, Martin G M, Mulligan J and Schellenberg G D (1996). "Positional cloning of the Werner's syndrome gene." Science **272**: 258-62.

Yuspa S H, Hawley-Nelson P, Koehler B and Stanley J R (1980). "A Survey of Transformation Markers in Differentating Epidermal Cell Lines." Cancer Research **40**: 4694-03.

Zarubin T and Han J (2005). "Activation and signaling of the p38 MAP kinase pathway." Cell Res. **15**: 11-8.

Appendix I

a) AG03141

Days	CPD
5	12.207029
9	13.790289
14	15.443668
21	16.231074
29	16.58834
43	17.270946
71	17.660852
89	18.675697

b) AG03141+ SB203580

Days	CPD
5	12.207029
9	14.06343
14	16.41096
21	18.46471
29	19.71301
43	21.55927
71	23.3649
89	25.29514

Table 5.1 CPD of primary Werner's syndrome fibroblasts treated with SB203580 and untreated Cumulative population doublings of Werner's syndrome fibroblasts (AG03141) a) untreated and b) treated with 10 μM SB203580.

a) HCA2.hTERT

Days	CPD
5	4.319419586
9	7.745930255
13	11.26744683
17	15.10652237
21	18.37376928
25	22.09043016
29	25.68130029
33	29.14526276
37	32.65418411
43	37.06665472
49	40.29998767
54	44.29466074
59	47.55580049

b) HCA2.hTERT+SB203580

Days	CPD
5	4.319419586
10	8.470814408
15	11.88648359
19	16.00372148
24	20.19637045
28	23.46748928
33	27.67839179
38	32.05666886
43	36.28303422
49	40.67050712
54	45.11418556
59	48.30873093

Table 5.2 CPD of telomerase immortalised normal fibroblasts treated with SB203580 and untreated Cumulative population doublings of hTERT immortalised normal fibroblasts (HCA2.hTERT) a) untreated and b) treated with SB203580.

a) AG03141.hTERT

Days	CPD
6	2.320580414
12	4.056535992
19	5.792491992
24	6.131432545
28	7.715475566
32	9.46934494
38	11.35577472
50	13.54300513
56	15.79971474

b) AG03141.hTERT+SB203580

Days	CPD
6	2.320580414
14	4.207009724
19	5.428690867
24	7.128143758
28	8.449304829
32	9.670713888
44	11.5176383
56	13.59709002

Table 5.3 CPD of telomerase immortalised Werner's syndrome fibroblasts treated with SB203580 and untreated Cumulative population doublings of hTERT immortalised Werner's syndrome fibroblasts (AG03141.hTERT) a) untreated and b) treated with SB203580.

Appendix II

a) 1BR.3neo

Passage	Days	CPD
1	6	3.997678
2	12	8.478376
3	17	12.23822
4	22	15.94756
5	26	19.24333
6	30	22.56813

b) WV-1

Passage	Days	CPD
1	6	4.669713
2	12	9.591288
3	17	13.57693
4	22	17.78654
5	26	21.33702
6	30	25.039

c) 1BR.3neo-WRN4

Passage	Days	CPD
1	6	4.562338
3	17	9.108135
2	12	12.38916
4	22	16.30655
5	26	19.34041
6	30	22.30216

d) 1BR.3neo-Rib3

Passage	Days	CPD
1	6	3.534001
2	12	7.356243
3	17	10.7738
4	22	14.09859
5	26	16.71375
6	30	19.75346

e) 1BR.3neo-WRN4/Rib3

Passage	Days	CPD
1	8	3.955113
2	14	8.068877
3	19	10.99927
4	24	14.58066
5	30	19.05603

Table 5.4 CPD of SV40 immortalised normal, Werner's syndrome, shRNA expressing, ribozyme expressing and both shRNA and ribozyme expressing fibroblasts Cumulative population doublings of SV40 immortalised fibroblasts a) 1BR.3neo (normal), b) WV-1 (Werner's syndrome), c) 1BR.3neo-WRN4 (shRNA expressing), d) 1BR.3neo-Rib3 (ribozyme expressing) and e) 1BR.3neo-WRN4/ Rib3 (shRNA and ribozyme expressing).

Appendix III

a) normal keratinocytes (SK206AK)

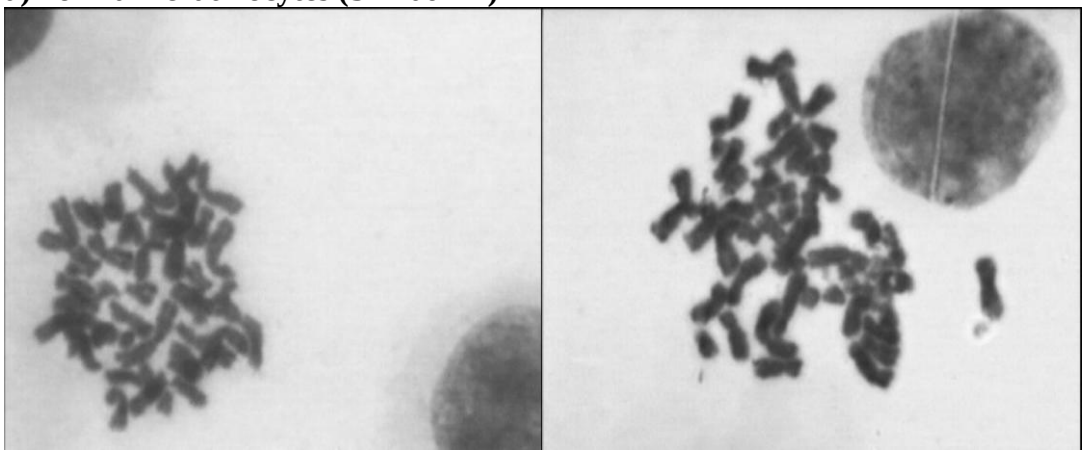

b) Werner's syndrome keratinocytes (WSK368)

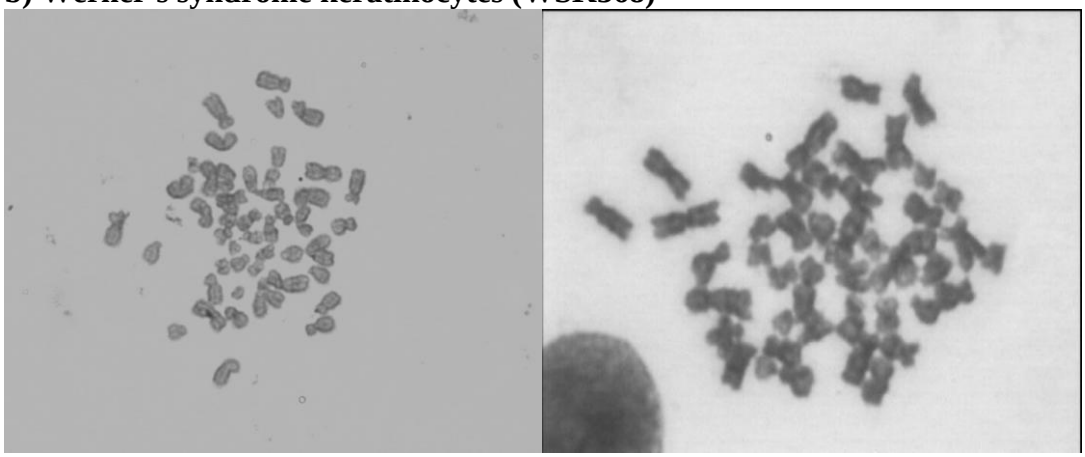

Figure 5.1 Photographs of metaphase chromosomes in normal and Werner's syndrome keratinocytes Metaphase photographs of a) normal keratinocytes (SK206AK) (CPD) and b) Werner's syndrome keratinocytes (WSK368) (CPD).

a) SK206AK

Passage	Days	CPD
1	7	0
2	13	3
3	19	5.005747166
4	26	8.125034531
5	37	9.252211422
6	51	12.65966504
7	61	16.26428529
8	73	19.08513709
9	96	20.70424086
10	103	22.3946911
11	116	25.42369798
12	129	28.75829916
13	143	31.89520764
14	153	33.85151089
15	160	36.34597345
16	170	38.72600408
17	184	42.1854357
18	198	43.70839354
19	206	46.79315157
20	217	50.23027576
21	227	53.33085834
22	240	56.17391328
23	251	58.61937125
24	259	60.70541861

Table 5.5 CPD of normal and Werner's syndrome keratinocytes Cumulative population doublings of keratinocytes from a) SK206AK (normal patient) and b) WSK368 (Werner's syndrome patient).

b) WSK 368

Passage	Days	CPD
1	7	0
2	13	3.6
3	19	5.73
4	24	7.93614
5	31	10.08660494
6	38	12.19382683
7	47	12.58536729
8	52	12.99876373
9	66	15.283548
10	78	17.17495362
11	87	18.89619048
12	95	20.49635371
13	104	22.98185461
14	112	24.42434034
15	119	25.61244762
16	127	26.41991
17	132	25.12122712
18	146	27.95573262
19	152	29.52821431
20	159	31.51777159
21	167	35.06694789
22	178	37.95233213
23	192	42.0267582
24	202	45.60888625
25	214	48.58132934
26	228	52.11137256
27	237	55.74545474
28	244	58.80889765
29	254	62.54489212
30	263	66.44314534
31	273	70.29912419
32	284	74.34074009
33	294	78.71018516
34	300	82.17123489
35	310	86.0005907
36	318	89.61261709
37	324	92.46012914
38	331	96.2788169
39	342	100.2295256
40	351	104.5955356
41	360	108.8065389
42	368	109.8476227
43	375	113.8104017
44	384	118.2787685
45	391	122.4342132
46	399	126.3176719
47	407	130.0960737

Table 5.5 CPD of normal and Werner's syndrome keratinocytes Cumulative population doublings of keratinocytes from a) SK206AK (normal patient) and b) WSK368 (Werner's syndrome patient).

a) SK206AK

Passage	CPDL
5	6.25
6	9.66
7	13.26
8	16.09
9	17.70
18	40.71
20	47.23

b) WSK 368

Passage	CPDL
5	4.36
6	6.46
7	6.86
8	7.27
9	9.55
10	11.44
11	13.17
12	14.77
13	17.25
14	18.69
15	19.88
16	20.69
28	53.08
29	56.81
30	60.71
31	64.57
40	98.87
41	103.08

Table 5.6 Passage and CPD of normal and Werner's syndrome keratinocytes assayed for SA β-Gal List of passages and cumulative population doublings (CPD) at which a) normal (SK206AK) and b) Werner's syndrome (WSK368) keratinocytes were assayed for SA β-galactosidase. All samples were tested in triplicates.